Acta morphologica et anthropologica (19)

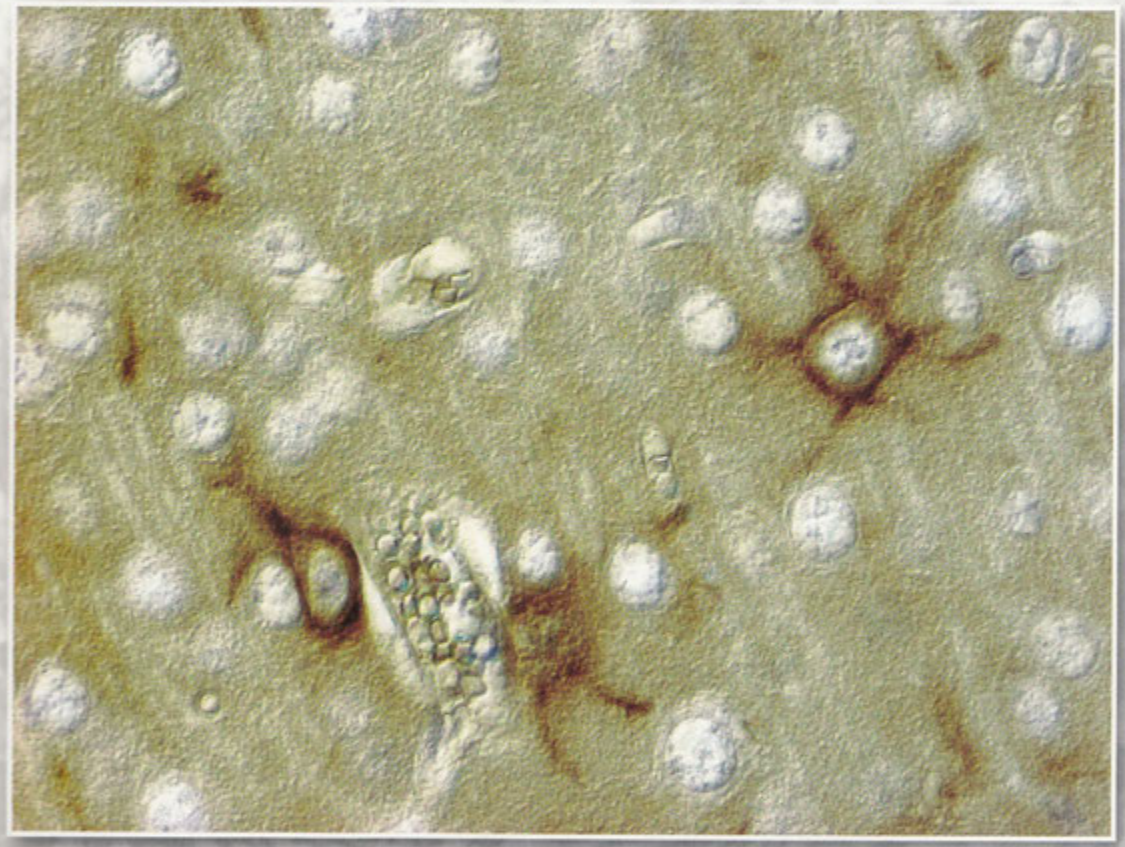

Prof. Marin Drinov Academic Publishing House

Acta morphologica et anthropologica

is the continuation of
Acta cytobiologica et morphologica

Издаването на настоящия брой на списанието е с финансовата подкрепа на Фонд „Научни изследвания" при Министерството на образованието и науката.

Prof. Marin Drinov Academic Publishing House
Bulgaria, 1113 Sofia, Acad. G. Bonchev Str., Bl. 6

Графичен дизайнер Д. Душанова
Формат 70×100/16 Печ. коли 17,75

Печатница на Академично издателство „Проф. Марин Дринов"
София 1113, ул. „Акад. Г. Бончев", бл. 5

ISSN 0861-0509

Acta morphologica et anthropologica (19)

19 • Sofia • 2012
Institute of Experimental Morphology, Pathology and Anthropology with Museum
Bulgarian Anatomical Society

Contents

Morphology

Anthropology

Institute of Experimental Morphology, Pathology and Anthropology with Museum
Bulgarian Anatomical Society

Acta morphologica et anthropologica, 19
Sofia • 2012

Morphology

Various morphological changes in the liver related to and resulting from prolonged intravenous heroin use

Al. Alexandrov[1], B. Landzhov[2], St. Hristov[1], D. Hinova – Palova[2], T. Todorov[3], A. Palov[2], L. Malinova[2], D Nikolov[1], T. Alexandrova[4]

[1]Department of Forensic Medicine and Deontology, [2]Department of Anatomy, Histology and embryology, [3]Department of Pathology, Medical University-Sofia 1431, Bulgaria, [4]Department of Dialysis, Hospital "Alexandrovska" – Sofia-1431, Bulgaria

Upon examining cadavers of addicts with a long history of intravenous heroin use, we found a number of macroscopic and microscopic morphologic pathological changes in the liver. Their characteristics, localization and severity depend on a number of key factors – the period of intravenous use of heroin; adhering to the main principles of aseptic treatment, such as using disposable needles, whether one or more people used the same needle, and the purity of and other substances in street heroin.

Key words: morphological changes, liver, heroin

Introduction:

With the progress made in the fields of chemistry and chemotherapy, a whole series of synthetic substances have come to fill the specter of drugs with such pharmaceutical properties. Misuse or abuse of these substances, referred to as "drugs", has created a major problem for society, namely drug addiction.

Medical texts contain descriptions of various morphological changes to different organs and tissues, related to and resulting from prolonged intravenous heroin use. These include different skin, cardiovascular, lung, liver, kidney and other morphological changes resulting from both the direct toxic impact of the drug and the way the dose is prepared, whether basic hygiene is maintained, and the type and amount of other substances present in the street dose. Morphological pathological changes within various organs include:

The pathogenesis of heroin-associated pathology is unknown, but the following factors are believed to play a role: the antigenic role of heroin and/or substances found

in it [6]; acute and chronic infections [1] and the related immune complex [2,6] or chronic hepatitis B and C with extrahepatic manifestations, direct damage from hepatitis and HIV to the glomerular structures with development of immune complex glomerulonephritis or HIV-associated nephropathy [1, 2]; unwanted side effects from interferon treatment of drug addicts with chronic viral hepatitis (appearance of autoimmune phenomena, provoking or exacerbating a preexisting autoimmune disease, thrombotic microangiopathy, tubulointerstitial nephritis, glomerulonephritis, acute renal failure). Acute and chronic forms of hepatitis are results from different types of viruses. Hepatitis C is the primary form of chronic hepatitis found in intravenous heroin addicts, which may develop into cirrhosis, liver failure and hepatocellular carcinoma [9].

The aim of our study was to establish morphological changes into liver of heroin addicts, who died following long-term intravenous use.

Material and methods

We studied 25 patients (16 men and 9 women), who died following long-term intravenous heroin use (between 8 and 106 months), at the Centers of forensic medicine and Clinical pathology of Alexandrovska University Hospital between 2007 and 2011. We traced the macro- and microscopic morphological changes to liver – to determine their type and the damage of the toxic substance to the body. We used light-microscopic study with Hematoxylin-eosin and PAS reaction. Thin slices were made (5 μm).

Results

In every case we studied, we found focal inflammatory changes to the skin and subcutaneous tissue in the areas where injections of the drug are most common (cubitals, groins, knee pits, forearms, thighs, legs).

In every case we found liver damage to various degrees. Lipid dystrophy was the most common morphological change to the liver, stemming from long-term heroin use. Less frequently, we found hepatitis of toxic genesis without fibrosis changes to the liver parenchyma (cirrhosis). The histological changes with such toxic liver damage are shown by means of vacuolization in the cytoplasm of the hepatocytes (fatty liver dystrophy, figs.1, 2), inflammatory infiltration of mononuclear cells and leucocytes with nuclear segmentation in the portal spaces of the liver (toxic hepatitis, figs. 3, 4). No morphological changes to the bile ducts were observed.

Discussion

Some authors [3, 7, 8] believe that the morphological pathological changes to multiple organs result from changes in the immune system, which are in turn due to the impact of painkiller drugs on the Humoral Immune Response and cell-mediated immunity. The direct effect of analgesic drugs on the immune system is lower resistance of the body to specific and non-specific infections, which is one of the main causes of morphological changes to the organs observed both during treatment of patients and upon examining the cadavers of long-term heroin addicts.

Chronic infections are believed to play a pathogenic role. Patients who inject cocaine and heroin under the skin develop nephrotic syndrome with increase of serum creatinine and creatinine clearance [8]. Hepatitis antibodies were found in the serum in 15

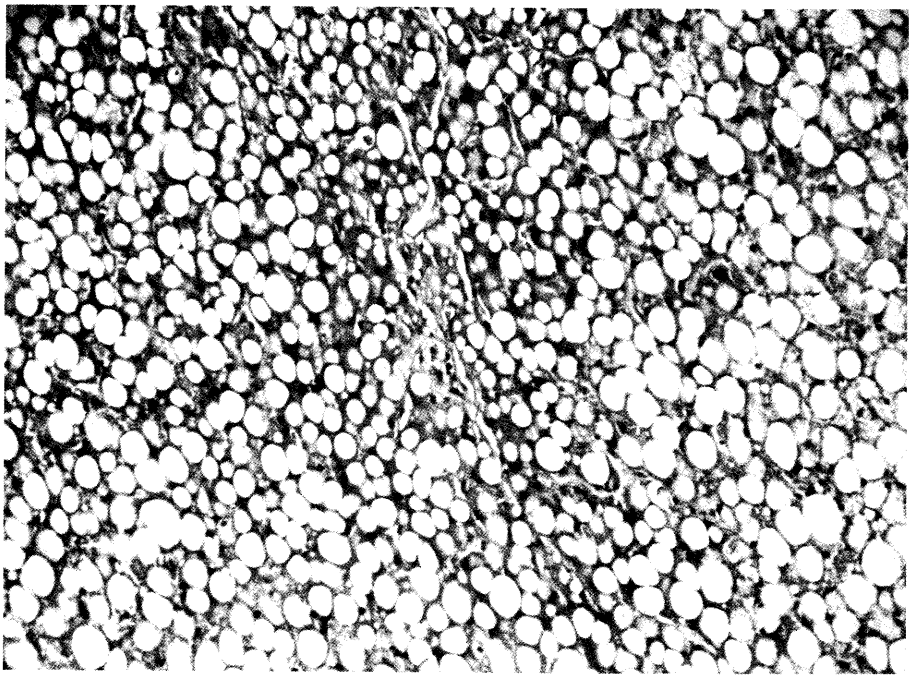

Fig. 1. Vacuolization in the cytoplasm of the hepatocytes (fatty liver dystrophy). HE, (x100)

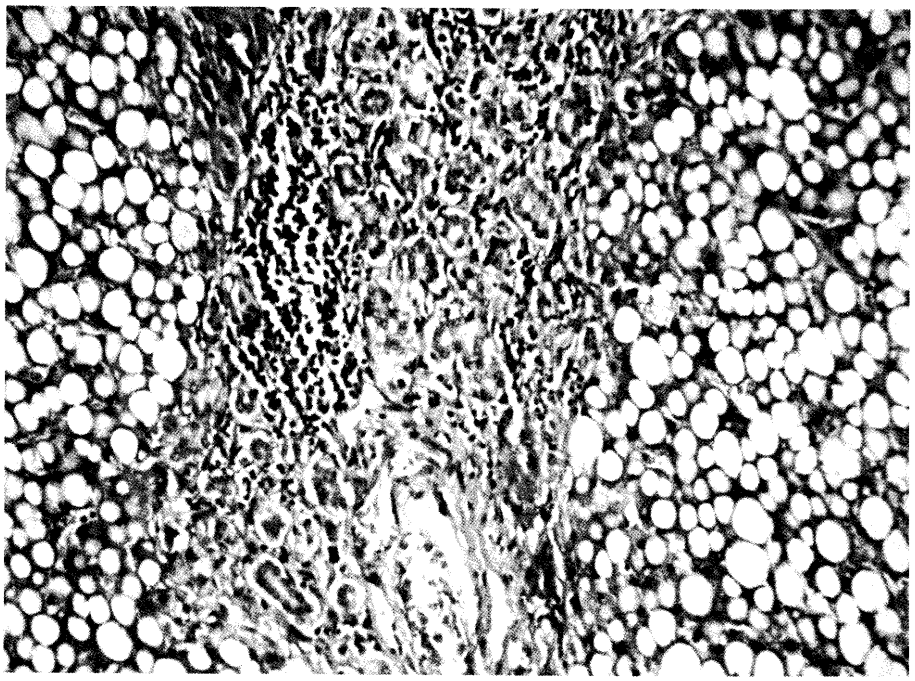

Fig. 2. Vacuolization in the cytoplasm of the hepatocytes (fatty liver dystrophy). HE, (x100).

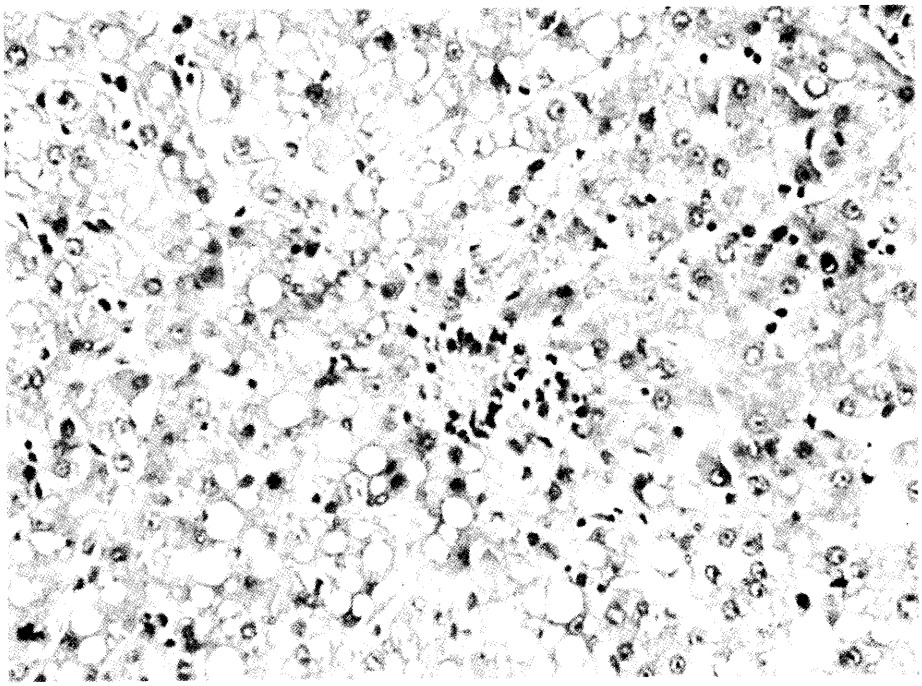

Fig. 3. Inflammatory infiltration of mononuclear cells and leucocytes with nuclear segmentation in the portal spaces of the liver (toxic hepatitis). PAS. (x200).

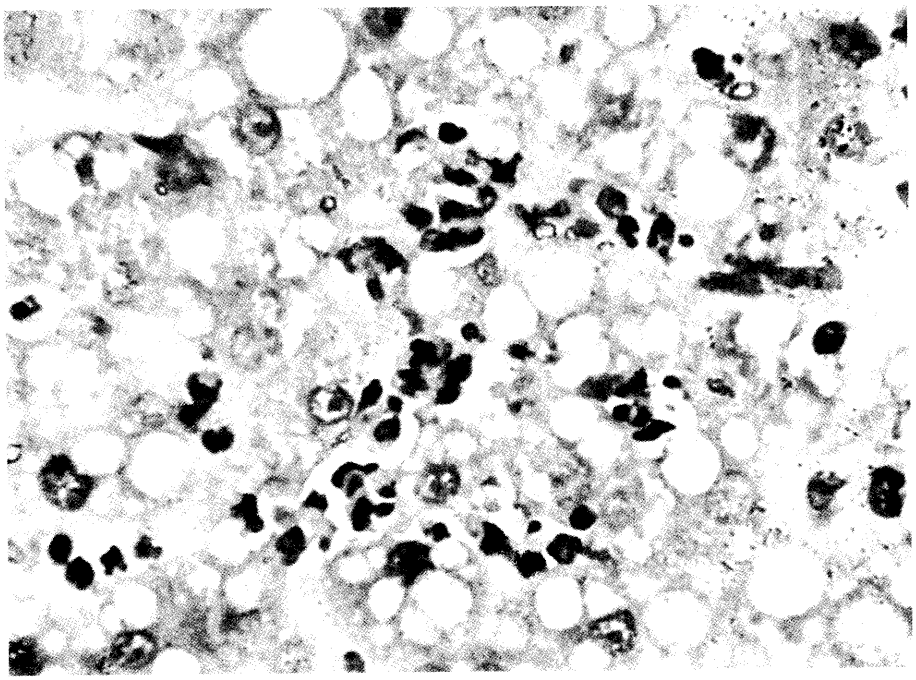

Fig. 4. Inflammatory infiltration of mononuclear cells and leucocytes with nuclear segmentation in the portal spaces of the liver (toxic hepatitis). PAS, (x400)

cases, while three of all patients were HIV-positive. Chronic hepatitis B and C are known to be connected to glomerulonephritis. Drug addicts in Europe develop monolymphocytic membrane-proliferative glomerulonephritis, in part due to heroin use or to the other substances mixed in with the drug and obviously independent of the hepatitis infection [2]. We must point out that these patients were not tested for hepatitis and HIV, which makes it possible to attribute the morphological changes to the kidneys and liver to these viruses. That aside, fatty liver dystrophy, which was observed in every case we studied, is usually caused by toxic substances. The combination of lipid dystrophy and inflammatory infiltration from mononuclear leucocytes and leucocytes with nuclear segmentation in the portal spaces of the liver could also be a morphological result of liver damage from toxic substances. The immunosuppressive effect of heroin is well known, which explains the specific and non-specific inflammatory changes observed in the lungs of deceased heroin addicts. It appears that prolonged abuse of "street" heroin is the most frequent cause of severe immunodeficiency along with HIV. This makes the user vulnerable to pneumocystic pneumonia, which is sometimes the direct cause of death. Opiate-induced asthma and other conditions provoked by drug abuse can make death more likely to occur [5]. Other authors describe the case of an HIV-positive intravenous addict with diffuse thrombosis of the superficial veins all over the body and periphlebitis with perivascular abscesses, who injected cocaine and heroin into his neck veins. He also suffered from oral candidiasis, Hepatitis C, bronchopneumonia, endocarditis and tricuspid valve insufficiency [4].

Conclusion

As the evidence shows, the most common "hard" drug – heroin – causes morphological changes and damage of varying intensity and clinical significance to different tissues and organs in the body when injected over a long period of time. Possessing knowledge of the morphological substrate of these changes enables experts of forensic medicine and pathoanatomy to give a quick and correct diagnosis of cases in their practice, thereby assisting clinicians, law enforcement officials and investigators.

References

1. Bakir, A. A., G. Dunea. Drugs of abuse and renal disease. – Curr Opin Nephrol Hypertens., 5, 1996, 122-126.
2. Crowe, A. V., M. Howse, G.M. Bell, J. A. Henry. Substance abuse and the kidney. – Q. J. M., 24, 2000, 147-152.
3. Downie, J. B., D. P. Dicostanzo, S. R. Cohen. Pemphigus vegetans neumann variant associated with intranasal Heroin abuse. – J. Am. Acad. Dermatol., 39, 1998, 872-875.
4. Maggi, P., M. Fullone, M. Federico, G. Angarano, G. Pastore, G. Regina. Drug injection in jugular veins: a new risk factor for vascular diseases in HIV-infected patients? A case report. – Angiology, 46, 1995, 1049-1052.
5. Merigian, K., K. Blaho. The role of pharmacology and forensics in the death of an asthmatic. – J. Anal. Toxiol., 19, 1995, 522-528.
6. Perneger, T. V., M. J. Klag, P. K. Welton. Reactional drug use: a neglected risk factor end-stage renal disease. – Am J Kidney Dis., 38, 2001, 49-56.
7. Simonart, T., D. Parent, M. Heenen, C. M. Farber, J. P. Van Vooren. Decreased skin reactivity to codeine in patients with the acquired immunodeficiency syndrome. – Clin. Immunol. Immunopathol., 81, 1996, 12-15.
8. Tan, A. U. Jr., A. H. Cohen, B. S. Levine. Renal amyloidosis in a drug abuser. – J. Am. Soc. Nephrol., 5, 1995, 1653-1658.
9. Tennant, F., D. Moll. Seroprevalence of hepatitis A, B, C and D markers and liver function abnormalities in intravenous heroin addicts. – J. Addictive Dis., 14, 1995, №3, 35-49.

Institute of Experimental Morphology, Pathology and Anthropology with Museum
Bulgarian Anatomical Society

Acta morphologica et anthropologica, 19
Sofia • 2012

Application of Various Cytotoxicity Assays for the Initial Evaluation of Biocompatibility of a Sr-modified dicalcium phosphate dihydrate

B. Andonova-Lilova, T. Zhivkova*, L. Dyakova**, M. Alexandrov* D. Rabadjieva***, S. Tepavitcharova***, R. Alexandrova**

**Institute of Experimental Morphology, Pathology and Anthropology with Museum, Bulgarian Academy of Science, Acad. G. Bonchev Str., Block 25, Sofia, Bulgaria;*
***Institute of Neurobiology, Bulgarian Academy of Science, Sofia, Bulgaria;*
****Institute of General and Inorganic Chemistry, Bulgarian Academy of Sciences, Sofia, Bulgaria*
Corresponding author e-mail: rialexandrova@hotmail.com

The aim of the present study was to evaluate the effect of strontium-modified dicalcium phosphate dihydrate ($CaHPO_4.2H_2O$, brushite) on viability and proliferation of cultured human Lep 3 cells using various cytotoxicity assays: thiazolyl blue tetrazolium bromide (MTT) test, neutral red uptake cytotoxicity assay (NR), crystal violet staining (CVS) and double staining with acridine orange and propidium iodide (AO/PI). The results obtained reveal high survival rate of the cells after 72 h cultivation in a $CaHPO_4.2H_2O$-modified medium – 81.5% ± 3.4 (CVS), 98.3% ± 4.6 (MTT) and 110.3% ± 4.6 (NR). No cytopathological changes were observed in the treated cells after staining with AO/PI.

Key word: Sr-modified dicalcium phosphate, cytotoxicity assays, cell culture, Lep 3 cell line, bone implants

Introduction

Bone disease is a serious health condition that directly impacts on the quality of life of sufferers. Diseases such as arthritis, tumours, and trauma can lead to defects in the skeleton requiring an operation to replace or restore the lost bone. As the population ages, the number of operations performed on bone is expected to increase (11). Bone is a tissue with a strong regenerative potential but when an area of damaged bone is too large for self-repair, the damaged bones must be repaired by using alternative materials, such as autografts, allografts and artificial materials. Bone harvested from donor sites is the gold standard for this procedure but there are limitations and complications from the use of autograft, including the limited quantity and associated chronic donor site pain. Allografts, which are transferred from other people, have problems related to not only limited availability but also with foreign body reactions and infections. As a result there is an impetus for the development of artificial bone substitute materials that do

not damage healthy tissue, do not pose any viral or bacterial risk to patients, and can be supplied at any time, in any amount (7, 8, 9, 10).

Calcium phosphate materials are widely used in surgery and dental medicine as replacements for hips, knees, teeth, tendons and ligaments, as well as repair for periodontal disease, maxillofacial reconstruction, augmentation and for stabilization of the jawbone, spinal fusion and bone fillers after tumor surgery (2). The ion-modified calcium phosphates possess some specific biologically important characteristics. For instance, it has been established that stroncium (Sr) activates osteoblats but decreases the number of osteoclasts, thus abolishing bone resorption and enhancing formation (15). The aim of the study presented was to evaluate the influence of a newly synthesized Sr-modified dicalcium phosphate dihydrate (Sr-DCP) on viability and proliferation of cultured human Lep 3 cells.

Materials and methods

Chemicals and materials

Dulbecco's modified Eagle's medium (DMEM) and fetal bovine serum (FBS) were purchased from Gibco-Invitrogen (UK); dimethyl sulfoxide (DMSO), thiazolyl blue tetrazolium bromide, neutral red, crystal violet, trypan blue, acridine orange, propidium iodide and trypsin were obtained from AppliChem (Germany). The other chemicals of the highest purity commercially available were purchased from local agents and distributors. All plasticware and syringe filters (0.2 μm) were from Orange Scientific (Belgium).

Sample preparation

Sr-dicalcium phosphate ($CaHPO_4.2H_2O$, brushite) was prepared by the biomimetic method (13, 14) at continuous co-precipitation in aqueous solution with pH 4.7 and room temperature. The modifications of the popular conventional simulated body fluid (SBFc) (6) were used as solvents for K_2HPO_4 and for the mixture of $CaCl_2$ and $SrCl_2$ in order to ensure electrolyte medium similar to blood plasma. The molar ratios in the initial solutions were (Ca+Sr)/P = 1.67 and Sr/(Sr+Ca) = 0.2. The solutions were added to precipitate with a rate of 4 ml/min. The precipitant was water washed (solid:water = 1:600), filtrated and dried at 75°C for 24 hours. Analytical reagents A.R. were used in the both synthesis.

For biological experiments 100 mg of the compound was mixed with 0.33 ml distilled water and placed on glass slide (5 cm^2) in petri dish (10 cm in diameter). After incubation for 30 min at room temperature 10 ml DMEM medium containing 10% FBS and antibiotics (100 U/mL penicillin and 100 μg/mL streptomycin) was added to the petri dish and incubated for 4 h at 37°C. Then the medium (so called calcium phosphate modified medium, Sr-CPM-medium) was filtered twice: with a paper filter (FILTRAK) and then a syringe filter (0.2 μm). This Sr-CPM-medium was used in the biological experiments.

Experimental design

The permanent cell line Lep 3 (Cell Culture Collection, IEMPAM – BAS), established from a 3-month old human embryo, was cultured in DMEM medium, supplemented with 5-10% FBS, 100 U/mL penicillin and 100 μg/mL streptomycin. The cells were maintained at 37 °C in a humidified CO_2 incubator. The exponentially growing cells

were seeded in 96-well flat-botommed microplates at a concentration of 1×10^4 cells/well. On the 24 h the culture medium was removed and changed with Sr-CPM-medium. The biocompatibility investigations were performed using thiazolyl blue tetrazolium bromide (MTT) test, neutral red uptake cytotoxicity assay (NR), crystal violet staining (CVS) double staining method with acridine orange (AO) and propidium iodide (PI) as it was previously described (1). The data are presented as mean ± standard error of the mean. Statistical differences between control and treated groups were assessed using one-way analysis of variance (ANOVA) followed by Dunnett post-hoc test.

Results and Discussion

The experimental data obtained by MTT, NR and CVS assays are summarized in Fig. 1. The percent of viable human Lep 3 cells cultured for 72 h in the presence of Sr-CPM-medium has been found to be > 80% (81.5% ± 3.4, CVS), with no changes as compared to the control (98.3% ± 4.6, MTT) and > 100% (110.3% ± 4.6, NR). The variations observed could be explained by the different nature of the methods applied – MTT reflects damage to mitochondria), NR indicates damage to lysosomes and Golgi apparatus whereas CVS shows the growth rate reduction reflected by the colorimetric determination of the stained cells. The combined staining with acridine otrange and propidium iodide did not reveal any cytopathological changes in the cells after 72 h treatment period (Fig. 2).

Calcium phosphate materials have been found to be osteoconductive, and they can be made osteoinductive with the appropriate morphology, specifically the macroporos-

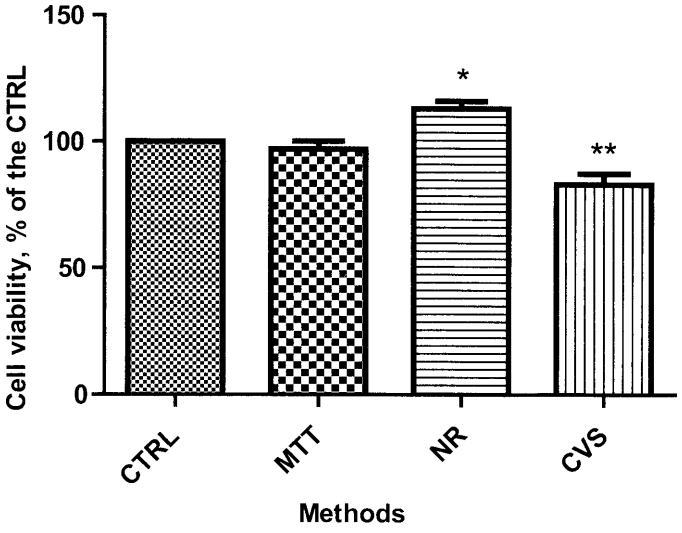

Fig. 1. Effect of Sr-modified dicalcium phosphate medium on viability and proliferation of Lep 3 human cells. The evaluation was performed by thiazolyl blue tetrazolium bromide (MTT) test; neutral red uptake cytotoxicity assay (NR) and crystal violet staining (CVS) after 72 h treatment period. Cell viability is expressed as a percent of the untreated control (CTRL). * – $p < 0.05$ ** – $p < 0.01$

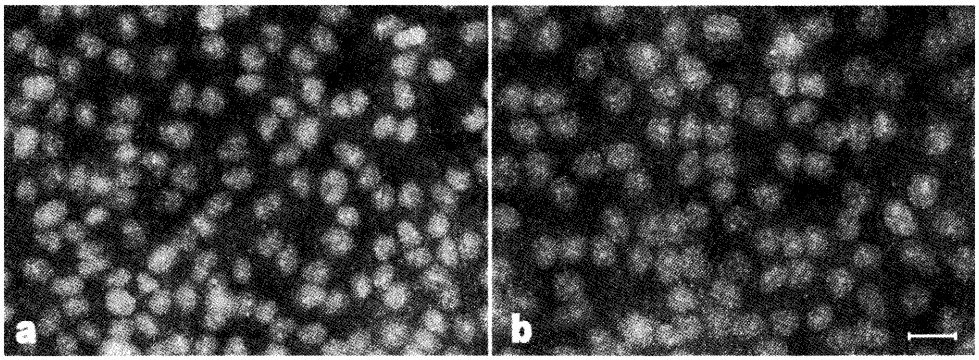

Fig 2. Untreated (Control) human Lep 3 cells (A) and cells cultured for 72 h in a Sr-modified dicalcium phosphate medium (B)

ity and microporosity (3, 4, 5, 12). It has been found in our previous investigations that Sr-modified dicalcium phosphate dehydrate, tested in the present study, does not decrease the number of viable murine fibroblasts (BALB/c 3T3) and cultured cells from bone explants (Data in press). Additional experiments are underway to clarify whether this compound will be suitable for biomedical purposes.

Acknowledgement: Supported by Grant DTK-02-70/2009, National Science Fund, Bulgaria; and European Social Fund and Republic of Bulgaria, Operational Programme "Development of Human Resources" 2007-2013, Grant № BG051PO001-3.3.06-0048 from 04.10.2012.

References

1. Alexandrova R., T. Zhivkova, M. Alexandrov, G. Miloshev, M. Georgieva, I. Pantcheva, M. Mitewa. Cytostatic and cytotoxic properties of monensic acid and its biometal(II) complexes against human tumor / non-tumor cell lines, Cent. Eur. J. Chem., **10(5)**, 2012,1464-1474
2. Dorozhkin SV. Bioceramics of calcium orthophosphates. Biomaterials. **31(7)**, 2010, 1465-85.
3. Dorozhkin SV. Biphasic, triphasic and multiphasic calcium orthophosphates. Acta Biomater., **8(3),** 2012, 963-77.
4. Daculsi G., P. Layrolle Osteoinductive properties of micro macroporous biphasic calcium phosphate bioceramics Key Eng Mater, **254–256,** 2004, pp. 1005–1008
5. Shin H.I., K.H. Kim, I.K. Kang, K.S. Oh Successful osteoinduction by cell– macroporous biphasic HA–TCP ceramic matrix Key Eng Mater, **288–289,** 2005, pp. 245–248
6. Kokubo T., Surface Chemistry of Bioactive Glass-Ceramics. J Non-Cryst Solids., **120,** 1990, 138 – 15
7. Kokubo T., Kim H.– M., Kawashita M. Novel bioactive materials with different mechanical properties Biomaterials, **24,** 2003, 2161-217.
8. Laurencin C, Khan Y, El - Amin SF. Bone graft substitutes. Expert Rev Med Devices., **3(1),** 2006, 49-57.
9. Le Guehennec L., Layrolle P., Daculsi G.. A Review Of Bioceramics And Fibrin Sealant European Cells and Materials, **8**, 2004, 1-11.
10. Nandi SK, Roy S, Mukherjee P, Kundu B, De DK, Basu D. Orthopaedic applications of bone graft & graft substitutes: a review. Indian J Med Res., **132**, 2010, 15-30.
11. Navarro M., A. Michiardi, O. castaño, J.A. Planell. J.R. Soc. Interface, 2008, **5**, 1137-1158.
12. Le Geros R.Z. Calcium phosphate-based osteoinductive materials, Chem Rev, 2008, **108**, pp. 4742–4753

13. Rabadjieva D., Tepavitcharova S., Gergulova R., Sezanova K., Titorenkova R., Petrov O., Dyulgerova E., Mg- and Zn-modified calcium phosphates prepared by biomimetic precipitation and subsequent treatment at high temperature., J Mater Sci: Mater Med **22,** 2011 (2011a.), 2187–2196.
14. Rabadjieva D., Tepavitcharova S., Sezanova K., Gergulova R., Titorenkova R., Petrov O. and Dyulgerova E.. Biomimetic Modifications of Calcium Orthophosphates, Chapter 7 in book "On Biomimetic", InTech, Rijeka, Croatia, 2011 (2011b), p. 135 – 162.
15. Zofková I, Kanceva RL. New drugs with positive effects on bones., Cas Lek Cesk., **136(15),** 1997, 459-63.

Institute of Experimental Morphology, Pathology and Anthropology with Museum
Bulgarian Anatomical Society

Acta morphologica et anthropologica, 19
Sofia • 2012

Expression of Some Neuropeptides in the Rat Carotid Body

D. Atanasova[1], N. Lazarov[1, 2]

[1]*Institute of Neurobiology, Bulgarian Academy of Sciences, Sofia, Bulgaria*
[2]*Department of Anatomy and Histology, Medical University of Sofia, Sofia, Bulgaria*

The carotid body (CB) is a polymodal oxygen sensor strategically positioned at the bifurcation of the common carotid artery and endowed with the ability to detect broadly the chemical composition of arterial blood. The chemoreceptor glomus cells of the carotid body work in concert with the opposing afferent nerve endings of the petrosal ganglion cells and together they form a functional unit. Evidence to date suggests that the chemoreceptor cells utilize various chemical substances for the afferent transmission of chemosensory information. The presence and distribution of substance P, neuropeptide Y and methionine-enkephalin immunoreactive nerve structures in the CB of rats were identified at a light microscopical level using immunohistochemistry. All the three examined neuropeptides were expressed in both the glomus cells and nerve fibers, albeit in a different manner. Our results provide immunohistochemical evidence that the rat CB utilizes sensory and autonomic peptides, which can modulate chemosensory activity through their actions on the glomus cells and vasculature.

Key words: carotid body, chemosensitivity, immunohistochemistry, neuropeptides, rat

Introduction

The carotid body (CB) is the main peripheral chemoreceptor responsible for monitoring changes in pO2, pCO2 and pH in arterial blood and participates in the ventilatory responses to hypoxia, hypercapnia and acidosis [5]. It is bilaterally located at the carotid bifurcation, between the external and internal carotid arteries. From a structural point of view, the organ is composed of lobules, which are organized in clusters of cells, surrounded by a dense meshwork of capillaries and penetrated by bundles of sensory nerve endings of the carotid sinus nerve, a branch of the glossopharyngeal nerve as well as by postganglionic sympathetic nerve fibers from the superior cervical ganglion [5].

The cell clusters, also known as glomeruli, consist of two major cell types: neurosecretory oxygen sensitive type I or glomus cells, which are round in shape and glial type II or sustentacular cells, which are fusiform and located at the periphery of the clusters. Type II cells mainly play a supportive role, but may also behave as stem cell precursors for type I cells [12]. Sustentacular cells have been suggested to co-ordinate chemosensory transduction through interactions with nerve endings, type I cells and blood vessels [14]

It has been proposed that the glomus cells in different animal species release a variety of transmitter candidates including classical and peptide transmitters. Previous studies have shown that the chemoreceptor cells contain diverse neuropeptides. Among them are sensory peptides such as substance P (SP) [7], autonomic neuropeptides like neuropeptide Y (NPY) [9] and the opioid peptide met-Enkephalin (mEnk) [17].

Materials and Methods

The experiments were carried out on adult Wistar rats of both sexes, weighing 250-300 g. All procedures were performed according to a standard protocol established by the Bioethical Commission of the Biomedical Research at the Institute of Neurobiology of the Bulgarian Academy of Sciences. All efforts were made to minimize the number of animals used and their suffering.

For the immunohistochemical experiments, the rats were deeply anesthetized and transcardially perfused first with 0.05 M phosphate-buffered saline (PBS), pH 7.3, followed by 4% paraformaldehyde (PFA) in 0.01 M phosphate buffer (PB), pH 7.3. The carotid bifurcations were dissected out and postfixed in the same fixative overnight at 4°C. Thereafter, the tissues were embedded in paraffin and cut into 7 μm thick sections. The samples were then deparaffinized with xylene and ethanol, and subsequently processed for avidin-biotin-horseradish peroxidase complex (ABC) immunohistochemistry. Briefly, the sections were treated with hydrogen peroxide (1.2% in absolute methanol; 30 min) to inactivate endogenous peroxidase and the background staining was blocked with 5% normal goat serum (NGS) in PBS for 1 hour. Between the separate steps, the sections were rinsed with cold PBS/Triton X-100. Afterward, they were incubated for 24 h at room temperature with the respective primary antibodies, rabbit anti-SP (diluted 1:1000, Abcam, Cambridge, UK), rabbit anti-NPY (1:500; Amersham International, Buckinghamshire, UK) and rabbit anti-mEnk (1:1000, Inc Star, Stillwater, MN, USA) overnight at 4°C in a humid chamber, followed by biotinylated goat anti-rabbit IgG (Sigma, 1:250) for 2 h at room temperature, and lastly the ABC complex (Vector Labs, Burlingame, CA, USA) was applied for 2 h at room temperature. Finally, the peroxidase activity was visualized using diaminobenzidine as a chromogen. After the immunoreaction, the sections were dehydrated in ethanols, cleared in xylene and coverslipped with Entellan (Merck, Darmstadt, Germany). The slides were observed and photographed with a Nikon research microscope equipped with a digital camera DXM1200c.

The specificity of the immunostaining was controlled by omission of the primary antiserum from the incubation medium or its replacement by PBS. No immunoreactivity was detected in either case.

Results

A dense plexus of substance P-immunopositive intraglomerular and periglomerular nerve fibers were observed throughout the CB and many of the varicose fibers were closely associated with glomus cells (Fig. 1A). At a higher magnification, a large number of SP-immunostained glomus cells were also seen within the CB (Fig. 1B).

In addition, abundant NPY-like immunoreactive nerve fibers were found throughout the parenchyma of the adult rat CB (Fig. 1C). The nerve fibers appeared as varicosities and most of them were associated with small vessels. On the other hand, only scattered glomus cells were NPY immunostained.

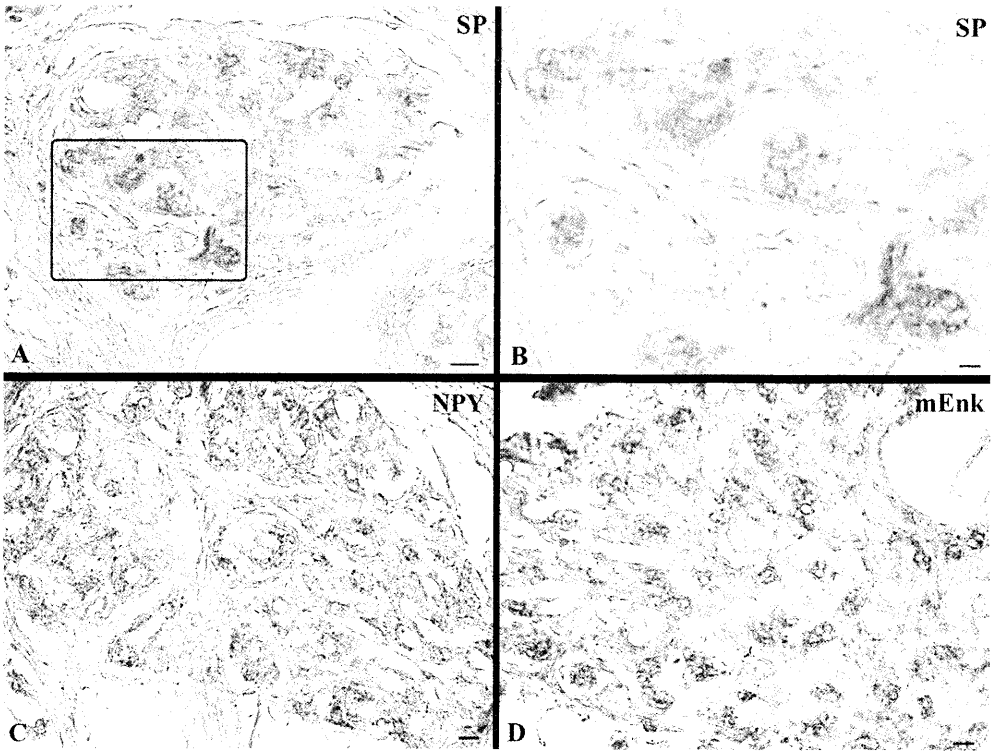

Fig. 1. (**A**) SP-immunoreactive intaglomerular and periglomerular nerve fibers in the rat CB. (**B**) A higher magnification of the boxed area in (A) showing a large number of SP-expressing glomus cells (**C**) NPY-immunoreactive perivascular nerve fibers and scattered immunostained glomus cells in the adult rat CB. (**D**) mEnk immunopositive glomus cells and nerve fibers. Scale bars = 25 μm (**A, C, D**); 50 μm (**B**).

Conversely, the immunohistochemical experiments demonstrated immunostaining for mEnk in the majority of glomus cells (Fig. 1D). Intraglomerular and periglomerular nerve fibers within and around the cell clusters were mEnk-immunostained as well.

Discussion

The present results demonstrate that all the three examined neuropeptides are expressed in the rat CB, albeit in a different manner. In this study, we find that the vast majority of glomus cells appear to contain certain sensory peptides like SP and mEnk. Moreover, the most numerous SP-immunoreactive fibers are associated with the glomus cells, though some immunostained varicosities were seen periglomerularly too. Hence, we have found SP immunoreactivity in both the glomus cells and nerve fibers in the rat CB in contrast with studies performed by other authors [2,7,17] which have been reported that SP immunoreactivity is only localized to the nerve fibers within the CB of this species. Furthermore, SP immunoreactivity has been found in the CBs from diverse animal species, although its specific cellular distribution to either carotid sinus nerve fibers or glomus cells appears to be species dependent. Indeed, SP has been reported to occur

in glomus cells of the human CB [13] or only in the glomic nerve fibers of this species [10]. Immunofluorescent studies [3] have also shown that SP is located in a few glomus cells and in nerve fibers present on the cat CB, while all previous studies have reported SP immunoreactivity exclusively in the nerve fibers within the rabbit CB [8]. These results suggest that SP is involved in chemosensory mechanisms in the CB of several animal species, including the rat CB. Taken together with previous immunohistochemical [7,17] and physiological [4] reports, our data indicate that SP probably modulates the CB chemosensitivity and indirectly increases carotid sinus nerve activity.

Our immunohistochemical data on the strong expression of mEnk immunoreactivity in both the glomus cells and nerve fibers innervating the CB of the rat are in contrast with the immunohistochemical findings of Heym and Kummer [6] who reported mEnk immunoreactivity only in the nerve fibers. Physiologically, it is likely that mEnk inhibits the sensory activity of the CB.

The present findings on the strong expression of NPY immunoreactivity in the perivascular nerve fibers and weak NPY-like immunoreactivity in the adult rat CB are in accordance with the immunocytochemical data of Oomory et al. [11]. These authors have reported that NPY immunoreactive glomus cells decrease rapidly from the first to the second postnatal week. On the other hand, NPY immunostained nerve fibers mainly increase after the second postnatal week [11]. From a functional point of view, as an autonomic neuroactive peptide, NPY possibly leads to the CB excitation by causing local vasoconstriction.

In conclusion, both excitatory and inhibitory neuropeptides are involved in the modulation of sensory response of the rat CB.

References

1. Atanasova, D. Y., M. E. Iliev, and N. E. Lazarov. Morphology of the rat carotid body. – Biomed. Rev., 22, 2011, 41-55.
2. Chen, I. V., R. D. Yates, J. T. Hansen. Substance P-like immunoreactivity in rat and cat carotid bodies: Light and electron microscopic studies. – Histol. Histopathol., 1, 1986, 203-212.
3. Cuello, A. C., D. S. Mc Queen. Substance P: A carotid body peptide. – Neurosc. Lett., 17, 1980, 215-219.
4. De Caro, R., V. Macchi, M. Sfriso, A. Porzionato. Structural and neurochemical changes in the maturation of the carotid body. – Respir. Physiol. Neurobiol., 2012, http://dx.doi.org/10.1016/j.resp.2012.06.012.
5. Gonzalez, C., L. Almaraz, A. Obeso, R. Rigual. Carotid body chemoreceptors: from natural stimuli to sensory discharges. – Physiol. Rev., 74, 1994, 829-898.
6. Heym, C., W. Kummer. Immunohistochemical distribution and colocalization of regulatory peptides in the carotid body. – J. Electron. Microsc. Tech., 12, 1989, 331-342.
7. Jacobowitz, D.M., C. J. Helke. Localization of substance P immunoreactive nerves in the carotid body. – Brain Res. Bull., 5, 1980, 195-197.
8. Kim D. K., E. K. Oh, B.A. Summers, N.R. Prabhakar, G. K. Kumar. Release of substance P by low oxygen in the rabbit carotid body: evidence for the involvement of calcium channels. – Brain Res., 892, 2001, 359-369.
9. Kondo, H., H. Kuramoto, T. Fujita. Neuropeptide tyrosine-like immunoreactive nerve fibers in the carotid body chemoreceptor of rats. – Brain Res., 372, 1986, 353-356.
10. Kummer, W., J. O. Habeck. Substance P- and calcitonin gene-related peptide-like immunoreactivity in the human carotid body studied at light and electron microscopical level. – Brain Res., 554, 1991, 286-292.
11. Oomory, Y., H. Murabayashi, K. Ishikawa, K. Miyakawa, K. Nakaya, H. Tanaka. Neuropeptide Y- and catecholamine-synthesizing enzymes: immunoreactivities in the rat carotid body during postnatal development. – Anat. Embryol., 206, 2002, 37-47.

12. Pardal, R., P. Ortega-Sáenz, R. Durán, J. López-Barneo. Glia-like stem cells sustain physiologic neurogenesis in the adult mammalian carotid body. – Cell, 131, 2007, 364-377.
13. Smith, P., J. Gosney, D. Heath, H. Burnett. The occurrence and distribution of certain polypeptides within the human carotid body. – Cell Tissue Res., 261, 1990, 565-571.
14. Tse, A., L. Yan, A. K. Lee, F. W. Tse. Autocrine and paracrine actions of ATP in rat carotid body. – Can. J. Physiol Pharmacol., 90, 2012, 705-711.
15. Wang, Z. Z., D. S. Bredt, S. J. Fidone, L. J. Stensaas. Neurons synthesizing nitric oxide innervate the mammalian carotid body. – J. Comp. Neurol., 336, 1993, 419-432.
16. Wang, Z. Z., L. J. Stensaas, B. Dinger, S. J. Fidone. The co-existence of biogenic amines and neuropeptides in the type I cells of the cat carotid body. – Neuroscience, 47, 1992, 473-480.
17. Wharton, J. J., J. M. Polak, A. G. E. Pearse, G. P. McGregor, M. G. Bryant, S. R. Bloom, P. G. Emson, G. E. Bisgard, J. A. Will. Enkephalin-, VIP-, substance P-like immunoreactivity in the carotid body. – Nature, 284, 1980, 269-271.

Institute of Experimental Morphology, Pathology and Anthropology with Museum
Bulgarian Anatomical Society

Acta morphologica et anthropologica, 19
Sofia • 2012

Cadmium bioaccumulation in kidneys of freshwater fishes from Kardzhali and Studen kladenets dams

Desislava Arnaudova, Emil Sapundzhiev

University of Plovdiv,Branch "L.Karavelov" – 6600 Kardzhali,
University of Forestry, Faculty of Veterinary Medicine – 1756 Sofia

Human interference upon or within water ecosystems has negative effect upon the quality of the water and brings considerable contamination which in turn damages the aquatic animals and organisms in general.

The present study has the aim to investigate the accumulation level of the heavy metal cadmium in the kidneys of the freshwater fishes from river Arda belonging dams.

The cadmium levels within tissue kidney samples from fishes common rudd (Scardinius erythrophthalmus), common bleak (Alburnus alburnus) and European perch (Perca fluviatilis) have been monitored by atomabsorpbing and spectrophotometric methods.

Increased levels of the cadmium in kidney tissue samples have been estimated which are upper than the acceptable limits in foods. Scardinius erythrophthalmus from Studen Kladnets dam and Perca fluviatilis from Kardzhali dam have the highest contamination indexes. This may be due to the fact that these fish species are highly adaptive and resistant against the changes and influences of the environmental sources even if they are severe and deadly.

A process of biomagnification of cadmium level has been accrued into fishes from Kardzhali dam compared to the ones in Studen Kladenets dam where biomagnification index (BMI) is above a unit.

Key words: kidney, fishes, accumulation, heavy metals

Introduction

Cadmium is consider as one of the most toxic heavy metals. Over recent decades, its content has considerably increased in areas affected by the refuse of a number of industrial enterprises.

The cadmium content in the water environment leads to its accumulation in the tissues and organs of various kinds of animals along the food chain [1]. As early as 1975, Ribelin and Migaki establish the fact of cadmium's causing the histopathological changes occurring on the kidney nephrons; later that was confirmed by other investigators [6]. In research done on the European bass (*Dicentrarchus labrax*) when heavily poisoned by cadmium showed the basic spots of toxicity are the lamellas of the gills and the kidney tubules, and in the case of subchronic poisoning, mainly the kidneys and the liver get affected [7]. When sublethal concentrations of cadmium are administered

to rainbow trout (*Salmo gairdneri*) chiefly the parenchyma tissue is affected and acute toxicity is caused [3].

The kidney is a basic organ with a hematopoietic function and in it the differentiation of all blood cells takes place [12]. In the case of chronic intoxication with heavy metals over the acceptable concentration limits, destructive alterations may be occur in the parenchyma organs of fishes and also anemia and exhaustion [10, 11].

Proceeding from these data, the aim of this research has been to trace the content of the heavy metal cadmium in the kidneys of three kinds of freshwater fish inhabiting the valley of the Arda River. The task was set to establish the bioaccumulation coefficient (BC) and the biomagnification index (BMI).

Materials and methods

The tests were done in the area of the Arda River, including stations in the two water basins – the Kardzhali and Studen Kladenets dams.

The chemical analysis for cadmium content in the water of the Kardzhali and Studen Kladenets dams was done using the method of flame atom-absorbent spectrophotometry air-acetylene (2100-2300° C) with a Perkin Elmer 3030 B apparatus. As test animals, three kinds of freshwater fish were used: common bleak (*Alburnus alburnus L.*), common rudd *(Scardinius erythrophtalmus L.*) and European perch (*Perca fluviatilis L.*), inhabiting the Kardzhali and Studen Kladenets dams.

The cadmium content in the organ samples of the freshwater fish investigated was determined via the method of atom-absorbent spectrophotometry (AAS „PERKIN-ELMER 3030 B") at the CLGE of the Bulgarian Academy of Sciences. The results were calculated in of air-dry sample and conform to the Regulation of Acceptable Concentration Limits (ACL) on the content of harmful chemical substances in foodstuffs [14, 15, 16].

The three kinds of fish belong to different trophic levels in the food chain, which enables one to trace the process of biomagnification by determining the biomagnification index (BMI) as set forth by Amiard and Amiard-Triquet, 1977. BMI boils down to a process of bioaccumulation on the higher tiers of the food-chain pyramid and is arrived at through the formula:

BMI = concentration of the metal at the trophic level X/ concentration of the metal at the trophic level X-1

The degree of bioaccumulation was determined via the bioaccumulation coefficient (BC) and arrived at through a formula representing the ratio of cadmium content in the organism to the cadmium content of water [9].

Results and discussion

The quantitative data established of cadmium content in the water of the Kardzhali and Studen Kladenets dams are shown in the enclosed tab. 1.

The data of cadmium content in the water of both dams indicate that the metal's content has not increased, its values being below ACL.

The research results of the cadmium content in the fish kidneys from the Kardzhali and Studen Kladenets dams are shown in tab. 2.

The analysis and dynamics of cadmium content in the kidneys of the three kinds of freshwater fishes from the Kardzhali and Studen Kladenets dams reveal data whose values are above ACL. As regards the hygienic norms for freshwater fish, the research

at the Kardzhali Dam indicates that the metal's bioaccumulation in the kidneys of common bleak is 42.42 times over the norm, the number for rudd being 50.64, and the one for perch 81.2. Comparing the cadmium content in the kidneys of, respectively, common bleak, rudd, and perch, the metal's content is highest in the kidneys of perch, followed by rudd and common bleak.

As regards the hygienic norms for freshwater fish, the research at the Studen Kladenets dam indicates that the metal's bioaccumulation in the kidneys of common bleak is 255.58 times over the norm, the number for rudd being 120.34, and the one for perch 118.9. Comparing the cadmium content in the kidneys of, respectively, common bleak, rudd, and perch, the metal's content is highest in the kidneys of rudd, followed by common bleak and perch (Tab. 2). The accumulation of cadmium in the organism of fish may lead to concentrations causing morphological changes in the kidneys.

The high affinity of organs with parenchymal structure towards cadmium is confirmed by other authors. It is consider that cadmium and copper are mainly accumulated in the liver and the kidneys [2, 4]. That may be explained by the individual adaptive stability of the fish species organism.

As regards the trophic level, the perch is considered as an unpretentious predator [13]. It feeds on small fishes and invertebrate, displacing, in some basins, most kinds of valuable fish. Its economic value is but insignificant while it is chiefly the object of sport fishing practice. The perch survives in waters poor of oxygen, too, where many other fishes would perish.

The rudd carry out a sedentary way of life. Young fish feed on plankton, and the adult ones on insects, larvae, small worms etc [13]. As regards the trophic level, the rudd is deemed a benthophage. Probably due to its sedentary way of life, in the Studen Kladenets dam rudd's kidneys high values of cadmium have been found.

Despite it being a plankton-eating species, the cadmium content in the kidneys of the common bleak is above ACL. Compared to ACL, the values of cadmium in the kidneys of the three fish species are above the acceptable concentration limits in both dams.

The results of analysis show that BMI for the Studen Kladenets dam is below 1. BMI for the Kardzhali dam is above value 1, for which reason we can point out that as regards cadmium there is a clearly defined process of biomagnification in the organism of the predatory species perch which is on a higher level in the food-chain pyramid (Tab. 3).

The bioaccumulation coefficient (BC) was calculated based on the average cadmium content in the three kinds of fish under research. According to the value of the bioaccumulation coefficient, the water inhabitants are defined as macroconcentrators (BC > 2), microconcentrators (BC = 1 to 2), and deconcentrators (BC < 2) [9]. The results of the bioaccumulation coefficient show that all three kinds of fish under research have a proven bioaccumulative capability and may be defined as macroconcentrators of cadmium (Tab. 4).

Of particular negative importance from the point of view of cadmium's ecological/toxicological influence is its accumulation on all levels of the food chains in those ecosystems, which creates a health hazard for humans, too.

It must be pointed out that that research serves as a basis for bio-monitoring and help towards improving the quality of waters in dams, the development of commercial fishing and fishing as a sport as well as for improving the safety of people using fish for consumption. When viewed as bio-monitoring, determining of the content and distribution of specific contaminants of an anthropogenic origin, as heavy metals in animal organisms, is a significant stage of the overall evaluation of the ecological state of the environment they inhabit [8].

Table 1. Average content of cadmium (mg/l) in the water of the dams Kardzhali and Studen Kladenets

№	Place of taking sample	ACL	Cadmium content
1.	the Kardzhali Dam	0.01	0.0003
2.	the Studen Kladenets Dam	0.02	0.0157

Table 2. Cadmium content (mg/kg) in the kidneys of common bleak, rudd, and perch from the Kardzhali and Studen Kladenets dams

№	Kind of fish	ACL	Place of taking sample	
			the Kardzhali Dam	the Studen Kladenets Dam
1.	*Scardinius erythrophtalmus*	0.05	2.121	12.779
2.	*Alburnus alburnus*	0.05	2.532	6.017
3.	*Perca fluviatilis*	0.05	4.060	5.945

Table 3. Biomagnification index (BMI) distributed among *Perca fluviatilis, Alburnus alburnus,* and *Scardinius erythrophtalmus*

Biomagnification index (BMI)	Kardzhali dam	Studen Kladenets dam
BMI_1 *Perca fluviatilis / Alburnus alburnus*	1.603	0.988
BMI_2 *Perca fluviatilis / Scardinius erythrophtalmus*	1.914	0.465

Table 4. Bioaccumulation coefficient (BC) of cadmium of *Scardinius erythrophtalmus, Alburnus alburnus,* and *Perca fluviatilis*

Kind of fish	Bioaccumulation coefficient	
	Kardzhali dam	Studen Kladenets dam
Scardinius erythrophtalmus	7070	813.949
Alburnus alburnus	8440	383.248
Perca fluviatilis	13533.333	378.662

Conclusions

1. The water values of the cadmium in Kardzhali and Studen Kladenets dams are below ACL.
2. Cadmium is accumulated in the kidneys of the investigated fishes and values are higher than ACL.
3. The cadmium bioaccumulation manifests a species-wise differentiation in the kidneys of the different investigated fishes and it is highest in perch from the Kardzhali dam and rudd from the Studen Kladenets dam.
4. The cadmium biomagnification is above value 1 in the kidneys of the three investigated fishes from the Kardzhali dam.
5. Cadmium BC above value 2 has been proved for the investigated rudd, common bleak and perch fishes, which qualifies them as macroconcentrators for this heavy metal.

References

1. Giles, M. A. Accumulation of Cadmium by Rainbow Trout, Salmo gairdneri, during Extended Exposure. Can. J. Fish. Aqut. Sci., 45, 1988, 1045-1053.
2. Hamza-Chaffai. A., R. P. Cossin, C. Amiard-Triquet, A. El-Abed. Physico-chemical forms of storage of metals (Cd – Cu and Zn) and metallothionein-like proteins in gills and liver of marine fish from the Tunisian Coast: ecotoxicological consequences. Comparative Biochemistry and Physiology, 102. 1995, 329–341.
3. Kay, J., D. G. Thomas, M. W. Brown, A. Cryer, D. Shurben, J. F. Solbe, and J. S. Garvey. Cadmium accumulation and protein binding patterns in tissues of the rainbow trout, Salmo gairdneri. Environ Health Perspect. March; 65, 1986, 133–139.
4. Protasowlcky, N. Bioaccumulation cadmium, lead, copper, zinc in Cyprinus carpio L. dependency f them concentration in the water in exposition term., 1991.
5. Ribelin, W. E. and Migaki, G. The Pathology of Fishes. The University of Wisconsin Press, Madison, Wisconsin, 1975, 537.
6. Tanimoto, A., T. Hamada, K. Higashi and Y. Sasaguri. Distribution of cadmium and metallothionein in $CdCl_2$–exposed rat kidney: Relationship with apoptosis and regeneration. Pathology International, 49, 1999, 125–132.
7. Thophon, S., M. Kruatrachue, E. S. Upatham, P. Pokethitiyook, S. Sahaphong and S. Jaritkhuan. Histopathological alterations of white seabass, Lates calcalifer, in acute and subchronic cadmium exposure. Environmental Pollution, 121, 2003, 307–320.
8. Марков Г., М. Господинова. Червената лисица (Vulpes vulpes Linnaeus, 1758) – биоиндикатор за екологичното състояние на агроекосистеми. Във: Втора научна конференция с международно участие "Космос, екология, сигурност", 14-16 юни, Варна 2006.
9. Никаноров, А. М., А. В. Жулидков, А. Л. Покаржевский. Биомониторинг тяжелых металлов в пресноводных экосистемах.- Л. Гидрометеоиздет, 1985.
10. Онищенко, Г. Г. "Вода и здоровье", Первый заместитель Министра здравоохранения РФ, главный государственный санитарный врач РФ «Экология и жизнь» 4, Научно-популярный и образовательный журнал, 1999.
11. Стоянов, С т. Тежки метали в околната среда и хранителните продукти, токсично увреждане на човека, клинична картина, лечение и профилактика "Екология и здраве" П. 2, 1999, 70-87.
12. Хамидов, Д. С., А. Т. Акилов, А. А. Турдиев. Кров и кроветворение у позвоночних животних, ФАН, Ташкент, 1978, 165.
13. Царев, Р. Книга за ловеца и риболовеца, Земиздат, София, 1977, 467.
14. Наредба № 5 за хигиенните норми за пределно допустимите количества от химични и биологични замърсители в хранителните продукти, Издадена от Министерството на народното здраве, ДВ, бр. 39 от 18. 05. 1984 г.
15. Наредба № 12 за норми за максимално допустими количества от тежки метали като замърсители в храни ДВ бр. 55 / 2002 г.
16. Наредба № 31 от 29 юли 2004 г. за максимално допустимите количества замърсители в храните. Приложение 1, Министерство на здравеопазването ДВ, бр. 88, 8.10. 2004.

Institute of Experimental Morphology, Pathology and Anthropology with Museum
Bulgarian Anatomical Society

Acta morphologica et anthropologica, 19
Sofia • 2012

Changes of bcl-2, bax and caspase-3 expression in the microvascular endothelium of derma in patients with mediterranean spotted fever

*S. Delchev, I. Baltadzhiev**

*Department of Anatomy, Histology and Embryology, *Department of Infectious Diseases, Parasitology and Tropical Medicine, Medical University, 4002, Plovdiv, Bulgaria*

The aim of the present study was to examine the expression of Bcl-2 family of proteins and Caspase-3 in dermal capillary endothelial cells of the skin rash papules of patients with Mediterranean spotted fever (MSF) in order to reveal apoptotic processes in MSF and the time of their onset and progress. Punch-biopsies, obtained from rash papules of patients with MSF, were used to apply immunohistochemical reactions for Bcl-2, Bax and Caspase-3. Weak expression of the immune reaction for Bcl-2 in the capillary endothelial cells of patients was revealed, which did not differ from the healthy controls ($p>0.05$). The expression of Bax was strongly increased in comparison with the controls ($p<0.001$). The immune reaction for Caspase-3 also showed increased intensity ($p<0.001$). The Bcl-2/Bax ratio in the patients was significantly decreased ($p<0.001$). The changes of the expression of Bax and Caspase-3 are indicators for already initiated apoptotic processes in patients with MSF.

Key words: Mediterranean spotted fever, Rickettsia conorii, endothelium, apoptosis, immunohistochemistry

Introduction

In the different stages of the development of infectious processes bacteria are able to either induce or inhibit the apoptotic processes aiming at their own survival [4]. The etiological agent of Mediterranean spotted fever (MSF), *Rickettsia conorii,* is a microorganism with obligate intracellular parasitism and prominent positive tropism to the vascular endothelial cells of the host [8, 9]. The problems of programmed host-cell death in rickettsial diseases are among the not fully un-encoded phenomena of these disorders [9]. The availability of pretty few publications on the problems of apoptosis in micro-vascular endothelial cells in rickettsial diseases and practically missing reports on studies of patients with MSF in vivo was the reason to realize this survey. Our investigations are the first ones in Bulgaria in that relation [1] and we have not found any similar surveys in the available foreign literature.

The aim of the present study was to examine the expression of the Bcl-2 family of proteins and Caspase-3 in the dermal capillary endothelial cells of the skin rash papules

in patients with Mediterranean spotted fever in order to establish whether apoptotic processes occur and the time of their onset and progress.

Materials and methods

In eight patients with a diagnosis of Mediterranean spotted fever capillary endothelial cells of the dermis, taken by punch-biopsy from skin rash papules were investigated. Punch-biopsies from the corresponding skin sections of 4 healthy individuals were used for controls. The biopsy material was processed by a standard method and was embedded into paraffin. Consecutive slices 5μm in thickness were prepared and mounted on microscope slides and immunohistochemical technique was applied. A "Mouse ABC Staining system" (sc-2017, Santa Cruz Biotechnology, Inc.) kit was used as well as the following primary antibodies: Bcl-2 monoclonal antibody (sc-509, Santa Cruz Biotechnology, Inc.), dilution 1:100; Bax monoclonal antibody (sc-7480, Santa Cruz Biotechnology, Inc.), dilution 1:100; Caspase-3 monoclonal antibody (sc-56046, Santa Cruz Biotechnology, Inc.), dilution 1:100. Additionally the slices were processed by staining with Hematoxylin (sc-24973). The so prepared slices were covered with Vector mount (Vector Lab, USA). The applied micro-photographic pictures were taken with the help of a Nikon Microphot-SA (Japan), which was equipped with a Camedia-5050Z digital camera (Olympus, Japan). The expression of the immune reaction for Bcl-2, Bax and Caspase-3 in the dermal vascular endothelial cells was read with the help of the specialized soft ware "DP – Soft" 3.2 (Olympus, Japan). The mean intensity of reaction was analyzed as 50 sections were randomly selected of each slice. The results were processed with the help of the Independent samples *t*-test and $p<0.05$ was considered significant.

Results

The immune reactions for Bcl-2, Bax and Caspase-3 in the capillary endothelial cells were manifested by slightly expressed to missing brownish colour for Bcl-2 and dark-brown to black colour for Bax and Caspase-3 (Fig. 1), which corresponded to the data of other authors who used the same method [6]. The values of intensity of the immunochemical reaction are presented in relative units (Fig. 2). There was weak expression of the immune reaction for Bcl-2 in the capillary endothelial cells of the skin rash papules of patients with MSF and a very weak expression in the controls, without statistically significant difference ($p>0.05$). The expression of the immune reaction for Bax in the capillary endothelial cells of skin rash papules was strongly manifested in comparison with the controls ($p<0.001$). The analysis revealed increased intensity of the immunohistochemical reaction for Caspase-3 in the capillary endothelial cells of skin rash papules in comparison with the control ($p<0.001$). The analysis of the Bcl-2/Bax ratio revealed that it was significantly decreased in the patients ($p<0.001$) mainly on the account of increased levels of the pro-apoptotic protein Bax.

Discussion

One of the diagnostic features of MSF is the characteristic papular (boutonneuse) skin rash. There are capillary and lymphatic networks, and nerve endings in the superficial papillary layer of the connective part of the skin – dermis [11]. Searching for signs of

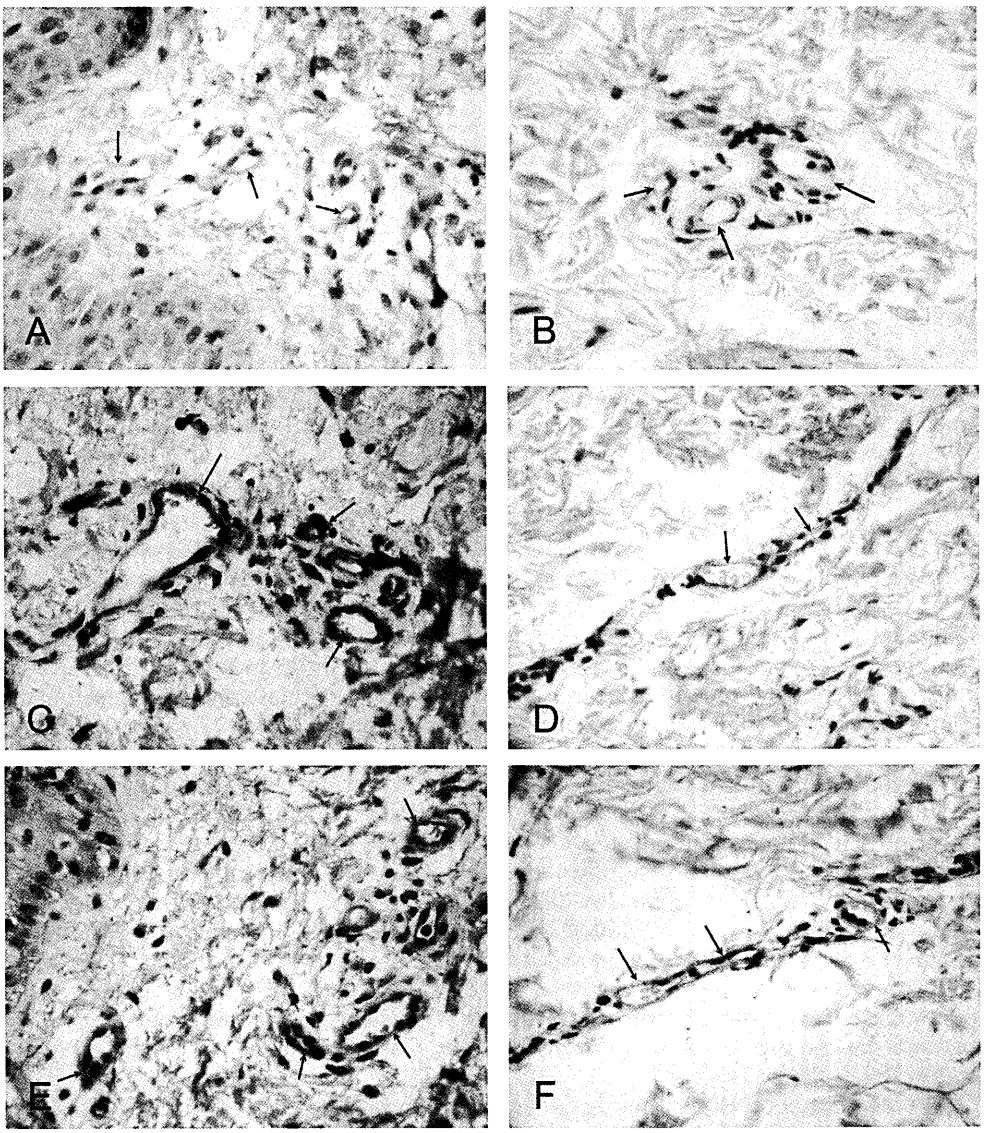

Fig. 1. Immunohistochemical reactions for Bcl-2 (A, B), Bax (C, D) and Caspase-3 (E, F) in the derma of skin rash papules of patients with Mediterranean spotted fever (A, C, E) and controls of healthy individuals (B, D, F). *Arrows* – reaction in the dermal capillary endothelial cells. Magnification x 400.

apoptosis in the microvascular endothelial cells we selected for biopsy the patient's rash papules as they are an expression of the intracellular pathogen activity i.e. increased capillary permeability, exudation and focal cell infiltration.

In the regulation of programmed host-cell death the B-cell lymphoma-2 (Bcl-2) family of proteins, which includes both pro- and anti-apoptotic factors, plays a critical role by controlling mitochondrial permeability. The anti-apoptotic proteins Bcl-2 and Bcl-xL reside in the outer membrane of mitochondria and they inhibit the release of

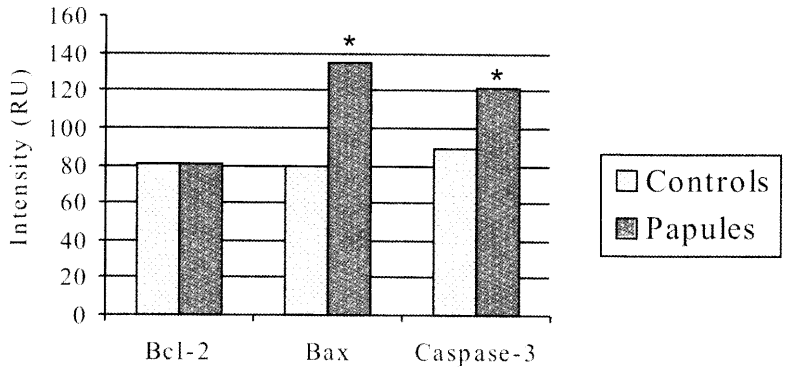

Fig. 2 Intensity of the immune expression of Bcl-2, Bax and Caspase-3 in the dermal capillary endothelial cells of the skin rash papules and controls (in relative units). *p<0.001 in comparison with the control.

cytochrome-C. In contrast, the pro-apoptotic proteins Bad, Bid and Bax are present in the cytosol and their translocation to mitochondria promotes cytochrome-C release [10]. The determination of the effects of Bcl-2 family on nuclear factor NF-kB reveals significant changes in the expression of various pro- and anti-apoptotic proteins and the ultimate outcome of it is the so called «equilibrium shift» in relation to apoptosis [7, 9]. This was the basis for the origin of the concept of regulation of the mechanisms of programmed endothelial cell death by intracellular *Rickettsie* [2]. The inhibition of apoptosis is necessary in the early stages of disease, when *Rickettsiae* begin to proliferate in the micro-vascular endothelial cells. Later on, when adoptive immunity has fully developed, there is intensification of apoptosis in the infected endothelial cells. The expression of the immune reaction for Bcl-2, Bax and Caspase-3 in skin tissue from papules was examined two days after the onset of the rash. It was estimated that the time period till the second day after the onset of the skin rash (5-6-th day after the initial symptoms of MSF) should be enough for the development of cell-mediated immune response and the effect on *Rickettsia* concerning its anti-apoptotic activity [1]. These presumptions gave us reasons to search for some elements of apoptosis in the endothelial cells of the dermal micro-vessels with the help of immunohistochemical reactions for the pro-apoptotic proteins Bax and Caspase-3 and for the anti-apoptotic protein Bcl-2.

In the dermal capillary endothelial cells of skin rash papules of patients with MSF the expression of Bcl-2 was weak, and the expression of Bax was strongly increased in comparison with the controls. Bax is an essential factor for mitochondria-mediated apoptosis [3]. The decreased Bcl-2/Bax ratio on the account of increased levels of the pro-apoptotic protein Bax is an indicator for intensified apoptotic tendencies and initiation of processes of programmed host-cell death.

While Bcl-2 inhibits apoptosis and Bax promotes it, Caspase-3 is known to be an executioner enzyme in the apoptotic processes. The activation of this executioner protease gives rise to a cascade of proteolytic processes, which lead to digestion of structural proteins in the cytoplasm, degradation of chromosomal DNA and phagocytosis of the cell [5]. The increased expression of Caspase-3 revealed in the capillary endothelial cells of the papules in patients with MSF is an indicator for the activation of apoptotic processes and is an initial distinguishing mark for moving to the next final stage of the apoptosis cascade, which leads to cell death.

Conclusion

The decreased Bcl-2/Bax ratio in patients with MSF is related to increased susceptibility to apoptosis, while the elevated levels of Caspase-3 are associated with the apoptosis itself. These markers alone at this stage of the development of the pathological process are not enough to definitely predict the destiny of the endothelial cells, as there are other factors too, which later may have effect on the final result – cell survival or cell death. Nevertheless, the changes of the expression of Bcl-2, Bax and Caspase-3 are indicators for already initiated apoptotic processes, and respectively for the progress of cell-mediated immune reactions in the MSF rickettsiosis within the indicated time limits.

References

1. Baltadzhiev, I., Apoptosis processes in the endothelial target cells of patients with MSF. – In: Clinical, epidemiological and pathogenetic aspects of the tick-borne rickettsiosis Mediterranean spotted fever. – PhDThesis, Plovdiv, 2012, 143-153.
2. Bechelli, J. B., E. Rydkina, P. M. Colonne, S. K. Sahni. Rickettsia rickettsii infection protects human microvascular endothelial cells against staurosporine-induced apoptosis by cIAP2-independent mechanisms. – J. Infect. Dis., 199(9), 2009, 1389-1398.
3. Chiu, S. M., L.Y. Xue, J. Usuda, K. Azizuddin, N. L. Oleinick. Bax is essential for mitochondrion-mediated apoptosis but not for cell death caused by photodynamic therapy. – Br. J. Cancer., 89(8), 2003, 1590-1597.
4. Faherty, C., A. Maureli. Stayng alive: bacterial inhibition of apoptosis during infection. – Trends Microbiol., 16(4), 2008, 173-180.
5. Finucane, D. M., E. Bossy-Wetzel, N. J. Waterhouse, T. G. Cotter, D. R. Green. Bax-induced caspase activation and apoptosis via cytochrome c release from mitochondria is inhibitable by Bcl-xL. – J. Biol. Chem., 274(4), 1999, 2225-2233.
6. Hsia, J. Y., C. Y. Chen, C. P. Hsu et al. Expression of apoptosis-regulating proteins p53, Bcl-2, and Bax in primary resected esophageal squamous cell carcinoma. – Neoplasma, 48(6), 2001, 483-488.
7. Joshi, S. G., C. W. Francis, D. J. Silvermann, S. K. Sahni. NF-kB activation suppresses host cell apoptosis during Rickettsia rickettsii infection via regulatory effects on intracellular localization or levels of apoptogenic and anti-apoptotic proteins. – EMS Microbiol. Lett., 234, 2004, 333-341.
8. Popivanova, N. Mediterranean spotted fever. Plovdiv, Ed: IK-VAP, 2006, 8-136.
9. Sahni, S., E. Rydkina. Host-cell interactions with pathogenic Rickettsia species. – Future Microbiol., 4, 2009, 323-339.
10. Scorrano, L., S. J. Korsmeyer. Mechanisms of cytochrome c release by proapoptotic Bcl-2 family members. – Biochem. Biophys. Res. Commun., 304, 2003, 437-444.
11. Vassilev, V., G. Baltadjiev, A. Baltadjiev. Human Anatomy – Atlas Textbook, (Ed. G.Baltadjiev), Plovdiv, IK-VAP, 2009, 230-233.

Institute of Experimental Morphology, Pathology and Anthropology with Museum
Bulgarian Anatomical Society

Acta morphologica et anthropologica, 19
Sofia • 2012

Morphological changes in biologically active Point /BAP/ ST36 after acupuncture in rat

N. Dimitrov

Department of Anatomy, Faculty of Medicine, Stara Zagora, Bulgaria

Biologically active points (BAP) ST 36 is treated with various methods of Chinese medicine. One of the most used is acupuncture. The aim of this study is to clarify the effect of the acupuncture needle on the structure of the BAP ST 36 in rat by the use of classic histological techniques. The impact of the acupuncture needle in the BAT ST36 induces morphological changes in the tissues studied. The methods used allow to explore the construction of acupuncture needle channel and the changes induced by it. The seen defect has a minimal size and the living tissue fast recovers its integrity upon with drawl of the needle.

Key words: biologically active points (BAP), histology, rat, ST 36, Acupuncture needle.

Introduction

Changes that occur in the tissues under the influence of acupuncture needle is not sufficiently investigated [14].Research efforts are focused on the study of morphological features in acupuncture points [2, 6, 8], the role of connective tissue under the skin of the reflex response [10, 11], the construction of Mechanoreceptors at the cellular level [1].Special attention is paid to the morphological characteristics [9, 10] and the skin changes that occur in it by mechanical [7] and electrical [13] influences. Some authors seek identity between energy channels in humans and animals [4] and follow the general mechanisms involved in Ayurvedic and Chinese medicine [3].

Aim and objectives

Target of this study is using the classic histological techniques [15] to identify any changes that occur in the tissues under the influence of acupuncture needle.

Materials and Methods

Experiments

Were carried out on five adult normotensive rats, Wistar strain of either sex weighing ranging between 220 and 350 g. and 2 adult spontaneously hypertensive rats, (SHR) of

both sexes, weighing 180 to320g. The area around the BAP was epilated, defined and marked with the method of standard proportion of anatomical structures [5] under the control of the apparatus KWD-808 measuring skin resistance. The material was taken and treated without removing the needle for better visualization of the acupuncture channel. Samples are cut into freezing microtomes thickness 20 and 30 mm and paraffin slice thickness of 5, 7 and 10 mm. We used the following 6 stains: routine staining with Hematoxylin-eosin (H&E), a connective tissue with van Gieson (V.G), three colour staining by Mallory, Toluidine blue, the elastic fibers with Orcein, three colour staining by Masson.

Results

The tissue recover fast its integrity upon withdrawal of the needle and the channel is difficult to discern **Fig 1**.Clearly distinct channel from the prick is seen if the needle is kept in the tissue during its processing. In this case, the observed channel penetrates the dermis, subcutaneous connective tissue, fascia, and reaches the muscle, without affecting the deeper lying vessels. The integrity of the epithelium, subcutaneous loose connective tissue, the fascia and the muscle is damaged. **Fig 2** In the subcutaneous connective tissue partial destruction of elastic and collagen fibers is observed **Fig 3** and increased degranulation of mast cells in the acupuncture area **Fig. 4**. The cells are deformed, the intercellular distances are reduced, the glands and the hair follicles are pressed. Pressed and with reduced cross section blood vessels are found, rupture, deformation and sag of the epithelium and deep subcutaneous connective tissue and condensing of the loose connective tissue, and the lying in it cells, collagen and elastic fibers. **Fig 5**. Changes in the structure of loose connective tissue are most pronounced near the channel formed by the acupuncture needle, but also occur in adjacent areas of skin **Fig 6**. There is a minimal swelling in the area around the needle and some red blood cells in the nearby to the acupuncture channel tissues . In depth a large blood vessels could be found that are not affected by the needle **Fig. 7, 8, 9.**

Discussion.

The channel of the acupuncture needle penetrates the dermis, subcutaneous connective tissue, fascia, and up to the muscle without affecting the deep larger blood vessels. The skin defect remains visible when holding the needle into the tissue during its processing. The results obtained by other authors for two types of amendments: destruction in the channel caused by the needle and deformation in the adjacent layers and tissues are confirmed [12]. The nearest to the needle tissues are destroyed. Cells shape and position is altered, intercellular distances are reduced, the glands and hair follicles are presssed, blood vessels are deformed and their diameter is reduced. In depth larger vessels are found, which confirms the results of other authors [7, 13]. They are not affected and there were no major bleeding. Similar changes in the loose connective tissue are described in the literature [7]. We also detected degranulation of mast cells in the acupuncture area, which is confirmed by other researchers [12].

Conclusions

1. The influence of the acupuncture needle in the BAP ST36 induces morphological changes in the examined tissues. The defect seen is with a minimum size and the tissue integrity recovers fast after the removal of the needle.

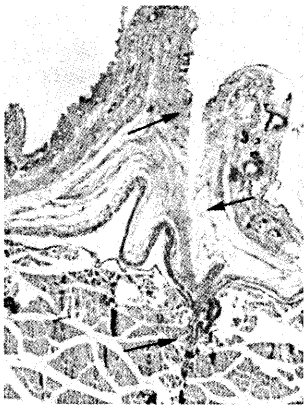

Fig 1. Acupuncture needle channel and deformation and sag of the epithelium, the fascia and deep subcutaneous tissue (arrow) (Mallory)

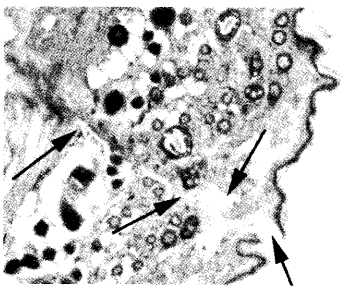

Fig 2. Acupuncture needle channel (arrow) and mast cells (toluidine blue)

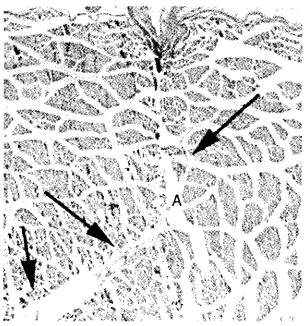

Fig 3. Acupuncture needle channel (A) and blood vessels (arrow) (Mallory)

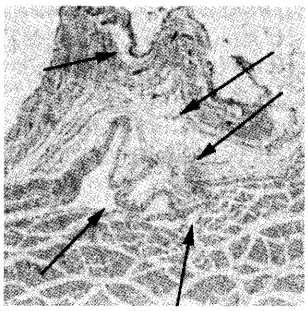

Fig 4 Deformation and sag of the epithelium and deep subcutaneous connective tissue near the channel formed by the acupuncture needle (arrow) (HE)

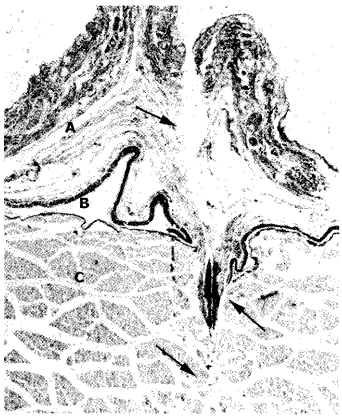

Fig 5. Acupuncture needle channel (arrow) (VG)

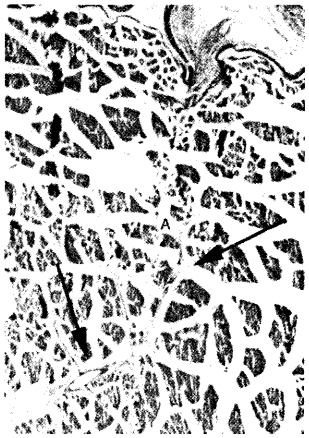

Fig 6. Large blood vessels (arrow) and acupunctureneedle channel (A) (Masson)

Fig 7. Destruction of elastic and collagen fibers (Orcein

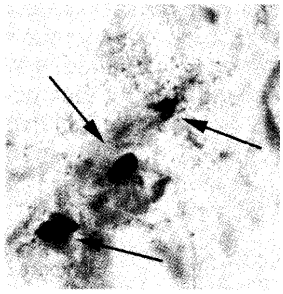

Fig 8. Degranulation of mast tissue (arrow) (Mallory)

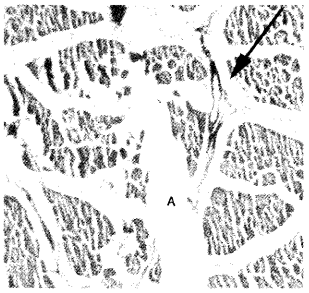

Fig 9. acupuncture needle channel (A) and blood vessels (arrow) (Mallory)

2. The main changes are related to the destruction and deformation in the adjacent tissues near the channel , accompanied by degranulation of mast cells in the prick area.

References

1. Banes, A.J., Tsuzaki, M., Yamamoto, J., Fischer, T., Brigman, B., Brown, T. and Miller, M. (1995). Mechanoreception at the cellular level: the detection, interpretation and diversity of responses to mechanical signals. Biochem Cell Biol. 73, 349-365.
2. Bossy, Jean. Morphological data concerning the acupuncture–points and channel network. Elektrother. Res, 9/1984.
3. Dimitrov, N., N. Pirovski, D. Sivrev. Application of ajurveda and traditional chinese medicine in the present medical practice. Scientific conference with international participation, scientific researchers volume III, part I, 2008, 346- 350.
4. Dimitrov, N., D. Sivrev, Y. Staykova, Z. Goranova. Comparative analysis of biological active channeles in humans and animals. Scientific conference with international participation, scientific researchers volume III, part I, 2008, 351- 357.
5. Dimitrov, N., D. Sivrev D, N. Pirovski, A. Georgieva, Methods for localization of BAP of the human body. 19-21.Jurnal of Biomedical &clinical Research, MU – Pleven, 2009
6. Dung, H.C. (1984). Anatomical features contributing to the formation of acupuncture points. Am J Acup. 12, 139-143.
7. Jeong, K., P. Min, C. Kuang, J. Hae. Histological Changes of the Acupoint by Acupuncture Stimulation. Korean Journal of Electron Mycroscopy, 2000, 30(1): 81-87.
8. Heine, H. Morphologie der Ohrakupunkturpunkte. Deutsche Zeitschr. für Akupunktur Nr. 36/1993.
9. Kurabayashi, Y. Histological studies on the skin elective resistance decreased point (SERDP). Okayama Igakukai Zasshi. 1980, 92: 635-657.
10. Langevin, H.M., Churchill, D.L., and Cipolla, M.J. (2001). Mechanical signaling through connective tissue: a mechanism for the therapeutic effect of acupuncture. FASEB J. 15, 2275-2282.
11. Langevin, H., D. Churchill, J. Wu, G. Badger, J. Yandow, J. Fox, M. Krag. Evidence of Connective Tissue Involvement in Acupuncture. The FASEB Journal, 2002.
12. Peter Chin Van Fung. Probing the mystery of Chinese medicine meridian channels with special emphasis on the connective tissue interstitial fluid system, mechanotransduction, cells durotaxis and mast cell degranulation
13. Yung-Kyoung, Y., H. Lee, K. Hong, Y. Kim, B. Lee. Electroacupuncture at acupoint ST36 reduces inflammation and regulates immune activity in Collagen-induces Arthritic mice. eCAM, 2007, 4(1): 51-57.
14. Лувсан, Г. Традиционные и современные аспекты восточной рефлексотерапии, Наука, Москва, 1992 (in Russian)
15. Чучков, Хр., Д. Сиврев, М. Недева. Хистологични техники. Универс прес, 2007.

Institute of Experimental Morphology, Pathology and Anthropology with Museum
Bulgarian Anatomical Society

Acta morphologica et anthropologica, 19
Sofia • 2012

Normal morphology of biologically active point BAP/ST36 rat.

N. Dimitrov

Department of Anatomy, Faculty of Medicine, Stara Zagora, Bulgaria

Point ST 36 is one of the most important and most commonly used in acupuncture biologically active point (BAP) [3] The purpose of this study is using the classic histological techniques to visualize normal morphology in the BAP ST 36 in rat. The methods used allow the study of normal anatomic structures in the BAP ST 36 – dermis, subcutis, fascia, muscle, blood vessels and nerves. The observed differences are in the thickness of the dermis and subcutis, loose connective tissue layer, the presence of indentations and differences in the thickness of the epidermis. Larger blood vessels could be found in depth in the underalaying striated muscle tissue, clusters of mast cells in certain areas of the dermis, subcutis, fascia and striated muscle.

Key words: acupuncture, biologically active point (BAP), histology, rat, ST 36.

Introduction

ST36 is one of the most important [2] and the most commonly used acupuncture in BAP [11].To establish any changes in it after acupuncture its normal morphology should be known.

Aim and objectives

The aim of this study is to establish the normal morphology of BAP ST 36 in rat by using a classic histological techniques [12].

Materials and Methods

Experiments

Were carried out on 14 normotensive rats, Wistar strain of either sex weighing 220-350 g and 7 adult spontaneously hypertensive rats, (SHR) of both sexes, weighing 180 to 320 g. The point ST 36 is localized by determining the ratio of standard anatomical structures [3, 4] and with device KWD-808 to measure the skin resistance.

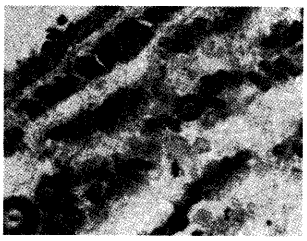

Fig. 1. Skin, subcutaneous adipose tissue (Sudan III)

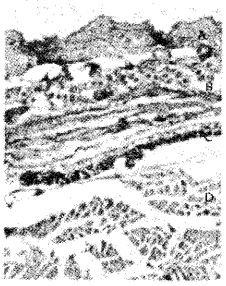

Fig. 2. Dermis (A), subcutis (B), fascia (C), muscles D) (V.G)

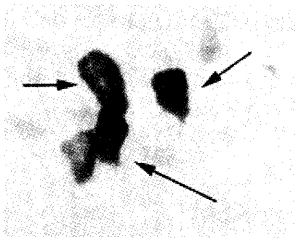

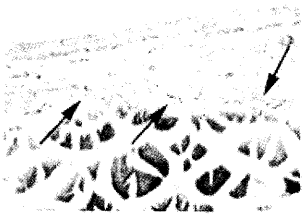

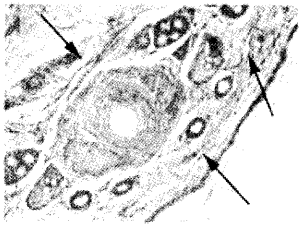

Fig. 3, 4. Mast cells (arrow) (toluidine blue) Fig. 5. Elastic fibers (arrow)

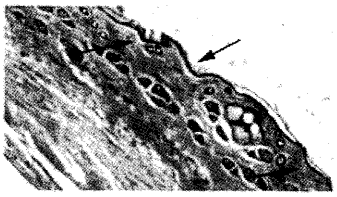

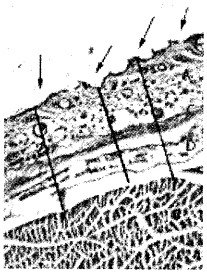

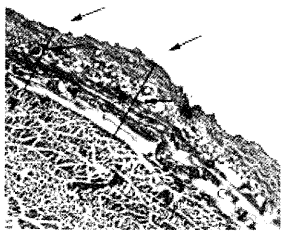

Fig. 6. Skin, Indentations and Fig 7. Dermis (A), subcutis (C), Fig. 8. Dermis (A), muscles (B), differences in the thickness of fascia(D), muscles (B) fascia(C), (arrow- the epidermis (arrow) (HE) (arrow-differences in the in the thickness of the thickness of the dermis and dermis and subcutis) subcutis) (Mallory) (Masson)

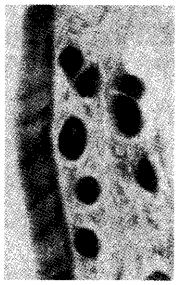

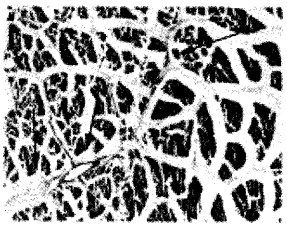

Fig. 9. Free nerve endings Fig 10. Cluster of large blood (Bodyan) vessels (arrow) (Masson)

The material is cut into freezing microtome with a thickness of 20 to 30 mm, and paraffin cut – thickness 5, 7 and 10 μm. Eight different types of staining is applied.

Hematoxylin-eosin (H&E); for the connective tissue- van Gieson (VG); three colour staining by Mallory; Toluidine blue for mast cells; elastic fibers with Orcein; Bodyan for nerve fibers;three colour staining by Masson; Sudan III for fat tissue.

Results

Normal anatomical structures was visualized [5]: skin, subcutaneous adipose tissue in **Fig 1**, fascia, striated muscles, blood vessels and nerves. **Fig 2** and accumulation of mast cells in certain areas **Fig 3, 4**. In the connective tissue [8, 9] elastic fibers are found around the glands, the hair follicles **Fig. 5** and fascias and collagen fibers also. In some areas of the skin we see a thicker layer of loose connective tissue, indentations and differences in the thickness of the epidermis and folding of the deep fascia. **Fig 6, 7, 8** Around the glands and the hair follicles free nerve endings are found [1], **Fig 9** and in the depth of the cross-striated muscle – a cluster of large blood vessels **Fig 10**.

Discussion

In BAP ST36 we observe an accumulation of mast cells, primarily – in the vicinity of blood vessels and the deep fascia, which is confirmed by other authors [7, 10]. Big blood vessels are not detected superficially, unlike earlier studies [6], and we find such in striated muscle[2].

Conclusion

Under normal conditions there is a difference between the normal structure in BAP and the adjacent tissues, but this difference is not pronounced.

References

1. Banes, A.J., Tsuzaki, M., Yamamoto, J., Fischer, T., Brigman, B., Brown, T. and Miller, M. (1995). Mechanoreception at the cellular level: the detection, interpretation and diversity of responses to mechanical signals. Biochem Cell Biol. 73, 349-365.
2. Dimitrov, N., N. Pirovski, D. Sivrev. Application of aiurveda and traditional chinese medicine in the present medical practice. Scientific conference with international participation, scientific researchers volume III, part I, 2008, 346- 350.
3. Dimitrov, N., D. Sivrev, Y. Staykova, Z. Goranova. Comparative analysis of biological active channeles in humans and animals. Scientific conference with international participation, scientific researchers volume III, part I, 2008, 351- 357.
4. Dimitrov. N., D. Sivrev D, N. Pirovski, A. Georgieva, Methods for localization of BAP of the human body. 19-21.Jurnal of Biomedical &clinical Research, MU – Pleven, 2009
5. Dung, H.C. (1984). Anatomical features contributing to the formation of acupuncture points. Am J Acup. 12, 139-143.
6. Jeong, K., P. Min, C. Kuang, J. Hae. Histological Changes of the Acupoint by Acupuncture Stimulation. Korean Journal of Electron Mycroscopy, 2000, 30(1): 81-87.
7. Kurabayashi, Y. Histological studies on the skin elective resistance decreased point (SERDP). Okayama Igakukai Zasshi. 1980, 92: 635-657.

8. Langevin, H.M., Churchill, D.L., and Cipolla, M.J. (2001). Mechanical signaling through connective tissue: a mechanism for the therapeutic effect of acupuncture. FASEB J, 15, 2275-2282.
9. Langevin, H., D. Churchill, J. Wu, G. Badger, J. Yandow, J. Fox, M. Krag. Evidence of Connective Tissue Involvement in Acupuncture. The FASEB Journal, 2002,
10. Yung-Kyoung, Y., H. Lee, K. Hong, Y. Kim, B. Lee. Electroacupuncture at acupoint ST36 reduces inflammation and regulates immune activity in Collagen-induces Arthritic mice. eCAM, 2007, 4(1): 51-57.
11. Лувсан, Г. Традиционные и современные аспекты восточной рефлексотерапии, Наука, Москва, 1992 (in Russian)
12. Чучков, Хр., Д. Сиврев, М. Недева. Хистологични техники. Универс прес, 2007.

Institute of Experimental Morphology, Pathology and Anthropology with Museum
Bulgarian Anatomical Society

Acta morphologica et anthropologica, 19
Sofia • 2012

The Challenge of the Brain Tumors – Searching for New Therapeutic Opportunities

L. Dyakova[1], D.-C. Culita[2], G. Marinescu[2], L. Patron[2], R. Kalfin[1], R. Alexandrova[3]

[1]Institute of Neurobiology, Bulgarian Academy of Sciences, Acad. Georgi Bonchev Str., Block 23, Sofia 1113, Bulgaria;
[2]Institute of Physical Chemistry "Ilie Murgulescu", Splaiul Independentei 202, Sect. 6, Bucharest 060021, Romania;
[3]Institute of Experimental Morphology, Pathology and Antropology with Museum, Bulgarian Academy of Sciences, Acad. Georgi Bonchev Str., Block 25, Sofia 1113, Bulgaria

The aim of our study was to evaluate the influence of newly synthesized metal (Zn, Cu, Ni) complexes of ursodeoxycholic acid (UDC) on viability and proliferation of cultured 8 MG BA human glioblastoma cells. The investigations were carried out by thiazolyl blue tetrazolium bromide (MTT) test. The results obtained revealed that applied at concentrations of 10-200 μg/ml for 24 h the compounds examined decreased in a time- and concentration- dependent manner the viability of the treated cells. The copper complex $Cu(UDC)_2 \cdot 2H_2O$ showed relatively the highest cytotoxic/antiproliferative potential. Independently tested, the ursodeoxycholic acid was found to be less active cytotoxic agent as compared to its complexes.

Key words: glioma, cell line, deoxycholic acid, metal complexes, cytotoxicity

Introduction

Gliomas are the most frequent primary neoplasms of the central nervous system (CNS) in adults, consisting of 63% of all primary CNS tumors. The majority of them remain difficult to cure because of the infiltrative growth of cancer cells and their resistance to standard therapy. This is the 3rd leading cause of death from cancer in persons aged 20 to 39 and also the most common solid tumors in children [3, 6, 7]. At the same time there are data revealing that some derivatives of cholic acids decrease the viability and proliferation of cultured human glioblastoma cells [12]. That is why the aim of our study was to evaluate the putative cytotoxic and cytostatic properties of newly synthesized metal complexes of ursodeoxycholic acid in cultured 8 MG BA human glioblastoma cells.

Matherials and Methods

Chemicals and other materials. Dulbecco's modified Eagle's medium (DMEM) and fetal bovine serum (FBS) were purchased from Gibco-Invitrogen (UK). Dimethyl sulfoxide (DMSO) and trypsin were obtained from AppliChem (Germany); thiazolyl blue tetrazolium bromide (MTT) were from Sigma-Aldrich Chemie GmbH (Germany). All other chemicals of the highest purity commercially available were purchased from local agents and distributors. All sterile plasticware were from Orange Scientific (Belgium).

Synthesis of metal ursodeoxycholate complexes. The metal complexes containing the anion of ursodeoxycholic acid (UDC) as ligand have been synthesized by the reaction of sodium ursodeoxycholate dissolved in water (at room temperature) with aqueous solution of metal salt $Cu(NO_3)_2 \cdot 3H_2O$; $Ni(NO_3)_2 \cdot 6H_2O$; $Zn(NO_3)_2 \cdot 6H_2O$), under vigorous stirring for one hour. The precipitates were filtered, washed several times with distilled water to eliminate unreacted metal salt and sodium ursodeoxycholate and then desiccated over P_4O_{10}. All of the solid complexes obtained were characterized by elemental chemical analysis and different physico-chemical methods (FTIR, UV-VIS, magnetic measurements, EPR spectroscopy) [5]. The complex compounds have the following formula: $Zn(UDC)_2 \cdot 3H_2O$, $Ni(UDC)_2 \cdot 11H_2O$, and $Cu(UDC)_2 \cdot 2H_2O$. The compounds were initially dissolved in DMSO and then diluted in culture medium. The final concentration of DMSO in stock solutions of the compounds tested (1 μg/ml) was 1-2 %

Experimental part. The permenent human cell line (8 MG BA) established from glioblastoma multiforme was used as an experimental model in our investigations [10]. The cells were grown as monolayer cultures in DMEM medium, supplemented with 5-10% fetal bovine serum, 100 U penicillin and 100 μg/ml streptomycin. The culture was maintained at 37°C in a humidified CO_2 incubator. For routine passages adherent cells were detached using a mixture of 0.5% trypsin (Gibco) and 0.02% ethylendiaminotetraacetic acid (EDTA). The experiments were performed during the exponential phase of cell growth. The effects of the compounds investigated on cell viability and proliferation were evaluated by thiazolyl blue tetrazolium bromide (MTT) test [Mosman]. Relative cell viability, expressed as a percentage of the untreated control (100% viability), was calculated for each concentration and "concentration – response" curves were prepared. All data points represent an average of three independent assays.

Statistical analysis. The received data are presented as mean +/- standard error of the mean. Statistical differences between control and treated groups were assessed using one-way analysis of variance (ANOVA) followed by Dunnett's *post-hoc* test.

Results

The results obtained by MTT test (Fig. 1) revealed that applied at concentrations of 10-200 μg/ml for 24 h the compounds examined decreased in a time- and concentration-dependent manner the viability and proliferation of the treated 8 MG BA glioblastoma cells. The copper complex $Cu(UDC)_2 \cdot 2H_2O$ was found to express relatively the highest cytotoxic/cytostatic propertis. Independently tested, ursodeoxycholic acid was shown to be the less active cytotoxic/cytostatic agent.

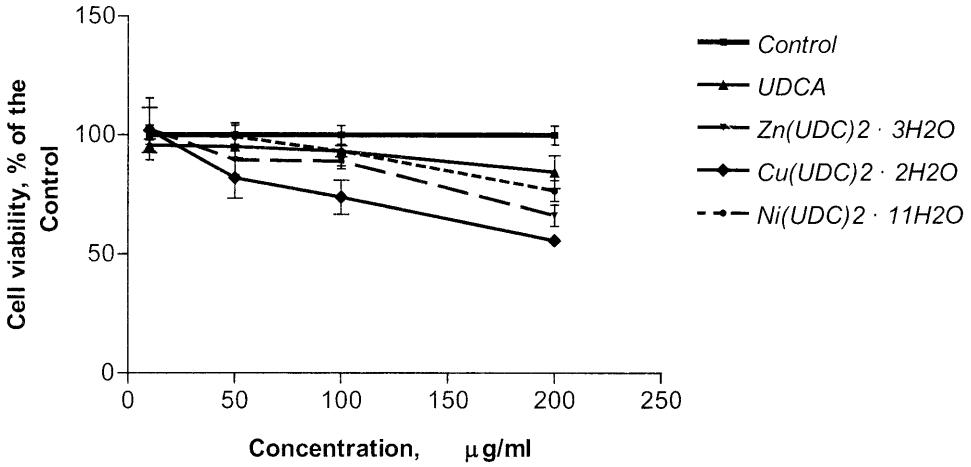

Fig. 1. Influence of ursodeoxycholic acid and its metal complexes on viability and proliferation of cultured human 8 MG BA glioblastoma cells. The compounds are applied at concentrations of 10, 50, 100 and 200 μg/ml for 24 h. The investigations were performed by MTT test.

Discussion

In recent years steroidal structures have become increasingly important in a number of fields such as pharmacology, medicinal chemistry, biomimetic, supramolecular chemistry and also in nanotechnology. There are well known the pharmacological applications of bile acids and their derivatives, including their use in the treatment of liver diseases, in dissolution of cholesterol gallstones, antiviral and antifungal properties, as well as their potential to act as carriers of liver specific drugs and cholesterol level lowering agents. Some of the latest applications in the area of the use of bile acids and their derivatives in cancer therapy are bile acids-*cis*-platin compounds [9] and chenodeoxycholylglycinato derivatives of Pt(II) and Au(III) [4].

A new family complex compounds of transition metals with bile acids and NH_3, named Bamets, have been shown to be promising cytostatic agents [2]. In our investigations the copper complex $Cu(UDC)_2 \cdot 2H_2O$ showed relatively the highest cytotoxic/antiproliferative activity. Copper is known as a trace element which plays a fundamental role in the biochemistry of the human nervous system. On the other hand there are data that some copper containing compounds may possess antineoplastic activity [2, 8, 11]. Something more, since copper is an essential metal for humans it has been suggested that its compounds will be relatively less toxic as compared to those of platinum. In this regard, the compound $Cu(UDC)_2 \cdot 2H_2O$ could be a promising cytostatic agent in glioblastoma treatment.

Acknowledgements: Supported by a bilateral grant between Bulgarian Academy of Sciences and Romanian Academy.

References

1. Alexandrova, R., G. Rashkova, I. Alexandrov, W. Tsenova, R. Tudose, O. Costisor. Briefly about copper. – Exp. Pathol. Parasitol., **6**, 2003, 3-12.

2. Ballestero, M.R., M.J. Monte, O. Briz , F. Jimenez , F. Gonzalez-San Martin , J.J. Marin. Expression of transporters potentially involved in the targeting of cytostatic bile acid derivatives to colon cancer and polyps. – Biochem Pharmacol., **72**, 2006, 729-738.
3. Candolfi, M., J.F. Curtin, W.S. Nichols, AKM. G. Muhammad, G.D. King, G.E.Pluhar, E.A. McNiel, J.R. Ohlfest, A.B. Freese, P.F. Moore, J. Lerner, P.R. Lowenstein, M.G. Castro. Intracranial glioblastoma models in preclinical neuro-oncology: neuropathological characterization and tumor progression. – J. Neurooncol., **85**, 2007, 133–148.
4. Criado, J.J., M.C. Garcia-Moreno, R.R. Macias, J.J.G. Manin, M.Medara, E. Rodriguez-Fernandez. – Biometals, **12**, 1999, 281-288.
5. Culita, D. C., G. Marinescu, L. Patron, F. Tuna, N. Stanica, M. Yun. – Rev. Roum. Chim., **55**, 2010, 63-67
6. Dai, C., E.C. Holland. Glioma models. – Biochim. Biophysica Acta, **1551**, 2001, M19-M27.
7. Furnari, F.B., T. Fenton, R.M. Bachoo et al. Malignant astrocytic glioma: genetics, biology, and paths to treatment. – Genes Dev., **21**, 2007, 2683-2710.
8. Marzano, C., M. Pellei , F. Tisato, C. Santini . Copper complexes as anticancer agents. Anticancer Agents Med. Chem., **9**, 2009, 185-211.
9. Paschke, R., J. Kalbitz, C. Paetz. – Inorg. Chim. Acta, **304**, 2000, 241-249.
10. Perzelova, A., I. Macikova, P. Mraz, I. Bizik, J. Steno. Characterization of two new permenant glioma cell lines 8-MG-BA and 42-MG-BA. Neoplasma, **45**, 1998, 25-29.
11. Ruiz-Azuara, L., M.E. Bravo-Gómez .- Copper compounds in cancer chemotherapy. Curr Med Chem., **17**, 2010, 3606-15.
12. Yee S.B., W.J. Yeo , B.S. Park , J.Y. Kim , S.J. Baek , Y.C. Kim , S.Y. Seo , S.H. Lee, J.H. Kim , H. Suh, N.D. Kim , Y.J. Lim , Y.H. Yoo . – Synthetic chenodeoxycholic acid derivatives inhibit glioblastoma multiform tumor growth in vitro and in vivo. – Int. J. Oncol., **27**, 2005, 653-659.

Institute of Experimental Morphology, Pathology and Anthropology with Museum
Bulgarian Anatomical Society

Acta morphologica et anthropologica, 19
Sofia • 2012

Pathomorphological approach to alopetic lesions on the scalp

Mary Gantcheva

Institute Experimental Morphology Pathology and Anthropology with Museum, Bulgarian Academy of Sciences

Hair loss is a common disorder but without enough knowledge in the evaluation of hair diseases. The differential diagnosis includes a lot of disorders causing cicatricial or noncicatricial alopecias.

We present two casuistic cases of patients with alopetic lesions on the scalp. The clinical examination signifies alopecia areata in both cases but with disappearance of visible follicular ostia. Pathomorphological findings clarifies the lesions as scarring or cicatricial alopecias, an uncommon and clinically diverse set of disorders that result in permanent and irreversible hair loss.

Key words: alopecia, cicatricial alopecia, sclerodermia "en coup de sabre", psoriasis vulgaris, lupus erythemathosus capilitii

Introduction

Alopecias of the scalp is divided into two groups, namely non-scarring or non-cicatricial and scarring or cicatricial forms. Pathomorphologically, a scar constitutes the end point of reparative fibrosis with permanent destruction of the preexisting tissue [4].

Non-scaring alopecia represents a complex group of hair disorders in which the hair shafts fall out, but the hair follicles are still alive and from this point of view the prognosis is better. The clinical entities include androgenic alopecia, telogen effluvium, alopecia areata, trichotillomania and traction alopecia.

Cicatricial alopecia encompasses a group of disorders characterized by permanent destruction of the hair follicle, which is replaced by fibrous tissue leading to progressive and permanent hair loss. According to the initially location of the inflammatory process cicatrical alopecia can be primary and secondary. In primary cicatricial alopecias the pilosebaceous follicle is the target of the destructive process. In secondary forms the follicular destruction is a consequence, and due to numerous aetiologies (Table 1) [1].

Table 1. **Secondary scarring alopecia**

- Aplasia cutis congenita
- Cicatricial bullous pemphigoid
- Infectious (kerion, staphylococcal)
- Neoplastic (primary, metastasis)
- Connective tissue disease (morphea)

- Trauma (burn)
- Metabolic (amyloid, mucin)
- Granulomatous (sarcoid)

Primary cicatricial alopecias are divided into several categories, including lymphocytic, neutrophilic and mixed (Table 2) according the current working classification proposed by the North American Hair Research Society [3]. The cause and pathogenesis are largely unknown, but the target is the hair follicle itself [6].

Table 2. **Working classification proposed by the North American Hair Research Society**

1. Lymphocytic
- Chronic cutaneous lupus erythematosus
- Lichen planopilaris (LPP)
  - Classic LPP
  - Frontal fibrosing alopecia
  - Graham–Little syndrome
- Classic pseudopelade (Brocq)
- Central centrifugal cicatricial alopecia
- Alopecia mucinosa
- Keratosis follicularis spinulosa decalvans

1. Neutrophilic
- Folliculitis decalvans
- Dissecting cellulitis / folliculitis (perifolliculitis capitis abscedens et suffodiens)

1. Mixed
- Folliculitis (acne) keloidalis
- Folliculitis (acne) necrotica
- Erosive pustular dermatosis

Materials and Methods

We present two different cases of alopetic lesions of the scalp.

First case is nine years old girl. She complains of hairless well-defined solitary lesion with linear form localized on the fronto-parietal part of the scalp. She and her parents treated it according medical prescription with local creams and solutions almost one year without visible effect.

Second case is 67 years old woman. She has red raised skin plaques covered with silvery white squamas on the skin of the knees, elbows and trunk. She is diagnosed as having psoriasis and the diagnosis is clinically and histological proven more than ten years ago. She has also psoriatic lesions on the scalp, presented as inflammatory plaques with white squamas which are not hairless. Last two months the patient has noticed another type of skin lesions on her capillicium, characterized with small oval alopetic maculae with very soften and thin skin without any visible hair.

Both patients followed laboratory and immunological investigations. The girl followed also examination of X-ray cranium and study for antibodies for Borrelia burgdoferi. All the results were in normal limits.

Skin biopsies of hairless lesions were obtained from the two patients. The biopsy tissue was fixed in 10% neutral buffered formaldehyde solution, processed routinely, and stained with hematoxyline-eosin.

Results and discussion

The histology of the first patient demonstrate thickening and moderate hyalinization of the collagen in middle and lower part of the dermis. Perivascular infiltrate are seen in middle and upper dermis (Fig. 1).

The clinical and histological characteristics of the skin lesions lead us to diagnosis of linear scleroderma, often called scleroderma en coup de sabre (SCS) for its resemblance to a sword-strike scar. The differential diagnosis include chronic cutaneous lupus erythematosus, frontal fibrosing cicatricial alopecia, pseudopelade of Brocq, or lichen sclerosus et atrophicus. The lack of surface changes, such as scaling, follicular plugging or perifollicular erythema, the linearity of the lesion and the extension of sclerosis onto the forehead help to distinguish it from the other alopetic lesions. According to Soma et al frontoparietal scleroderma, may occur along the lines of Blaschko [5]. Since both the unilateral distribution and the lesions along Blaschko's lines are the patterns created by genetic mosaicism, they suggest that a significant part of linear scleroderma and perhaps a smaller part of multiple morphea could be related to cutaneous mosaicism. We follow the patient till now because 25% of the cases with SCS could be worsened with Central Nervous System complications [2]. Alopetic lesion persists as it is classified as secondary cicatricial alopecia due to connective tissue disease- morphea but fortunately there is not involvement of any other organ or system.

Two biopsies were performed from the skin of the second patient. The first one was obtained from a lesion localized on the hand. The findings demonstrates hyper and parakeratosis, epidermal acathosis and elongation of rete ridges and moderate perivascular inflammatory infiltrate in upper derma (Fig. 2). All these characteristics are typical for psoriasis. The other biopsy was taken from alopetic lesion of the scalp. The findings were quite different and showed epidermal atrophy, moderate vacuole degeneration of the basal layer and lymphocytic infiltrate in upper derma (Fig.3). Direct immunofluo-

Fig. 1 Thickened connective tissue septae in hypoderma and hyalinization of the collagen (HE, x 20)

Fig. 2. Hyper and parakeratosis, epidermal acathosis and elongation of rete ridges and moderate perivascular inflammatory infiltrate in upper derma (HE, x 20)

Fig.3. Epidermal atrophy, vacuole degeneration of the basal layer and lymphocytic infiltrate in upper derma (HE, x 20)

rescense revealed granular Ig M (+) deposit on the layer of dermo-epidermal junction. These findings correlate with the diagnosis of cutaneous form of lupus erythematosus chronicus discoides (LECD). We conclude that this patient has psoriasis vulgaris in association with LECD on the scalp. The two diseases are very different from clinical, morphological and therapeutic point of view. However, they both have multifactor immunological background and their pathogenetic pathway is disputable. Clearly is

that the alopetic lesions are due to LECD and are classified to lymphocytic subtype of primary cicatricial alopecia.

Conclusion

Alopetic lesions on the scalp are clinically similar but pathomorphologicaly quite different. Their correct interpretation from all points of view leads to correct diagnosis and consequently to correct treatment. Our cases have histologic and clinical overlap of cicatricial alopecia – due to a connective tissue disease, secondary subtype and lymphocytic primary subtype in association with systemic disease. The both have permanent destruction of the hair follicle that result in irreversible hair loss.

References

1. Finner, A.M., N. Otberg, J. Shapiro. Secondary cicatricial and other permanent alopecias. – Dermatol. Ther., 21, 2008, 279–294.
2. Jablonska, S. Long-lasting follow up favors a close relationship between PFH and LSCS. – JEADV, 19, 2005, 4-9.
3. Olsen, E. A., W. F. Bergfeld, G. Cotsarelis. Summary of North American Hair Research Society (NAHRS)-sponsored Workshop on Cicatricial Alopecia, Duke University Medical Center. – J. Am. Acad. Dermatol., 48, 2003, 103–110.
4. Sellheyer, K., W.F. Bergfeld. Histopathologic Evaluation of Alopecias. – Am J Dermatopathol., 28, 2006, 236–259.
5. Soma, Y., K. Tamihiro, E. Yamasaki, R. Sasaki, M. Mizoguchi. Linear Scleroderma Along Blaschko's Lines in a Patient with Systematized Morphea. – Acta Derm Venereol, 83, 2003, 362–364.
6. Sperling, L.C., S.E. Cowper. The histopathology of primary cicatricial alopecia. -Semin. Cutan. Med. Surg., 25, 2006, 41–50.

Institute of Experimental Morphology, Pathology and Anthropology with Museum
Bulgarian Anatomical Society

Acta morphologica et anthropologica, 19
Sofia • 2012

Effects of cadmium and monensin on the morphology of lung of mice, subjected to subacute cadmium intoxication

A. Gegova[1], D. Mitkov[1], Y. Gluhcheva[2], S. Arpadjan[3], M. Mitewa[3], Ju. Ivanova[1*]*

[1*] corresponding authors: Faculty of Medicine, Sofia University "St. Kliment Ohridski"
[2]Institute of Experimental Morphology, Pathology and Anthropology with Museum – BAS
[3]Faculty of Chemistry and Pharmacy, Sofia University "St. Kliment Ohridski"

The effects of cadmium (Cd) and monensin on the lungs of mice, subjected to subacute Cd intoxication were studied on ICR mouse model. The data demonstrated that Cd induced elevation of the lungs weight in Cd-intoxicated mice compared to the normal controls. The treatment of Cd-intoxicated mice with monensin recovered lungs weight to normal values, suggesting an ameliorative effect of the antibiotic on the lung function. Histopathological analysis of the lung tissue demonstrated that Cd induced circulatory and inflammatory alterations. Monensin administration to Cd-treated animals reduced the morphological alterations and restored histology of the lungs to normal in a great extent. These data were well correlated with the results from the atomic absorption that showed that monensin reduces the concentration of Cd in the lungs of the Cd-intoxicated animals by 30 % compared to the toxic control. Taken together the results presented in this study prove that monensin could be a promising chelating agent for the treatment of Cd-induced lung dysfunction.

Key words: lung, cadmium, monensin, ICR mice, chelating agents

Introduction

The development of modern industry led to a rapid increase of the concentrations of toxic elements in our environment [9]. Among them, cadmium (Cd) is extremely dangerous for the human health because of its long biological half-life (40 years for humans) [8, 9]. Humans could be exposed to Cd either by inhalation or ingestion. 90 % of inhaled Cd is absorbed by the lungs [4]. Studies on animal model have been proven that the accumulation of Cd in the lungs initiates inflammation via cytokine production [4]. High levels of lipid peroxidation have been observed in the lungs of Cd-intoxicated mice [6]. Cd has been demonstrated to induce obstructive lung disorder and at prolonged exposure – lung cancer [2, 5, 7].

To the best of our knowledge, there is no effective chelating therapy for humans exposed to Cd intoxication [1]. Recently we have demonstrated that the polyether

ionophorous antibiotic monensin significantly reduces the concentration of Cd in organs of mice, subjected to subacute intoxication [3]. These results motivate as to conduct extensive research on the potential application of this antibiotic as chelating agent for the treatment of Cd-intoxications. Herein we present novel data that demonstrate that monensin significantly attenuates Cd-induced morphological alterations in the lungs of mice, subjected to subacute Cd intoxication.

Material and Methods

Chemicals

The sodium salt of monensin was provided by Biovet Ltd. (Peshtera, Bulgaria). Tetraethylammonium hydroxide (Et_4NOH), nitric acid (HNO_3), and diethyl ether (Et_2O) were purchased from Merck (Darmstadt, Germany).

Preparation of monensic acid

Monensic acid A monohydrate was prepared from sodium monensin (711 mg, 1 mmol) applying the procedure previously described.

Animal model

The animal model is described in details in Ivanova et al [3]. Briefly sixty-day old adult male ICR mice were housed at the Institute of the Experimental Morphology, Pathology and Anthropology with Museum (Bulgarian Academy of Sciences, Sofia) under conventional conditions. The animals were divided into three groups with six mice in each group. The first (normal control) group received standard diet and had free access to distilled water during the experimental protocol. The second group animals (toxic control) was subjected to treatment with 20 mg/kg body weight $Cd(CH_3COO)_2 \times 2H_2O$ once daily for 2 weeks. The compound was dissolved and obtained in drinking (distilled) water. During the next 14 days of the experiment, the animals from this group were received distilled water and food *ad libitum*. The third group (monensin-treated mice) was administrated with $Cd(CH_3COO)_2 \times 2H_2O$ as described above followed by treatment with tetraethylammonium salt of monensic acid (16 mg/kg body weight in distilled water) during the 15^{th} to the 28^{th} days of the experimental protocol. On the 29^{th} day of the experimental protocol, all the animals were sacrificed under light ether anaesthesia and the samples were collected for the analysis. The lungs for atomic absorption spectrometry were stored at -20 °C prior to analysis. The animal studies were approved by the Ethics Committee of the Institute of the Experimental Morphology, Pathology and Anthropology with Muzeium, BAS.

Atomic absorption analysis

The organs were digested with concentrated HNO_3 (free of metal ions) as previously described [3]. The determination of Cd in the lungs was preformed by electrothermal (Zeeman Perkin Elmer 3030, HGA 600) analyzer. Certified Reference Materials were used to control for analytical accuracy.

Histopathological analysis

Lung tissue materials from the experimental animals were embedded in paraffin using routine histological practice. Tissue sections (thickness 5μm) were deparaffinised and stained with haematoxylin and eosin.

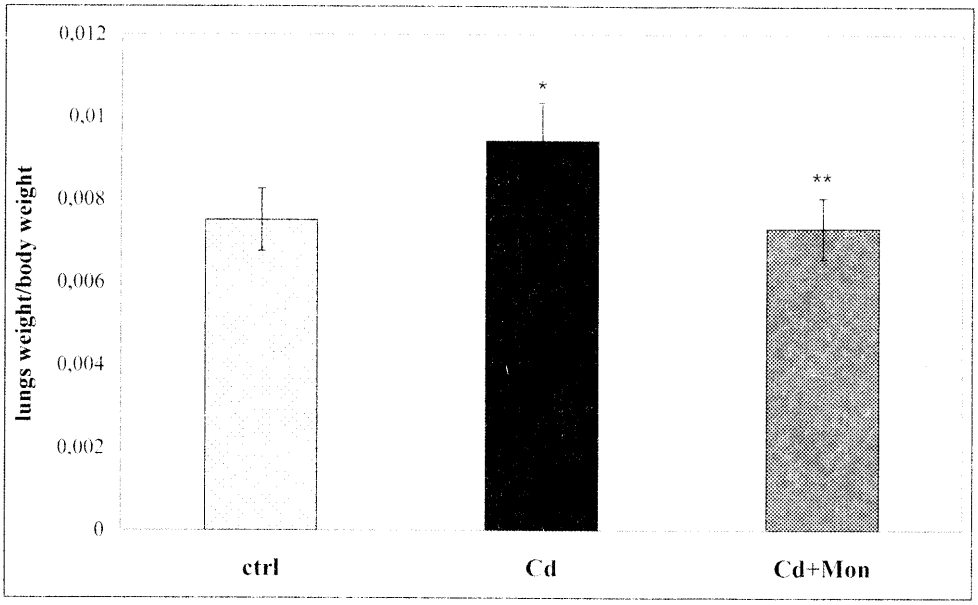

Fig. 1. Lung weight/body weight ratio of the experimental animals. Each column represents mean ± SD, $n = 6$. Asterisk (*) represents statistical differences between the Cd-treated group and normal controls ($p<0.05$); Double asterisk (**) represents significant differences between monensin-treated group and the Cd-intoxicated animals ($p<0.05$)

Statistical analysis

The obtained results are presented as mean value ± SD. Statistical significance between the experimental groups was determined using Student's *t*-test. Difference was considered significant at $p < 0.05$.

Results and Discussion

The data on the effect of cadmium and monensin on the lungs weight of mice, subjected to subacute Cd intoxications are presented on Fig. 1. As could be seen, Cd induced a significant increase (by 20 %) of the lungs weight/body weight index compared to the normal control. The treatment of Cd-intoxicated mice with monensin restored the lungs weight to normal values. These results suggest that the antibiotic most likely improved the lung function in Cd-intoxicated mice.

The morphological analysis of the lung tissue from the experimental animals demonstrated severe pathological changes of lung morphology in the subacute Cd intoxication of adult mice. Cd exerts its effect in the lung tissue by perturbing blood circulation and inducing inflammatory alterations.

The pathological changes were significantly manifested in Cd-treated animals (Fig. 3) compared to corresponding control animals (Fig. 2). Bronchioli with lesions and desquamations of the respiratory epithelium and many large focuses of inflammatory and circulatory alterations (haemorrages) were observed in the lung tissue of the Cd-treated mice (Fig. 3). After monensin administration to Cd intoxicated animals we

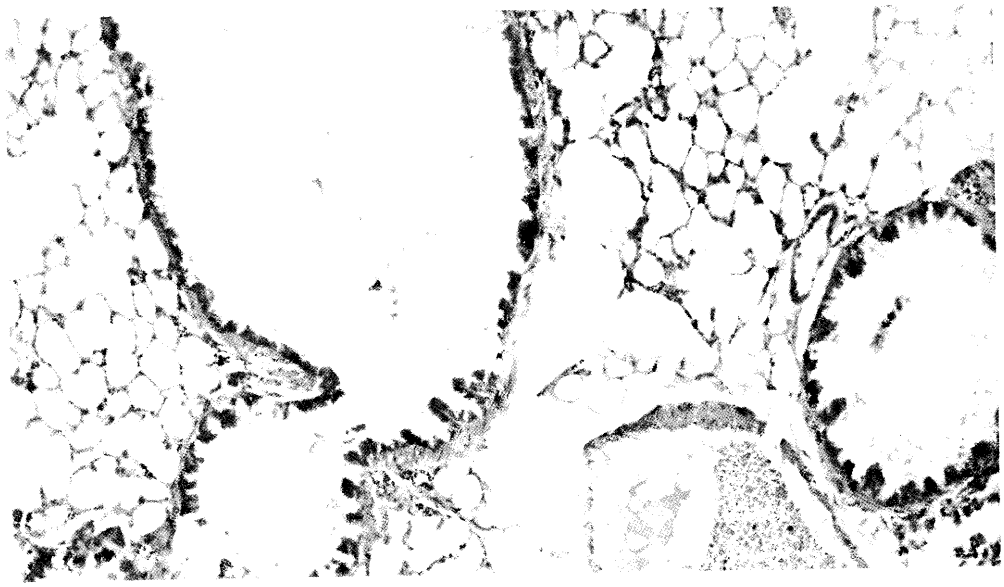

Fig. 2. Morphology of lung in a control animal (tissue section stained with haematoxylin and eosin)

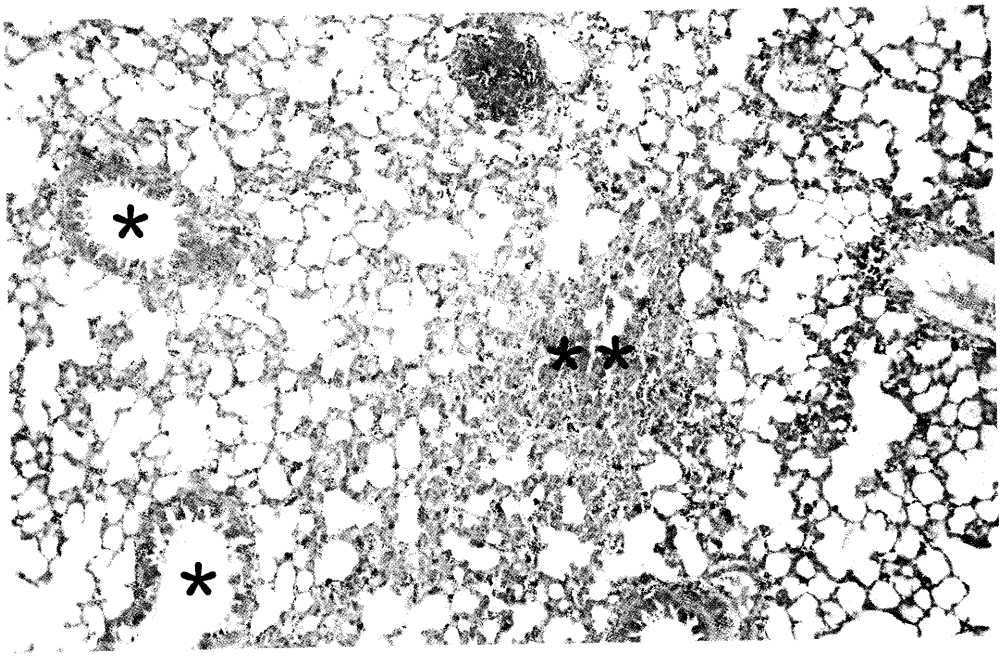

Fig. 3. Morphology of lung in a Cd-intoxicated animal. Asterisk (*) marks bronchioli with lesions and desquamations of the respiratory epithelium; Double asterisk (**) marks a large focus of inflammatory and circulatory alterations (haemorrage) (tissue section stained with haematoxylin and eosin)

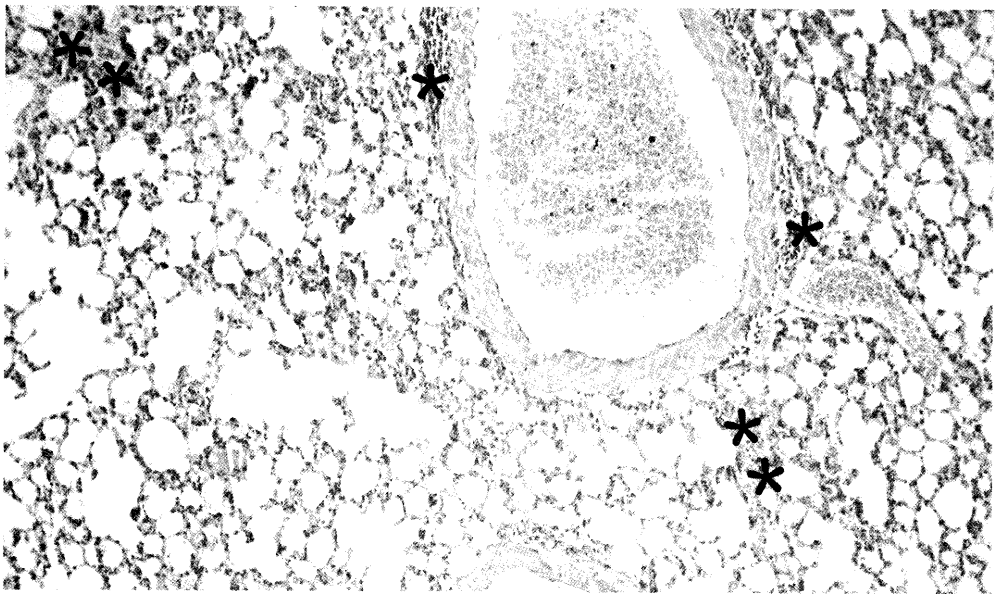

Fig. 4. Morphology of lung in monensin-treated group. Asterisk (*) marks scanty perivasal inflammatory infiltrates. Double asterisk (**) marks single small disseminated residual focuses of inflammatory and circulatory alterations (tissue section stained with haematoxylin and eosin).

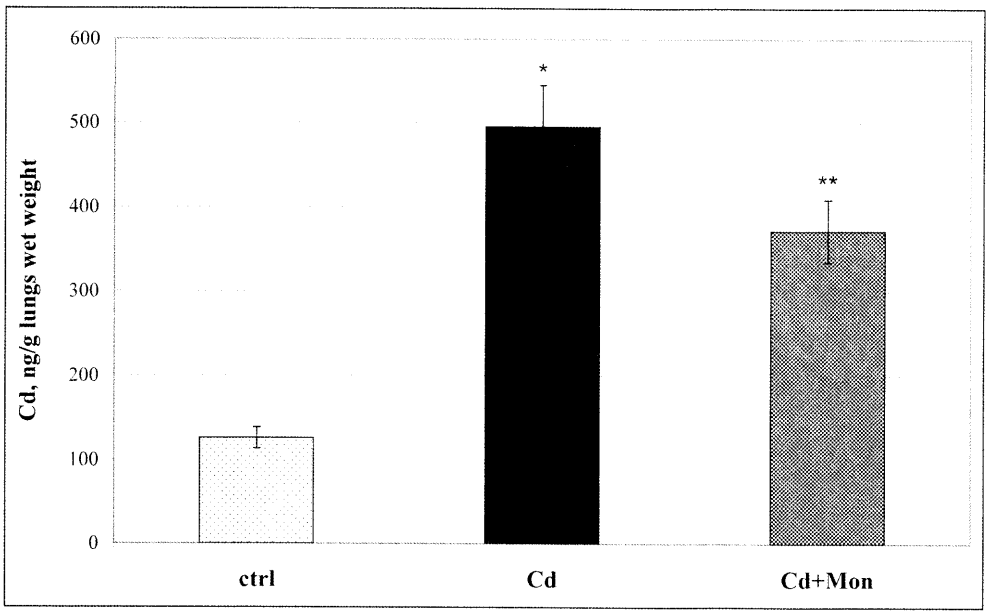

Fig. 5. Cd concentration in the lungs of the experimental animals. Each column represents mean ± SD, $n = 6$; Asterisk (*) represents statistical differences between the Cd-treated group and normal controls ($p<0.05$); Double asterisk (**) represents significant differences between monensin-treated group and the Cd-intoxicated animals ($p < 0.05$)

established reduction of the pathological alterations and tendency towards restoration of the normal morphology of the lungs to a great extent (Fig. 4).

The atomic absorption analysis of the lungs of the experimental animals revealed that monensin decreases the concentration of Cd in the lungs of the Cd-intoxicated animals by 30 % compared to the toxic control ($p < 0.05$) (Fig. 5).

In conclusion our investigation demonstrated that subacute Cd intoxication induced severe changes in lung morphology, especially in the blood circulation and in the epithelium of the bronchial tree and of the alveols. Monensin reduced lung injuries and recovered its morphology to a great extent that can suggest monensin as a candidate in chelating therapy of some heavy metal intoxications.

Acknowledgements. The work is supported by a grant No 72/2012 from University of Sofia "St. Kliment Ohridski" Fund for Science Research (project leader: Juliana Ivanova).

References

1. Andujar, P., L. Bensefa-Colas, A. Descatha. Acute and chronic cadmium poisoning. Rev. Med. Interne. 31, 2010, 107-15.
2. Huff, J., R.M. Lunn, M.P. Waalkes, L. Tomatis, P. F. Infante. Cadmium-induced cancers in animals and in humans. Int J Occup Environ Health 13(2), 2007, 202-12.
3. Ivanova, Ju., Y. Gluhcheva, K. Kamenova, S. Arpadjan, M. Mitewa. The tetraethylammonium salt of monensic acid – an antidote for treatment of subacute cadmium intoxication. A study using ICR mouse model. J. Trace Elem. Med. Biol. (2012), in press.
4. Kundu, S., S. Sengupta, S. Chatterjee, S. Mitra and A. Bhattacharyya. Cadmium induces lung inflammation independent of lung cell proliferation: a molecular approach. J Inflamm., 6, 2009, 19.
5. Lin, Y.S., J. L. Caffrey, M. H. Chang, N. Dowling, J. W. Lin. Cigarette smoking, cadmium exposure, and zinc intake on obstructive lung disorder. Respir Res., 11, 2010, 53.
6. Luchese, C., R. Brandão, R. de Oliveira, C.W. Nogueira, F.W. Santos. Efficacy of diphenyl diselenide against cerebral and pulmonary damage induced by cadmium in mice. Toxicol Lett., 2007, 173(3),181-90.
7. Nordberg, G. F. Lung cancer and exposure to environmental cadmium. The Lancet Oncology, 7(2), 2006, 99-101.
8. Suwazono, Y., T. Kido, H. Nakagawa, M. Nishijo, R. Nonda, E. Kobayashi, M. Dishi, K. Nogawa. Biological half-life of cadmium in the urine of inhabitants after cessation of cadmium exposure. Biomarkers 14, 2009, 77-81.
9. World Health Organization (WHO). Cadmium: Air Quality Guidelines, second ed. World Health Organization, Regional Office for Europe, Copenhagen, Denmark (chapter 6.3), 2000.

Institute of Experimental Morphology, Pathology and Anthropology with Museum
Bulgarian Anatomical Society

Acta morphologica et anthropologica, 19
Sofia • 2012

Morphological studies of rat foetus skeletons: test for teratogenicity of nootropic drug pyramem.

M. Georgieva[1], M. Gabrovska[2]

[1]Department of Pharma`cology and Toxicology
[2]Department of Anatomy, Histology and Embriology
Medical University "Prof. Paraskev Stoyanov" – Varna

The teratogenic effect of the nootropic drug Pyramem on the skeleton and internal organs of rats was investigated. Pregnant Wistar rats were treated orally by 200 mg/kg b. m. Pyramem and 200 mg/kg b. m. during the period of organogenesis since the 7th until 15th day of pregnancy. The effect of Pyramem on the fetuses in terms of malformations, skeletal fragility and abnormalities in the internal organs (lungs, liver, spleen and kidneys) close to delivery (day 20-21) was analyzed. The nootropic Pyramem failed to prove to be embryotoxic agents at all.

Key words: toxicology, teratogenicity, "Double staining method", "Wilson section method", nootropic drugs.

Introduction

Nootropics are a relatively new class of drugs developed actively in recent years in the hope that they will assist in the impaired nerve cell regeneration, enhance the intellectual and memory capacities as well strengthen the adaptive possibilities of the CNS towards extreme requirements because of their antioxidant effect (3). This study aims at investigating the nootropic drug „Pyramem" for evaluation its teratogenic effect and its skeletal and organ toxicity, in particular.

Material and methods

Experimental model for evaluation of the teratogenicity in rats.

The study of teratogenicity required application of the studied substances on pregnant female Wistar rats (n=30) during the organogenesis (day 7-17) according to the International Conference on Harmonisation (2) (Fig. 1).

Pregnant Wistar rats (15 per group) were dosed by intraperitoneal application with Pyramem 200 mg/kg b. m. and physiological solution 10 ml/kg b.m. during the period of organogenesis (days 7-15), taking day one when the female was found to be sperm

+...Dose application...+

mating ↓↓↓↓↓↓↓↓↓↓↓↓

0.....7.....17.....20 (21) – euthanasia

..... days after coitus ..... examination of the fetuses fixation of the internal organs and the skeleton

Fig. 1. Teratologic studies in rats (according to EEC, FDA, OECD, etc.).

positive. On day 21 after conception were extracted via caesarian section and were explored for skeletal toxicity, using the method of "Double skeleton staining" with Alcian blue and Alizarin red (4,5) (Fig. 2). The fetuses were studied microscopically to detect any internal organ abnormalities (lung, liver, spleen etc.), using 20 body slices with thickness 1 mm. (Wilson Section Method) (Fig. 3).

Fig. 2. Double skeleton staining method.

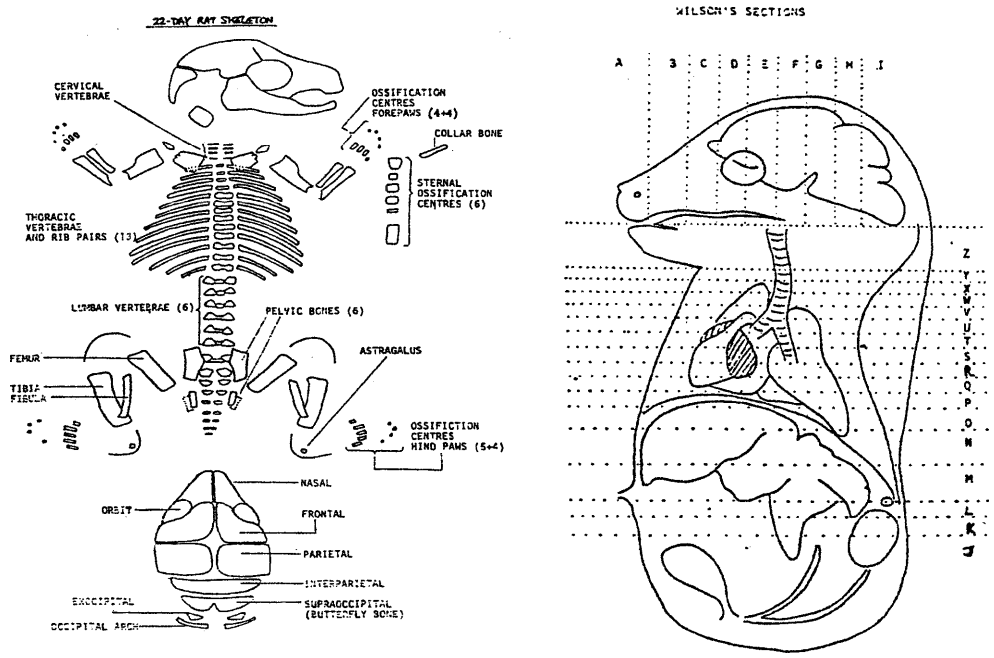

Fig. 3. "Wilson Section Method

"Double staining" method for skeletal examination

Staining of the skeleton was made with 0,15 % of Alcian blue and 0,005 % of Alizarin red S. All the cartilages were stained in blue but the ossified bones in red. The entire fetal skeleton was examined and all the abnonnalities, variations in degrees of ossification and lack of cartilage were recorded. Each bone was assessed for its size, shape, relative position and number of bones, and ribs and data were compared with the controls (Fig. 2).

Bouin's fixation for internal examination using the Wilson section method

Fetuses for visceral examination were processed using Bouin's solution to allow examination of the internal organs. Sections were then examined using a microscope to find out any abnormalities in the internal organs such as liver, lungs, kidneys and spleen (Fig. 3). Data were statistically processed by using the variation analysis and Student's /-test.

Results

Pyramem showed no evidence of teratogenicity. The body weight and the length of the fetuses, the weight of the placentas and livers of adult rats treated with Pyramem showed no statistically significant differences from controls with physiological solution (Table 1).

Table 1. Weight and length of fetuses, weight of placentas and livers.

	Weight fetuses (g)	Length fetuses (mm)	Weight placentas (g)	Weight livers (g)	n
Controls (phys. sol.)	2.81 ± 0.24	33.48 ± 1.21	0.45 ± 0.07	0.2 ± 0.017	29
Pyramem	2.72 ± 0.28	33.69 ± 1.02	0.46 ± 0.08	0.18 ± 0.01	38
	$p > 0.05$	$p > 0.05$	$p > 0.05$	$p > 0.05$	

On inspection of the fetuses from the group with Pyramem no anomalies were seen regarding the skeleton: head, body, extremities. Lack of teratogenic effect was detected, using following indices: Gross appearance – external: Coloration of the fetus; Subcutaneous hemorrhages; Gross abnormalities as: spina bifida, anencephaly, exencephaly, arhinencephaly; cebocephaly; Head: eyes, ears, nostrils, tongue, palate, mouth. Extremities: anterior, posterior (number of fingers, syndactyly, micromelia). Rear part of the body: anus (abnormalities) – atresia ani; tail (deformities, lack of tail; genitals (2 mm for male gender, 1 mm for female gender).

Test for skeletal toxicity

When the nootropic drug Pyramem was tested for skeletal toxicity with the "double staining method" all cartilages stained in blue, and the ossified bones in red. The examination of the whole skeleton for variations in the level of ossification, lack of cartilages and any possible abnormalities no deviations from the norm were found. For each bone the dimensions, type, relative position, number of bones and ribs were denoted and compared to controls. The nootropic drug Pyramem that was tested did not induce skeletal toxicity.

Microscopy

On microscopy examination of the fetuses for abnormalities of the internal organs (lung, liver, spleen, kidneys etc.) using the Wilson section method no anomalies were found in any of the explored organs.

Discussion

In the current experiment a test for fetal and maternal toxicity of the Pyramem was done. The body weight, and the length of the fetuses, the weight of the placentas, and livers of rats treated with Pyramem, did not show statistically significant difference compared to parameters with controls. The inspection of the fetuses showed no abnormalities.

The nootropic drug Pyramem was tested for skeletal toxicity using double skeleton staining method with alizarin red and alcian blue (1,4,5). All cartilages stained in blue, and the ossified bones in red. Thus the cartilaginous and the bone part of the skeleton were examined, and any possible abnormalities could be detected. The animals treated with Pyramem showed no difference compared to the controls with physiological solution.

The Wilson section method, which is standard teratological method and still represents the most utilized technique to examine the visceral organs, was used to explore the soft tissues. No impairment was found in any of the examined internal organs in animals treated with Pyramem.

Conclusion

This experiment convincingly demonstrates that nootropic drug Pyramem does not manifest data indicative for teratogenicity.

The double staining method used in the current study is a fundamental part of the teratological studies for assessment of the toxicity of the xenobiotics and non-chemical factors for the individual development.

References

1. Christian M.S Test methods for assessing female reproductive and developmental toxicology. In: Hayes AW (ed.). Principles and method of toxicology. 4th Ed. Taylor & Francis, Philadelphia, 2001, 1301–1381.
2. ICH ICH Harmonised tripartite guideline. Maintenance of the ICH guideline on toxicity to male fertility. 2000, An addendum to ICH tripartite guideline on detection.
3. Malykh AG, Sadaie MR. Piracetam and piracetam-like drugs: from basic science to novel clinical applications to CNS disorders. Drugs. 2010 Feb 12;70(3):287-312.
4. Whitaker J, K.M. Dix. Double staining technique for rat foetus skeletons in teratological studies. Lab Anim. 13(4), 1979, 309-10.
5. Young A.D, D.E. Phipps, A.B. Astroff, Large-scale double-staining of rat fetal skeletons using Alizarin Red S and alcian blue. Teratology. 61(4), 2000, 273-6.

Institute of Experimental Morphology, Pathology and Anthropology with Museum
Bulgarian Anatomical Society

Acta morphologica et anthropologica, 19
Sofia • 2012

Transmission electron microscopy study of benign giant cell tumor of bone

G.P. Georgiev[1], B. Landzhov[2]

[1]University Hospital of Orthopaedics "Prof. B. Boychev", Medical University Sofia, Bulgaria
[2]Department of Anatomy, Histology and Embryology, Medical University Sofia, Bulgaria

Giant cell tumor of bone is still one of the most obscure and intensively examined tumors of bone. The World Health Organisation has classified it as "an aggressive, potentially malignant lesion", which means that its evolution based on its histological features is unpredictable and there are still many unanswered questions with regard to both its treatment and prognosis. In the report a detailed investigation of the ultrastructure of benign giant cell tumor of bone in five cases is presented.

Key words: giant cell tumor of bone, ultrastructural characteristics.

Introduction

Giant cell tumor of bone (GCTB) is defined as a primary intramedullary bone tumor composed of mononucleated cells and osteoclast-like multinucleated giant cells and presenting as a locally aggressive lesion with unpredictable behavior [2, 3, 4, 8]. It accounts for around 5% of primary bone tumors [8]. Nearly 50% of cases occur in the region of the knee, but other frequent sites are the distal part of the radius, the proximal humerus and fibula, and the pelvic bones [8]. It is usually situated in the epiphysis, and may later also affect the metaphysis. It appears most often in the third and fourth decade of life with a slight predilection for females. The definite treatment of GCTB varies from intralesional curettage followed by bone grafting and/or bone cement packing to wide resection [2, 3, 4, 8].

The aim of this study is to investigate the ultrastructural characteristics of giant cell tumor of bone.

Materials and Methods

We examined material from 5 patients with benign GCTB (3 female and 2 male). A musculoskeletal pathologist verified all tissue specimens for the pathologic diagnosis.

Electron microscopy preparation protocol: Tumor tissues were fixed in 3% glutaraldehyde for 2 h. After that the tissue samples were postfixed in 1% OsO_4 in PBS

for 2 h. Then the slices were dehydrated and embedded in Durkupan (Fluka, Buchs, Switzerland). All slices were processed with disectional microscope and cut with ultramicrotome (LKB, Stockholm-Bromma, Sweden). Finally, they were mounted, covered, contrasted and examined with an electron microscope Hitachi 500.

Results

Our study revealed different cell types:
Multinucleated, osteoclast-like giant cells:

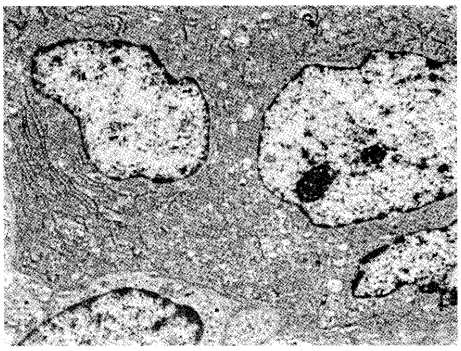

Fig. 1. Electron micrograph of multinucleated, osteoclast-like giant cell x 6000.

Ultrastuctural study of GCTB revealed large multinucleated, osteoclast-like giant cells with round or ovoid form. They had numerous nuclei with oval or irregular shape. The nuclear chromatin is finely granular and arranged in clusters in the peripheral nuclear area. The cytoplasm contained a large number of mitochondria, distinct lysosome-like bodies and large vacuoles (Fig. 1). In some instances, pseudopode-like vili covering parts of cell surface were found. Degenerating multinucleated giant cells were also observed. The cytoplasm of these cells consisted many vacuoles. Mitochondria in stages of degeneration were detected.

Fig. 2. Electron micrograph of mononuclear spindle-shaped cell x 15000.

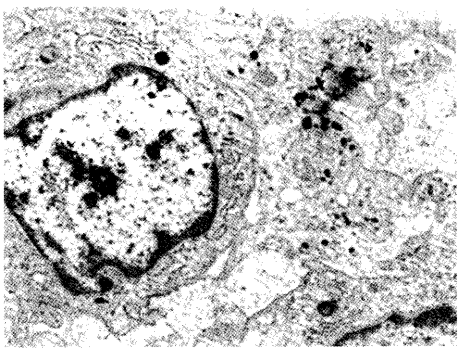

Fig. 3. Electron micrograph of mononuclear polygonal cell x 7000.

Mononuclear spindle-shaped cells

The mononuclear spindle-shaped tumour cells resemble fibroblastic cells at the ultrastructural level. Their nuclei displayed a very delicate chromatin structure, clearly visible heterochromatin in the peripheral nuclear area. The cytoplasm contained expanded rough endoplasmic reticulum, free ribosomes, polysomes and irregularly shaped mitochondria (Fig. 2).

Mononuclear polygonal cells

The ultrastructural features of the mononuclear polygonal cells are similar to those of macrophages. Their nuclei are oval with low chromatin density. The cytoplasm had relatively abundant rough endoplasmic reticulmn, well developed Golgi apparatus, variable number of mitochondria, lysosomes, vesicles, and free ribosomes (Fig. 3).

Other cells resembling lymphocytes and monocytes were also detected. They were characterized by with scanty rough endoplasmic reticulum, few mitochondria and a small Golgi apparatus.

Discussion

In 1818 Sir Astley Cooper first described GCTB as an expansive lesion of the fibular head and named the lesion "fungus medullary exostosis". He documented the natural history, gave detailed anatomic descriptions, and provided the first pathologic drawings of this lesion [1]. In 1845 Lebert described the first microscopic observations of GCTB presented by multinucleated giant cells and fusiform cells and termed it "tumeur fiblastique" [6]. The first electron microscopic description of GCTB was reported by Miller and Monteleone in 1957. The authors concluded that the giant cells were highly differentiated because of the large number of organelles they contained [7]. Since then, several reports have appeared, all in the Japanese literature, the majority of them emphasizing the variety of stromal cells and the ultrastructural similarity of giant cells to osteoclasts [5]. Later, however it was accepted that the multinucleated giant cells differ from osteoclasts of normal bone in their degree of multinucleation and the presence of pseudopode-like vili covered the cell surface [5, 9]. The majority of mononuclear tumor cells of the GCTB have the ultrastructural features that are seen in adult connective tissue cells. In conclusion, we defined ultrastructurally three main cell types: multinucleated osteoclast-like giant cells, mononuclear spindle-shaped cells that resemble fibroblastic cells and polygonal cells similar to macrophages.

References

1. Cooper, A., B. Travers. Part I. – In: Surgical Essays, London, Cox and Son; 1818, 186–208.
2. Georgiev, G. P., L. Stokov. Giant cell tumor of bone: review. – Bulg. J. Orthop. Trauma., 49, 2012, 34-39.
3. Georgiev, G. P., B. Landzhov, S. Slavchev, P. Rashev, L. Stokov, W. Ovtscharoff. Localization of matrix metalloproteinase-2 in giant cell tumor of bone. – Compt. rend. Acad. bulg. Sci., 65, 2012, 1285-1288.
4. Georgiev, H., B. Matev, N. Dimitrov, P. Georgiev. Osteoclastoma of metacarpal bones. – Acta Med. Bulg., 38, 2011, 3-7.
5. Hanaoka, H., B. Friedman, R. P. Mack. Ultrastructure and histogenesis of giant-cell tumor of bone. – Cancer, 25, 1970, 1408-1423.
6. Lebert, H. Physiologie pathologique ou recherches cliniques, expérimentales et microscopiques sur l'inflammation, la tuberculisation, les tumeurs, la formation du cal, etc., Paris, J.B. Bailliere, 1845.
7. Miller, F., M. Monteleone. Fine structure of polynuclear giant cells in genign giant cell tumors of bone. – Frankf. Z. Pathol., 68, 1957, 49-54.
8. Niu, X., Q. Zhang, L. Hao, Y. Ding, Y. Li, H. Xu, W. Liu. Giant cell tumor of the extremity: retrospective analysis of 621 Chinese patients from one institution. – J. Bone Joint Surg. Am., 94, 2012, 461-467.
9. Zheng, M. H., P. Robbins, J. Xu, L. Huang, D. J. Wood, J. M. Papadimitriou. The histogenesis of giant cell tumour of bone: a model of interaction between neoplastic cells and osteoclasts. – Histol. Histopathol., 16, 2001, 297-307.

Institute of Experimental Morphology, Pathology and Anthropology with Museum
Bulgarian Anatomical Society

Acta morphologica et anthropologica, 19
Sofia • 2012

Creating of 3D anatomical phantoms with En and Pn plastinated slices

A. Georgieva, D. Sivrev

Department of Anatomy, Faculty of Medicine, St. Zagora, Bulgaria

This visual educational method is being developed in a three-year project of Thracian University dating back to 2012 year. After the approval of S10 plastic technique in teaching morphology E12, R35 and R40 were introduced as new techniques for making plates of brain and slices of the body and limbs. In these techniques by means of Biodur through participation of ultraviolet light are made thin (up to 10 mm) transparent plates of natural biological material. The plates preserve the natural ratio of the organs placed at the appropriate topographic level.

Three-dimensional anatomical forms can be made from all parts of the body – head, neck, legs, chest, abdomen and pelvis. Ranking them in the order in which they are separated from the human or animal body restores bodily structure but with perennial topographic products. A circuit on which is marked skeletotopiya slice constituting the human body can be added to the anatomical phantom.

Keywords: Biodur, plastination, P40, impregnation, brain slices.

Introduction

After approval of S10 plastination technique in teaching morphology introduced the new E12, R35 and R40 plastination techniques for making plates of brain [3, 13, 15] and slices of whole body, brain or limbs [6, 8]. They using Biodur, featuring ultraviolet light, natural biological material is produced thin (10 mm) transparent plates that retain the natural ratio of organs located at the appropriate topographic level [5, 14].

This is a three-years project from 2012 of the University of Thrace for an educational method development – 5132 levs value [16].

Purpose

The purpose of this presentation is to introduce the scientific society with the possibilities of En and Pn plastination techniques.

Material and Methods

We use organic material that is available in the Laboratory of plastination. The material freezes at -25°C and it cuts with a band saw plates with thickness up to 10 mm. The size of the cuts made in compliance with the size of impregnation cameras we have.

En plastination techniques are rarely used because the epoxy techniques are more suitable for research in histology, although it is possible their use for making cuts from the whole body, limbs or parts thereof. Dehydration performs step-wise with acetone at room temperature. Impregnation is carried out with a mixture of Biodur E12 and Biodur E1 in the ratio 4:1. Forced impregnation achieves gradually to vacuum 5 mm Hg. Gas-curing occurs within 24 hours at room temperature.

Pn plastination techniques, especially R40 technology is applied more often, but predominantly in brain slices due to the high quality of the products. Fixation, dehydration and impregnation are standard, but drying is carried out with the participation of ultraviolet light. Glass casting chamber is filled with P35 or P40 resin and biological material was put into the chamber. It was exposed to UV light sources until cured.

Results

Fig. 1. The P40 polymer in chambers formed a solid gel by 30 minutes of exposure with UV light and cured completely 40 minutes later. The plates, made with En plastination technologies are translucent, but they are distinguished by high strength. Pn cuts are primarily used for studying the brain. They are highly transparent polymer plate. Both En and Pn have pronounced details and preserve the natural ratio of the organs placed at the appropriate topographic level.

Fig. 2. A circuit on which is marked skeletotopiya slice constituting the human body can be added to the anatomical phantom.

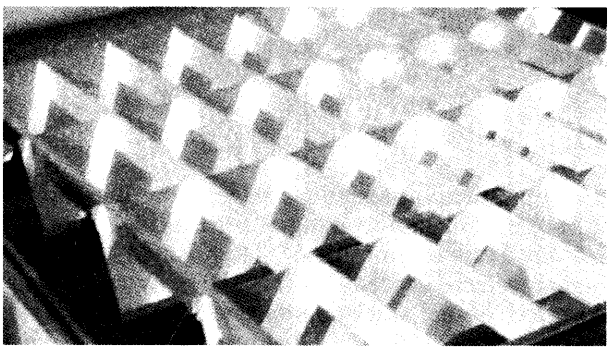

Fig. 1. UV chamber for P40 plastination technique.

Legend: Abdomen preparations		
Slice number	**Sceletotopy**	**Objects**
P7	**9-th right rib cartilage**	**Liver, Diaphragm, Stomach**
P8	**11-th right rib cartilage**	**Gall-bladder, Transv. colon**
P9	**1-st lumbal vertebra**	**Pylorus, Spleen**
P10	**2-nd lumbal vertebra**	**Duodenum**

Fig 2. A sample legend to slices of the human body.

Discussion

Although the study of individual cuts shows topographic relations of a certain level, it dose not give accurate perceptions about the overall structure of the human body. This can be achieved by building a three-dimensional anatomical forms. This is according to publications of other authors [1].

They can be made (via E12 plastination technique)) [2, 7, 10] from all parts of the body – head, neck, legs, chest, abdomen and pelvis [2, 11, 12].. Ranking them in the order in which they are separated from the human or animal body [4] restores bodily structure but with perennial topographic products [1, 6]. Some investigators use 3D plastination atlas for parallel study to MRI [4].

A corpse which is fully build can be placed in a natural vertical construction or lying down, and limbs – in special racks. Brain plates [9, 13, 15] may be arranged in the skull in their natural state.

Conclusions

1. 3D models are a better idea of anatomical detail, demonstrated with preparations compared with two-dimensional models.

2. They are made easily and are an excellent resource for studying the human body.

References

1. Beyersdorff, D., T. Schiemann, M. Taupitz, H. Kooijman, B. Hamm, V. Nicolas. Sectional depiction of the pelvic floor by CT, MR imaging and sheet plasination: Computer-aided correlation and 3D model. Eur Radiol, 11(4): 659-664.
2. Fasel J, Mohler R, Lehmann B. 1988: A technical note for improvement of the E12 technique. J Int Soc Plastination 2(1):4-7.
3. Henry RW, Latorre R. 2007: Polyester plastination of biological tissue: P40 technique for brain slices. J Int Soc Plastination 22:59-68.
4. Latorre R, Váquez J M, Gil F, Ramírez G, López-Albors O, Ayala M, Arencibia A. 2002: Anatomy of the equine tarsus: A study by MRI and macroscopic
5. Latorre R, Arencibia A, Gil F, Rivero M, Ramírez G, Váquez-Auton JM, Henry RW. 2004: Sheet Plastination with Polyester: An Alternative for All Tissues. J Int Soc Plastination 19:33-39.
6. Latorre R, Henry RW. 2007: Polyester plastination of biological tissue: P40 technique for body slices. J Int Soc Plastination 22:69-77.
7. Reed R.B. 2003: Effects of reduced pressure on components of epoxy (E12) reaction mixture. J Int Soc Plastination 18:3-8.
8. Steinke, H., S. Pfeiffer, K. Spanel-Borowski. A new plastination technique for head slices containing brain. Annals of Anatomy, 184(4), 2002, 353-358.
9. Sora MC, Brugger P, Traxler H. 1999: P40 plastination of human brain slices: Comparison between different immersion and impregnation techniques. J Int Soc Plastination 14(1) 22-24.
10. Sora MC, Brugger PC, Strobl B. 2002: Shrinkage during E12 Plastination. J Int Soc Plastination 17:23- 27.
11. Sora M.C., Cook P. 2007: Epoxy plastination of Epoxy discoloration 9 biological tissue: E12 technique. J Int Soc Plastination 22:31-39.
12. Sora M.C. 2007: Epoxy plastination of biological tissue: E12 ultra-thin technique. J Int Soc Plastination 22:40-45.
13. von Hagens G. 1994: Plastination of brain slices according to the P40 procedure. A step-by-step description. 23 pages.

14. W e b e r W, H e n r y RW. 1993: Sheet plastination of body slices – E12 technique, filling method. J Int Soc Plastination 7:16-22.
15. W e i g l e i n AH, F e i g l G. 1998: Sheet plastination of brain slices according to the P35 and P40 procedures. J Int Soc Plastination 13(2):30.
16. Колектив. Проучване и приложение на пластинационни методи за изработване на безвредни и дълготрайни анатомични препарати за обучението по морфология. Инфраструктурен проект на стойност 5132.00 лв на Тракийски университет – Стара Загора за 2012.

Institute of Experimental Morphology, Pathology and Anthropology with Museum
Bulgarian Anatomical Society

Acta morphologica et anthropologica, 19
Sofia • 2012

Changes in the mouse spleen after long-term treatment with cobalt(II) compounds

Y. Gluhcheva[1], E. Pavlova[1], R. Nizamova[2], V. Atanasov[2], Ju. Ivanova[3], M. Mitewa[2]

[1]Institute of Experimental Morphology, Pathology and Anthropology with Museum – BAS
[2]Faculty of Chemistry and Pharmacy, Sofia University "St. Kliment Ohridski"
[3]Faculty of Medicine, Sofia University "St. Kliment Ohridski"

Chronic treatment with cobalt(II) compounds induced changes in the spleen index of exposed mice. The compounds showed diverse effect on immature and mature animals. Administration of low and/or high doses of $CoCl_2$ or Co-EDTA reduced the index in d18 mice which proved that at this age they are the most sensitive.

Key words: cobalt(II) compounds, chronic exposure, *in vivo* model, mice, spleen

Introduction

The wide use of cobalt alloys in medical devices requires full elucidation of its biological role and cells, tissues and organs after long-term exposure [6, 9]. It accumulates in organs such as spleen, kidney, heart, liver, intestines, stomach, muscles, brain, testes, etc. [1]. Data show that cobalt is transferred from food into the mother's milk [7, 10]. Young animals (rats and guinea pigs) have 3- to 15-fold greater absorption than adult animals (aged 200 days or more) [11]. Although widely spread diet is the main source of cobalt(II) to humans and animals. The average daily intake of cobalt ranges from 5-45 μg with relatively high concentrations of the metal occurring in fish and in vegetables [2].

The spleen has a key role in hematopoiesis and in the immune response. In rodents the red pulp is a site for hematopoiesis especially in fetal and neonatal animals. Since it is also a storage site for iron, erythrocytes and platelets [3] alterations in its functions will affect iron metabolism, blood cell production, etc. The ratio of splenic weight to body weight remains fairly constant regardless of age [3].

The aim of the present study is to investigate the effect of long-term treatment with cobalt chloride ($CoCl_2$) and cobalt-EDTA (Co-EDTA) on the spleen of developing mice.

The study was approved by the Ethics Committee of the Institute of Experimental Morphology, Pathology and Anthropology with Museum – Bulgarian Academy of Sciences.

Material and Methods

Animal model

Pregnant ICR mice in late gestation were subjected to cobalt chloride ($CoCl_2.6H_2O$) or Co-EDTA treatment at daily doses of 75 mg/kg or 125 mg/kg. Cobalt(II) compounds were dissolved and obtained from drinking tap water. Animals were fed a standard diet and had access to food *ad libitum*. Mice were maintained in the institute's animal house at 23°C ± 2°C and 12:12 h light-dark cycle in individual standard hard bottom polypropylene cages to ensure that all experimental animals obtained the required dose. The newborn pups were sacrificed on days 18, 25, 30, 45, 60 and 90 which correspond to different stages of development. Mice were weighed weekly and the experimental cobalt concentration was adjusted accordingly. The spleens were excised, weighed and processed for histological analysis. Spleen index (SI) was calculated as a ratio of spleen weight to body weight.

Statistical analysis

The obtained results are presented as mean value ± SD. Statistical significance between the experimental groups was determined using Student's t-test. Difference was considered significant at $p<0.05$.

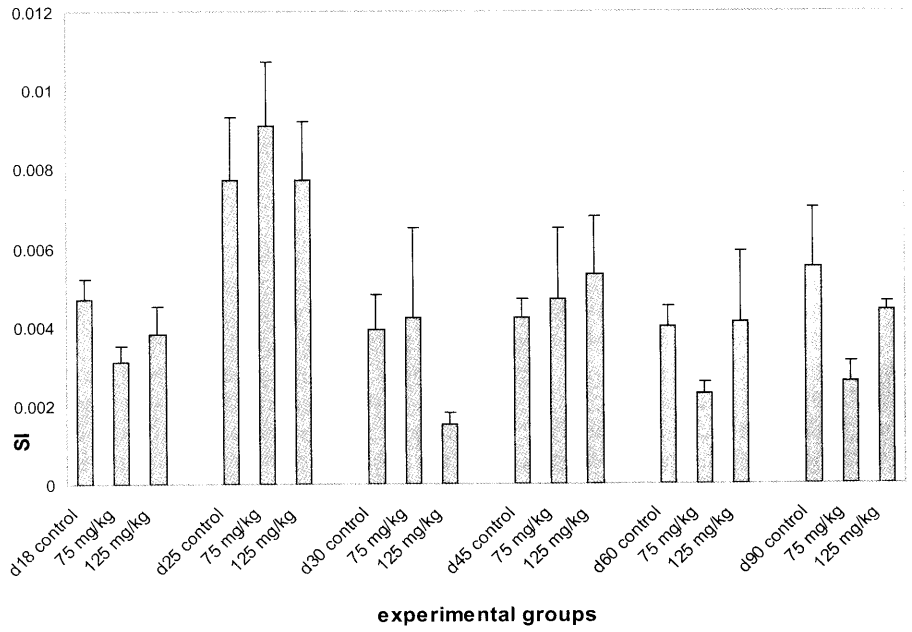

Fig. 1. Spleen index (SI) changes of mice treated with low and/or high daily dose $CoCl_2$. Each column represents data as mean ± SD. Asterisk (*) represents statistical difference $p<0.05$ and triple asterisk (***) $p<0.001$.

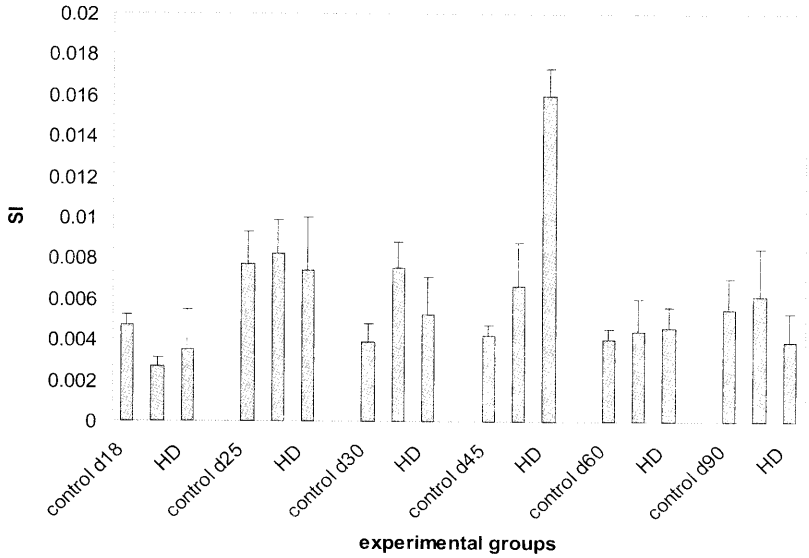

Fig. 2. Spleen index (SI) changes of mice treated with low and/or high daily dose Co-EDTA. Each column represents data as mean ± SD. Asterisk (*) represents statistical difference $p<0.05$ and triple asterisk (***) $p<0.001$. LD represents low dose (75 mg/kg) Co-EDTA and HD is for high dose (125 mg/kg) Co-EDTA.

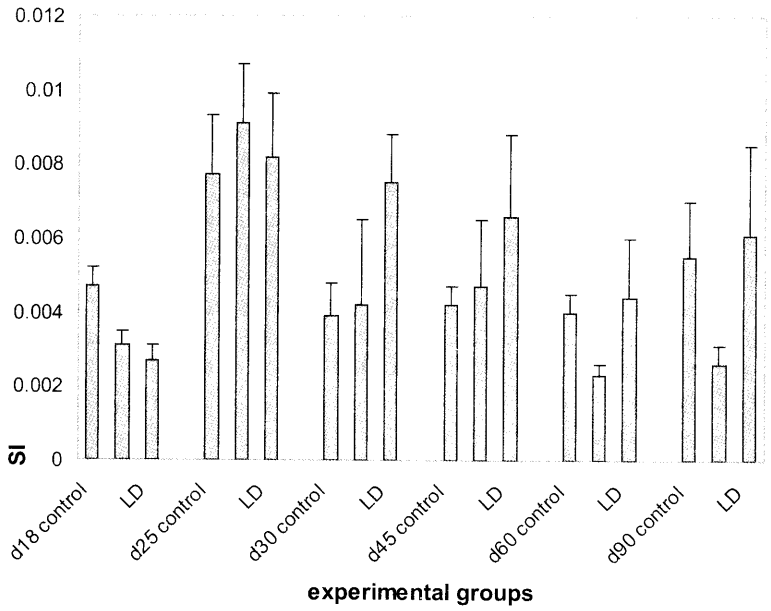

Fig. 3. Comparison of spleen index (SI) changes of mice after chronic treatment with low daily dose $CoCl_2$ and/or Co-EDTA. Each column represents data as mean ± SD. Asterisk (*) represents statistical difference $p<0.05$. LD represents low dose (75 mg/kg) Co-EDTA.

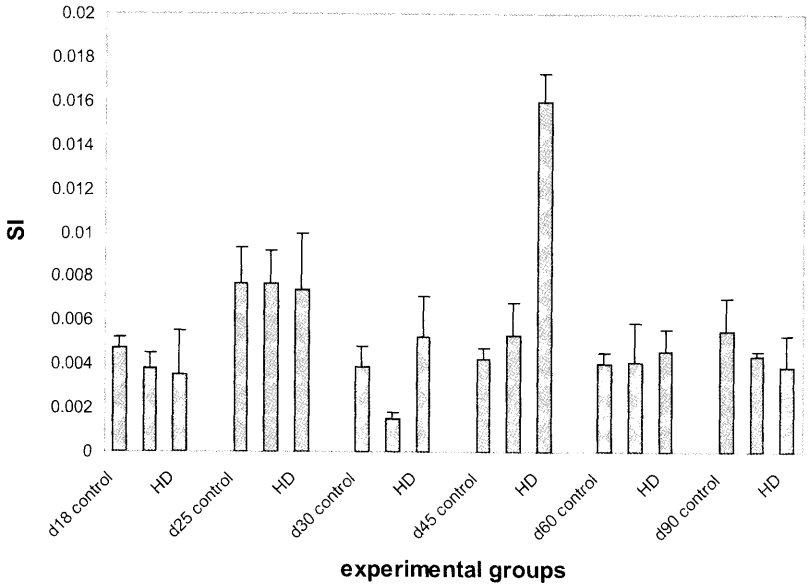

Fig. 4. Comparison of spleen index (SI) changes of mice after chronic treatment with high daily doses $CoCl_2$ and/or Co-EDTA. Each column represents data as mean ± SD. Triple asterisk (***) represents statistical difference $p<0.001$. HD stands for high dose (125 mg/kg) Co-EDTA.

Results and Discussion

Long-term exposure to Co(II) compounds induced changes in the spleen index (Figs. 1,2). SI was significantly decreased in immature mice. Day18 and d25 treated with $CoCl_2$ have increased SI compared to Co-EDTA (Figs.3,4). In mature mice (d30 – d90) treatment with Co-EDTA increased SI. Our results are in agreement with Simonyte et al. [8] and Dkhil [4] demonstrating increased SI in mice after long-term exposure to heavy metals and infections. Increased SI is associated with changes both in the white and red pulp [4]. The increased splenic index in our studies could be due to increased number of macrophages in the spleen. As a transition metal cobalt enhances oxidative stress which can further damage the organ. The results could explain the observed by us disturbed extramedullar hematopoiesis in the spleen after long-term treatment of mice with low or high dose Co-EDTA [5].

Conclusions

Long-term exposure to $CoCl_2$ and Co-EDTA alters SI of treated mice. The compounds affect differently immature and mature mice. They reduced SI in d18 mice which are the most sensitive.

Acknowledgements: The work is supported by a grant No DOO2 – 351/2008 for Young scientists from the Bulgarian National Science Fund.

References

1. Ayala-Fierro, F., J. M. Firriolo, D. E. Carter. Disposition, toxicity, and intestinal absorption of cobaltous chloride in male Fischer 344 rats. – J. Toxicol. Environ. Health A., 56, 1999, 571-591.
2. Barceloux, D.G., Barceloux, D. 1999. Cobalt. – Clin. Toxicol., 37, 1999, 201-216.
3. Cesta, M. Normal structure, function, and histology of the spleen. – Toxicol. Pathol., 34, 2006, 455-465.
4. Dkhil, M. Apoptotic changes induced in mice splenic tissue due to malaria infection. – J. Microbiol. Immunol. Infect., 42, 2009, 13-18.
5. Gluhcheva, Y., V. Atanasov, Ju. Ivanova, M. Mitewa. Cobalt- induced changes in the spleen of mice from different stages of development. – JTEH, 2012 (in press)
6. Guilford, A.L., T. Poletti, L.H. Osbourne, A. Di Cerbo, A.M. Gatti, M. Santin. Nanoparticles of a different source induce different patterns of activation in key biochemical and cellular components of the host response. – J. R. Soc. Interface, 6, 2009, 1213–1221.
7. Kincaid, R.L., M.T. Socha. Effect of cobalt supplementation during late gestation and early lactation on milk and serum measures. – J. Dairy Sci., 90, 2006, 1880-1886.
8. Simonyte, S., R. Planciuniene, G. Cherkashin, G. Zekonis. Influence of long-term cadmium and selenite exposure on resistance to Lysteria monocytogenes during acute and chronic infection in mice. – Biologija, 3, 2006, 92-95.
9. Tanaka, Y., K. Kurashima, H. Saito, A. Nagai, Y. Tsutsumi, H. Doi, N. Nomura, T. Hanawa, 2009. In vitro short-term platelet adhesion on various metals. – J. Artif. Organs, 12, 2009, 182-186.
10. Wappelhorst, O., I. Kuhn, H. Heidenreich, B. Markert. Transfer of selected elements from food into human milk. – Nutrition, 18, 2002, 316-322.
11. World Health Organization. Cobalt and inorganic cobalt compounds. In: Concise International Chemical Assessment Document 69, 2006, 13-21.

Institute of Experimental Morphology, Pathology and Anthropology with Museum
Bulgarian Anatomical Society

Acta morphologica et anthropologica, 19
Sofia • 2012

Proliferation and Apoptosis during Early Postnatal Neurogenesis in Rat Brain

V. Goranova[1], O. Uckermann[2] and C. Ikonomidou[3]

[1]Dept. of Anatomy, Histology and Embryology, Medical University, Varna, Bulgaria; [2]Department of Pediatric Neurology, Childrens' Hospital, Technical University, Dresden, Germany; [3]Waisman Center and Department of Neurology, University of Wisconsin, Madison, WI, USA

We studied neurogenesis in the developing brain using the thymidine analog, 5-bromo-2'-deoxyuridine (BrdU) to assess proliferation and terminal deoxynucleotidyl transferase-mediated deoxyuridine triphosphate nick end labeling (TUNEL) method to evaluate apoptosis.

Wistar rats between postnatal day 0 (P0) and P30 received single or multiple BrdU injections by various survival time points. Peroxidase or fluorescence immunohistochemistry were applied on paraffin sections to label BrdU+ cells, neuronal markers such as nestin, Dcx, MAP(2) and NeuN or for TUNEL. Cell proliferation and neuronal apoptosis were analyzed using standard or confocal microscopy and stereology. Peak neurogenesis was found in the dentate gyrus during the first postnatal week with a progressive decline after P9. Colocalization of BrdU with neuronal markers was found mainly within the dentate gyrus and cerebellum. Most of the newly generated cells became nonneuronal cells (endothelial and glial cells). Apoptosis did not contribute to cell death of the newly generated neuronal progenitors.

Key words: BrdU, TUNEL, neurogenesis, developing brain

Introduction

In the mammalian brain, prenatal (embryonal) neurogenesis continues after birth as early and adult postnatal events of generation and functional integration of new neurons. It occurs intensively during the first weeks after birth picking at P7-P9. Thereafter, it remains longlife in the subventricular zone (SVZ) of the lateral ventricle and subgranular zone (SGZ) of the dentate gyrus (DG)[4,8,9]. Neurogenesis includes several processes such as proliferation, migration, differentiation, maturation and apoptosis that play crucial roles in the final physiological outcome. Apoptosis, or programmed cell death, is the death of excess or unwanted cells that could be activated also in the presence of appropriate stimuli in time of detrimental stress[5,6,10]. Coordination between cell proliferation and apoptosis maintains tissue homeostasis in the brain. TUNEL method is widely used for demonstration of apoptotic cell death opposite to necrotic cell death. In this study, we investigated the rate of proliferation and apoptosis as well as if apoptosis contributes significantly to cell death of newly generated neuronal progenitors and mature neurons during the early postnatal period.

Material and Methods

Wistar rats (BgVV, Berlin) at different age between P0 and P30 received single or multiple 100 or 50 mg/kg BrdU (Sigma, St. Louis, MO) injections by various survival time points between P1 and P51. Animals were anesthetized and transcardially perfused with 0.01M PBS, followed by 4% paraformaldehyde in 0.1M PB. The brains were removed and postfixed in the same fixative. Paraffin sections were processed for single or double peroxidase or fluorescence immunostaining. TUNEL was performed using ApopTag® Peroxidase or Fluorescein *In Situ* Apoptosis Detection kit. First antibodies against BrdU, Nestin, Dcx, MAP(2) and NeuN were used followed by biotinylated second antibodies, ABC reagent and DAB or VNR substrate. Alexa Fluor 594 or 488 and Vectashield mounting medium with DAPI were used by fluorescence labeling. Morphometric countings evaluating BrdU+ nuclei on P9, P12, P15 and P23 were done in a blinded fashion. Confocal microscopy was applied for colocalization of BrdU with neuronal markers or TUNEL.

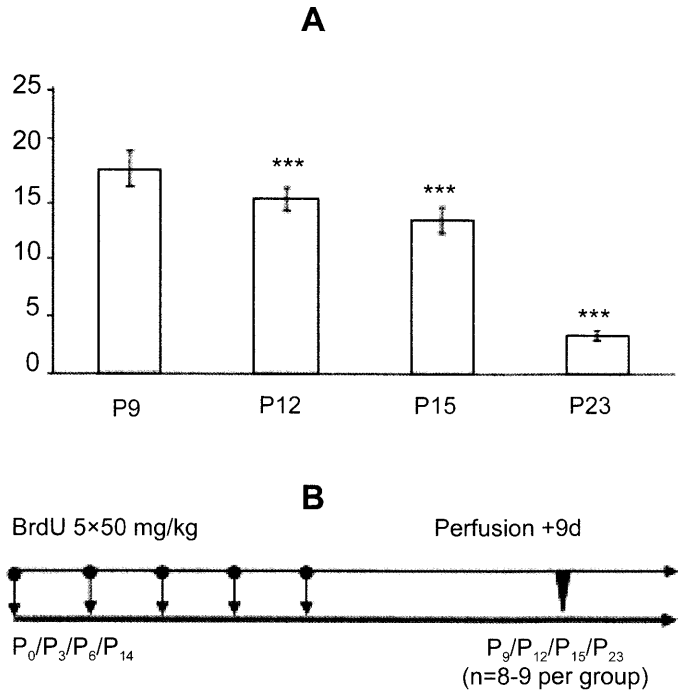

Fig. 1. (A) Summarized total proliferative scores of BrdU+ cell counts by peroxidase immunohistochemistry on P9, P12, P15 and P23; ten brain regions are included (frontal cortex layer I, frontal cortex layer II, parietal cortex layer I, parietal cortex layer II, caudate nucleus, mediodorsal thalamus, corpus callosum, molecular layer of cerebellum, subgranular zone of the dentate gyrus, granular cell layer of the dentate gyrus). Cell countings have shown a significant decrease in the proliferative rate to each previous age group. Student't *t*-test; ***P<0.001, values are presented as mean ± S.E.M. **(B)** BrdU paradigm: 50 mg daily for 5 days starting on P0, P3, P6 and P14; perfusion is performed 9 days later on P9, P12, P15 and P23 respectively.

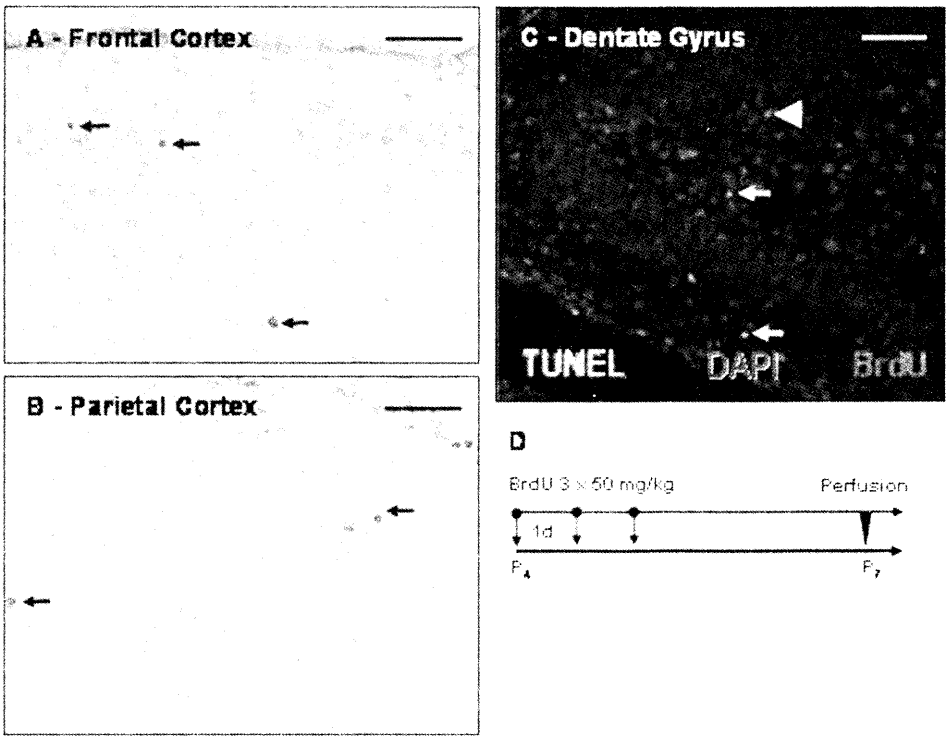

Fig. 2. (A, B) Single TUNEL+ nuclei detected by peroxidase immunostaining with DAB located in the brain cortex; **(C)** confocal image after fluorescein immunohistochemistry for TUNEL (green), BrdU (red) and DAPI (blue) in DG **(D)** BrdU paradigm applied in C; arrow = TUNEL+ cell, arrowhead = BrdU+ cell, bar = 50μm.

Results

We analyzed cell proliferation comparing same age groups with different BrdU paradigms, i.e., ages, dosages or survival timings. By same ages, higher dosages of BrdU produced a more intensive immunostaining when survival times were equal. By same dosage, younger animals showed a more expressed staining, whereas longer survival times showed reduced labeling. This was demonstrated by summarized total proliferative scores of BrdU+ cell counts in ten brain regions on P9, P12, P15 and P23 (Fig. 1). At the end of the second postnatal week, frequent colocalization for BrdU+/Nestin+ and BrdU+/Dcx+ was mainly found in specific regions such as the SVZ, cerebellum, corpus callosum and DG-SGZ. BrdU+/MAP+ and BrdU+/NeuN+ colocalization was occasionally seen by later timings (data not shown). Many of the newly generated cells were negative for the neuronal markers applied.
TUNEL method showed a relatively low level of cell death in the early postnatal period except for the first week. Single TUNEL+ nuclei were found maily in the gray matter areas such as thalamus, caudate and cortex (Fig. 2A,B). No colocalization of BrdU or any of the neuronal markers with TUNEL was found in the brain regions analyzed (Fig. 2C,D).

Discussion

During the early postnatal period, cell proliferation and neuronal differentiation in the rat brain are very intensive. Together with apoptosis, they play an important role in shaping the developing nervous system. Not all BrdU labeled cells observed in our study belong to the neuronal lineage. Colocalization of BrdU with some of the neuronal markers applied is an indice for neuronal differentiation. The newly generated cells that were negative for neuronal markers become mainly endothelial and glial cells. After the first two to three postnatal weeks, neurogenesis in the rat brain is attenuated but remains lifelong in the SVZ of the lateral ventricle and SGZ of the DG. In both zones multipotent neural precursors are preserved and may serve to repair injuries to the brain[1-3,7].

Apoptosis does not contribute significantly to cell death of the newly generated neuronal progenitors and mature neurons during the early postnatal period. Our data on early postnatal neurogenenic processes might be helpful for a better understanding of the adult neurogenesis in the mammalian brain.

Acknowledgements: Supported by BMBF grants 01GZ0305 and PBZ-MN-001/P05/2002/25-28.

References

1. Danzer, S. C., 2008. Postnatal and adult neurogenesis in the development of human disease. – Neuroscientist, 14(5), 446-458.
2. DeCarolis, N. A., A. J. Eisch, 2010. Hippocampal neurogenesis as a target for the treatment of mental illness: a critical evaluation. – Neuropharmacology, 58(6), 884-893.
3. Eisch, A. J., H. A. Cameron, J. M. Encinas, L. A. Meltzer, G. L. Ming, L. S. Overstreet-Wadiche, 2008. Adult neurogenesis, mental health, and mental illness: hope or hype? – J. Neurosci., 28(46), 11785-91.
4. Gage, F. H., 2002. Neurogenesis in the adult brain. – J. Neurosci., 22(3), 612–613.
5. Liou, A. K., R. S. Clark, D. C. Henshall, X. M. Yin, J. Chen, 2003. To die or not to die for neurons in ischemia, traumatic brain injury and epilepsy: a review on the stress-activated signaling pathways and apoptotic pathways. – Prog. Neurobiol., 69(2), 103-142.
6. Raff, M., 1998. Cell suicide for beginners. – Nature, 396, 119-122.
7. Snyder, J. S., A. Soumier, M. Brewer, J. Pickel, H. A. Cameron, 2011. Adult hippocampal neurogenesis buffers stress responses and depressive behaviour. – Nature, 476(7361), 458-461.
8. Toni, N., E. M. Teng, E. A. Bushong, J. B. Aimone, C. Zhao, A. Consiglio, H. van Praag, M. E. Martone, M. H. Ellisman, F. H. Gage, 2007. Synapse formation on neurons born in the adult hippocampus. – Nat. Neurosci., 10(6), 727-734.
9. van Praag, H., A. F. Schinder, B. R. Christie, N. Toni, T. D. Palmer, F. H. Gage, 2002. Functional neurogenesis in the adult hippocampus. – Nature, 415(6875), 1030-1034.
10. Yuan, J., B. A. Yankner, 2000. Apoptosis in the nervous system. – Nature, 407, 802-807.

Institute of Experimental Morphology, Pathology and Anthropology with Museum
Bulgarian Anatomical Society

Acta morphologica et anthropologica, 19
Sofia • 2012

Neurotrophic factors and schizophrenia

Lilia Grozlekova, Yvetta Koeva and Stefan Sivkov

Department of Anatomy, Histology and Embryology, Medical University, Plovdiv

Neurotrophins have an essential role in neuronal development, synaptogenesis, and response to stress/anxious stimuli. Furthermore, these agents are neuromodulators of monoaminergic, GABAergic, and cholinergic systems. There is a growing interest of the developmental neurobiology of schizophrenia, as well as the tendency for progressive brain changes and abnormalities in the expression of neurotrophins in schizophrenia. The role of neurotrophins and their precursor, pro-neurotrophins in the pathophysiology of several CNS disorders, including depression and schizophrenia is derived from current genetic, neurochemical and therapeutic research. The present research aims to demonstrate immunoreactivity for the neurotrophic factor neurotrophin-3 (NT-3) in brain structures of rats in an experimental model of schizophrenia by neonatal lesion with *i*- butenic acid and to attempt connection between obtained results and disontogenetic hypothesis of the origination of schizophrenia.

Key words: NT-3, schizophrenia, experimental model, rat

Introduction

Schizophrenia is a complex disease characterized by disturbances of thinking, emotional disorders and severe functional disabilities. There is a theory, called neuroontogenetic theory, which explains the emergence of disease during intra-uterine period. It leads to brain structural and functional alterations, expressed in appearance of typical disease symptoms decades later. Morphological damage of brain structure is caused by abnormal expression of factors regulating the proliferation and differentiation of neuroectodermal cells and chronology of these processes (7). This pathological process translates into a reduction in the amount of neurons and glial cells and functional connections between different neuronal phenotypes therefore functional disorders can reveal at a large stage in the mature nervous system (1,11).

Hypothesis of neurotrophic factors

Abnormalities in fetal neurogenesis result from pathological changes of genetic code of certain neurotrophic factors (NTF) and their corresponding receptors. These changes consist in primary and secondary violations of biologically active substances, neurotrophic factors, under the influence exogenous effects. Developmental role of NTF during embryogenesis and in adult isn't well studied. Data for these factors are insufficient in the context of schizophrenia accompanying structural and functional abnormalities

in certain brain structures which occur only after complete maturation of the brain. Our research aims to:

- To demonstrate immunoreactivity for the neurotrophic factor neurotrophin-3 (NT-3) in brain structures of rats in an experimental model of schizophrenia by neonatal lesion with *i*- butenic acid.
- To attempt connection between obtained results and disontogenetic hypothesis of the origination of schizophrenia.

Materials and methods:

Experimental model of neonatal hippocampal lesion by Lipska et. al., (5)
7-day old Wistar rats (n=20) are divided into control and experimental groups. After hypothermic anesthesia using Hamilton needle and infusion pump 0.3 μl of 10 μg / μl solution of *i*- butenic acid (experimental animals) or artificial spinal liquor (control animals) was injected bilaterally in the area of hippocampal formation (AP – 3.0 mm, ML +_ 3.5 mm, VD – 5.0 mm, from bregma) at rate of 0.15 μl/min.

35 and 56 days rats (control and with neonatal lesion) after deep anesthesia were perfused intracardial, through the ascending aorta with Zamboni fixative. After the experiment, the brains are removed and cut into 4-5mm thick fragments of the frontal cortex and hippocampal formation. Brain fragments are placed in cryoprotective solution at 4° C overnight, frozen in liquid nitrogen and prepared for routine histological (staining with hematoxylin-eosin and impregnation techniques) and immunohistochemical analyses. Immunohistochemical techniques, amplified by the combination of ABC and PAP methods on cryostat and paraffin slices of rat brain (frontal cortex and hippocampal formation) were applied using polyclonal anti- NT-3 antibody, Santa Cruz, USA, 1:1000 and kits for detection and visualization of the immunochistochemical reactions- Vectastain® *Elite* ABC detection kit (Vector, USA) and DAB Peroxidase Substrate kit, (Vector, USA).

Results

NT- 3 immunoreactivity is visualized in hippocampal pyramidal cells (CA-1, CA-2 and CA-3 fields), cells of granular layer of the dentate gyrus cortex (GrDG) of 35 and 56 day injured rats. Reaction intensity is reduced compared with control animals (**Fig.1**). Declination in the immune reactivity of NT-3 is more pronounced on 56 day injured experimental animals, especially in the cells from CA-3, GrDG and cells in the hilus of gyrus dentatus (**Fig.2**).

Discussion

In this research is used an animal developmental model obtained by bilateral infusion of the glutamatergic agonist *i*-botenic acid. This is a molecular trigger of the excitotoxic cascade in the ventral hippocampus of 7 days old male rats (5). Fundamental features of schizophrenia are wide spectrum of structural and physical abnormalities and they are very similar to that caused by neonatal damage of the hippocampal formation with *i*-botenic acid (4,5). Our routine morphological analysis does not show any damages in the hippocampal cytoarchitectonic pattern of the lesioned rats compared to rats in the control group. A possible explanation of this fact is the low dose of *i*-botenic acid

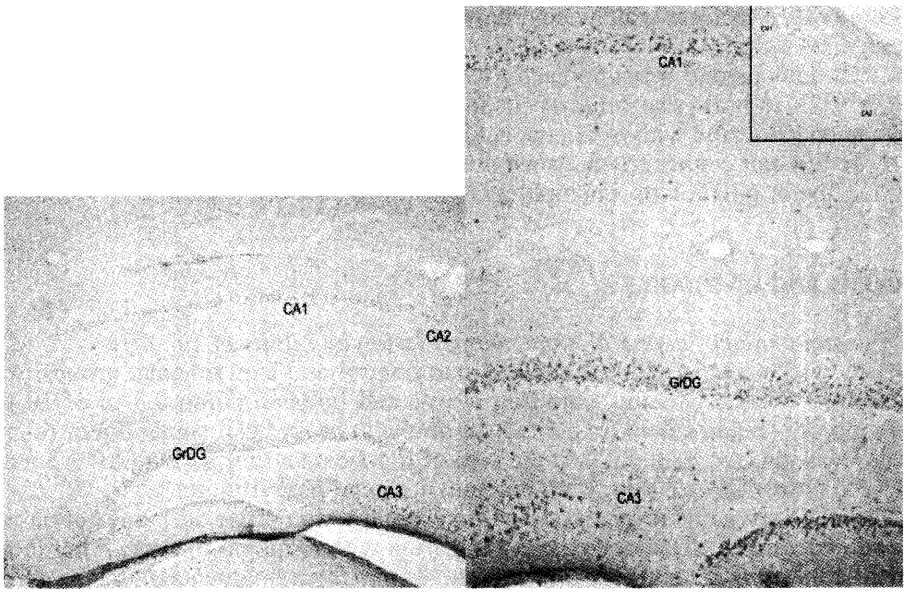

Fig.1. 35 days rats. Group of lesioned animals. NT-3 expression in hippocampus and dentate gyrus. x 200; x 400.

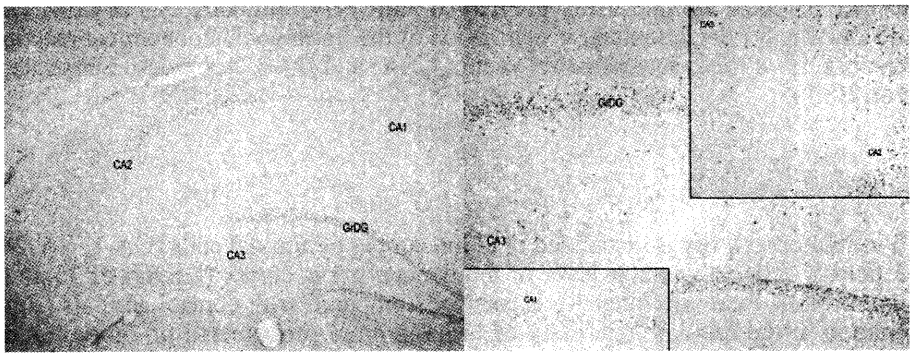

Fig. 2. 56 days old rats. Group of lesioned animals. Immunostaining for NT-3 in hippocampus and dentate gyrus. x 200; x 400.

used in the experimental procedure. Our opinion that disturbances of cytoarchitectonic depend on the used dose of *i*-botenic acid confirmed previously reported results (8). The highest levels of NT-3 expression were detected in the cerebellum and hippocampus of adult brains (6). Our findings are related with data which demonstrate that the expression of NT-3 in hippocampal formation prevails largely in the vast of dentate granule cells as well as in subpopulations of pyramidal neurons located in CA1 and CA2 (2). Low levels of NT-3 mRNA have also been detected in CA3 and CA4. In the current study, immunohistochemical staining for NT-3 shows that the NT-3 immuno-

reactivity localized in the hippocampal pyramidal cells (CA1, CA2 and CA3 fields), dentate granule cell layer (GrDG) and cells of the polymorph layer of the dentate gyrus (PoDG) of the 35 and 56 days old lesioned rats is with markedly reduced intensity than that of the control animals. The decrease in NT-3 immunoreactivity is more obvious in the hippocampal formation of the 56 days lesioned animals, especially in the cells of CA3, PoDG and dentate hilar cells. This fact suggests a change or a kind of alteration in regulatory mechanism of NT-3 expression as a consequence of neonatal hippocampal lession. The hippocampal dentate gyrus is one of the few areas of the rat brain that continues to generate neurons postnatally whereas the neuronal progenitor cells divide at the border between the hilus and inner and outer blade of the GrDG (3,9). The current data reveal reduced NT-3 expression in the hippocampal formation of the lesioned animals, especially in the cells of dentate gyrus and indicate that the dysfunction of the neurotrophins may contributes to impaired brain development, neuroplasticity and synaptic neurotransmitter system leading to the schizophrenic syndrome (10).

Conclusion

The present study reveals additional evidence in support of the neurodevelopmental model and neurotrophic factor hypothesis for schizophrenia. Our data prove the role of neurotrophins in normal brain development and their possible relevance in the neuropathology and neuropharmacology of schizophrenia.

References

1. De Lisi E. Is schizophrenia a life-time disorder of brain plasticity, growth and aging?- Schizophr. Res., 23, 1997, 119-129.
2. Ernfors P., C. F. Ibanez, T. Ebendal, L. Olson, H. Persson. Molecular cloning and neurotrophic activities of a protein with structural similarities to nerve growth factor: Developmental and topographical expression in the brain. – Proc. Natl. Acad. Sci. USA, 87, 1990, No 14, 5454-5458.
3. Kuhn H.G., H. Dickinson-Anson, F. H. Gage. Neurogenesis in the dentate gyrus of the adult rat: age-related decrease of neuronal progenitor proliferation. – J. Neurosci., 16, 1996, No 6, 2027-33.
4. Lipska B.K., D. R. Weinberger. Genetic variation in vulnerability to the behavioral effects of neonatal hippocampal damage in rat. – Proc. Natl. Acad. Sci. U S A, 92, 1995, No 19, 8906-10.
5. Lipska B.K., G. E. Jaskiw, D. R. Weinberger. Postpubertal emergence of hyperresponsiveness to stress and to amphetamine after neonatal excitotoxic hippocampal damage: a potential animal model of schizophrenia. – Neuropsychopahrmacology, 9, 1993, No 1, 67-75.
6. Maisonpierre P.C., L. Belluscio, B. Friedman, R. F. Alderson, S. J. Wiegand, M. E. Furth, R. M. Lindsay, G. D. Yancopoulos. NT-3, BDNF, and NGF in the developing rat nervous system: parallel as well as reciprocal patterns of expression. – Neuron, 5, 1990, No 4, 501-509.
7. Marenco S. and D. R. Weinberger. The neurodevelopmental hypothesis of schizophrenia: following a trail of evidence from cradle to grave. – Dev Psychopathol., 12(3), 2000, 501-27.
8. Marret S., P. Gressens, P. Evrard. Arrest of neuronal migration by excitatory amino acids in hamster developing brain.- Proc. Natl. Acad. Sci. USA, 93, 1996, No 26, 15463-15468.
9. Sharp F. R., J. Liu, R. Bernabeu. Neurogenesis following brain ischemia.- Brain Res. Dev. Brain. Res., 134, 2002, No 1-2, 23-30.
10. Wakade C. G., S. F. Mahadik, J. L. Waller, F. C. Chiu. Atypical neuroleptics stimulate neurogenesis in adult ra.- J. Neurosci. Res., 69, 2002, No 1, 72-9.
11. Weinberger D. R. From neuropathology to neurodevelopment. – Lancet, 346, 1995, 552-557.

Institute of Experimental Morphology, Pathology and Anthropology with Museum
Bulgarian Anatomical Society

Acta morphologica et anthropologica, 19
Sofia • 2012

A doubled palmaris longus muscle: case report

Alexandar Iliev, Lazar Jelev, Boycho Landzhov, Lina Malinova , Dimka Hinova-Palova, Adrian Paloff, Wladimir Ovtscharoff*

Department of Anatomy, Histology and Embryology,
Medical University of Sofia, BG-1431 Sofia, Bulgaria

During routine anatomical dissection of the left anterior forearm of an elderly female cadaver, two separate muscles having characteristics of palmaris longus have been observed. The lateral of the muscles had a typical palmaris longus composition – small proximal muscular belly and a long distal tendon continuing into the palmar aponeurosis. The second, medial muscle started with a thick tendon from the medial epicondyle of the humerus. Its muscular belly occupied the middle third of the forearm; in the lower third it turned into a short, broad tendon attached to the flexor retinaculum and to the proximal attachment sites of the thenar and hypothenar muscles. The clinical importance of this variation is due to the close relations of the distal tendons with the neurovascular structures in the anterior wrist.

Key words: palmaris longus, variation, clinical significance, entrapment

Introduction

Reports on variations of the muscles, arteries and nerves of the upper limb may have both academic and clinic relevance [11]. In the anatomical literature different variations of the palmaris longus muscle have been documented [1, 11, 12]. There are many clinical case reports presenting the significance of these muscular variations for traumatologists, plastic surgeons and neurologists [2, 3, 7, 8].

Herewith, we describe an interesting case of palmaris longus variation.

Case report

During routine anatomical dissection of the left upper limb of an elderly formol-carbol fixed Caucasian female cadaver, from the autopsy material available at the Department of Anatomy, Histology and Embryology of the Medical University of Sofia, an unusual muscular variation was found. After removal of the forearm fascia and presentation of the individual muscles from the superficial anterior group, we noted with surprise the presence of two separate muscles with characteristics of palmaris longus (Fig.1,2).

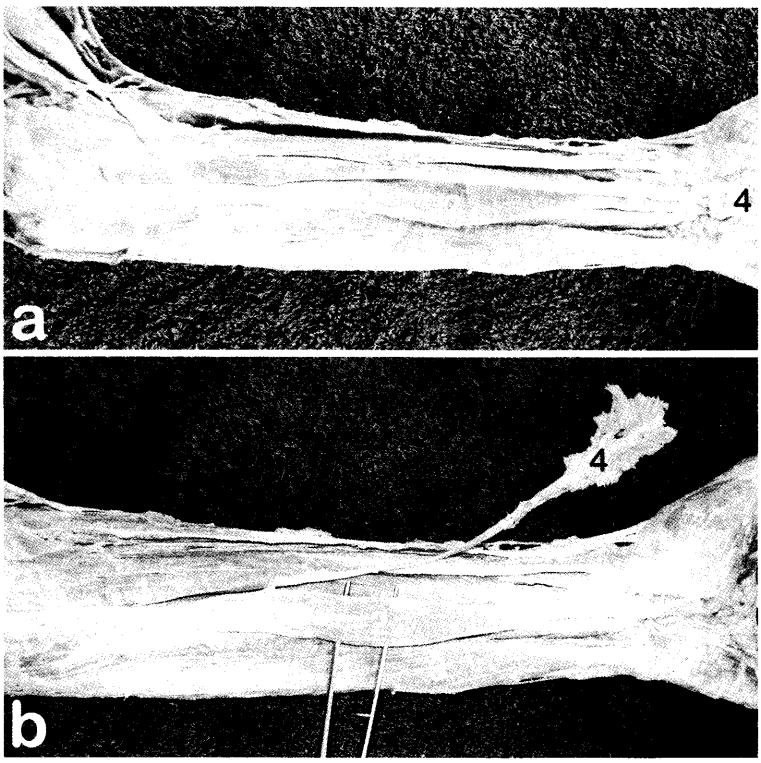

Fig. 1. Photographs of the reported variation of the palmaris longus in situ (a) and after cutting and retracting the palmar aponeurosis (b). Muscles – 1, lateral palmaris longus; 2, medial palmaris longus; 3, flexor carpi ulnaris.

The first muscle, located on the lateral side, had a small proximal muscular belly starting from the medial epicondyle of the humerus, which at mid-forearm turned into a long thin tendon continuing into the palmar aponeurosis. The second muscle, located on the medial side, started with a long thick tendon from the medial epicondyle of the humerus. Its strong muscular belly occupied the middle third of the forearm and was located slightly below and medial to the distal tendon of the lateral palmaris longus. In the lower third of the forearm, the muscle belly turned into a short, broad tendon, which was divided into several bundles attached to the flexor retinaculum and to the proximal attachment sites of the thenar and hypothenar muscles. These tendinous bundles arched over the median nerve and the ulnar artery and nerve at the canal of Guyon.

Discussion

The plamaris longus is probably the most variable muscle in the human arm and one of the most variable muscles in the human body [7, 8, 12]. The most common variations concerning this muscle are the following: absence (in around 10% of the individuals), presence of digastric muscle, reversed muscle, bifid reversed variation and duplication [7, 8, 10, 12]. There are also reports of variations in the origin and insertion of the palmaris longus [5].

In the clinical practice, the aberrant palmaris longus could be incidentally found during clinical examination without provoking any symptoms and may simulate a soft tissue tumor [10]. The clinical importance of the palmaris longus variations is mainly due to the close relations of its distal tendon with the neurovascular structires in the anterior wrist. In the literature, there are many reports of the median and/or ulnar nerve compression due to the existence of a variant palmaris longus [4, 7, 8, 10, 12]. Such patients usually present with swelling, reduction of the hand's muscular power, pain and numbness in the area of distribution of the compressed nerves [6, 9]. In addition, the palmaris longus is often considered as an ideal donor in reconstructive and plastic surgery and the knowledge of its variations is important to provide safe and successful surgical procedures [7]. This muscle could be used for tendon grafts in the replacement of the long flexors of the fingers, the flexor policis longus tendon, dorsal finger injuries involved with both soft tissue loss and extensor tendon defects [12]. It is also utilized as a simple static support in the treatment of facial paralysis, in digital pullay reconstruction, lip augmentation, and in various nerve palsies as a tendon transfer [7, 12].

In conclusion, the aberrant palmaris longus muscles, reported in this study, may cause entrapment neuropathies, cosmetics defects and functional disability, and may also play an important role in plastic and reconstructive surgery.

References

1. Coskun N, Sarikcioglu L, Donmez BO, Sindel M. Arterial, neural and muscular variations in the upper limb. Folia Morphol (Warsz) 2005; 64: 347-352.
2. Kaufmann RA, Pacek CA. Pulley reconstruction using Palmaris longus autograft after repeat trigger release. J Hand Surg Br 2006; 31: 285-287.
3. Lin CH, Wei FC, Lin YT, Chen CT. Composite palmaris longus venous flap for simultaneous reconstruction of extensor tendon and dorsal surface defects of the hand-long-term functional result. J Trauma 2004; 56: 1118-1122.
4. Lisanti M, Rosati M, Maltinti M. Ulnar nerve entrapment in Guyon's tunnel by an anomalous palmaris longus muscle with a persisting median artery. Acta Orthop Belg 2001; 67: 399-402.
5. Macalister A. Additional observations on muscular anomalies in human anatomy (third series), with a catalogue of the principal muscular variations hitherto published. Trans Roy Irish Acad 1875; 25: 85-86.
6. Netsher D., Cohen V., Ulnar nerve compression at the wrist secondary to anomalous muscles: a patient with a variant of abductor digiti minimi, Ann Plast Surg, 1997, 39(6):647-651.
7. Sebastin SJ, Lim AY, Bee WH, Wong TC, Methil BV. Does the absence of the palmaris longus affect grip and pinch strength? J Hand Surg Br 2005; 30: 406-408.
8. Seyhan T. Median nerve compression at the wrist caused by reversed 3-headed palmaris longus muscle: case report and review of the literature. Am J Orthop 2005; 34: 544-546.
9. Simodynes E. E., Cochran R.M. 2nd, Anomalous muscles in the hand and wrist – reports of three cases, J Hand Surg Am, 1981, 6(6):553-554.
10. Turner MS, Caird DM. Anomalous muscles and ulnar nerve compression at the wrist. Hand 1977; 9: 140-142.
11. Wadhwa S, Vasudeva N, Kaul JM. A rare constellation of multiple upper limb anomalies. Folia Morphol (Warsz) 2008; 67: 236-239.
12. Zeybek A, Gürünlüoglu R, Cavdar S, Bayramiçli M. A clinical reminder: a palmaris longus muscle variation. Ann Plast Surg 1998; 41: 224-225.

Institute of Experimental Morphology, Pathology and Anthropology with Museum
Bulgarian Anatomical Society

Acta morphologica et anthropologica, 19
Sofia • 2012

In vitro antiproliferative activity and subcellular distribution of recently synthesized anthracene-derived Schiff base and anthracene-containing aminophosphonate

I. Iliev[a], A. Georgieva[a], I. Kraicheva[b], I. Tsacheva[b], E. Vodenicharova[b], E. Tashev[b], T. Tosheva [b], A. Kril[a]

[a]*Institute of Experimental Morphology, Pathology and Anthropology with Museum, Bulgarian Academy of Sciences, Acad. G. Bonchev Str., Bl. 25, 1113 Sofia, Bulgaria*
[b]*Institute of Polymers, Bulgarian Academy of Sciences, Acad. G. Bonchev Str., Bl. 103A, 1113 Sofia, Bulgaria*

Organophosphorus compounds have wide range of commercial applications ranging from agriculture to medicine owing to their unique physicochemical and biological properties. The α-aminophosphonates, as structural analogues of natural α-amino acids, constitute a valuable class of compounds with a wide spectrum of biological activities. A recently synthesized anthracene-derived Schiff base – 9-anthrylidene-furfurylamine and novel anthracene-containing aminophosphonate – [N-methyl(diethoxyphosphonyl)-1-(9-anthryl)]-p-toluidine were tested for *in vitro* antitumor activity on HT-29 cell line. *In vitro* safety testing of the compounds was performed by Balb/c 3T3 Neutral Red Uptake Assay. The aminophosphonate and the Schiff base showed high *in vitro* antitumor activity towards HT-29 cell line. Both tested compounds were found to exert moderate cytotoxicity on the Balb/c 3T3 cells. In addition, the fluorescent properties of these compounds allowed precise observation of their subcellular distribution in the normal and tumor cells.

Keywords: Aminophosphonic acid, Schiff base, Antiproliferative activity, Subcellular distribution

Introduction

The α-aminophosphonates are organophosphorus compounds, which have found a wide range of applications in the areas of industrial, agricultural and medicinal chemistry owing to their biological and physical properties as well as their utility as synthetic intermediates. As analogues of natural amino acid, α-aminophosphonates constitute an important class of compounds with diverse biological activities, including enzyme inhibitory, antibacterial, antifungal, antiviral and antitumor effects [3, 4, 8, 9]. Some aminophosphonate derivatives inhibit bone resorbtion, delay the progression of bone metastases, exert direct cytostatic effects on a variety of human tumour cells and have found clinical application in the treatment of bone disorders and cancer [2].

Anthracene-bearing α-aminophosphonates might be of particular interest in the design of new antitumor therapeuticals considering the fact that the DNA-intercalating anthracene-derived planar structure is the main pharmacophoric fragment of some cytostatic drugs, which have found clinical applications in the treatment of human cancers [5]. Some of these anthracene-containing substances have been reported to display strong antiproliferative activity against several tumor cell lines, including multidrug resistant phenotypes [7]. The fluorescent properties of anthracene-based aminophosphonates could find valuable bioanalytical application in studying of their subcellular distribution and binding in normal and tumor cells.

The aim of the present work was to assess the *in vitro* antiproliferative activity of recently synthesized [4] anthracene-containing aminophosphonate [N-methyl (diethoxyphosphonyl)-1-(9-anthryl)]-p-toluidine and its synthetic precursor – an anthracene-derived Schiff base 9-anthrylidene-furfurylamine on HT-29 cell line and on Balb/c 3T3 cell line. In addition, we report data about subcellular distribution of the tested compounds in normal and tumor cell culture systems.

Materials and methods

Cell lines and culture conditions

The cell lines Balb/c 3T3 (mouse embryo fibroblasts) and HT-29 (human colon carcinoma) were used for *in vitro* safety assessment and *in vitro* antitumor activity testing, respectively. All cells were grown as monolayers in DMEM (*Sigma*), supplemented with 10% fetal bovine serum (*Gibco*) and antibiotics in usual concentrations. Cultures were maintained in a humidified atmosphere with 5% CO_2 at 37°C.

Test chemicals preparation

The tested compounds were dissolved in DMSO and further diluted in complete culture medium to reach the desired test concentrations. A constant dilution factor ($\sqrt[6]{10}$) was used in each experiment for the preparation of eight test concentrations of both compounds.

Safety assessment

The cytotoxicity testing was performed by the Balb/c 3T3 Neutral Red Uptake (Balb/c 3T3 NRU) Assay [1]. Optical density was measured after 24 h of treatment by microplate reader at wave length 540 nm.

In vitro antitumor activity

The antitumor activity of the tested compounds was assessed by MTT-dye reduction assay [6] on the HT-29 cell line. Cultures treated with the referent antineoplastic drug Doxorubicin hydrochloride (*Lemery*) and non-treated cultures were used as positive and negative controls, respectively. The MTT-formazan absorption was measured at wave length 580 nm after 24 hour treatment. All experiments were performed in triplicate.

Statistical analysis

The relative cell cytotoxicity/viability, expressed as a percentage of the untreated negative controls, was calculated for each concentration. The statistical analysis included application of One-way ANOVA followed by Bonferroni's *post hoc* test. $p < 0.05$ was accepted as the lowest level of statistical significance. IC_{50} values were calculated using non-linear regression analysis (*GraphPad Prizm5 Software*).

Fluorescent studies

HT-29 and Balb/c 3T3 cells were seeded on sterile 12 ring diagnostic slides and treated with non-toxic concentrations of the Schiff base and the aminophosphonate for 24 h. After fixation in cold (20°C) acetone the slides were air-dried, covered and examined with fluorescent microscope.

Results and discussion

In vitro safety testing

The results from the Balb/c 3T3 NRU Assay revealed dose-dependent cytotoxic activity of both tested compounds (Fig. 1). The Schiff base and the aminophosphonate showed statistically significant ($p<0.001$) cytotoxic effect on Balb/c 3T3 cells in a wide concentration range (1–0.07 mg/ml), compared to untreated control cell cultures. The aminophosphonate appeared to be more toxic than its synthetic precursor and the mean IC_{50} values from three consecutive experiments were 0.095 ± 0.002 mg/ml and 0.16 ± 0.006 mg/ml, respectively. The results from these experiments indicate that tested compounds exert moderate cytotoxic activity on the Balb/c 3T3 cells.

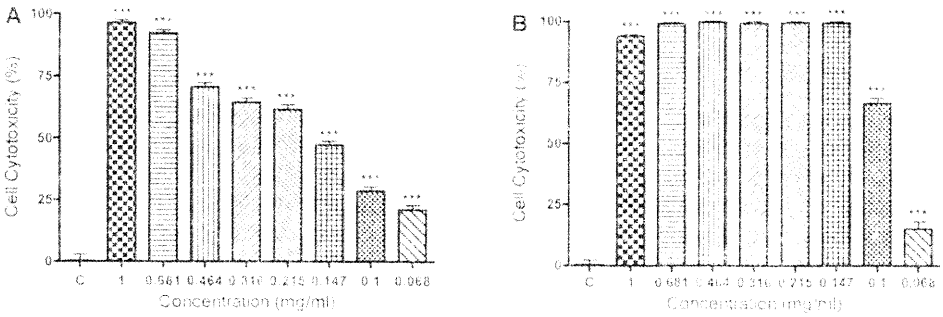

Fig. 1. Cytotoxicity of Schiff base (A) and aminophosphonate (B). Neutral Red Uptake assay. C – negative control; ***p <0.001, compared to C.

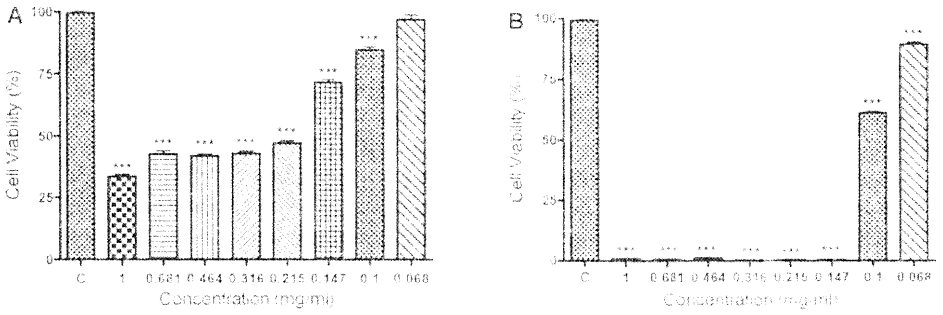

Fig. 2. Antiproliferative activity of Schiff base (A) and aminophosphonate (B) on HT-29 cell line. MTT-dye reduction assay. C – negative control; ***p <0.001, compared to C.

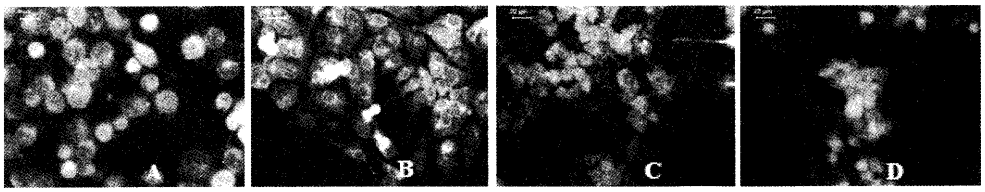

Fig. 3. Subcellular distribution of 9-anthrylidene-furfurylamine (A, C) and [N-methyl (diethoxyphosphonyl)-1-(9-anthryl)]-p-toluidine (B, D) in Balb/c 3T3 (A, B) and HT-29 (C, D) cells; Fluorescent microscopy.

In vitro antitumor activity

The Schiff base and the aminophosphonate exerted concentration-dependent antiproliferative effects after 24 h exposure (Fig. 2) and the mean IC_{50} values from three consecutive experiments were 0.2± 0.003 mg/ml and 0.11± 0.002 mg/ml, respectively. Both compounds were found to have significantly higher antiproliferative activity than the positive control substance Doxorubicin (mean IC_{50} = 0.58 ± 0.013 mg/ml). As evident from the cytotoxicity data, the tested compounds proved to be potent cytotoxic agents towards colon carcinoma cell line HT-29. The results obtained imply that these compounds could be considered as promising leads for further development of agents active in chemotherapy of malignant colon disease.

Fluorescent studies

The fluorescent signal of the Schiff base was observed in the nucleus, the perinuclear region and in the nucleoli of Balb/c 3T3 cells (Fig. 3 A), while the aminophosphonate was distributed mainly perinuclearly in the cytoplasm (Fig. 3 B). In contrast, the most intensive fluorescence was found in the cytoplasm and nucleoli of the HT-29 cells treated with the Schiff base (Fig. 3 C) and in the nuclei of aminophosphonate-treated tumor cells (Fig. 3 D). The latter observation confirms the fact that DNA-intercalating anthracene-derived planar structure is the main pharmacophoric fragment of the recently synthesized aminophosphonate [N-methyl (diethoxyphosphonyl)-1-(9-anthryl)]-p-toluidine.

Conclusion

In vitro safety assessment of the anthracene-derived Schiff base – 9-anthrylidene-furfurylamine and the aminophosphonate [N-methyl(diethoxyphosphonyl)-1-(9-anthryl)] furfurylamine revealed that the compounds exert moderate toxicity to normal mouse cells. Both compounds were found to be cytotoxic to HT-29 human colon carcinoma cells. The aminophosphonate exhibited higher antiproliferative activity than its synthetic precursor. Therefore, the novel substances are promising for future work on the development of agents active in chemotherapy of malignant colon disease. In addition, the fluorescent properties of anthracene ring allow adequate and precise studies on the cellular uptake and intracellular distribution of the novel compounds in malignant and normal cells.

Acknowledgment. This work was supported by grant DTK-02/34 (2009) from Ministry of Education and Science, Bulgaria

References

1. 3T3 Neutral Red Uptake (NRU) Phototoxicity Assay. Invittox protocol no. 78, http://ecvam-dbalm.jrc.ec.europa.eu
2. Djokic, D. D., D. L. Jankovic, N. S. Nikolic. Labeling, characterization, and in vivo localization of a new 90Y-based phosphonate chelate 2,3-dicarboxypropane-1,1-diphosphonic acid for the treatment of bone metastases: comparison with 99mTc-DPD complex. – Bioorg. Med. Chem., 16, 2005, 4457-4465.
3. Kafarski P, B. Lejczak. The Biological Activity of Phosphono- and Phosphinopeptides. – In: Aminophosphonic and aminophosphinic acids: chemistry and biological activity. (Kukhar, V. P., H. R. Hudson, Eds.), Chichester, Wiley, 2000, 407-435.
4. Kraicheva, I., I. Tsacheva, E. Vodenicharova, E. Tashev, T. Tosheva, A. Kril, M. Topashka-Ancheva, I. Iliev, Ts. Gerasimova, K. Troev. Synthesis, antiproliferative activity and genotoxicity of novel anthracene-containing aminophosphonates and a newanthracene-derived Schiff base. – Bioorg. Med. Chem., 20, 2012, 117–124.
5. Martinez, R., L. Chacon-Garcia. The search of DNA-intercalators as antitumoral drugs: what it worked and what did not work. – Curr. Med. Chem., 12, 2005, 127-151.
6. Mosmann, T. Rapid colorimetric assay for cellular growth and survival: application to proliferation and cytotoxicity assays. – J. Immunol. Methods., 65(1-2),1983,; 55-63.
7. Nickel H., P. Schmidt, K. Böhm, S. Baasner, K. Müller, M. Gerlach, E. Unger, E. Günther, H. Prinz. Synthesis, antiproliferative activity and inhibition of tubulin polymerization by 1,5- and 1,8-disubstituted 10H-anthracen-9-ones bearing a 10-benzylidene or 10-(2-oxo-2-phenylethylidene) moiety. – Eur. J. Med. Chem., 45(8), 2010, 3420-38.
8. Rezaei, Z., S. Khabnadideh, K. Zomorodian, K. Pakshir, S. Nadali, N. Mohtashami, E. Mirzaei. Design, Synthesis, and Antifungal Activity of New α-Aminophosphonates. – Int. J. Med. Chem., 2011, Article ID 678101, 11 p.
9. Zhou, J., H. Fan, B. Song, L. Jin, P. Bhadury, D. Hu, S. Yang. Synthesis and Antiviral Activities of α-Aminophosphonate Derivatives Containing a Pyridazine Moiety. – Phosphorus, Sulfur, 168 (1), 2010, 81-87.

Institute of Experimental Morphology, Pathology and Anthropology with Museum
Bulgarian Anatomical Society

Acta morphologica et anthropologica, 19
Sofia • 2012

Effect of chronic Epididymitis inflammation on maturity spermatozoa and male fertilizing ability

I. Ilieva, St. Ivanova, P. Tzvetkova, B. Nikolov, L. Vojvodova

Department of Experimental Morphology, Institute of Experimental Morphology, Pathology and Anthropology with Museum, Bulgarian Academy of Sciences, Sofia

According to the clinical data chronic epididymitis leads to impaired fertility.

The aim of the present study is to determine specific changes in sperm structure and the level of male infertility with chronic epididymitis.

Spermatological studies on ejaculates of 94 patients with Epididymitis chr. and 20 healthy men were carried out according to the WHO criteria.

Changes in the quality and quantity of ejaculate are expressed mainly in higher percentage of gametes with microcephal and round heads, cells without tails and a high percentage of immotile sperm in conditions of Normo- and Oligozoospermia (Gr. I-III).

Integrated application of different methods for qualitative and quantitative assessment of sperm appears appropriate for better monitoring of patients with infertility.

Key words: sperm, morphology, Epididymitis, fertility

Introduction

The most common disorders of the reproductive system are chronic non-specific inflammation processes – orchitis, epididymitis, prostatitis, urethritis. Based on the clinical data, chronic epididymitis leads to impaired fertility in 42% of cases [Kerr, 1998].

The inflammatory process in epididymis can be located in the head, tail, or affects the whole organ. It causes infiltration of the epithelium, forming lymph-epithelium complexes, fibroses changes (with or without the presence of sperm) and epididymal duct obstruction [Jones, 1999]. Morphological and functional damages influence on epididymis role to serve as a sperm depot and thus on spermatozoa post-testicular maturation and motility. There are changes in the quality and quantity of ejaculate [Ilieva et al., 2009]. They are expressed in deviation from the state of Normospermia to the state of Oligoastenozoospermia (Gr. I-III) and to obstructive azoospermia or even aspermia [Bedford, 1994; Jones, 1999].

The **aim** of the present study is to determine specific changes in sperm structure and the level of male infertility in chronic Epididymitis.

Material and Methods

Spermatological studies on ejaculates of 94 patients (mean age 34.8 ± 4.56 years) with Epididymitis chr. were carried out according to the WHO criteria (2010). The results were compared with those of 20 healthy men (mean age 30.12 ± 1.22 years old).

The following methods were used:

- *Medical history and physical examination;*
- *Light microscopic studies of spermatozoa after routine staining with Yashkovski, Papanicolaou, hematoxyline-eosin, and*
- Cytochemical study according to the method of E. Zvetkova [2000];
- *The following criteria for evaluation of the fertilizing ability in Epididymitis chr. patients were used:* Preserved fertilizing ability, Relatively Preserved fertilizing ability, Poor fertilizing ability, Missing fertilizing ability

Results were reported as *mean values ± SD* and as relative part in percentage, and statistically analyzed by *Student's t-test* using statistical package SPSS. Difference was considered significant at $p<0.001$.

Results

Spermatological parameters

In 46.81% of patients with Epididymitis chr we found reduced ***concentration*** *of the mature germ cells* in the semen plasma – various grades of Oligozoospermia (Gr. I-III) with mean number of gametes 19.64 million/ml (1 – 39 million/ml) (Table 1). The reduced number of spermatozoa in Oligozoospermia (Gr. I-III) was above four times lower in comparison to the control group and the cases with Normospermia.

The relationship between the number of spermatozoa and the percentage of gametes with normal and abnormal morphology in the ejaculate samples from Epididymitis chr. patients is shown in Table 1. The results demonstrated a significant increase in the number of the abnormal germ cells in the Epididymitis chr. groups with Normo- and Oligozoospermia.

The pathology of Epididymitis chr. was characterized by a combination of a low cellular concentration and an increased content of abnormal spermatozoa in the semen. However, in 6.38% of patients with Oligozoospermia we found relatively low quantity of metamorphic gametes and, at the same time, the number of morphologically normal and vital germ cells predominated. These differences are statistically significant ($p<0.001$).

Besides, the comparison between the *number of spermatozoa and sperm* ***motility*** *in the semen plasma* made possible to draw a conclusion on the degree of the functional disturbances in this disease, and the degree of man infertility (Table 2).

In most patients with *Normospermia*, the sperm motility is recognized as progressive (25.60%) and non-progressive (24.20%) with velocity values between 5 and 6 μm/sec, and immotility – 50.20%. In 17 cases of *Oligozoospermia*, there were no spermatozoa with high motility, the percentage of poorly motile gametes was between 10% and 30% with velocity >5 μm/sec, and the akinetic germ cells were 70% and 90%. There were 100% immotile cells in six patients with *Normospermia* and in seven cases with *Oligozoospermia*. In all other cases, there were no substantial changes in sperm motility in comparison to *Normospermia*.

The results were statistically significant ($p<0.001$).

Table 1. Number and morphology of spermatozoa in cases with Epididymitis chr.

Epididymitis chr. (n=94)	Concentration (million/ml)	Gametes with normal morphology (%)	Gametes with impaired morphology (%)
Normospermia (53.19 %)	*63.24 ± 20.59*	*50.22*	*49.78*
Oligozoospermia Gr. I-III (46.81 %)	*19.64 ± 11.71*	*36.05*	*63.95*
Control group	**78.73 ± 18.45**	**78.63**	**21.37**

Table 2. Motility, number and velocity of spermatozoa in cases with Epididymitis chr.

Epididymitis chr. (n=94)	Motility (%)			Velocity
Number gametes *(%)*	**Progressive motile**	**Non-progressive**	**Immotility**	**(μ/sec)**
Normospermia (53.19)	**25.60 ± 2.51**	**24.20 ± 1.54**	**50.20 ± 2.86**	**6**
Oligozoospermia (46.81)	**20.75 ± 2.18**	**17.22 ± 1.81**	**62.03 ± 3.23**	**4.47 ± 0.32**
Control group *(n=20)*	**64.17 ± 5.07**	**15.90 ± 5.13**	**19.93 ± 4.04**	**16.52 ± 2.93**

Table 3. Morphological changes in germ cells

I. Anomalies in head spermatozoa	*37%*
II. Anomalies in tail spermatozoa	*11%*
III. Cytoplasmic droplet	*4%*
IV. Mixed anomalies	*5%*
Total percentage of ♂ with impaired morphology	*57%*

Morphological changes in germ cells.

Changes in the shape of the spermatozoa head

The morphological studies in Epididymitis chr. showed two predominant types of *abnormal head*: microcephalic, and round (Fig. 1A, Fig. 2). The first configuration had the highest percentage (19%), and the round-headed gametes represented 9% of the abnormal shapes. Macrocephalic (6%) and elongate-headed (3%) spermatozoa were also observed. The other atypical forms (amorphous and double head) were rare.

Another morphological alterations in shape of the spermatozoa

Other anomalies in the sperm morphology such as cytoplasmic residue or flagellum malformation were rarely registered in comparison to the head abnormalities.

Gametes with no tail (6%) or coiled tail (3%) were most commonly observed, the short and broken tail could rarely be seen (Figure 1B and Figure 2C).

The cytoplasmic droplet as a particular deformation was most frequently found around the neck, embracing the postacrosomal section of the head or the anterior part of the mitochondrial sheath (Figure 2D).

The results showed the highest percentage of sperm head anomalies (37%), less commonly observed tail anomalies (11%) and rarely seen cytoplasmic droplet (Table 3).

Besides spermatozoa with single defects, a small percentage of gametes with two or more nomalies in the sperm head and tail (5%) accompanied by cytoplasmic droplet was observed in Epididymitis chr. (Fig. 2C).

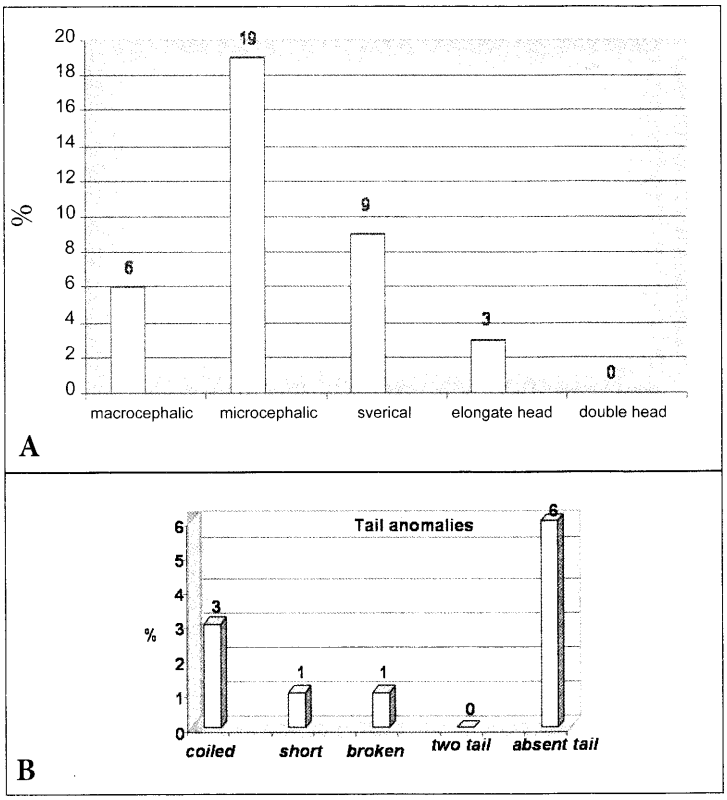

Fig. 1 Anomalies (%) in spermatozoa's head (A) and tail (B)

Cytochemical research of semen

We carried out a cytochemical research on semen plasma for meanwhile proving both nucleoproteins (DNP, RNP) and basic proteins in germ cells in order to follow up the maturity/immaturity of chromatin and basic proteins-containing (mainly protamine) cytoplasm.

In the control group of healthy men we found a large number of mature differentiated sperm intensively stained for basic proteins (Fig. 3A). The acrosome area, the nucleus and to a less extent, the area of the tail, were well visible. Basic proteins were stained in green by fast-gryin. The seminal plasma showed slight staining, and the nuclear chromatin – blue-purple, depending on the degree of decondensation (activation).

In semen samples from cases with Epididymitis, significantly reduced number of germ cells, immature sperm and dominated spermatids were observed (Fig. 3B) with a reduced amount of the basic proteins in the nucleus and chromatin decondensation.

Another sign indicating insufficient differentiation of gametes was the presence of so-called "oversize multinuclear cells" in the ejaculate which could be interpreted as similar to clusters, microcolony of undifferentiated spermatid cells, respectively. The nuclei of these cells probable are likely to be left in a common cytoplasm, "during the incomplete cell differentiation (Fig. 3D).

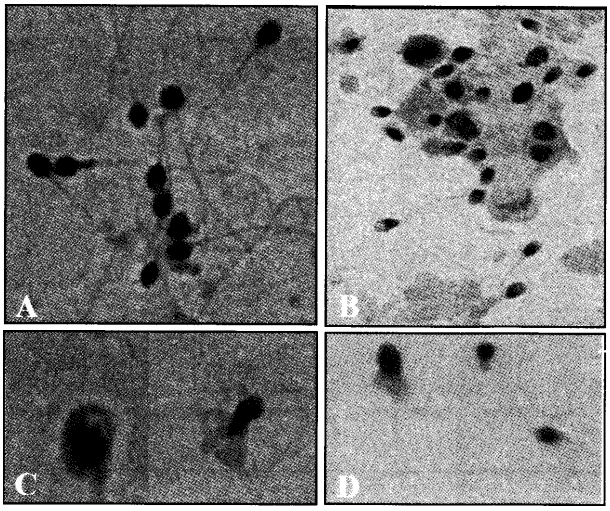

Fig. 2. Morphological changes in sperm in cases with Epididymitis chr. A-B – spermatozoa with normal, small, round and amorphous head and spermatids – (B); C – coiled tail and mixed anomalies; D – cytoplasmic droplet . Papanicolau, XE. X 450

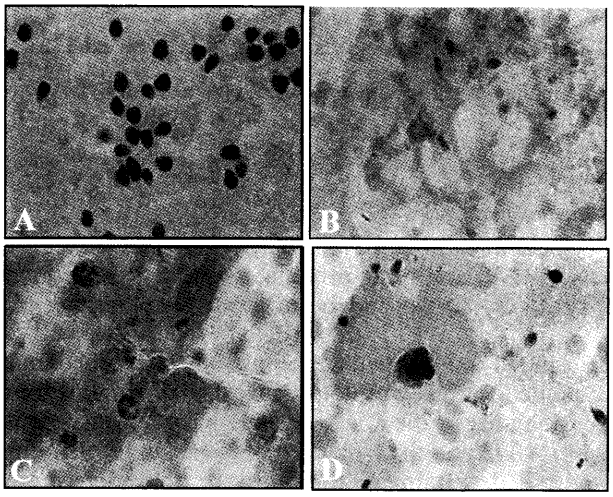

Fig. 3. Cytochemical research of semen plasma. A – normal spermatozoa, B-C – immature sperm, D – immature sperm and clusters of multinuclear cells. X 250; X 450; Immersio

Based on the above mentioned criteria for the degree of male infertility we can assess the fertilizing ability of patients with Epididymitis chr. We estimated it preserved in 46.67% of the cases, relatively preserved – in 38.09% and poor – in 14.28% fertilizing ability.

Discussion

Studies on the motility of gametes give a reason to some researchers to perceive this quality as a marker for good prognosis of male fertility – in vivo and especially in vitro fertilization [Auger et al., 1994; Elzanaty et al., 2002]. According to other authors [Lin et al., 1990] motility of sperm is the first visible indicator that changes with disturbance of the physico-chemical conditions of sperm regardless of etiologies factors. The studies in this area indicate that the epididymis and accessory sex glands play an important role in the formation of the functional status of the male gametes [Elzanaty et al., 2002; Gonzales et al., 1992].

Another major factor affecting the motility and fertility of germ cells appears their concentration and morphology. It is reported that in diseases of the male reproductive system changes occur in the morphology of germ cells, eg. increasing the number of immature gametes with abnormal shape [Fukuda et al., 1989].

Our results show a large number of Epididymitis patients with low concentration of sperm in the ejaculate. In different stages of Oligospermia (Gr. I-III), the number of spermatozoa decreased by about 3 times compared to the cases of Normospermia and about 4 times compared to the control group. It is notable the large proportion of gametes with abnormal morphology, both in Normospermia and Oligospermia. These data correlate with the results for the motility of the germ cells, demonstrating a lasting trend in the two groups (Normospermia and Oligozoospermia) to a very low number of normokinetic and hypokinetic gametes. Explanation of Oligo- and astenozoospermia could be the disadvantages that occur as a result of the presence of microorganisms (and their toxins) in the affected tissue, the entire range of elements of inflammation (high temperature etc.) and duration the disease process leading to the suppression and/ or inhibited sperm maturation [Viviani et al., 1991].

In our study on patients with Epididymitis chr. we found an increased number of morphologically damaged sperm. The most common changes in the structure of gametes concern the shape and size of the head and rarely the flagella.

Our results show a tendency to cells with small head and combination between small and round head, suggesting that the disease process affects the final stage of spermiogenesis. The presence of high percentage of small heads in inflammatory processes in the epididymis is usually the result of acrosome anomaly [Holstein et al., 2003] in the late spermatid stage. We can assume that these changes are dependent on the severity and duration of the disease and have individual character [Ilieva et al., 2009].

The cytochemical study according to the method of Zvetkova (2000) allows, on the one hand, a good differentiation of the nuclei with highly condensed chromatin from those with destructive DNA, and on the other, visualization of insufficient differentiated cells (spermatitds and prespermatids) and multicore claster similar forms with intense violet staining. Data for the seminal plasma quality are also obtained, which is strongly positive (green color by fast – green) for basic proteins with a probable origin from apoptotic or damaged spermatids or spermatogenic line cells. The results show a close correlation between the etiological factor of the infectious process and the extent of damage to the morpho-functional properties of gametes.

Moreover (even by electron microscopy), isolated large cytoplasmic residues are often seen, dispersed in semen. The reason for their appearance could be the presence of other cell types (lymphocytes, granulocytes and macrophages) and the influence of various biologically active substances, products of chronic inflammation [Giamarellon et al., 1984] and altered physico-chemical state of the ejaculate.

The injuries of the head and especially of the various segments of flagella decreased sperm motility and fertility, respectively [Weidner & Krause, 1999; Rives, 2005] and represent a common cause of male infertility.

References

1. Auger J., C. Serres, J. Wolf, P. Jouannet. Sperm motility and fertilization. Contracept. Fertil. Sex., 22, 1994, 3, 314-8.
2. Bedford J. The status and the state of the human epididymis. Hum. Reprod. Update., 9, 1994, 9, 2187-2199.
3. Cooper T. In defence of a function for the human epididymis. Fert. Ster., 54, 1990, 6, 964-975.
4. Elzanaty S., J. Richthoff, J. Malm, A. Giwercman. The impact of epididymal and accessory sex gland function on sperm motility. Human Reproduction, 17, 2002, 10, 2904-2911.
5. Fukuda M., P. Morales, J. Overstreet. Acrosomal function of human spermatozoa with normal and abnormal head morphology. Gamete Res., 24, 1989, 1, 59-65.
6. Giamarellon H., K. Tympanidis, N. Bitos. Infertility and chronic prostatitis. Andrologia, 16, 1984, 6, 417-422.
7. Gonzales G., G. Kortebani, A. Mazzolli. Leukocytospermia and function of the seminal vesicles on seminal quality. Fertil. Steril., 57, 1992, 6, 1058–1065
8. Holstein A., W. Schulze, M. Davidoff. Understanding spermatogenesis is a prerequisite for treatment. Reprod Biol Endocrinol., 1, 2003, 1, 107-109.
9. Ilieva I., P. Tzvetkova, N. Bojilova-Kirkova, S. Ivanova, B. Nikolov, Y. Gluchcheva. Morphometric measurements of spermatozoa on inflammatory male genital diseases. Journal of Biomedical & Clinical research, 2, 2009, 1, Suppl. 1, 7-10.
10. Jones R. To store or mature spermatozoa? The primary role of the epididymis. Int. J. Androl., 22, 1999, 3, 57-67.
11. Kerr J. Male reproductive system, In: Atlas of functional histology, Mosby – London, St. Lonis, Philadelphia, Sydney, Tokyo, 1998, 339-358.
12. Lin C., W. Chen, H. Chiang. Mump associated with nephritis. Child Nephrol. Urol., 10, 1990, 2, 68-71.
13. Rives NM. Chromosome abnormalities in sperm from infertile men with normal somatic karyotypes: asthenozoospermia. Cytogenet Genome Res., 2005, 111(3-4), 358-62.
14. Viviani S., G. Ragni, A. Santoro, L. Perotti,, E. Caccamo, E. Negretti, P. Valagussa, G. Bonadonna. Testicular dysfunction in Hodgkin's disease before and after treatment. Eur. J. Cancer, 27, 1991, 11, 1389–13921.
15. Weidner W., W. Krause. Orchitis. In: Encyclopedia of Reproduction. Knobil E. and Neill J. (eds), Academic Press. San Diego, 1999, 92-95.
16. Zvetkova E. Cytochemical studies of DNP, RNP and some basic proteins in mouse spermatozoa. Macedonian Journal of Reproduction, 6, 2000, 2, 123-128.

Institute of Experimental Morphology, Pathology and Anthropology with Museum
Bulgarian Anatomical Society

Acta morphologica et anthropologica, 19
Sofia • 2012

Two interesting variations of the rhomboid muscles

Lazar Jelev, Boycho Landzhov, Lina Malinova*

Department of Anatomy, Histology and Embryology, Medical University of Sofia
BG-1431 Sofia, Bulgaria

During routine student dissections two cases with unusual composition of the rhomboid muscles were observed. In the first case, the rhomboid major layers on both sides of a 65-y-old male cadaver were extremely well developed with and increased spinal attachment from T1-T7 spinous processes. In the second case, an additional to the rhomboids muscle was described bilaterally in a 72-year-old male cadaver. This aberrant muscle arose by a thin aponeurosis from the spinous processes of the mid-thoracic vertebrae and was attached laterally to the lowest part of the medial border of the scapula. The reported in the literature variations of the rhomboids are summarized and their possible clinical importance is discussed as well.

Key words: rhomboid muscles, variation, human

Introduction

The rhomboids are flat muscles from the superficial muscle group of the back that connect the scapula with the spinal column [3]. They are located under the trapezius layer and usually can be divided into two portions – the rhomboid minor, arising from C6-C7 (C7-T1) spinous processes and the rhomboid major arising from T1-T4 (T2-T5) spinous processes [2]. Despite the rhomboids' morphology seems to be quite constant [7], some interesting variations of these muscles have been reported in the anatomical literature. With this report, we present two such cases.

Case report

In the first case, after removal of the trapezius of a 65-y-old male cadaver, an extremely were developed rhomboids layer was observed on both sides (Fig.1). The following dissection revealed an increased spinal attachment of the rhomboid major, which in this case arose from the T1-T7 spinous processes.

In the second case, an interesting aberrant muscle (Fig. 2) was observed bilaterally during routine anatomical dissection of the superficial back structures of a 72-year-old male cadaver. The unusual muscle belonged to the layer of levator scapulae and rhom-

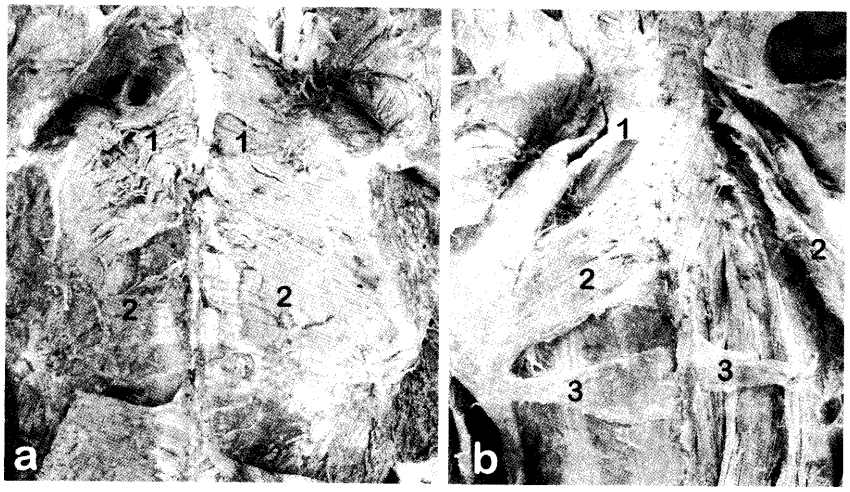

Fig. 1. Photographs of the findings described in Case 1(a) and Case 2(b). Muscles – 1, rhomboideus minor; 2, rhomboideus major; 3, rhomboideus tertius.

boids and was located below the lower border of the rhomboideus major. On the left side the aberrant muscle was slightly larger and started with a thin aponeurosis from the T6-T8 spinous processes, while on the right side it started from T6-T7 spinous processes. On both sides the muscle fibers directed nearly horizontally to insert into the lowest part of the medial border of the scapula. Careful dissection revealed an innervation by the dorsal scapular nerve.

Discussion

Numerous variations concerning the rhomboids have been reported in the literature: 1) absence (more frequently the rhomboid minor); 2) complete fusion of the two muscles; 3) separation into several bundles; 4) splitting into a superficial and deep layers; 5) extension of the vertebral origins in both a cranial and caudal direction [2,3,5-7]. There are also reports on the presence of small muscular slips of rhomboids that fused with some of the neighboring muscles – teres major, latissimus dorsi, serratus anterior [2,5,6]. Some authors described interesting aberrant muscles in the posterior neck related to the rhomboids – "rhomboideus occipitalis" [2,6] and "atlanto-rhomboideus" [9]. Two other unusual muscles have been described below the lower border of the rhomboid major and termed "m. rhomboideus minimus" [10] and "m. rhomboideus minus" [7]. A similar location had the aberrant muscle reported here in the second case. Because of its size, however, being larger than the rhomboid minor, a more plausible term for such a muscle would be "m. rhomboideus tertius".

In the clinical practice the variations of the rhomboids, despite being rare occasions, might have importance during particular surgical interventions such as intrathoracic muscle flap transfer [4] or muscle transfer for paralysis of the trapezius [1,8].

References

1. Bigliani LU, Compito CA, Duralde XA, Wolfe IN. Transfer of the levator scapulae, rhomboid major, and rhomboid minor for paralysis of the trapezius. J Bone Joint Surg Am 1996; 78: 1534-1540.
2. Bryce TH. Myology. In: Shafer ES, Symington J, Bryce TH, editors. Quain's Anatomy. Vol. VI, Part II. 11th Ed. New York, Toronto: Longmans, Green and Co., 1923, pp 90-96.
3. Clemente CD (ed.). Anatomy of the Human Body. 30th Ed. Philadelphia: Lea and Febiger, 1985, pp 515-516.
4. Grima R, Krassas A, Bagan P, Badia A, Le Pimpec Barthes F, Riquet M. Treatment of complicated pulmonary aspergillomas with cavernostomy and muscle flap: interest of concomitant limited thoracoplasty. Eur J Cardiothorac Surg 2009; 36: 910-913.
5. Le Double A-F. Muscles de la nique et du dos. In: Traité des Variations du Système Musculaire de l'Homme. Tome I. Paris: Schleicher Frères, 1897, pp 191-242.
6. Macalister A. Additional observations on muscular anomalies in human anatomy (third series), with a catalogue of the principal muscular variations hitherto published. Trans Roy Irish Acad 1875; 25: 1-130.
7. Mori M. Statistics on the musculature of the Japanese. Okajimas Fol Anat Jap 1964; 40: 195-300.
8. Romero J, Gerber C. Levator scapulae and rhomboid transfer for paralysis of trapezius. J Bone Joint Surg 2003; 85B: 1141-1145.
9. Ruge G. Anleitungen zu den Präparierübungen an der Menschlichen Leiche. I Bd. 4 Aufl. Leipzig: Verlag von Wilhelm Engelmann, 1908, pp 202-206.
10. von Haffner H. Eine seltene doppelseitige Anomalie des Trapezius. Internat Monatsschrift für Anat Physiol 1903; 20: 313-318.

Institute of Experimental Morphology, Pathology and Anthropology with Museum
Bulgarian Anatomical Society

Acta morphologica et anthropologica, 19
Sofia • 2012

Rare variety of additional right testicular vein rushing into right suprarenal vein and into right inferior suprarenal vein – a case report

M. Kalniev[1], D. Krystev[2], N. Krystev[3]

Department of Anatomy and Histology, MU – Sofia[1], College of Medicine "Jordanka Filaretova", MU – Sofia[2], Department of Anatomy and Histology, MU – Sofia[3]

During routine dissection, we came across a very interesting variation in the confluence of the right testicular vein. We saw additional right testicular vein which finally divided into two branches. The first branch flowed into the right lower phrenic vein and the second branch flowed into the right suprarenal vein. In addition we saw that right testicular artery passes behind the inferior vena cava. We made series of pictures and did literature. We did not find literature data describing a similar variation. Finally, we made a conclusion that a functional varicocele in the right side is possible very rarely.

Key words: testicular vessels, testicular veins, human, anatomical variation.

Introduction

The testis is an important organ upon which the survival of the human species depends. The testicular arteries and veins play major roles in the thermo-regulation that is essential for the efficient functioning of this organ. However, very little is found in the literature about the veins and their anatomical variations.

Material and Methods

During the dissections, we came across a very interesting variation in the confluence of the right testicular vein. We made a series of images that are presented below.

Results

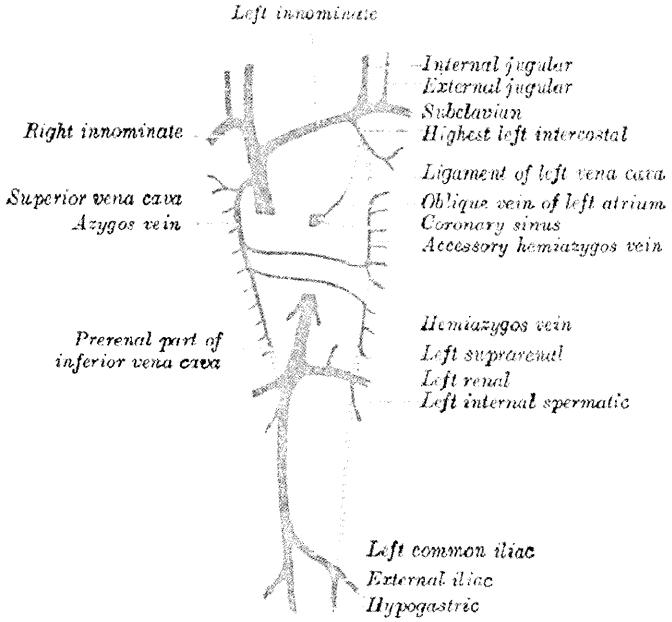

Fig. 1. A scheme showing system of superior vena cava and inferior vena cava in the human body.

Fig. 2. Presence of additional right testicular vein making the proximal direction. Clearly visible main right testicular vein rushing into inferior vena cava and right testicular artery.

Fig. 3. Presence of additional right testicular vein making the proximal direction. Main right testicular vein rushing into inferior vena cava. Right testicular artery passes behind the inferior vena cava.

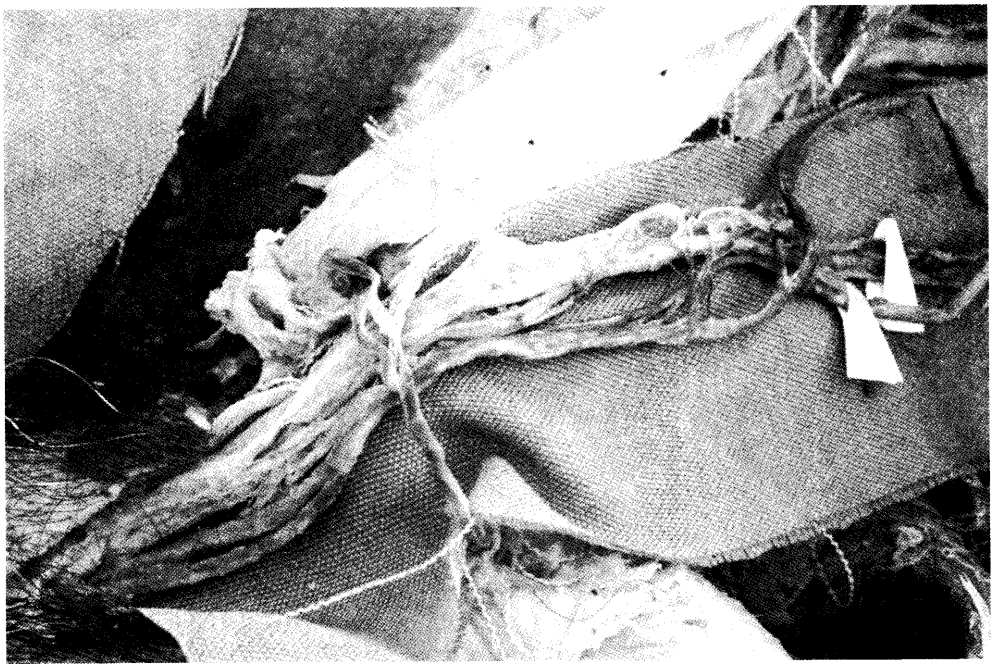

Fig. 4. Both right testicular veins are separate, but clinging to each other by connective tissue. We see the place where the general connective tissue „vagina" disappears and they go up alone.

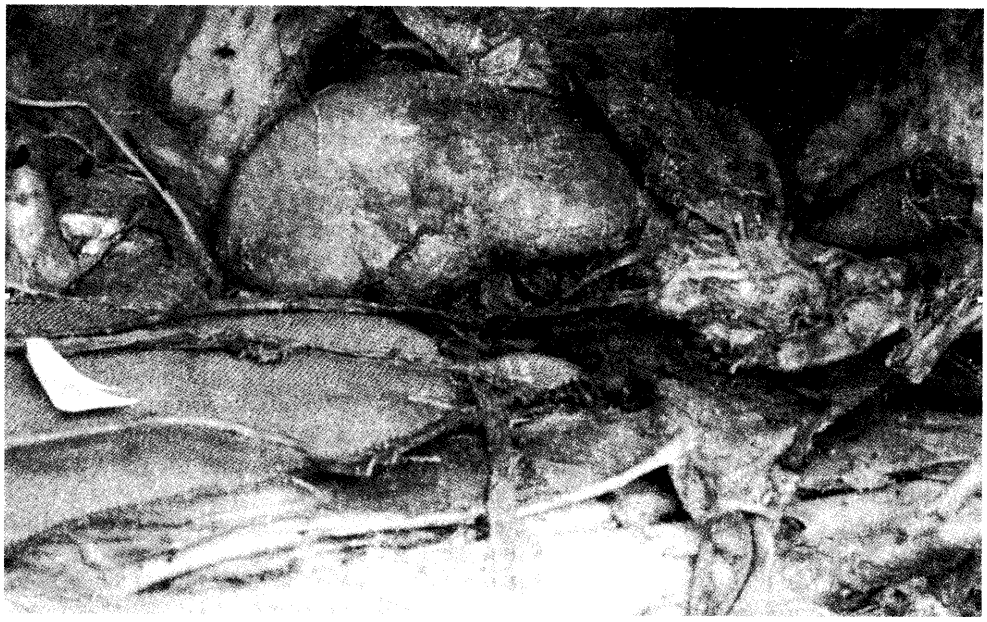

Fig. 5. Clearly visible side by side from top to bottom (right-left) additional right testicular vein, right testicular artery and main right testicular vein.

Fig. 6. Additional right testicular vein ends as two major pillars through: right lower phrenic (diaphragmatic) vein (which in turn splits) and the right suprarenal vein (which is behind the gland). You see the additional branches to the right kidney and right renal vein.

Discussion

Unlike the far more common variations of renal veins, which is written quite in the literature [4, 5, 6] the literature data about variations of testicular veins are much less. It is worth mentioning that the variations of testicular arteries are more common on the right side [8]. On the other hand according to literature data the variations of testicular veins are more common on the left side, 21.3% of people i.e. every fifth man has a variation in the testicular vein. In most of these cases, approximately in 16% variations are the left side [1]. In some of these cases the additional left testicular vein flows into lower tributary of left renal vein [2]. These variations are usually expressed in particular the presence of additional veins. Especially the veins were either completely or partially duplicated, with or without beading. The duplicated veins terminated in the corresponding renal veins either separately or after combining into one vein. In 4% of cases variations are bilaterally. Only about 1.3% of variations are in the right side [1]. As described previously in the literature, however, additional varieties the right testicular vein terminated in the right renal vein [3, 4, 7]. Sometimes the right testicular vein flows into the additional right renal vein [2].

Varieties in which the testicular vein flows into suprarenal vein or even in lower phrenic vein has not been described. The question arises whether the presence of this additional right testicular vein can contribute to the emergence of a functional varicocele on the right. Varicocele on the right side is generally symptomatic i.e. occurs in tumor processes in the pelvis or testicles e.g. – seminoma.

In general urology the presence of a varicocele on the right is a poor prognostic sign but as seen rarely is possible presence of a functional varicocele in the right side.

References

1. Asala, S., S.C. Chaudhary, N. Masumbuko-Kahamba, M. Bidmos. Anatomical variations in the human testicular blood vessels. – Ann. Anat., 183, 2001, №6, 545-549.
2. Biswas, S., J.C. Chattopadhyay, H. Panicker, J. Anbalagan, S.K.Ghosh. Variations In Renal And Testicular Veins – A Case Report. – J. Anat. Soc. India., 55, 2006-07 – 2006-12, №2
3. Merklin, R.J., N.A. Michels. The variant renal and suprarenal blood supply with data on inferior phrenic, ureteral and gonadal arteries. – J. Int. Coll. Surgeons., 29, 1958, 41-76.
4. Pick, J.W., B.J. Anson. Inferior Phrenic Artery: origin and suprarenal branches. – Anat. Rec., 78, 1940, 413- 427.
5. Rupert, R.R. Further study of irregular kidney vessels as found in one hundred cadavers. – Surg. Gynaecol. Obstet., 21, 1915, 471-480.
6. Satyapal, K.S. Classification of drainage pattern of renal veins. – J. Anat., 186, 1995, 329-333.
7. Satyapal, K.S. Additional renal vein: incidence and morphometry. – Clin. Anat., 8, 1995, 51-55.
8. Sylvia, S., S.V. Kakarlapudi, V.R. Vollala, B.K. Potu, R. Jetti, S.R. Bolla, M. Rao, N. Pamidi. Bilateral variant testicular arteries with double renal arteries. – Cases J., 2, 2009, 114.

Institute of Experimental Morphology, Pathology and Anthropology with Museum
Bulgarian Anatomical Society

Acta morphologica et anthropologica, 19
Sofia • 2012

Immunohistochemical study of the distribution of fibronectin in some zones of the meniscus

Manol Kalniev[1], Dimo Krystev[2], Nikolay Krystev[3], Kalin Vidinov[4]

Department of Anatomy and Histology, MU – Sofia[1], College of Medicine "Jordanka Filaretova", MU – Sofia[2], Department of Anatomy and Histology, MU – Sofia[3],Department of Endocrine Surgery, MU – Sofia[4]

The aim of our study was to trace out the distribution of the fibronectin in some different zones of the meniscus. The investigation was performed upon menisci of the knee joints of Wistar rats. A light microscopy, transmission electron microscopy and immunohistochemistry to demonstrate the fibronectin were used. We observed that fibronectin consisted of medium-sized granules located densely among themselves mainly in a row on the plasmalemma of cells in the SSZ. In TSZ the fibronectin consisted of fine and medium sized granules located not only on the cell membrane, but also near to the cells in the territorial matrix. Our observation revealed that in the deeper TPZ the fibronectin consisted by small granules situated in the territorial matrix of the cells.

Key words: meniscus, fibronectin, chondroblasts, fibroblasts, collagen.

Introduction

The fibronectin with the chondronectin and the ancorin is one of the adhesive glycoproteins in cartilage. They act as "cellular glue"[2, 8]. Very little has been written in the literature concerning the distribution of fibronectin in different areas of the meniscus [4, 5]. For this reason we aimed to investigate the presence and distribution of fibronectin in some areas of the meniscus.

Material and Methods

The materials of the investigation were menisci of the knee joint of 15 Wistar rats of both sexes, aged between 60 and 120 days, weighing about 250 g each. The animals were treated under the European Convention working with experimental animals. The fixation was carried out by glutaraldehyde and formaldehyde. Permanent histological preparations were obtained after appropriate procedures. They have been colored with HE and AZAN. Light microscopy (HE and AZAN), transmission electron microscopy (TEM) and immunohistochemistry to demonstrate the fibronectin were performed. We traced out the distribution of the fibronectin in some zones of the menisci.

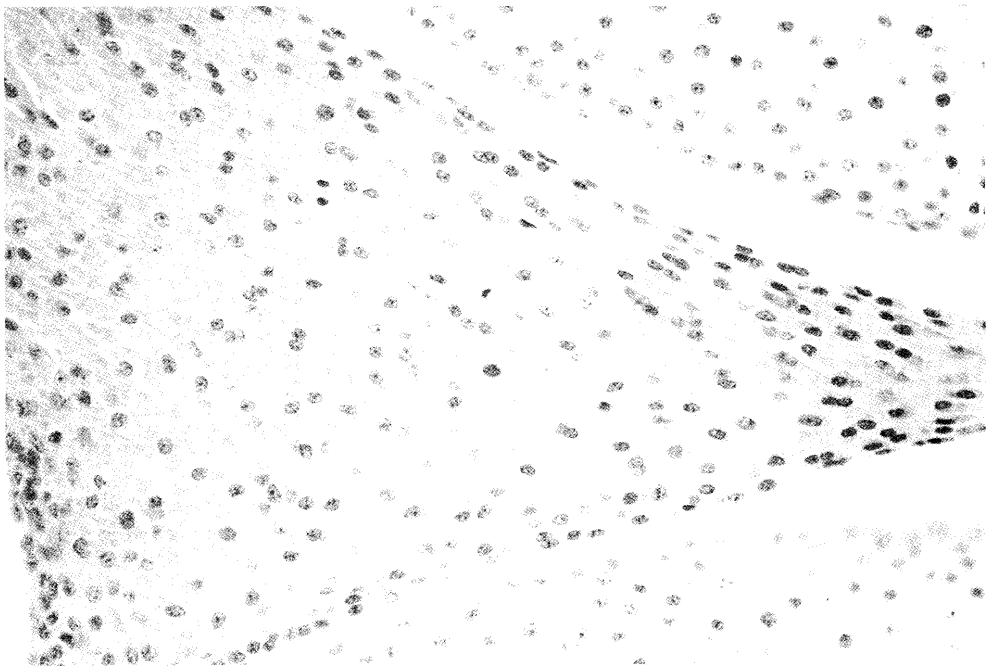

Fig.1. The Superficial Sliding Zone consists of 2 to 4 layers of elongated fibroblasts that have a longitudinal axis parallel to the articular cleft. The Transitional Sliding Zone is placed just below SSZ. It was composed of elliptical or oval cells with the character of chondroblasts and intercellular matrix represented by mixed network of collagen fibers type I and II. Staining – AZAN; X – 200.

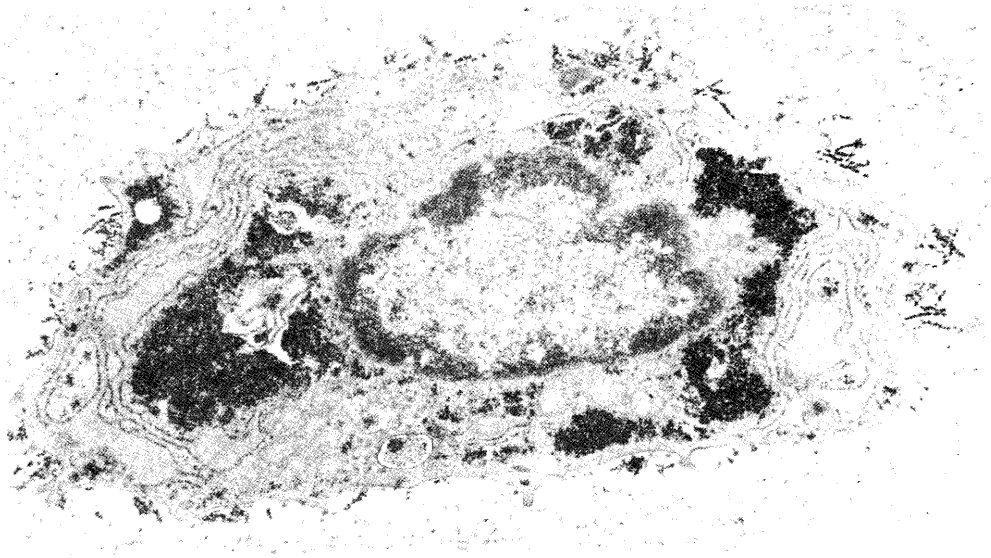

Fig. 2. Immunohistochemical study showed that the fibronectin is represented by medium-sized granules located densely among themselves mainly in a row on the plasmalemma of cells of the SSZ. TEM with immunohistochemistry for fibronectin; X – 11500

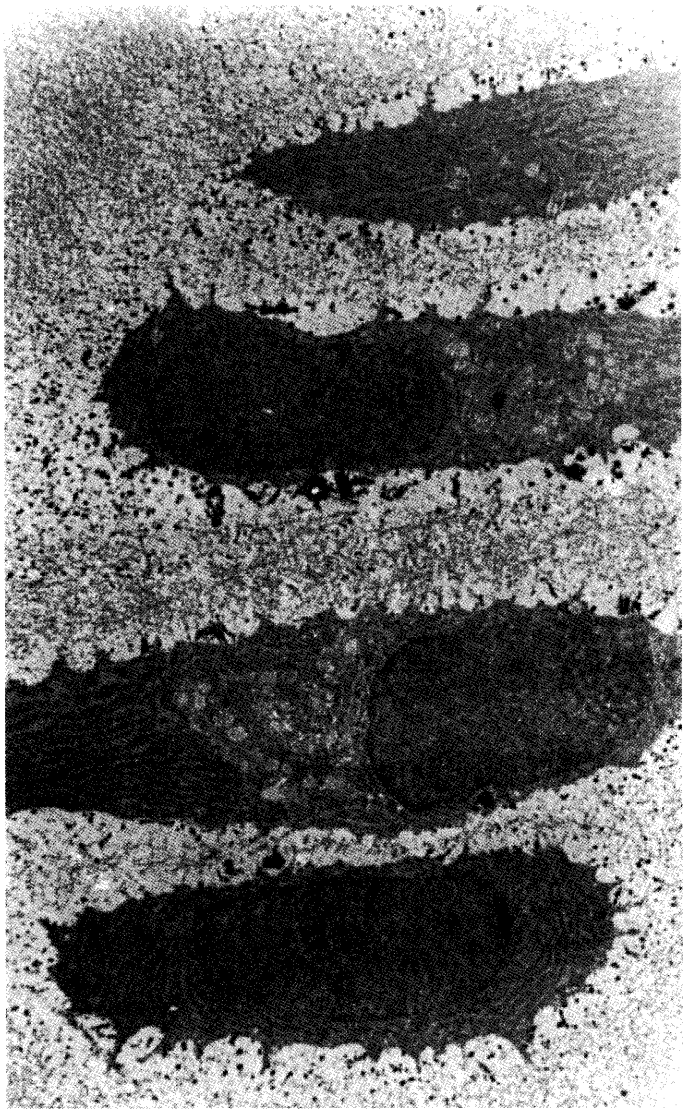

Fig. 3. Fine and medium sized granular fibronectin located near and on the cell membrane of TSZ. TEM with immunohistochemistry for fibronectin; X – 6000

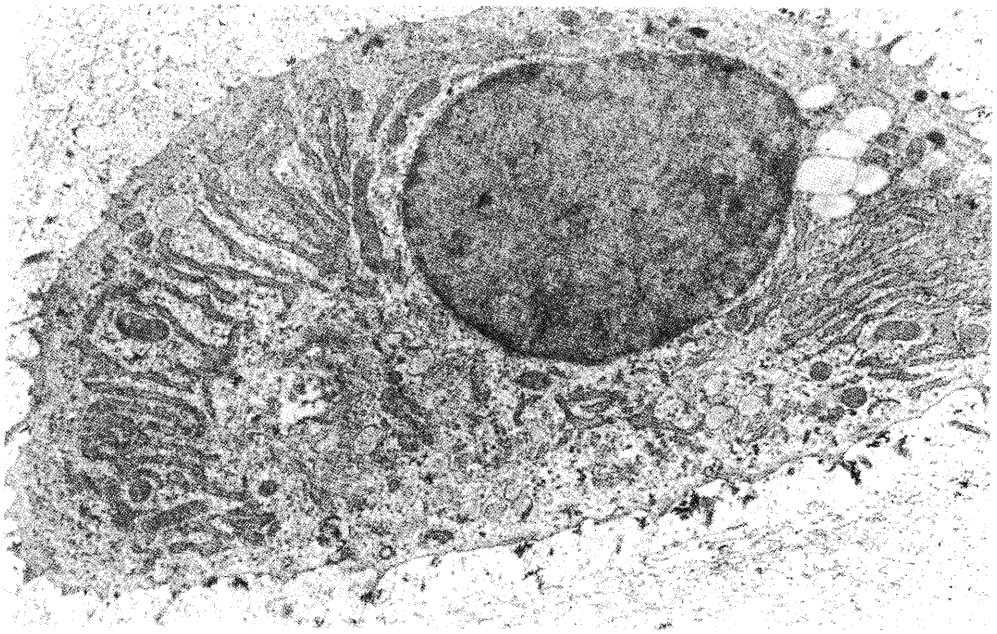

Fig. 4. Electron image showing the transitional pressure zone (TPZ) situated deeper in the meniscus. It is composed of chondroblasts with well-developed GER and Golgi complex. TEM; X – 8000

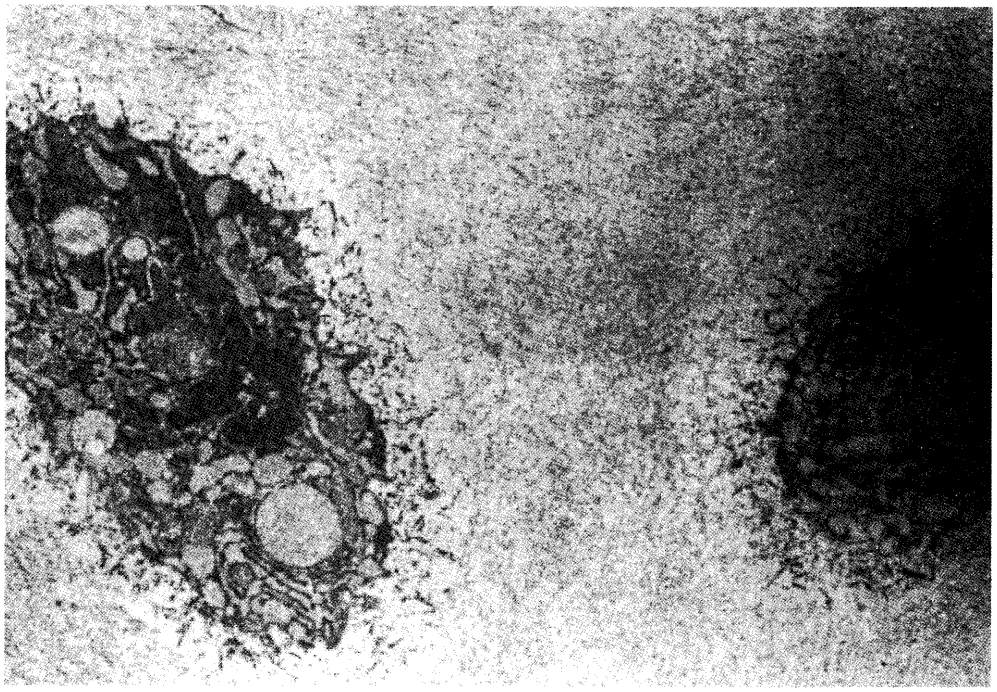

Fig. 5. Chondroblasts of TPZ. There were observed small granules of fibronectin in the territorial matrix. TEM with immunohistochemistry for fibronectin, X – 6000

Results

The results from light microscopic examination in AZAN showed the location of the Superficial Sliding Zone and the Transitional Sliding Zone in the meniscus.

Immunohistochemical study of fibronectin in SSZ indicates the presence of reaction product in the territorial matrix directly on the plasmalemma of cells. These are medium-sized granules located densely together most often in a row on the plasmalemma (Fig. 2). Sometimes it can be observed much granules in two or more lines, but in certain sections may be missing.

Immunohistochemical study of fibronectin in TSZ showed a similar picture as in SSZ. We observed fine and medium sized granular palisading arranged on the cell membrane of chondrocytes (Fig. 3).

The transitional pressure zone is composed by chondroblasts. They usually had well-developed GER and Golgi complex.

The study of fibronectin showed a large amount of reaction product in the territorial matrix of SPZ and TPZ. The reactionary granules are located densely and wrong without forming layers (Fig. 5).

Discussion

Unlike the chondronectin, which is available exclusively pericellular in the territorial matrix [2] and is associated with collagen type II and proteoglycan aggregates [7], our investigation shows that fibronectin is located both on the plasmalemma of cells and pericellular in the territorial matrix. Moreover, the fibronectin is placed in the territorial matrix of cells when the cells are chondroblasts [1, 3]. When the cells are fibroblasts as in SSZ the fibronectin is located upon plasmalemma itself moreover in a row. In TSZ the cells are chondroblasts [10] and the collagen is both type I and type II. The fibronectin in TSZ is situated both upon cell plasmalemma and in the territorial matrix. TPZ is composed by chondroblasts and collagen only type II [10]. The fibronectin in this zone is situated only in the territorial matrix around the cells but not on the plasmalemma of cells TPZ.

The distribution of the fibronectin is obviously related with the type of cells and collagen types in different zones of the meniscus. Cells are fibroblasts and the collagen is type I in SSZ [10]. Here the fibronectin is located only upon plasmalemma but not in the intercellular matrix. This fact confirms long-established concept, that fibronectin is a product of fibroblasts [9]. However its presence pericellular around chondroblasts shows that the fibronectin is also related with the chondrogenesis [6]. It is clear that further investigation about the distribution of the fibronectin in the other zones of the meniscus is necessary.

References

1. Clarke, I.C. Articular cartilage: a review and scanning electron microscope study. II The territorial fibrilar architecture. – J. Anat., 118, 1974, 268-280.
2. Hewitt, A.T., H.H. Varner, M.H. Silver, G.R. Martin. The role of chondronectin and cartilage proteoglycan in the attachment of chondrocytes to collagen. – Prog. Clin. Biol. Res., 110 B, 1982, 25-33.
3. Hunziger, E.B., W. Herrmann. In situ localization of cartilage extracellular matrix components by immunelectron microscopy after cryotechnical tissue processing. – J. Histochem. Cytochem., 35, 1987, №6, 647-655.

4. Mc Devitt, C.A., R.J. Webber. The ultrastructure and biochemistry of meniscal cartilage. – Clin. Orthop. Rel. Res., 252, 1990, 8-18.
5. Miller, R.R., C.A. Mc Devitt. The presence of thrombospondin in ligament, meniscus and intervertebral disc. – Glycoconjugate J., 5, 1988, p. 312.
6. Vasan, N.S. Analysis of perinotochordal materials. 2. Studies on the influence of proteoglycans in somite chondrogenesis. – J. Embryol. Exp. Morphol., 73, 1983, 263-274.
7. Vasan, N.S., J.W. Lash. Monomeric and aggregate proteoglycans in the chondrogenic differentiation of embryonic chick limb buds. – J. Embryol. Exp. Morphol., 49, 1979, 47-59.
8. Wu, J.J., D.R. Eyre, H.S. Slatter. Type VI collagen of the intervertebral disc: biochemical and electron microscopic characterization of the native protein. – Biochem. J., 248, 1987, 373-381.
9. Yoshimura, M., J.W. Lash, N. Vasan, A. Kaji. Inhibition of precartilaginous chick somites by oncogenic virus. – Dev. Biol., 97, 1983, №1, 70-80.
10. Калниев, М. Дисертация за ДМ. 2008, 73-97.

List of the most used abbreviations:
AZAN – azocarmine aniline orange
GER – granular endoplasmic reticulum
HE – haematoxylin eosin
SPZ – superficial pressure zone
SSZ – superficial sliding zone
TEM – transmission electron microscopy
TPZ – transitional pressure zone
TSZ – transitional sliding zone

Institute of Experimental Morphology, Pathology and Anthropology with Museum
Bulgarian Anatomical Society

Acta morphologica et anthropologica, 19
Sofia • 2012

Unusual insertion of the pectoralis minor muscle

Yuliyan Kartelov, Lazar Jelev, Dimka Hinova-Palova, Adrian Paloff, Wladimir Ovtscharoff*

Department of Anatomy, Histology and Embryology, Medical University of Sofia
BG-1431 Sofia, Bulgaria

In this report the authors described an interesting variation in the insertion of the pectoralis minor muscle. It was found during routine anatomical dissections of the upper limbs and shoulder joints. In one left upper limb and one dissected left shoulder joint the pectoralis minor tendon was divided into a lateral portion attached as usual to the coracoid process and a small medial portion attached to the capsule of the shoulder joint and the glenoid labrum. The possible clinical implications of the abnormal pectoralis minor tendon is discussed.

Key words: pectoralis minor muscle; abnormal tendon; variation; clinical significance

Introduction

The pectoralis minor is a flat triangular muscle located on the upper-lateral part of the thorax, posterior to pectoralis major muscle. It is commonly composed of three muscular slips arising from the third, fourth and fifth ribs near their cartilages. Upwards and laterally the muscular slips converged to insert into the medial border and superior surface of the coracoid process of the scapula. In some rare cases, however, the pectoralis minor may have some additional insertion points [3-5,7,8].

Case report

Two cases of unusual insertion of the pectoralis minor were accidentally found during routine anatomical dissections of the upper limbs and shoulder joints from the autopsy material available at the Department of Anatomy, Histology and Embryology of the Medical University of Sofia. In both cases, one left upper limb (Fig. 1) and one left dissected shoulder joint (Fig. 2), the tendon of the pectoralis minor was divided into two portions – a medial and lateral. The lateral portion was attached to the medial border and superior surface of the coracoid process of the scapula. The small aberrant medial portion turned around the upper surface of the coracoid process and inserted into the capsule of the shoulder joint and the upper-posterior part of the glenoid labrum. We found also an interesting synovial bursa between the lower surface of the medila tendinous portion and the upper surface of the coracoid process.

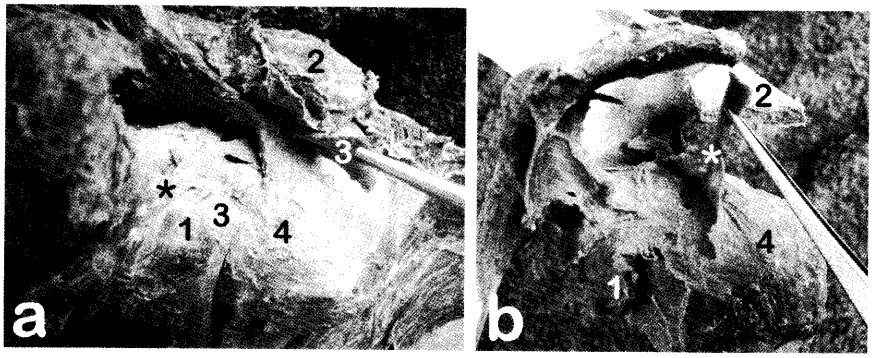

Fig. 1. Photographs of the reported variant incertion (asterisk) of the pectoralis minor found in a dissected upper limb (a) and isolated shoulder joint (b). 1, coracoid process of the scapula; 2, acromion; 3, coracoacromial ligament; 4, humeral head covered by the shoulder joint capsule.

Discussion

Many insertional variations of the pectoralis minor have been described in the literature. In addition to the usual coracoid insertion, some portion of the tendon have been found attached to the acromioclavicular ligament, the supraspinatous tendon, the glenoid labrum, the shoulder joint capsule, the greater or lesser tubercules of the humerus [3-5,7,8]. Most of these variations were described on cadaver dissection, but recently such unusual insertions have been also observed in patients by means of modern imaging techniques. By ultrasonographic and CT methods, Homsi et al. [2] found that in 9.6% of the patients the pectoralis minor showed some variations in its insertion. Moreover, an ectopic tendon of the pectoralis minor was observed during exploratory surgery in a patient reporting pain during shoulder movement [6]. By that reason, some authors claimed the variations in the insertion of the pectoralis minor as a possible cause of antero-internal conflict of the scapula [1].

References

1. Apoil A. Le conflit antero-interne de l'epaule. Ann Radiol (Paris) 1992; 35:161-166.
2. Homsi C, Rodrigues MB, Silva JJ, Stump X, Morgan G. Aspect echographic des anomalies d'insertion du muscle pectoralis minor (petit pectoral). J Radiol 2003 ;84:1007-1011.
3. Le Double A-F. 1897. Muscles des parois de la poitrine. In: Traité des Variations du Système Musculaire de l'Homme. Tome I. Paris: Schleicher Frères. pp 243-286.
4. Macalister A. Additional observations on muscular anomalies in human anatomy (third series), with a catalogue of the principal muscular variations hitherto published. Trans Roy Irish Acad 1875;25:85-86.
5. Musso F, Azeredo RA, Tose D, Marchiori JGT. Pectoralis minor muscle. An unusual insertion. Braz J morphol Sci 2004;21:139-140.
6. Samuel P, Blanchard JP. Syndrome de la coiffe des rotateurs par anomalie d'insertion du petit pectoral.Rev Chir Orthop 1984;70:401-404.
7. Uzel AP, Bertino R, Caix P, Boileau P. Bilateral variation of the pectoralis minor muscle discovered during practical dissection. Surg Radiol Anat 2008; 30:679-682.
8. Wood J. On human muscular variations and their relation to comparative anatomy. J Anat Physiol 1867;1:44-59.

Institute of Experimental Morphology, Pathology and Anthropology with Museum
Bulgarian Anatomical Society

Acta morphologica et anthropologica, 19
Sofia • 2012

Fat embolism during hip replacement. Risk Reduction

Y. G. Kolev[1], St. R. Rachev[2], P. S. Kinov[3], D. D. Radoinova[4]

[1] *Department of Forensic medicine, District Hospital MBAL, Gabrovo*
[2] *Department of Clinical Pathology, District Hospital MBAL, Gabrovo*
[3] *Clinic of Orthopaedics and Traumatology, University Hospital "Tsaritsa Yoanna – ISUL", Sofia*
[4] *Department of Forensic medicine and Deontology, Medical University, Varna*

Fat embolism is a complication of long bone fractures, intramedullary fixation and joint arthroplasty. It may progress to fat embolism syndrome, which can occasionally be fatal. Thrombembolic complications, which include the fat embolism syndrome, are well-known consequences of femoral total hip replacement. The increase in intramedullary pressure in the femur is the most decisive pathogenic factor for the development of embolic phenomena. Three cases of intraoperative death during total hip replacement of patients aged over 65 are reported. The efficiency of new techniques developed to prevent the risk of intraoperative pulmonary embolism was assessed. The observed mortal cases were discussed and the increased risk in elderly patients addressed. All the options to reduce the amount of fatty tissue in the medullary cavity and pressure during total hip arthroplasty should be considered. Application of jet lavage is to be a regular practice in all clinics.

Key words: fat embolism, hip arthroplasty, elder patients, intraoperative death

Introduction

Fat microembolism is a complication with embolism of the vessels of internal organs with fat drops, entering the veins around fractures of long tubular bones and pelvis, extensive subcutaneous fat tissue trauma, or during intramedullary fixation and arthroplasty.

This phenomenon may progress to the development of fat embolism syndrome, which is relatively rare but leads to prominent clinical manifestations and in some cases to death [4, 5].

Thromboembolic complications that include fat embolism syndrome are well known for hip arthroplasty.

There are several theories about the pathogenesis of fat embolism.

The main mechanism (classical pathophysiologically confirmed theory) is entering in the veins of fat droplets from the site of tissue damage. They pass by the bloodstream through the heart and enter the arterioles and capillaries in the lungs, leading to obstruction (Fig. 1). Drops (to approx. 20%) can undergo pulmonary arterio-venous anastomoses and reach other internal organs – brain, kidneys (Fig. 2).

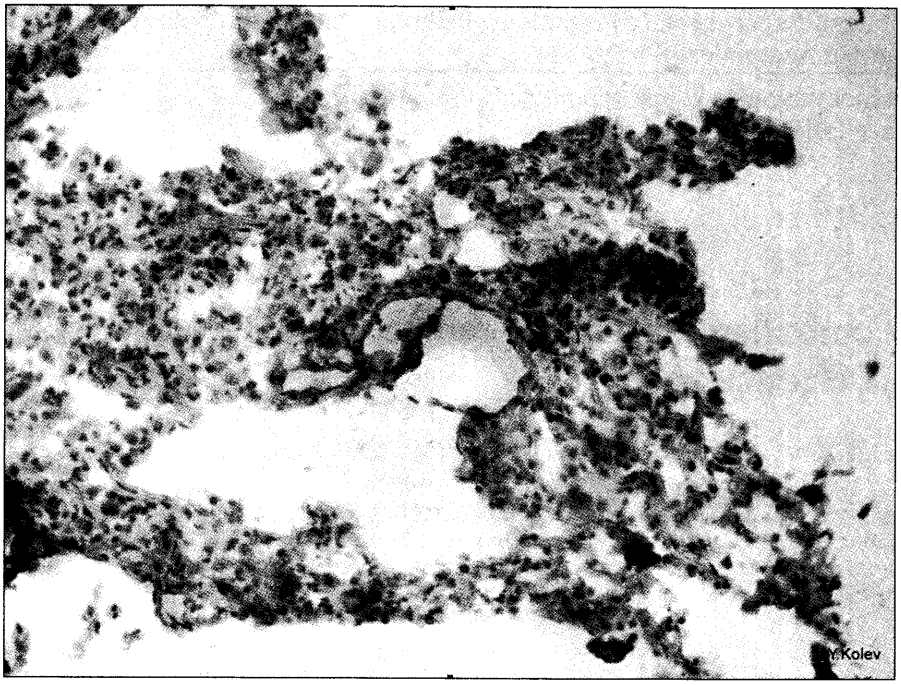

Fig. 1 Fat microembolism in lungs (Sudan III staining)

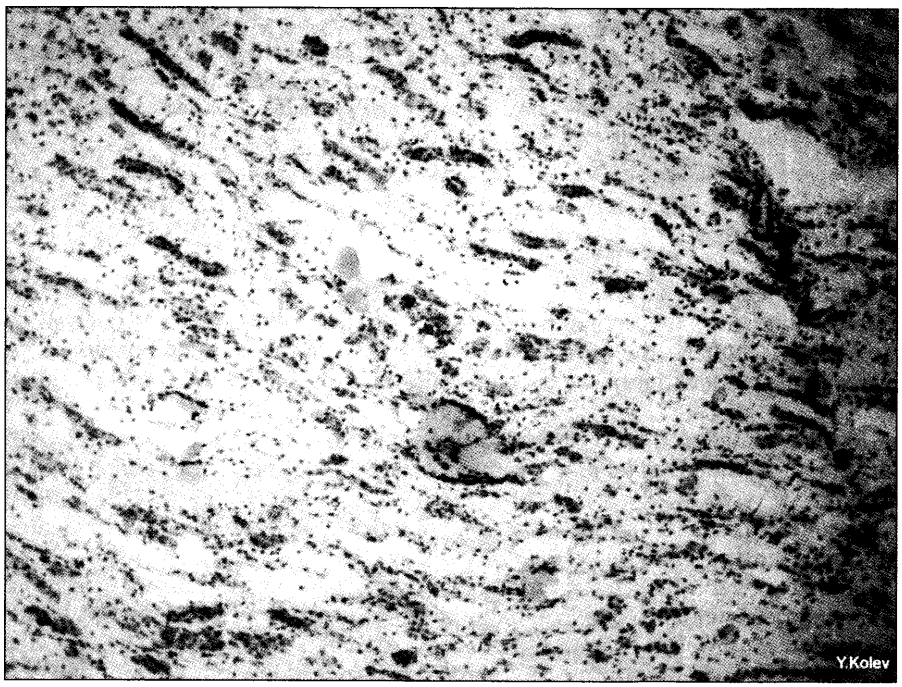

Fig. 2 Fat microembolism in kidney (Sudan III staining)

Clinical forms of fat embolism:

- Fulminant – leads to death within minutes
- Acute – developing in the first hours after trauma or intervention
- Subacute – a latency period of 12 to 72 hours

Clinical features of fat embolism:

- Cerebral disorders similar to hypoxic encephalopathy, disturbances in consciousness in the form of mental inadequacy
- Cardio-respiratory dysfunction
- Capillaropathy (petechial hemorrhages on skin and mucous membranes)
- Hyperthermia, which is unaffected by conventional therapy

Fat microembolism and total hip arthroplasty

According to Maxeiner, the hip arthroplasty is the most common cause of fatal fat embolism in the lungs [8].

Due to a well-developed venous system, especially in supracondylar area, the increased pressure in the femoral cavity leads to embolization by the contents of the bone marrow.

Pressure rise during the implantation of prosthetic joint with cement is an output of this mechanism [1, 2, 15].

Logical therapeutic measure is to avoid biological spontaneous drainage of the femur.

Several cases of perioperative death during total hip arthroplasty drew our attention:

- Case 1: A 69-year-old woman with coxarthrosis and rheumatoid arthritis, died at the end of the operation. The autopsy showed that the cause of death was a massive fat embolism in the lung vessels (Sudan III staining).
- Case 2: 75-year-old woman with a fracture of the femoral neck, died at the end of the operation. Autopsy and microscopic findings also suggest fat embolism in the lungs.
- Case 3: 72-year-old man with a basicervical hip fracture died at the end of the operation. Again, the cause of death was massive pulmonary fat microembolism.

Common to these cases, which are for a period of three years (2010-2012), was a case of death in people aged over 65.

Discussion

A specific feature in adults is the change of bone marrow substance (*medulla ostium rubra*) in the bone cavity of the femur to adipose tissue (*medulla ostium flava*).

The main factor for higher mortality in adults with total hip arthroplasty is the above mentioned anatomical feature [16]. Embolism occurs in most cases during the implantation of the femoral component. The polymerization of cement increases the volume and temperature, the pressure rises.

Over the past 15 years there have been publications about such cases [6, 7, 11]. There are implemented suggestions for improvement in surgical techniques. The goal is risk reduction.

Implemented improvements:

- Better preparation of the intramedullary cavity, lavage, drainage
- Jet lavage [3] (Fig.3)

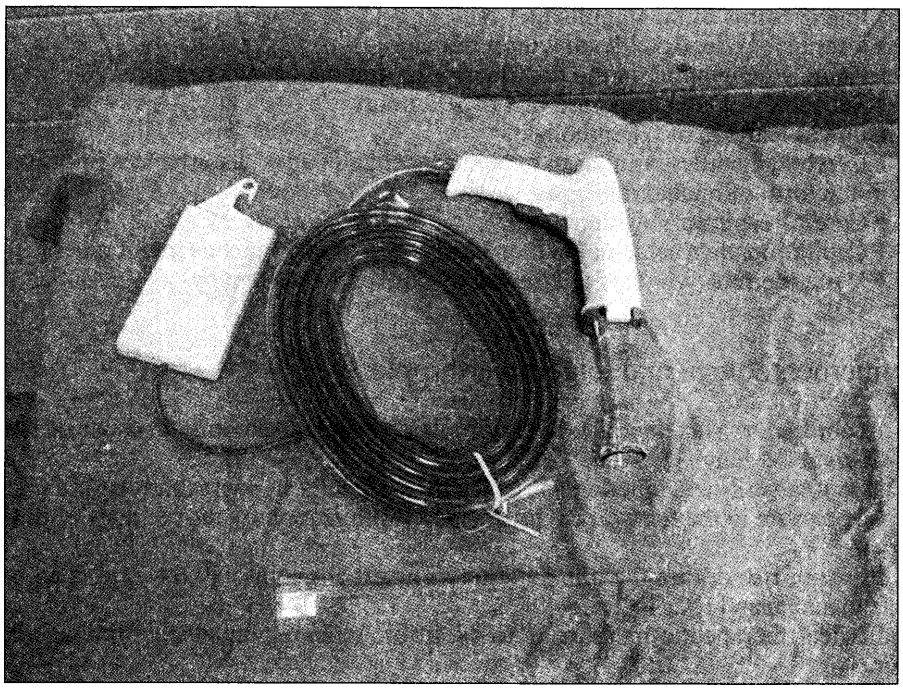

Fig. 3 Set for jet-lavage

- Trans-prosthetic + vacuum drainage system [14]
- Proximal drainage placed along the *Linea aspera* and distal drainage placed in the diaphysis, by creating a vacuum in the medullary cavity during insertion of the stem [12]

The improved technique reduces the risk substantially and actually allows almost no mortality in these operations [17, 18].

Conclusion

The observed mortal cases were discussed at clinical conferences and addressed the increased risk in elderly patients. All the options to reduce the amount of fatty tissue in the medullary cavity and pressure during total hip arthroplasty should be given. Application of jet lavage is not a regular practice in all clinics, but obviously should be, despite the increased expenses.

References

1. Byrick R. J., J. B. Mullen, C. D. Mazer, C. B. Guest. Transpulmonary systemic fat embolism. Studies in mongrel dogs after cemented arthroplasty. Am. J. Respir. Crit. Care Med. 150(5 Pt 1), 1994, 1416-22.
2. Hagley S. R., F. C. Lee, P. C. Blumbergs. Fat embolism syndrome with total hip replacement. Med. J. Aust. 145(10), 1986, 541-3.

3. Heisel C., H. Mau, T. Borchers, J. Müller, S. J. Breusch. Fat embolism during total hip arthroplasty. Cementless versus cemented – a quantitative in vivo comparison in an animal model. Orthopade. 32(3), 2003, 247-52.
4. Khandheria B. K., J. B. Seward, A. J. Tajik. Transesophageal echocardiography. Mayo Clin. Proc. 69(9), 1994, 856-63.
5. Koch S., A. Forteza, C. Lavernia, J. G. Romano, I. Campo-Bustillo, N. Campo, S. Gold. Cerebral fat microembolism and cognitive decline after hip and knee replacement. Stroke. 38(3), 2007, 1079-81.
6. Marshall P. D., D. L. Douglas, L. Henry. Fatal pulmonary fat embolism during total hip replacement due to high-pressure cementing techniques in an osteoporotic femur. Br. J. Clin. Pract. 45(2), 1991, 148-9.
7. Maxeiner H. Fatal intraoperative lung fat embolism in endoprosthesis of the hip joint. Beitr. Gerichtl. Med. 47, 1989, 415-27.
8. Maxeiner H. Significance of pulmonary fat embolism in intra- and early postoperative fatal cases following femoral fractures of the hip region. Orthopade. 24(2), 1995, 94-103.
9. Modig J., C. Busch, S. Olerud, T. Saldeen, G. Waernbaum. Arterial hypotension and hypoxaemia during total hip replacement: the importance of thromboplastic products, fat embolism and acrylic monomers. Acta Anaesthesiol. Scand. 19(1), 1975, 28-43.
10. Patel R., J. Stygall, J. Harrington, S. Newman, F. Haddad. Intra-operative cerebral microembolisation during primary hybrid total hip arthroplasty compared with primary hip resurfacing. Acta Orthop. Belg. 75(5), 2009, 671-7.
11. Pitto R. P., M. Koessler. The risk of fat embolism during cemented total hip replacement in the elderly patient. Chir. Organi Mov. 84(2), 1999, 119-28.
12. Pitto R. P., M. Koessler, K. Draenert. The John Charnley Award. Prophylaxis of fat and bone marrow embolism in cemented total hip arthroplasty. Clin. Orthop. Relat. Res. (355), 1998, 23-34.
13. Renne J., R. Wuthier, E. House, J. C. Cancro, F. T. Hoaglund. Fat macroglobulemia caused by fractures or total hip replacement. J Bone Joint Surg Am. 60(5), 1978, 613-8.
14. Schmidt J., C. Sulk, C. Weigand, K. La Rosée, T. Schneider. Preventing fat embolism syndrome (FES) in implantation of cemented hip endoprosthesis shafts with a trans-prosthetic drainage system (TDS). Biomed. Tech. 46(11), 2001, 320-4.
15. Wenda K., J. Degreif, M. Runkel, G. Ritter. Pathogenesis and prophylaxis of circulatory reactions during total hip replacement. Arch. Orthop. Trauma Surg. 112(6), 1993, 260-5.
16. Wenda K., G. Ritter, J. Ahlers, W. D. von Issendorff. Detection and effects of bone marrow intravasations in operations in the area of the femoral marrow cavity. [article in German] Unfallchirurg. 93(2), 1990, 56-61.
17. Wenda K., M. Runkel, L. Rudig, J. Degreif. The effect of bone marrow embolization on the choice of procedure in the stabilization of femoral fractures. [article in German] Orthopade. 24(2), 1995, 151-63.
18. Ulrich C. Value of venting drilling for reduction of bone marrow spilling in cemented hip endoprosthesis. [article in German] Orthopade. 24(2), 1995, 138-43.

Institute of Experimental Morphology, Pathology and Anthropology with Museum
Bulgarian Anatomical Society

Acta morphologica et anthropologica, 19
Sofia • 2012

Serum IgG and IgM antibodies to GD1a ganglioside in adults – preliminary data

V. Kolyovska, D. Deleva

Institute of Experimental Morphology, Pathology and Anthropology with Museum, Bulgarian Academy of Sciences, Sofia

Over the past few years it is of critical importance to establish the clinical significance of serum IgG and IgM anti-GD1a antibodies as potential biomarkers of neuronal damage in immune-mediated neuropathies and neurodegenerative diseases. In this study the diagnostic value of IgG and IgM anti-GD1a antibodies was determined by ELIZA method in the serum of 11 adult patients (70-81 years). Significantly elevated serum antiganglioside IgG and IgM antibodies titers were detected only in three patients. These data suggest the immune-mediated neurodegeneration and antibody -mediated neuropathies. Therefore, IgG and IgM anti-GD1a antibodies can serve as hallmarkers lead to nervous system dysfunction.

Key words: serum IgG and IgM anti-GD1a antibodies

Introduction

Gangliosides are a family of acidic glycosphingolipids highly concentrated in the nervous system, where they represent about 10% of the total lipid content. The ganglioside spectra of normal blood plasma are remarkably stable, but show pronounced changes in pathological conditions [5]. GD1a is one of the major central nervous system neuronal ganglioside fraction. In our previous studies a considerable increase of serum GD1a ganglioside was determined in MS (neurodegenerative multifactorial disorder with an autoimmune component) [9,10,11]. Autoantobodies against gangliosides GM1 or GD1a are associated with acute motor axonal neuropathy and acute motor-sensory axonal neuropathy [7]. That'swhy, over the past few years it is of critical importance to establish the clinical significance of serum IgG and IgM anti-GD1a antibodies as potential biomarkers for the diagnosis, classification, disease activity and prediction of clinical courses in anti-ganglioside antibody-mediated neurodegenerative disorders.

No immunological studies about the possible role of serum IgG and IgM anti-GD1a antibodies in adults (over 70 years old) have been performed so far. Therefore, the aim of this study was to evaluate the levels of IgG and IgM anti-GD1a antibodies in the serum of these adult patients.

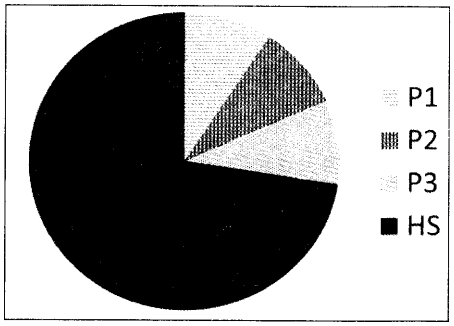

Fig.1. Percentage distribution of antiganglioside antibodies of the IgG and IgM class against GD1a ganglioside in adult patients
P1, P2, P3 – Adult patients; HS – Healthy subjects

Materials and Methods

Serum samples were obtained from 32 healthy subjects (middle age) and from 11 adult patients (70– 81 years) without neurological clinical symptoms. We determined antiganglioside antibodies (AGA) of the IgG and IgM class against GD1a ganglioside. The presence of anti-GD1a antibodies in the serum was measured by the enzyme-linked immunosorbent assay (ELISA). We made slight modifications of the method of Mitzutamari et al. [4,6]. As AGA were found in low titers in some healthy subjects we estimated a reference range for the healthy controls. Adult patients were considered strongly positive only if the optical density of their sera exceeded $x \pm 2$ SD of the healthy controls. The Student test was used to determine statistical differences between the groups using $p<0.05$ as the level of confidence.

Results and Discussion

The difference of optical density of serum IgG and IgM anti-GD1a antibodies between two groups (strongly positive adults and healthy subjects) was statistically significant. Elevated serum IgG and IgM titers to GD1a gangliosides were detected only in three adult patients (27.3 %) of the 11 studied adults. The remaining eight patients (72.7 %) had values similar to those of healthy controls (Fig. 1). Significantly elevated serum IgG and IgM antibodies titers to GD1a gangliosides in three adult patients in comparison with healthy subjects are shown in Fig. 2 and Fig. 3. Anti-ganglioside complex antibodies may be useful diagnostic and prognostic markers of the neuropathy [2]. Patients with a positive titer of anti-ganglioside antibodies had significant alterations of motor conduction parameters and contribute to the neuropathy [3]. In immune mediated neuropathies associated with antibodies to GM1, GD1a and GD1b the common mechanism is a complement mediated dysfunction and disruption of the nodes of Ranvier which causes a pathophysiological continuum from early reversible conduction failure to axonal degeneration [8]. These findings confirm a disease specific correlation between specific neuropathies and antiganglioside antibodies clinically useful [1].

In conclusion, our preliminary study permits us to find that: elevated titers of IgG and IgM anti– GD1a antibodies suggest the immune-mediated neurodegeneration; IgG and IgM anti–GD1a antibodies can serve as a biological marker for neuronal and

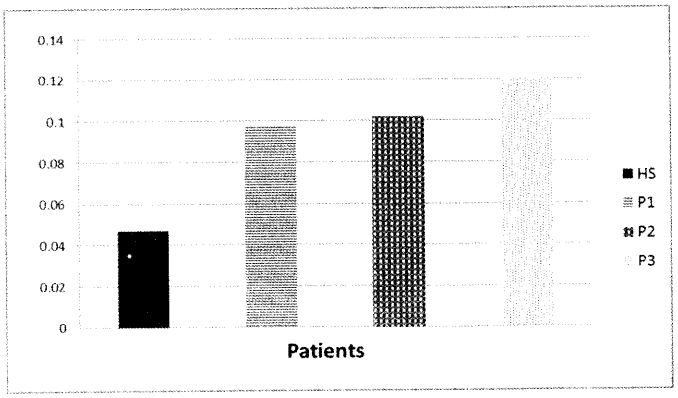

Fig.2. Serum IgG antibodies to GD1a in adults in comparison with healthy subjects

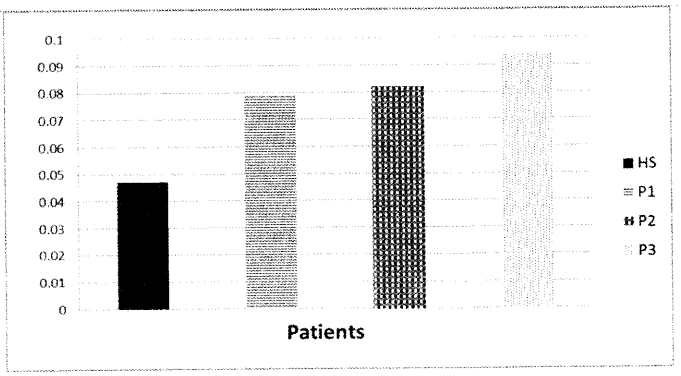

Fig.3. Serum IgM antibodies to GD1a in adults in comparison with healthy subjects

axonal damage, a very important indication for immediate neuroprotective treatment and its efficacy; there is not direct relationship between patient's age and the presence of symptomatic neurological damage.

References

1. Gallardo, E., R. Rojas-García, R. Belvís, C. Serrano-Munuera, E. Ortiz, N. Ortiz, J. Grau, I. Illa. Antiganglioside antibodies: when, which and for what. -Neurologia, 16 (7), 2001, 293-297.
2. Kusunoki, S. Immune-mediated neuropathies. – Rinsho Shinkeigaku., 49 (11), 2009, 956-958.
3. Matà, S., E. Betti, G. Masotti, F. Pinto, F. Lolli. Motor nerve damage is associated with anti-ganglioside antibodies in diabetes. – J Peripher Nerv Syst., 9 (3), 2004, 138-143.
4. Mizutamari, R.K., H. Wiegandt, G. Nores. Characterization of antiganglioside antibodies present in normal human plasma. – J. Neuroimmunol., 50 (2), 1994, 215-220.
5. Prokazova, N., L. Bergelson. Gangliosides and atherosclerosis. – Lipids, 29, 1994, 1-5.

6. Ravindranath, M.H., S. Muthugounder. Human antiganglioside autoantobodies: validation of ELISA. – Ann NY Acad Sci., 1050, 2005, 229 – 242.
7. Susuki, K., N. Yuki, D.P. Schafer, K. Hirata, G. Zhang, K. Funakoshi, M.N. Rasband. Dysfunction of nodes of Ranvier: a mechanism for anti-ganglioside antibody-mediated neuropathies. – Exp Neurol., 233 (1), 2012, 534-542.
8. Uncini, A. A common mechanism and a new categorization for anti-ganglioside antibody-mediated neuropathies. – Exp. Neurol., 235 (2), 2012, 513-516.
9. Zaprianova, E., D. Deleva, B. Sultanov, V. Kolyovska. Biological markers of neuronal damage and disturbed axon-oligodendroglial interactions in early multiple sclerosis. – Compt. Rend. Acad. Bulg. Sci., 61 (3), 2008, 407-412.
10. Zaprianova, E., D. Deleva, B. Sultanov, V. Kolyovska. Current knowledge of multiple sclerosis pathogenesis. – Acta morphol. et anthropol., 14, 2009, 136-140.
11. Zaprianova, E., S.S. Sergeeva, O.S. Sotnikov, D. Deleva, B. Sultanov, V. Kolyovska, T.V. Krasnova. Evidence of early neuronal damage in the serum of multiple sclerosis patients. – Compt. Rend. Acad. Bulg. Sci., 63 (3), 2010, 447-454.

Institute of Experimental Morphology, Pathology and Anthropology with Museum
Bulgarian Anatomical Society

Acta morphologica et anthropologica, 19
Sofia • 2012

NOS positive mast cells in the pelvic urethra of male pigs

G. Kostadinov, A. Vodenicharov, I. Stefanov, N. Tsandev

Department of Veterinary Anatomy, Histology and Embryology, Faculty of Veterinary Medicine, Trakia University, 6000 Stara Zagora, Bulgaria

With regard to our thorough research on mast cells in the pelvic urethra of male pigs, the aim of the present study was to obtain more data about the histochemical features of these cells by finding out whether they were positive for nitric oxide. The incentive of the study was the key role of nitric oxide (NO) and the closely related isoenzymes of nitric oxide synthase for a number of physiological and pathological events in the animal body. The study of NOS would also contribute to obtaining more information for the innervation of the organ in this animal species.

Key words: nitric oxide (NO), mast cells, pelvic urethra, pig.

Introduction

It is known that nitric oxide synthases (NOS) are haemoproteins which catalyse the oxidation of L-arginine and L-citrulline to nitric oxide. The synthesis of its isoenzymes is regulated by specific genes. Three isoforms are known, two of which are cell-bound – the neuronal and endothelial (nNOS and eNOS) and the third – free (iNOS). All three NOS are used as diagnostic markers of various vascular disorders, pathological deviations in the function of endocrine and exocrine glands (Quesada et al. 2002). NOS expression was established by Kawamoto et al. (1998) in the epithelium of human nasal mucosa, nasal glands, nerve fibres and the endothelium. Persson et al. (1998) assayed the possible co-presence of nitric oxide (NO) and acetylcholine in the major pelvic ganglia in rats by immunohistochemistry with antiserum against NO and acetylcholine esterase (AChE). Data from similar studies in the urethra of female pigs have demonstrated the presence of nitrergic, peptidergic and acetylcholine esterase-positive nerves in its distal part. Further, immunoreactivity to catecholamines containing various peptides, as well as immunoreactive nerves were established in the muscle layers of the urethra, in the propria, ureter and near the blood vessels (Crowe et al. 1989, Persson et al. 1995, Vodenicharov et al. 2005).

The important role of nitric oxide for a number of physiological and pathological events in the animal body, and the lack of data about NOS-positive mast cells in the pelvic urethra of domestic pigs motivated the present study aimed at completing the available information about the histochemical features of mast cells and the innervation of this organ in pigs.

Material and Methods

The specimens (pelvic urethras) were obtained from 12 healthy male Belgian Landrace pigs, 6–8 months of age, weighing 90–110 kg, slaughtered at the licensed slaughterhouse for a meat consumption of Dimes 2000 Ltd in compliance with all Bulgarian legislative norms. Immediately after the slaughter, the material was fixed by immersion in 10 % neutral formaldehyde (Merck, Darmstadt, Germany) for 48h. Further, the material was dehydrated in ascending ethanol series, cleared in xylene and embedded in paraffin. Cuts 5-6 μm thick were treated according to the routine ABC-HRP method with antigen unmasking in 0.01 M citrate buffer, pH 6.0 (Atanassova et al. 2005). Initially, they were treated with 3% (v:v) hydrogen peroxide (H_2O_2) in methanol and then, blocked with Normal Swine Serum with 5% BSA (Sigma Chemical A3425, St Louis, MO, USA). The primary universal antibody – rabbit anti-nitric oxide synthase universal (N-217, Sigma-Aldrich, Chemie Gmbh, Germany) for detection of the three NOS isoforms: neuronal, endothelial and inducible; was applied diluted 1:100 overnight at 4°C. The subsequent incubation was done with Swine Antirabbit Biotinylated IgG (DAKO E0353 Glostrup, Denmark) and ABC-HRP (DAKO; K0355, Glostrup, Denmark). The reaction was developed with DAB (liquid DAB+Substrate-Chromogen System) (DAKO; K3468, Glostrup, Denmark) and controlled under microscope, and afterwards was stopped in water. Then followed contrast staining with Harris' haematoxylin, dehydration and covering with Pertex mounting medium (CellPath plc). Negative controls were run without the primary antibody or after preabsorption with immunogenic peptide at a ratio of 1:10.

Results and Discussion

The light microscopy demonstrated expression of nitric oxide synthase in almost all structures of the pelvic urethral wall. In mucosal epithelial cells, positive expression was observed only in the cytoplasm, but not in the nuclei (Fig. 1).

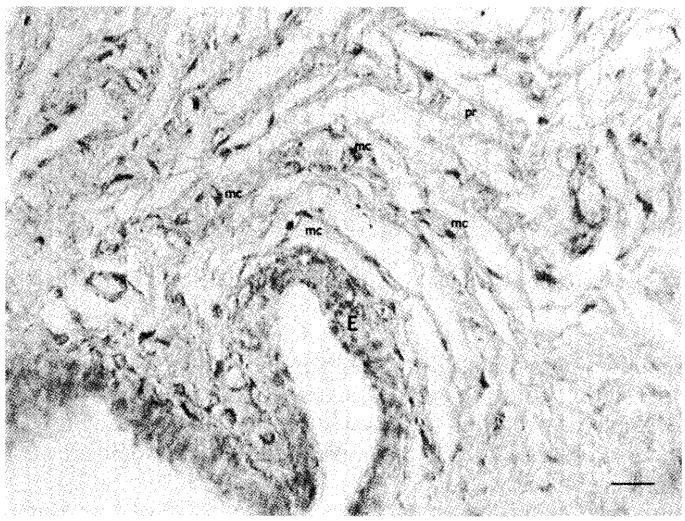

Fig. 1. Expression of nitric oxide synthase in epithelial cells (E) of the mucosa, as well as in mast cells (mc), located into the propria (pr). Bar = 20 μm.

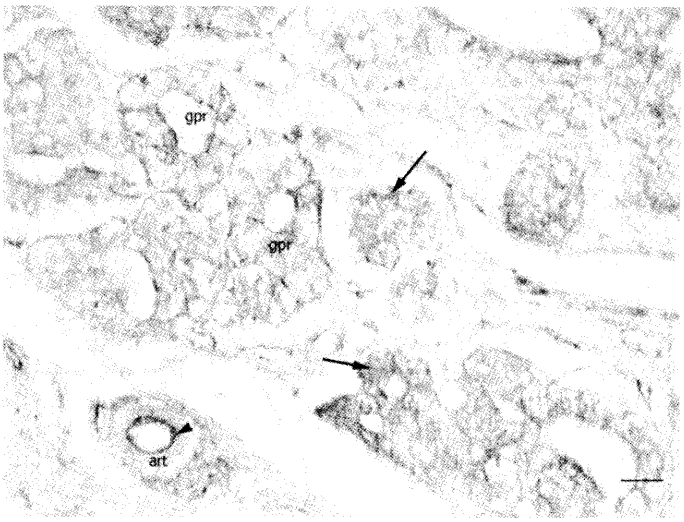

Fig. 2. Positive reaction in secretory cells (arrows) of glands (gpr), and in the endothelium (arrowhead) of the arteriole (art). Bar = 20 μm.

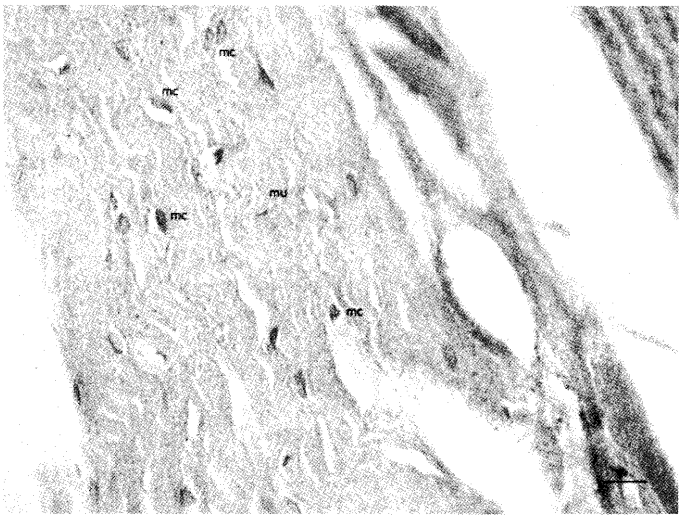

Fig. 3. Positive reaction in the cytoplasm of muscle cells (mu).

Immunohistochemical reactivity was observed also in secretory cells of glandular lobules of the prostate. From the studied arteries and veins of a various calibers, the strongest expression was observed in the endothelium of arteries (Fig. 2).

A well expressed reactivity was also observed in the cytoplasm of striated muscle cells of M. urethralis (Fig. 3).

Localisation of NOS-positive mast cells in M. urethralis (mu). Bar = 20 μm.

The presence of NOS-positive mast cells was also detected in the different layers of the pelvic urethra. These cells were observed in the propria, mainly in vicinity of

vessels from the microcirculatory vascular bed and near the organ's epithelium. Some mast cells were found out around the urethral glands. NOS-positive mast cells were also found in the connective tissue layers of *M. urethralis*. NOS expression was demonstrated in small and larger blood vessels, located in the urethral muscle and the connective tissue of the pelvic urethra. The strongest expression was detected in intimal endothelial cells, and a less strong one – in the adventitia. There were also numerous NOS-positive mast cells in the perimysium, among the muscle cells. Our findings are in agreements with data reported in female pigs and guinea pigs (Crowe et al. 1989, Werkstrom et al. 1998). In our experiment, NOS reactivity was also exhibited by the glandular epithelium of the disseminate part of the prostate gland and its excretory ducts. The reacted epithelial cells of the excretory ducts outlined clearly the pattern of their arrangement and their direction towards the urethral lumen.

In conclusion, the presented data allowed supporting the opinion of some researchers about the importance of investigating the distal urinary tract and the innervation patterns of *M. urethralis* and the pelvic urethra, as the domestic pig is an appropriate experimental model for studying pathological alterations in men. The results could be used in patients with complications following surgery of the urinary bladder or the urethra or after vertebral column injuries.

References

1. Barret, K., F. Pearce. Mast cells heterogeneity. – In: Immunopharmacology of mast cells and basophils, K. Barret and F. Pearce, eds., London: Academic Press, 1993, 29–38.
2. Crowe, R., G. Burnstock . A histochemical and immunohistochemical study of the autonomic innervation of the lower urinary tract of the female pig. Is the pig a good model for the human bladder and urethra? – Journal of Urology, 141, 1989, 414 – 422.
3. Kawamoto, A. H., C. T. Kello, R. Jones, K. Bame. Initial phoneme versus whole word criterion to initiate pronunciation: Evidence based on response latency and initial phoneme duration. – Journal of Experimental Psychology: Learning, Memory, and Cognition, 24, 1998. 862- 885.
4. Persson K., P. Alm, K. Johansson, B. Larsson, K. E. Andersson. Co-existence of nitrergic, peptidergic and acetylcholinesterase-positive nerves in the pig lower urinary tract. – Journal of the Autonomic Nervous System 52, 1995, 225 – 236
5. Persson K., P. Alm, B. Uvellus, K. E. Andersson. Nitrergic and cholinergic innervation of the rat lower urinary tract after pelvic ganglionectomy. – American Journal Physiology 274, 1998, 389 – 397
6. Quesada, A., J. Sainz, R. Wangensteen, I. Rodriguez – Gomez, F. Vargas, A. Osuna, Nitric oxide synthase activity in hyperthyroid and hypothyroid rats. – European Journal of Endocrinology, 147, 2002, 117-122.
7. Vodenicharov, A., R. Leiser, M. Gulubova, T. Vlaykova, Morphological and Immunocytochemical investigations on mast cells in porcine ureter. –Anatomia Histologia Embriologia, 34, 2005, 343–349.
8. Werkstrom V., P. Alm, K. Persson, K.E. Andersson. Inhibitory innervation of the guinea-pig urethra; roles of CO, NO and VIP. – Journal of the Autonomic Nervous System 74, 1998, 33 – 42

Institute of Experimental Morphology, Pathology and Anthropology with Museum
Bulgarian Anatomical Society

Acta morphologica et anthropologica, 19
Sofia • 2012

Experimental Model for Streptozotocin-Induced Diabetes Mellitus Neonatally or in Adulthood – Comparative Study on Male Reproduction in Condition of Hyperglycaemia

E. Lakova[1], S. Popovska[1], I. Gencheva[1], M. Donchev[1], G. Krasteva[1], E. Pavlova[2], D. Dimova[2], N. Atanassova[2].

[1] *Medical University, Pleven, Bulgaria*
[2] *Institute of Experimental Morphology, Pathology and Anthropology with Museum, Bulgarian Academy of Sciences, Sofia, Bulgaria*

Reproductive dysfunction is a consequence of diabetes mellitus (DM), but the underlying mechanisms are poorly understood. In this respect the aim of the present study is comparative evaluation of spermatogenesis in conditions of experimentally induced DM neonatally (NDM) or prepubertaly (PDM) or in adulthood (ADM) in relation to diabetes status. DM was induced by single i.p. injection of streptozotocin (65 mg/kg) Germ cell development/spermatogenesis was assessed by immunohistochemistry for tACE. Gross morphology of the testis in ADM rats is relatively normal whereas the histology of the testes from 50 day-old NDM rats is more altered than in ADM. Testicular morphology was most affected in 50 day-old PDM. Spermatogenesis is not completed and different degree of delay in spermatid development was observed. In conclusion the long-term diabetes with sustained hyperglycemia leads to significant testicular dysfunction that could be considered as a risk factor for male fertility.

Key words: ACE, diabetes, spermatogenesis, germ cells, testis

Introduction

Angiotensin I converting enzyme (ACE) is well-known component of rennin-angiotensin system (RAS) that plays an essential role in male reproduction [6]. This enzyme exists in two isoforms – somatic (sACE) and testis (tACE) specific and they are differently distributed in the male reproductive system [5]. The tACE is expressed in germ cells during spermiogenesis, particularly in elongating spermatids in a stage specific manner. Therefore tACE can be used as a good marker for spermatid differentiation [10, 1]. Our data from previous studies [1] indicated that tACE is a marker for developmental stage of germ cell differentiation in the course of the first spermatogenic wave. Our data from experimental models that affect spermatogenesis characterize tACE as a marker for germ cell depletion in pathological conditions [2, 3].

Reproductive dysfunction is a consequence of diabetes mellitus (DM), but the underlying mechanisms are poorly understood. Abnormal sperm production and failure of reproduction is a long time recognised consequence of DM, and it is accepted that infertility is a common complication in diabetic men [11]. In rats, DM induces decreased testicular weight, sperm number and motility, testosterone levels that are an expression of abnormal spermatogenesis [9]. Data from experimental model in rat revealed that spermatogenesis is more severely altered by DM induced prepubertally than DM induced in adulthood [8]. Nevertheless, the histological alteration of testes has never been deeply studied, and the molecular mechanisms underlying this dysfunction are poorly understood. In this respect the aim of the present study is comparative evaluation of spermatogenesis in conditions of experimentally induced DM neonatally or prepubertally or in adulthood in relation to diabetes status.

Materials and methods

DM was induced by single i.p. injection of streptozotocin (65 mg/kg) in adulthood (10 week-old rats) or neonatally on d1 p.p or prepubertally on d10 DM status confirmed by blood glucose > 15 mmol/l 2-3 days after injection. Testes were sampled at d50 (neonatal and prepubertal treatments); or at 1 and 2 months after injection (adult treatment) and they are fixed in Bouin's fluid and embedded in paraffin. Germ cell development/spermatogenesis was assessed by immunohistochemistry (ABC-HRP technique) for tACE using rabbit polyclonal antibody at dilution 1:500 (Santa Cruz) [2].

Results

Our data from experimental model for DM induced in adulthood (ADM) revealed significant reduction of body weight by 20-30% whereas the 10% decrease in testis weight was not significant. The similar tendency for testis weight was found in animals with induced DM neonatally (NDM) or prepubertally (PDM) (data not shown). Blood glucose levels were strongly elevated up to 4 times in ADM and they were higher by 20-30% in NDM and PDM compared to the controls. Plasma testosterone levels were not significantly lower than controls in all the experimental groups.

Histology and immunohistochemistry for tACE showed that on d50 p.p.in all the experimental group spermatogenesis is completed as indicated by full germ cell complement in the seminiferous tubules (ST) of the testis. The stage specific pattern of expression of tACE is intact starting in step 8 round spermatid at stage VIII of the spermatogenic cycle and reaching maximum in step 19 mature elongated spermatids at the same stage. Gross morphology of the testis in ADM rats is relatively normal and at some places shrinkage of seminiferous tubules is found accompanied by thickening of blood vessel wall. Histology of the testes from 50 day-old NDM rats is more altered than in ADM rats. Differential response to the hyperglycaemia was found as in some animals ST with enlarged lumen were seen and in others rats shrinkage of ST in stage VIII was found. Comparative analysis revealed that testicular morphology was most affected in 50 day-old PDM. Spermatogenesis is not completed and different degree of delay in Sd development was observed. It was indicated by lack of elongating spermatids in stages IV-VII or in early stages (I-VII) or total loss of elongating spermatids in all the fourteen stages was seen (Fig.1.).

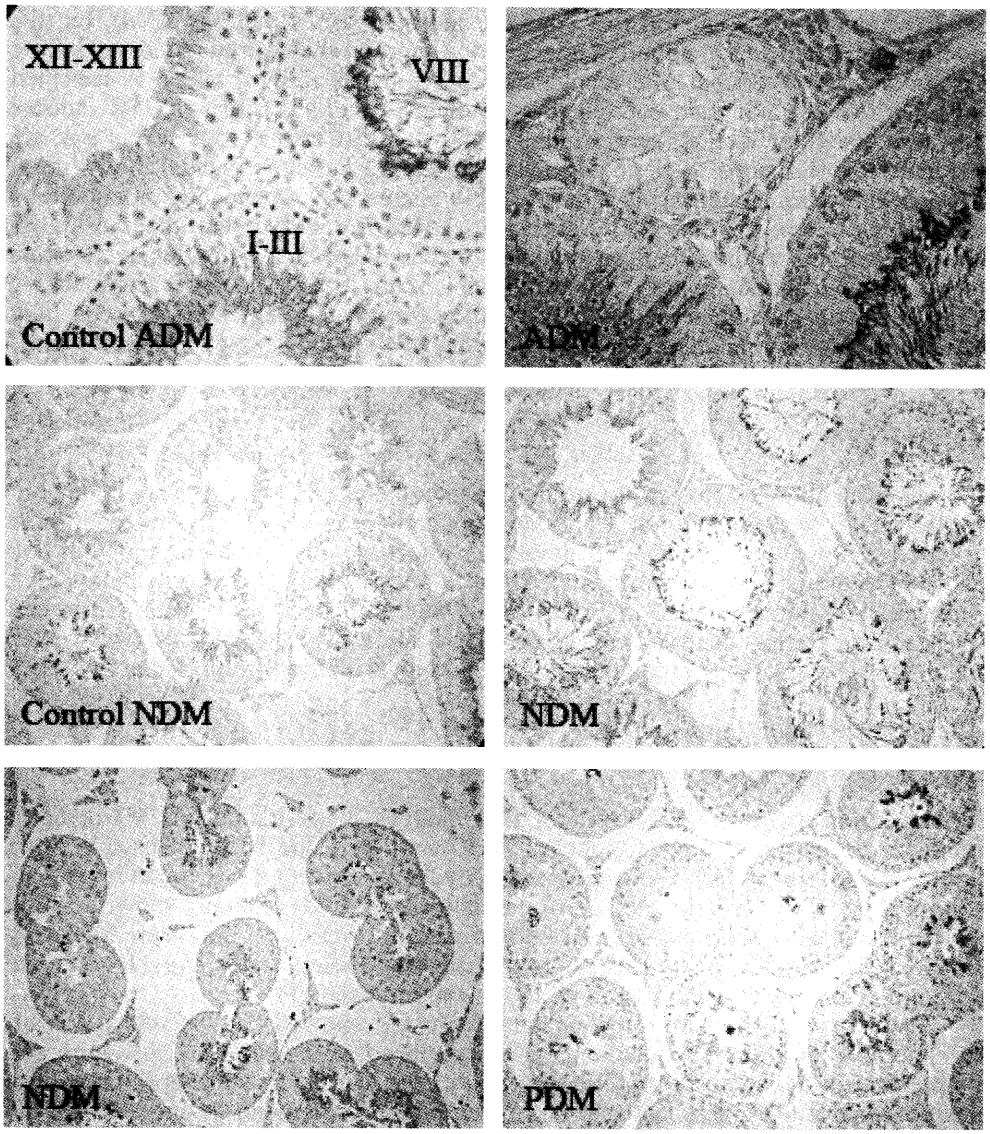

Fig.1. Immunohistochemical localization of tACE in the elongating spermatids of the testes from ADM, NDM and PDM. Enlarged ST lumen and shrinkage of ST is evident in NDM. Note lack of spermatids in PDM. Magnification: ADM – x400; NDM and PDM – x200.

Discussion

Our data provide evidence that diabetic state results in decreased body and testis weight and induced obvious changes on the testicular morphology, especially in neonatal and prepubertal diabetic animals. Recent study by Ricci et al [8] also reported frequent abnormal morphology of ST in which disorganized epithelium was present. As the authors found abnormal localization of occludin in Sertoli cells they conclude

that diabetes directly or indirectly impairs tight junctions and probably prevents the formation of peculiar microenvironment that in turn produce negative impact on germ cells.

It is a long time known that in diabetes, the cellular defense against toxic free radicals is reduced and induction of diabetes with streptozotocin dramatically decreased superoxide dismutase (SOD) in pancreatic islets [7] and in the testis [8]. The role of oxidative stress due to diabetic conditions in testicular function is not well understood.

It has been described that the anti-oxidant defence systems in rat Leydig cells decrease with age [4], and in the total testes the SOD activity is age-dependent [12]. Diabetes appears to mimic the effects of ageing, inducing an increase in OS in the testes. Therefore, the alteration in spermatogenesis in diabetic state is mainly due to Leydig cell functional impairment caused by oxidative stress. As a consequence decreased testosterone production is responsible for the suppression of germ cell development [8].

Our data provide new evidence for expression of t ACE in diabetic condition and demonstrated the dynamic of spermatid population, in particular the delay in development of postmeiotic stages of spermatogenesis. Previously we suggested tACE as a marker for germ cell depletion during aging and pathological conditions [2, 3]. In case of DM tACE also could be considered as a marker for assessment of developmental stage of delayed spermatogenesis. Moreover our comparative analysis provided the first evidence that neonatal and pubertal testis is more affected by hyperglycaemia that adult testis. Induction of DM on d10, when the first proliferative wave have started, affects germ cell development in a stronger extent compared to DM induced on day 1when gonocytes are still quiescent GC. Our data indicate that the spermatogenesis is more vulnerable to DM at the time of proliferative phase of spermatogonia (d4.5-d12) rather than the time of their mitotic arrest/quiescent period before d4.5 p.p.

In conclusion our results indicate that long-term diabetes with sustained hyperglycemia leads to significant testicular dysfunction associated with decreased fertility potential.

Acknowledgements. This study was supported by a grant from Medical University of Pleven №2/2010.

References

1. Atanassova, N., E. Lakova, Y. Bratchova, G. Krasteva. Stage specific expression of angiotensin-converting enzyme in adult and developing rat testis. – Acta morphol. anthropol., 15, 2008, 52-56
2. Atanassova, N., E. Lakova, Y. Bratchkova, G. Krasteva. Expression of testicular angiotensin-converting enzyme in adult spontaneously hypertensive rats. – Folia Histochem. Cytobiol., 47, 2009, 117-122.
3. Atanasova, N., E. Lakova, S. Popvska, M. Donchev, G. Krasteva, V. Nikolov. Expression of testicular angiotensin I-converting enzyme in ageing spontaneously hypertensive rats. – Acta morphol. anthropol., 17, 2011, 79-83.
4. Cao, L., S. Leers-Sucheta, S. Azhar. Aging alters thefunctional expression of enzymatic and non-enzymatic antioxidant defense systems in testicular rat Leydig cells. – J. Steroid Biochem. Mol. Biol., 88, 2004, 61–67.
5. Franke, F.E., K. Pauls, R. Metzger, S.M. Danilov. Angiotensin-converting enzyme and potential substrates in human testis and testicular tumors. – APMIS, 111, 2003, 234-244.
6. Paul, M., A. P. Mehr, R. Kreutz. Physiology of local rennin-angiotensin system. – Physiol. Rev., 86, 2006, 747-803.
7. Pedulla, M., R. d'Aquino, V. Desiderio, F. de Francesco, A. Puca, G. Papaccio. MnSOD mimic compounds can counteract mechanical stress and islet beta cell apoptosis, although at appropriate concentration ranges. – J. Cell Physiol., 212, 2007, 432–438.
8. Ricci, G., A. Catizone, R, Esposito, F.A. Pisanti, M.T. Vietri, M. Galdieri. Diabetic rats testis: morphological and functional alterations. – Andrologia, 41, 2009, 361-368.

9. Scarano, W.R., A.G. Messias, S.U. Oliva, G.R. Klinefelter, W.G. Kempinas. Sexual behaviour, sperm quantity and quality after short-term streptozotocin-induced hyperglycaemia in rats. – Int. J. Androl., 29, 2006, 482–488.
10. Sibony, M., J. Segretain, M. Gasc. Angiotensin-converting enzyme in murine testis: step-specific expresiionof the germinal isoforms during spermatogenesis. Biol. Reprod., 50, 1994, 1015-1026.
11. Steger, R.W. Testosterone replacement fails to reverse the adverse effects of streptozotocin-induced diabetes on sexual behavior in the male rat. – Pharmacol Biochem. Behav., 35, 1990, 577–582.
12. Vazquez-Memije M.E., R. Capin, A. Tolosa, M. El Hafidi M. Analysis of age-associated changes in mitochondrial free radical generation by rat testis. – Mol. Cell. Biochem., 307, 2008, 23–30

Institute of Experimental Morphology, Pathology and Anthropology with Museum
Bulgarian Anatomical Society

Acta morphologica et anthropologica, 19
Sofia • 2012

Alteration in nitric oxide activity in the ventrolateral periaqueductal gray after immobilization stress in rats

Boycho Landzhov, Elena Dzhambazova[1]

Medical University, Dept. of Anatomy, Histology and Embryology, Sofia-1431, Bulgaria;
[1]Sofia University "St. Kliment Ohridski", Dept. of Physiology and pathophysiology, Sofia-1407, Bulgaria

Nitric oxide (NO) synthesized by the enzyme nitric oxide synthase (NOS) affects the secretion of stress hormones and NO system is a stress-limiting system. Also, NO is involved in NO-molecular ways, which affect through auto regulation different signaling molecules – like opioids, endocannabinoids and others. Many stress models have been reported to affect the levels of nitric oxide and stimulate the expression of NOS engaged in their synthesis. Stimulation of opioid receptors within the periaqueductal gray (PAG) activates descending opioid and noradrenaline inhibitory pathways and suppresses nociception.

Because PAG has been identified as region that mediates the response to different stressful paradigms and contains distinct, longitudinally organised neural substrates, our goal was to investigate the effect of 3 hours immobilization stress (IS) on NO activity in rat ventrolateral PAG (vlPAG) by a histochemical procedure for nicotinamide adenine dinucleotide phosphate-diaphorase (NADPH-d). According to obtained data NADPH-d reactive neurons in rat's vlPAG and NO activity respectively was increased by stress model mentioned above.

Key words: Nitric oxide, immobilization stress, vlPAG

All animals, including humans, react with distinct emotional coping strategies to different types of stress. According literature data, immobilization stress (IS) is physical, inescapable stressor which usually evoke passive emotional coping. On the other hand, the midbrain periaqueductal gray (PAG) has been identified as region that mediates the response to different stressful paradigms and the main structure involved in pain modulation and perception. One of the mechanisms involved in PAG's stress response modulation is activation of opioidergic and nitric oxideergic pathways. PAG region also contains distinct, longitudinally organised neural substrates which mediate either active or passive emotional coping strategies. It's known that active emotional coping of stress is evoked by activation of either the dorsolateral (dl) or lateral (l) PAG columns, whereas passive coping is triggered by activation of the vlPAG column.

The aim of our study was to investigate the efect of 3h IS on NO activity in rat vlPAG by a histochemical procedure for nicotinamide adenine dinucleotide phosphate-diaphorase (NADPH-d).

Material and Methods

Nine male Wistar rats (180-220 g) were divided in three groups. Each group included 4 rats: Animals from first group (control group) were not submitted to stress procedure. Animals from second group were submitted for acute model of IS for 3 h.

Acute immobilization stress: The animals were placed in a plastic tube with adjustable plaster tape on the outside so that the animals were unable to move. There were holes for breathing. The control group was not submitted to restraint. The immobilization procedure was carried out for 3 hours.

Histochemical procedure: The animals of each group were anaesthetized with thiopental (40 mg/kg, i.p.). After perfusion through the heart with fixative (4% paraformaldehyde in 0.1M phosphate buffer, pH 7,2) brains were removed and coronal sections were cut on a freezing microtom at 40 mm, and collected in Tris-HCl buffer 0.05M, pH 7.6. The NADPH-d histochemical procedure was used as a marker of NO activity in the neurons. All animals were cared for in compliance with the Principles of Laboratory Animal Care of the Medical University, Sofia.

Statistical analysis: The data were entered in the computer program (Olympus CUE-2), recorded automatically and calculated. The values from controls and rats undergoing immobilization stress were compared by Student's t-test.

Results and discussion

Nitric oxide (NO) is a unique neurotransmitter, which participates in many physiological and pathological processes in the organism. It was synthesized by the family of enzymes called nitric oxide synthase (NOS), which belong to three subtypes – neuronal (nNOS), inducible (iNOS) and endothelial (eNOS)) and had widespread distribution in the brain [6, 9, 10, 11].

Our previous results revealed that some neuropeptides have modulating effects on acute immobilization stress-induced analgesia in rats maybe by opiod and non-opioid systems [2, 3, 4,]. Recent study have shown that the vlPAG can be activated by acute immobilization stress. 3 h immobilization stress significantly increased the number of NADPH-d neurons in the vlPAG compared to the control group (Fig. 1 and 2). This correlate with literature data that nNOS is increased in response to stress [1, 5, 7, 8, 12,]. There are no data available about the effects of IS in different columns of PAG. Our study have shown that acute immobilization stress activate mainly vlPAG.

Some investigators demonstrated that both nNOS and corticotrophin-releasing factor (CRF) are increased in response to stress [1, 7]. In our experiments the number of NADPH-d reactive neurons in vlPAG were significantly potentiated by investigated immobilization stress model. The obtained result correlate with literature data that nNOS is increased in response to stress.

During stress opioidergic system is strongly stimulated and also NO-ergic system because they have structural and functional relations within the PAG.

Conclusion

In conclusion our results showed that acute IS rises NADPH-d reactive neurons in rat's vlPAG and NO activity respectively. These data suggest that NO activity in rat's vlPAG may play an important role in the continuity of homeostasis disrupted by stress.

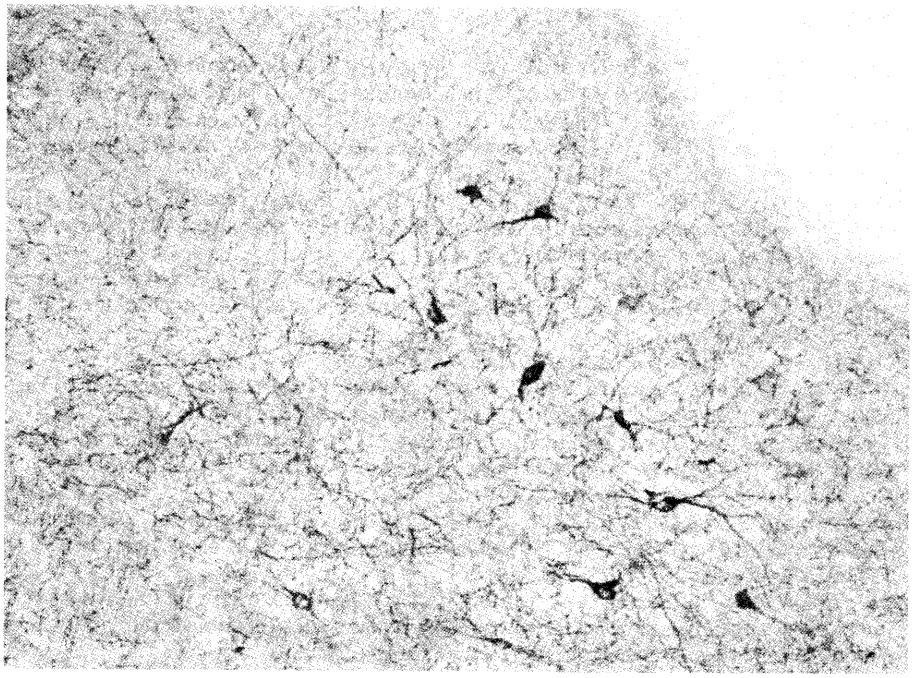

Fig. 1: NADPH-d reactive neurons in the vlPAG after 3 h immobilization stress. (x200).

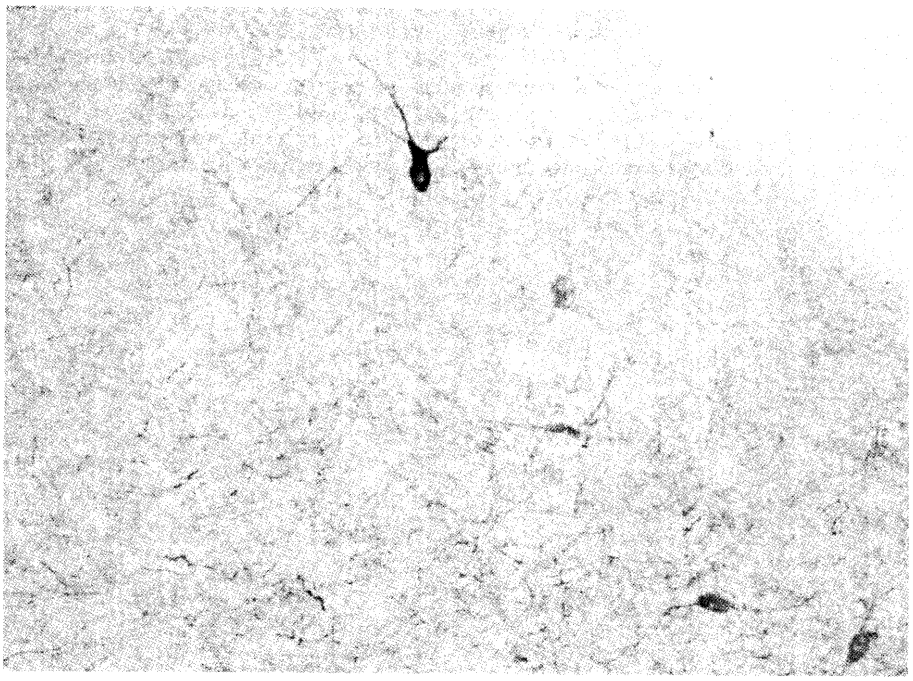

Fig. 2: NADPH-d reactive neurons in the vlPAG. Control group (x200).

References

1. Costa, A., P. Trainer, M. Besser, A.Grossman. Nitric oxide modulates the release of corticotropin-releasing hormone from the rat hypothalamus in vitro. – Brain Res., 605, 1993, 187-192.
2. Dzambazova, E., B. Landzhov, A. Bocheva, A. Bozhilova-Pastirova. Effects of kyotorphin on NADPH-d reactive neurons in rat's Cerebral cortex after acute immobilization stress. – Compt. Rend. Acad. Bulg. Sci., 64, 2012, 1779-1784.
3. Dzhambazova, E., B. Landzhov, A. Bocheva, A. Bozhilova-Pastirova. Effects of D-kyotorphin on nociception and NADPH-d neurons in rat's periaqueductal gray after immobilization stress. – Amino acids, 41, 2011, 937-44.
4. Dzambazova, E., A. Bocheva., B. Landzhov, A. Bozhilova-Pastirova. Effects of kyotorphin on NADPH-d reactive neurons in rats after cold stress. – Compt. Rend. Acad. Bulg. Sci., 61, 2008, 661-666.
5. Gilinsky, M. A., G. M. Petrakova, T. G. Amstislavskaya, L. N. Maslova, V. V. Bulygina. Hypothalamic monoamines in cold stress on the background of changes in the activity of the nitric oxide system. – Neurosci. Behav. Physiol., 35, 2005, 171–175.
6. Hinova-Palova, D.V., A. Paloff, T. Christova, W. Ovtscharoff. Topographical distribution of NADPH-diaphorase-positive neurons in the cat's claustrum. – Eur. J. Morphol., 35, 1997, 105–116.
7. Karanth, S., K. Lyson, S. M. McCann. Role of nitric oxide in interleukin 2-induced corticotropin-releasing factor release from incubated hypothalami. – Proc. Natl. Acad. Sci., 90, 1993, 3383-3387.
8. Landzhov, B., E. Dzambazova, L. Malinova, A. Bocheva, A. Bozhilova-Pastirova. Comparison between effects of two types of stress on nitric oxideactive neurons in rat's dlPAG. – Compt. Rend. Acad. Bulg. Sci., 65, 2012, 555-562.
9. Ovtscharoff, W., A. Bozhilova-Pastirova, T. Christova. Postnatal development of neurons expressing NADPH-diaphorase and parvalbumin in the parietal cortex of male and female rats. – Acta Histochem., 104, 2002, 23-28.
10. Papantchev, V., A. Paloff, D. Hinova-Palova, S. Hristov, D. Todorova, W. Ovtscharoff. Neuronal nitricoxide synthase immunopositive neurons in cat vestibular complex: a light and electron microscopic study. – J. Mol. Histol., 2006, 343–352.
11. Papantchev, V., A. Paloff, T. Christova, D. Hinova-Palova, W. Ovtscharoff. Light microscopicalstudy of nitric oxide synthase I-positive neurons, including fibresin the vestibular nuclear complex of the cat. Acta Histochem., 107, 2005, 113–120.
12. Uribe, R.M., S. Lee, C. Rivier. Endotoxin stimulates nitric oxide production in the paraventricular nucleus of the hypothalamus through nitric oxide synthase I: Correlation with HPA axis activation. – Endocrinology, 140, 1999, 5971-5981.

Institute of Experimental Morphology, Pathology and Anthropology with Museum
Bulgarian Anatomical Society

Acta morphologica et anthropologica, 19
Sofia • 2012

Correlation between cold stress procedure and expression of CB1 receptors in the rat's basal nuclei. An immunohistochemical study

Boycho Landzhov, Elena Dzhambazova[1], Lina Malinova, Anastasia Bozhilova-Pastirova, Wladimir Ovtscharoff

Medical University, Dept. of Anatomy and Histology, Sofia-1431, Bulgaria;
[1]Sofia University "St. Kliment Ohridski", Dept. of Physiology and pathophysiology, Sofia-1407, Bulgaria

The basal nuclei (BN) have been involved in stress response and nociceptive perception. They are complicated complex of internal anatomical and neurochemical organization that receive input from many brain areas includes the cortex and sends output to other components of the brain. They are designed to protect the individual through basic "drives" such as self preservation, bodily appetite and fear.

The endocannabinoid system is a recently identified neuromodulatory system involved in several physiological and pathopysiological processes. Endogenous cannabinoids are important signaling molecules in neuroendocrine control of homeostatic and reproductive functions including stress response and energy metabolism.

The aim of the present study was to examine the expression of endocannabinoid CB1 receptors after acute cold stress. We suggest that increased by cold stress CB1- immunoreactivity in rat's BN is possible protective role of CB1 receptors in stressful condition.

Key words: Basal nuclei, CB1 receptors, cold stress

When stress specifically activated one of these functions, the basal nuclei send a message to the limbic system – the part of the brain that initially processes emotions. Thus basal ganglia mediate the emotional coping of stress response to different stressful stimulus – physical or psychological. The cannabinoid CB1 receptor is the receptor that is expressed ubiquitously throughout most regions of the brain [5; 7; 9].

Literature data revealed that stress alters the levels of many biologically active substances including endocanabinoids. CB1 receptor is the major responsible for the behavioral effects of cannabinoids [3. 8]. Neuroanatomical studies have shown a very high density of cannabinoid CB1 receptors in neurons of the cerebellum, basal ganglia, limbic cortices.

Material and Methods

Ten adult eight-week old male Wistar rats were utilized for light microscopy. They were divided in two groups: control group – five animals were individually housed in an empty cage for three hours, cold stressed group – five animals were placed in a refrigerating chamber at 4°C for 1 h.

Immunohistochemistry: After stress termination three animals of each group were anaesthetized immediately with thiopental (40 mg/kg, i.p.). After perfusion through the heart with fixative (4% paraformaldehyde in 0.1M phosphate buffer, pH 7,2) brains were removed and coronal sections were cut on a freezing microtom at 40 μm, and collected in Tris-HCl buffer 0.05M, pH 7.6. Free-floating sections were preincubated for 1 h in 5% normal goat serum in PBS. Afterwards, incubation of the sections was performed in a solution of the primary antibody for 48 hs at room temperature. We used a polyclonal rabbit anti-CB1 antibody (Santa Cruz, USA), in a dilution of 1:1000. Then sections were incubated with biotinylated anti-rabbit IgG (dilution, 1:500) for 2 hs and in a solution of avidin-biotin-peroxidase complex (Vectastain Elite ABC reagent; Vector Labs., Burlingame CA, USA; dilution 1:250) for 1 h. This step was followed by washing in PBS and then in 0.05 M Tris-HCl buffer, pH 7.6, which preceded incubation of sections in a solution of 0.05% 3,3′-diaminobenzidine (DAB, Sigma) containing 0.01% H2O2 for 10 min at room temperature for the visualization.

The data were entered in the computer program (Olympus CUE-2), recorded automatically and calculated. The values from controls and rats undergoing cold stress were compared by Student's t-test. All animals were caried for in compliance with the "Principles of Laboratory Animal Care" of the Medical University, Sofia.

Results and Discussion:

The BN are key region for the control of nociception containing higher levels of endocannabinoids in the brain [2].Our immunohistochemical study present CB1 immunoreactivity throughout the basal ganglia which was different in controls (Fig. 1, 3) and cold stressed rats (Fig. 2, 4). We found CB1-immunoreactivity (CB1-IR) in axons and dendrites as well as in cell bodies where they presented as puncta on somata. The cells bodies were comprised of several distinct shapes: pyramidal, oval, fusiform and multipolar. The CB1-like immunoreactive neurons were divided into three categories:

Fig. 1. CB1 immunoreactivity throughout the basal ganglia in controls (x100).

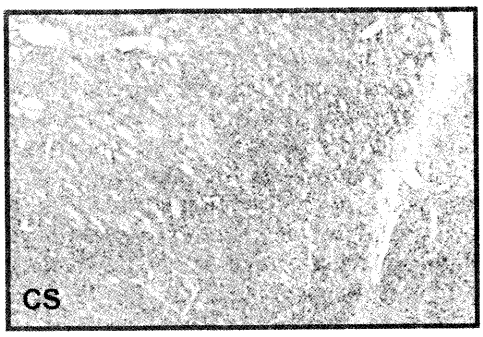

Fig. 2. CB1 immunoreactivity throughout the basal ganglia in cold stressed rats (x100).

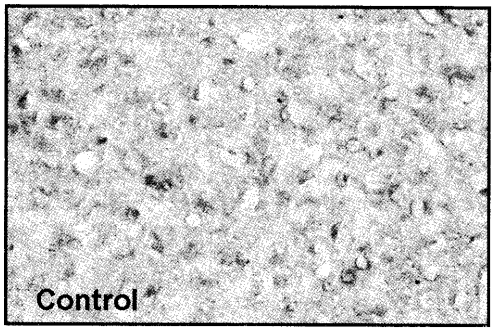

Fug. 3. CB1 immunoreactivity throughout the basal ganglia in controls (x200).

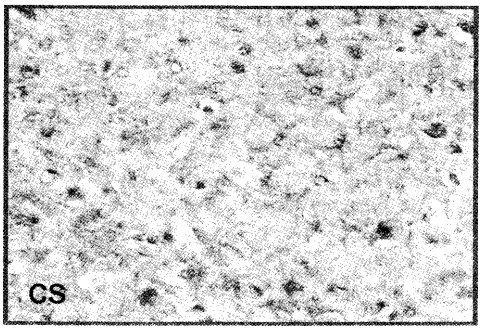

Fug. 4. CB1 immunoreactivity throughout the basal ganglia in cold stressed rats (x200).

small-sized (10-15μm in diameter; 25%), medium-sized (16-20μm in diameter; 60%) and large-sized (21-30μm in diameter; 15%).

The BN contained higher levels of endocannabinoids, parallel with a high densitie of CB1 receptors [1, 4, 5, 6].The BN contained sparsely distributed, thin, varicose, labeled processes, as well as a diffuse immunoreactivity that was morphologically indistinct and contained a very dense meshwork of thin, smooth, CB1-IR processes that encircled large unstained fascicles, cell bodies, and wooly fibers.

Immunoreactivity was most often seen in medium-sized neurons, in the form of puncta. Numerous fine-beaded fibers and puncta were also seen on a handful of pyramidal large-sized neurons, while many puncta were observed around the oval-shaped small- and medium-sized neurons. As well, CB1-positive fusiform-shaped neurons were noted, evidenced by unstained nuclei and stained perikarya.

Conclusion:

CB1-IR in rat BN were increased by cold stress. We suggest possible protective role of CB1 receptors in stressful condition. Further experiments and specific markers are needed to understand the phenotype of the endocannabinoid producing neurons in the basal ganglia.

References

1. Biegon, A., I. A. Kerman. Autoradiographic study of pre- and postnatal distribution of cannabinoid receptors in human brain. – Neuroimage, 14, 2001, 1463-1468.
2. Di Marzo V., T. Bisogno, L. De Petrocellis. Endocannabinoids: new targets for drug development. – Curr. Pharm. Design., 6, 2000, 1361–1380.
3. Gatley, S. J., A. N. Gifford, N. D. Volkow, R. Lan, A. Makriyannis, 23I-labeled AM251: a radioiodinated ligand which binds in vivo to mouse brain cannabinoid CB1 receptors. – Eur. J. Pharm., 1996, 3, 331–338,.
4. Glass M., J. M. Brodie, Y. P. Maneuf. Modulation of neurotransmission by cannabinoids in the basal ganglia. – Eur J Neurosci., 9, 1997, 199 –203.
5. Herkenham M., A. B. Lynn, M. R. Johnson, L. S.Melvin, B. R. de Costa, K. C. Rice. Characterization and localization of cannabinoid receptors in rat brain: a quantitative in vitro autoradiographic study. – J. Neurosci., 11, 1991, 563–583.
6. Matsuda L. A., T. I., Bonner, S. J. Lolait. Localization of cannabinoid receptor mRNA in rat brain. – J. Comp. Neurol., 327, 1993, 535–550.

7. Moldrich G, T. Wenger. Localization of the CB1 cannabinoid receptor in the rat brain. An immunohistochemical study. – Peptides, 21, 2000, 1735–1742.
8. Rinaldi-Carmona, M., F. Barth, M. Heaulme, D. Shire, B. Calandra, C. Congy, S. Martinez, J. Maruani, G. Neliat, D. Caput, P. Ferrara, P Soubrie, J. C. Breliere,G. Le Fur. SR141716A, a potent and selective antagonist of the brain cannabinoid receptor. – FEBS Letters, 350, 1994, 240–244.
9. Tsou, K., S. Brown, M. C. Sanudo-Pena, K. Mackie, J. M. Walker. Immunohistochemical distribution of cannabinoid CB1 receptors in the rat central nervous system. – Neurosci., 83, 1998, 393–411.

Institute of Experimental Morphology, Pathology and Anthropology with Museum
Bulgarian Anatomical Society

Acta morphologica et anthropologica, 19
Sofia • 2012

The Human Carotid Body in Health and Disease

N. Lazarov[1,2], *D. Atanasova*[2]

[1]*Department of Anatomy and Histology, Medical University of Sofia, Sofia, Bulgaria*
[2]*Institute of Neurobiology, Bulgarian Academy of Sciences, Sofia, Bulgaria*

The carotid body (CB) is a small paired organ located at the bifurcation of the common carotid artery. It is the only chemoreceptor sensitive to systemic hypoxia in humans. The CB parenchyma is organized in cell clusters (glomeruli), separated by septa of connective tissue and composed of two juxtaposed cell types: type I or glomus cells and type II or sustentacular cells. As a neurovascular structure, the CB is highly vascularized and densely innervated by sensory and autonomic nerve fibers. The neuron-like glomus cells contain numerous dense-cored vesicles storing and releasing neurotransmitters. These include both classical and peptide transmitters. There is evidence that chronic hypoxia induces gene expression, leading to marked morphological and neurochemical alterations in the human CB, thus implying its structural and neurochemical plasticity. These changes could be either physiological during the course of high altitude adaptation or pathological in patients with systemic hypertension or cardiopulmonary diseases with concomitant hypoxemia. Altered structural, neurotransmitter and functional profiles of the human CB are also implicated in various physiological and pathophysiological conditions, including sleep-disordered breathing, congestive heart failure and hypertension. The CB is a neurogenic center in adult life and its stem cells could be potentially useful for cell therapy against neurodegenerative diseases.

Key words: carotid body, chemoreception, chronic hypoxia, neurogenesis, structural and neurochemical plasticity, human

Introduction

The carotid body (CB), also known as the glomus caroticum, is a small, neural crest-derived paired ovoid mass of tissue, around 2 mm large in humans. It is situated in the loose connective tissue of the carotid bifurcation, between the external and internal carotid arteries [2]. This location is strategic for monitoring blood chemicals just before they reach the brain, an organ that is critically sensitive to oxygen and glucose deprivation.

The CB is the main peripheral chemoreceptor while the aortic bodies only play a limited role in chemoreception in humans. The carotid chemoreceptors register the arterial blood tension of O_2, CO_2 and pH, and respond to their level changes by regulating breathing. The organ also plays an essential role in initiating an appropriate cardiovascular response to hypoxia, hypercapnia and acidosis. It has recently been shown that the CB is a glucose sensor too, activated by hypoglycemia [reviewed in 11].

Embryologically, the CB develops from the mesenchyme of the third branchial arch next to the third arch artery [17], at the same time when neural crest cells, blood vessels, and nerve fibers from sympathetic and cranial nerve ganglia invade the mesenchymal primordia in its wall [8]. In addition, neural crest cells differentiate into the two cell types of the CB.

Structural organization of the human carotid body

The cellular parenchyma consists of two types of cells commonly arranged in clusters called glomeruli which represent the basic morphofunctional unit of the CB [5, 13]. The lobules of glomic tissue are separated from each other by septa of connective tissue, which converges upon the surface to form a capsule for the whole organ (Fig. 1A). Mast cells are commonly seen in the human CB and they are largely confined to the interlobular connective tissue, closely apposed to and around small blood vessels [7].

The most striking structural features of the CB are its rich vascularization and dense innervation. The CB contains the most abundantly vascularized tissue in the human body; hence it has the highest blood flow per tissue weight of any organ. It is supplied by one or more glomic arteries, arising from the external carotid artery [19]. A profuse capillary network travels in the fibrous stroma and gives a pink-colored ap-

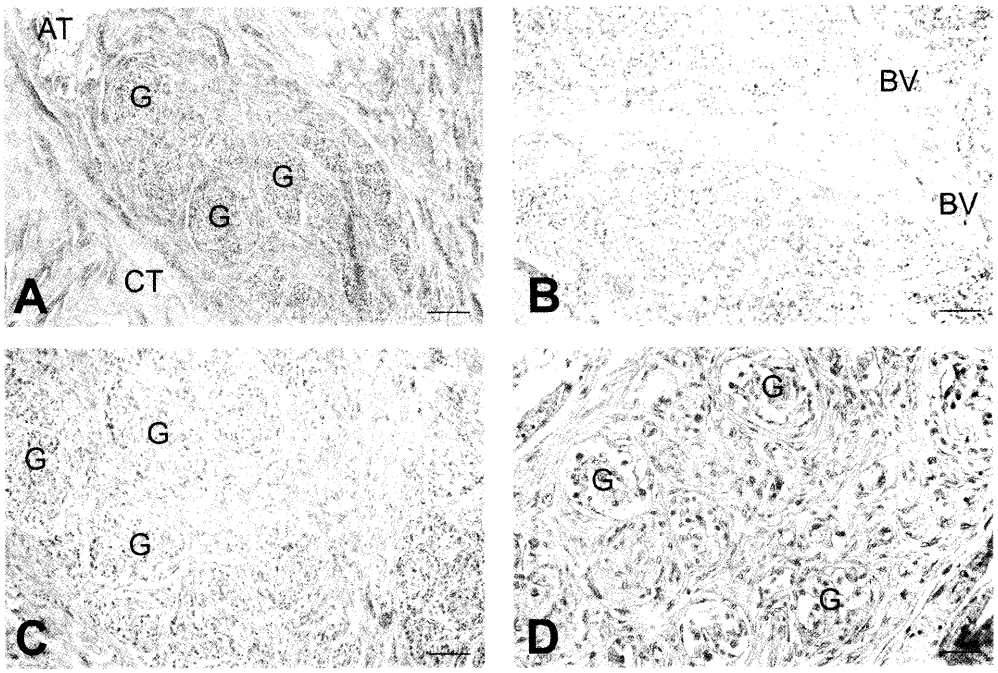

Fig. 1. Morphology of the human carotid body. (**A**) A conventional H&E staining showing the structural organization of the organ. Note the clusters, glomeruli (G) of parenchymal cells, the surrounding connective tissue (CT) and the adipose tissue located in the interlobular stroma. (**B**) A dense network of blood vessels (BV) is also dispersed in the stromal CT. (**C**) Juvenile human carotid body with compact glomic lobules (G) separated by thin septa of CT. (**D**) shows the carotid body of an elderly person. Note the denser and more compressed glomeruli (G) with progressive cellular degeneration. Scale bars = 200 μm (**A-C**); 50 μm (**D**).

pearance of the organ (Fig. 1B). The glomus cells are dually innervated by sensory and autonomic nerve fibers. Sensory innervation is provided by the carotid sinus nerve (also known as Hering's nerve), a branch of the glossopharyngeal nerve, while the sympathetic supply is provided by postganglionic neurons from the closely located superior cervical ganglion.

The principal cell type, the neuron-like type I or glomus cell, is considered to be the chemosensory cell of the organ [5, 19]. The glomus cells are round to oval in shape with a diameter of 10-16 μm and contain a large round, euchromatic nucleus and an abundant pale cytoplasm with numerous organelles. Amongst them, most notable are dense-cored secretory granules packed with putative neurotransmitters. Although smaller in size, they closely resemble the granules of paraneurons belonging to the diffuse neuroendocrine system cell family [13]. On the basis of the size and staining properties of their dense-cored vesicles, De Castro (1926) classically distinguished two types of glomus cells in the human CB: light and dark gomus cells [3]. Type II or sustentacular cells (~15-20% of all parenchymal cells) are glial-like supporting cells typically located at the periphery of the cell cluster. They are elongated cells with a disk-shaped hyperchromic nucleus and long cytoplasmic processes that partially envelop the glomus cells. Their cytoplasm lacks secretory granules but expresses glial marker enzymes such as the S-100 protein and glial fibrillary acidic protein [15]. Recently they have been assumed to be the stem cells in the adult CB [15].

The CB undergoes morphological changes with age. In general, it is best developed in children and young people [10], in which the characteristic cell clusters are more compact, separated by thin walls of connective tissue filled with a large number of fine blood vessels and nerve fibers (Fig. 1C). Aging leads to a decrease in the number of nerve fibers and glomus cells with a progressive cellular degeneration and an apparent increase in the surrounding connective tissue (Fig. 1D) [10, 17]. The organ also undergoes postmortal alterations, mostly associated with the nuclear morphology. Based upon differences in it, three distinct forms of glomus cells can be recognized in human glomic tissue: light, dark and pyknotic variants, the latter two representing postmortem changes [6, 18].

Neurochemistry of the human carotid body

A variety of neurochemical agents, both classical transmitters and neuropeptides, have been proposed to play a role in the chemosensory function [5, 9, 14]. Amongst them, the biogenic amines, including acetylcholine, norepinephrine, dopamine (Fig. 2A) and serotonin, represent the largest group in the human CB. In recent years, histamine has also been considered a putative transmitter in hypoxic chemosensitivity in humans (Fig. 2B) [10]. Other neuroactive substances such as some neuropeptides (substance P, VIP and enkephalins) and the gaseous neuromessengers nitric oxide and carbon monoxide also play a role as neuromodulators or second messengers, respectively, in oxygen sensing in the mammalian CB [16]. In their turn, the neurotransmitters contribute to the modulation of glomus cell function via autoreceptors as well.

Hypoxia-induced morphological and neurochemical plasticity of the human carotid body

There is convincing evidence that chronic hypoxia induces gene expression, leading to profound morphological changes in the human CB. In particular, long term hypoxic

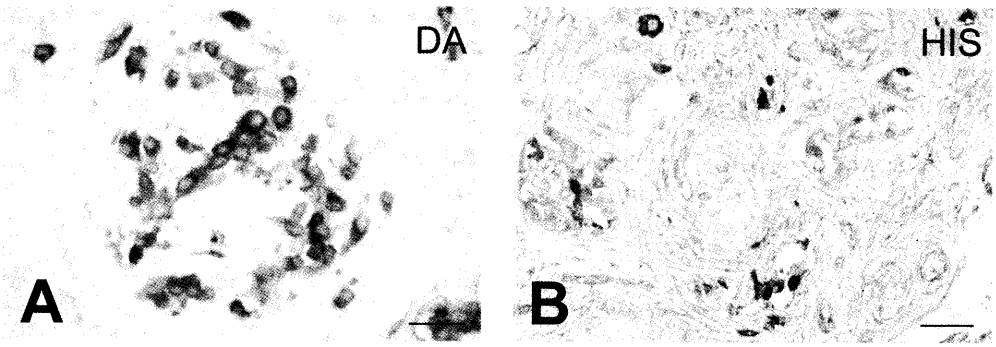

Fig. 2. Neurotransmitter traits in the human carotid body. (**A**) Immunohistochemical staining for dopamine (DA) in the mature carotid body. A subset of glomus cells is intensely immunostained. (**B**) A number of glomus cells exhibit strong immunoreactivity for histamine (HIS) in the adult carotid body. Scale bars = 25 μm (**A**); 50 μm (**B**).

exposure enlarges the CB, causing hypertrophy and mitosis of glomus cells, vasodilatation of the existing and growth of new blood vessels [20]. Such a physiological adaptive response to prolonged hypoxia occurs during acclimatization to high altitudes, or pathologically in patients suffering from systemic hypertension and/or cardiopulmonary diseases with concomitant hypoxemia [1].

In addition, it is well established that hypoxia causes glomus cells to depolarize and release transmitters, which bind to autoreceptors expressed by type I cells or postsynaptic receptors on apposed chemoafferent nerve terminals [5]. The predominant excitatory transmitters synthesized and released by glomus cells in response to hypoxia are acetylcholine and adenosine triphosphate while dopamine has a primarily inhibitory role in hypoxic chemosensitivity [9, 10, 14]. Our recent data have also proved the modulatory role of histamine as an essential excitatory modulator of the chemoreceptor activity upon hypoxia in man.

Carotid body chemotransduction mechanisms in disease

During the early postnatal life, human infants seem to be particularly vulnerable to hypoxic and hypercapnic episodes during sleep and to changes in peripheral chemoreception. This results in altered chemosensitivity which may be one of the factors contributing to a higher incidence of sudden infant death syndrome (SIDS), a disease responsible for unexpected deaths in newborns. Indeed, smaller than usual in size CBs or abnormalities in their transmitter content have been reported in victims of SIDS [4] and in subjects with congenital central hypoventilation syndrome. Conversely, an abnormal enlargement of the CB, elevated catecholamine synthesis and hypersensitivity to hypoxia have been shown in patients with essential hypertension, congestive heart failure and obstructive sleep apnea syndrome. It is likely that the CB tends to maintain oxygen homeostasis by marked morphological and neurochemical changes, and thus acts as a defense entity preventing the progression of morbidity associated with these diseases.

The carotid body neurogenic niche and its clinical applicability to cell therapy

The CB is the first neurogenic center identified outside the CNS. Recent research has demonstrated that the glia-like sustentacular cells sustain physiologic neurogenesis in the adult CB and in response to physiological hypoxia can proliferate and differentiate into new glomus cells [15]. The newly born neuron-like glomus cells are highly dopaminergic and produce neurotrophic factors such as GDNF, BDNF and NT3. Given their dopaminergic nature and ability to synthesize neurotrophins, CB stem cells could potentially be applied in cell replacement therapies in Parkinson's disease and in the treatment of other neurodegenerative disorders [reviewed in 12].

Conclusion

For over a century it has been known that the CB in man has an intricate internal structure. Due to several decades of extensive study, we are now aware of its remarkable ability to release a broad variety of transmitter agents in response to different chemostimuli. This provides clues on its important role in the homeostatic maintenance of the whole organism. Recent advances in human CB research and in understanding morphological and physiological mechanisms that operate in it have revealed that its histological structure and neurochemical profile alter upon hypoxia and certain cardiorespiratory disorders thus adapting the living organism to changing environmental or pathological conditions. Last but not least, the CB is a neurogenic center with a recognizable physiological role in adult life and, therefore, the cultivation of adult human CB progenitors in vitro should be a major task in future experimental work. Consequently, stem cell-derived glomus cells would enable successful autotransplantation of CB cell aggregates for tissue repair after injury or in neurodegenerative diseases.

References

1. Arias-Stell, J., J. Valcarcel. Chief cell hyperplasia in the human carotid body at high altitudes; physiologic and pathologic significance. – Hum. Pathol., 7, 1976, 361-373.
2. Atanasova, D. Y., M. E. Iliev, N. E. Lazarov. Morphology of the rat carotid body. – Biomed. Rev., 22, 2011, 41-55.
3. De Castro, F. Sur la structure et l'innervation de la glande intercarotidienne (glomus caroticum) de l'homme et des mammifères, et sur un noveau système d'innervation autonome du nerf glossopharyngien. – Trab. Lab. Invest. Biol. Univ. Madrid, 24, 1926, 365-432.
4. Gauda, E. B, E. Cristofalo, J. Nunez. Peripheral arterial chemoreceptors and sudden infant death syndrome. – Resp. Physiol. Neurobiol., 157, 2007, 162-170.
5. Gonzalez, C., L. Almaraz, A. Obeso, R. Rigual. Carotid body chemoreceptors: from natural stimuli to sensory discharges. – Physiol. Rev., 74, 1994, 829-898.
6. Heath, D., C. Edwards, P. Harris. Post-mortem size and structure of the human carotid body. Its relation to pulmonary disease and cardiac hypertrophy. – Thorax, 25, 1970, 129-140.
7. Heath, D., P. Lowe, P. Smith. Mast cells in the human carotid body. – J. Clin. Pathol., 40, 1987, 9-12.
8. Hempleman, S. C., S. J. Warburton. Comparative embryology of the carotid body. – Respir. Physiol. Neurobiol., 2012, http://dx.doi.org/10.1016/j.resp.2012.08.004.
9. Iturriaga, R., J. Alcayaga. Neurotransmission in the carotid body: transmitters and modulators between glomus cells and petrosal ganglion nerve terminals. – Brain Res. Rev., 47, 2004, 46-53.

10. Lazarov, N. E., S. Reindl, F. Fischer, M. Gratzl. Histaminergic and dopaminergic traits in the human carotid body. – Respir. Physiol. Neurobiol., 165, 2009, 131-136.
11. Lopez-Barneo, J. Oxygen and glucose sensing by carotid body glomus cells. – Curr. Opin. Neurobiol., 13, 2003, 493-499.
12. López-Barneo, J., R. Pardal, P. Ortega-Sáenz, R. Durán, J. Villadiego, J. J. Toledo-Aral. The neurogenic niche in the carotid body and its applicability to antiparkinsonian cell therapy. – J. Neural Transm., 116, 2009, 975-982.
13. McDonald, D. M. Peripheral chemoreceptors. Structure-function relationships of the carotid body. In: Regulation of breathing (Ed. T. F. Hornbein). New York, Dekker, 1981, 105-319.
14. Nurse, C. A. Neurotransmission and neuromodulation in the chemosensory carotid body. – Auton. Neurosci., 120, 2005, 1-9.
15. Pardal, R., P. Ortega-Sáenz, R. Durán, J. López-Barneo. Glia-like stem cells sustain physiologic neurogenesis in the adult mammalian carotid body. – Cell, 131, 2007, 364-377.
16. Prabhakar, N. R. Neurotransmitters in the carotid body. — Adv. Exp. Med. Biol., 360, 1994, 57-69.
17. Sarrat-Torres, M. A., A. Torres, J. Whyte, S. Baena, A. Cisneros, R. Sarrat. Structure, location, function and pathological features of the human carotid body. – Eur. J. Anat., 10, 2006, 1-5.
18. Seker, M., D. J. Pallot, J.-O. Habeck, A. Abramovici. Postmortem changes in the human carotid body. In: Arterial chemoreceptors: cell to system (Eds. R. G. O'Regan, P. Nolan, D. S. McQueen, D. J. Paterson). New York, Plenum Press, 1994, 349-351.
19. Verna, A. The mammalian carotid body: morphological data. In: The carotid body chemoreceptors (Ed. C. Gonzalez). Austin, Landes Bioscience, 1997, 1-29.
20. Wang, Z. Y., G. E. Bisgard. Chronic hypoxia-induced morphological and neurochemical changes in the carotid body. – Misrosc. Res. Tech., 59, 2002; 168-177.

Institute of Experimental Morphology, Pathology and Anthropology with Museum
Bulgarian Anatomical Society

Acta morphologica et anthropologica, 19
Sofia • 2012

Quantity and Distribution of de novo Generated Cells in the Spinal Cord of Adult Macaque Monkeys

D. Marinova[*], *M. Angelova*[*], *I. Velikov*[*], *V. Goranova*[*], *T. Yamashima*[**], *A. B. Tonchev*[*1]

[*]*Dept. of Anatomy, Histology and Embryology, Medical University, Varna, Bulgaria*
[**]*Department of Restorative Neurosurgery, Kanazawa University Graduate School of Medical Science, Kanazawa, Japan*
[1]Corresponsdence: Anton B. Tonchev, Department of Anatomy, histology and embryology, Medical University – Varna, Marin Drinov-str. 55 Varna, BG-9002, Bulgaria, E-mail: anton.tonchev@mu-varna.bg

The existence of multipotent progenitors in the adult forebrain of mammals, including primates, has been widely documented. However, the data on the spinal cord are limited. We used bromodeoxyuridine (BrdU) to label *de novo* generated cells in adult (5-10 year old) non-human primates. We studied the quantity and distribution of BrdU-positive cells on histological sections from cervical, thoracic and lumbar spinal cord segments at 2h, 2, 5 or 10 weeks after exposure to BrdU. We report a significant reduction of BrdU-labeled cells at the 2/5/10-week post-injection time points as compared to the 2-hour time point. Further, we performed a subregional tracing of the BrdU-stained cells in gray matter, white matter, and around the central canal. This represents the first analysis of *in vivo* cell proliferation in normal adult primate spinal cord.

Key words: BrdU, proliferation, spinal cord, adult.

Introduction

Recently, mounting evidence using both i*n vitro* and *in vivo* experiments suggested the existence of adult stem cells in the mammalian brain. These cells are self-propagating and capable of producing all major cell types in the nervous system. In the spinal cord, adult stem/progenitor cells can be isolated, expanded and differentiated *in vitro* [7, 8]. Evidence suggests that a stem-like cell type can be localized in or near the ependymal layer of the spinal cord [1, 3]. Ependymal astrocytes appear the primary source of stem cell activity *in vitro* [2]. While most studies use rodent models, evidence in primates regarding the existence of spinal cord progenitors is scarce.

The aim of this study was to investigate the quantity and distribution of *de novo* generated cells at different levels and zones in the intact spinal cord of adult non-human primates (macaque monkeys).

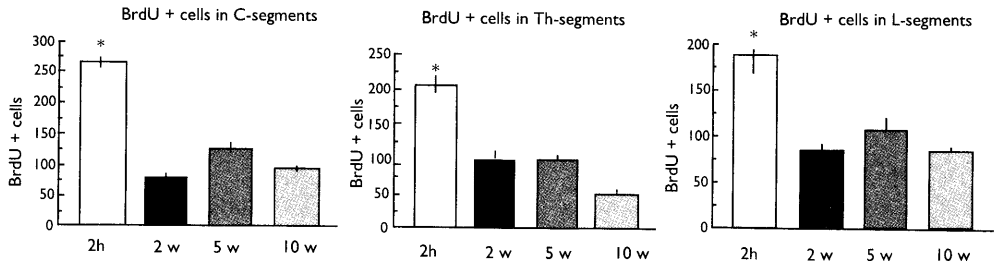

Fig. 1. Total number of BrdU+ cells on histological sections from cervical (C), thoracic (Th) and lumbar (L) segments of spinal cord 2 hours, 2, 5 and 10 weeks after BrdU injection.* P<0.05, Tukey-Kramer test.

Materials and methods

Female monkeys (*Macaca fuscata*) were used in accordance with the institutional guidelines of the Kanazawa University (Japan). Eleven adult (5-9 years-old) monkeys received daily injections (100 mg/kg, i.v.) of BrdU for 5 consecutive days. The animals in the short-term survival group (n = 3) were sacrificed 2 h after the last injection. The animals in the long-term survival groups were sacrificed 2 weeks (n = 3), 5 weeks (n = 3) and 10 weeks (n = 2) after the last injection. Under general anesthesia, the monkeys were intracardially perfused with 4% paraformaldehyde in 0,1 M phosphate buffer saline, pH 7,4. Spinal cord tissues were postfixed for 2 – 3 h in paraformaldehyde and cryoprotected. After embedding, transverse 40 μm thick sections were sequentially cut and stored at -20°C until staining. For BrdU labeling, DNA was denaturated in 50% formamide/2x SSC buffer and 2N HCl for 30 minutes at 37°C and mouse anti-BrdU (1:100) or rat anti-BrdU (1:100) first antibodies was then applied followed by appropriate secondary antibodies conjugated to biotin.

Image analysis of BrdU+ cells was performed on every 12th section from cervical, thoracic and lumbar segments of all groups with an Axovert S100 microscope (Carl Zeiss Co, Tokyo). We counted all BrdU+ cells on the section. Further, the gray matter and white matter were divided into specific regions of interest as follows: 1) gray matter (ventral horn, dorsal horn, central canal); 2) white matter (anterior funicle, lateral funicle, posterior funicle). Statistical analysis was performed using one-way ANOVA followed by Tukey – Kramer's post hoc comparisons and two-sided *t* test. Data expressed as the mean ± SEM. Differences were considered significant when $p \leq 0.05$.

Results

The total number of BrdU+ cells per section showed a significant reduction in the monkey groups with a long-term (weeks) survival after BrdU in all investigated spinal cord segments with more cells in the gray matter compared to the white matter (Fig. 1). Within the three zones of the gray matter we found more positive cells in the ventral horns of the cervical segments in short-term survival group and in lumbar segments 2 h and 10 weeks post infusion (Fig. 2). In the dorsal horns of gray matter, the number of BrdU+ cells was significantly higher in the 2h-survival group, in all segments. In the zone around the central canal, we found more BrdU+ cells only in the cervical segments of short-term (2h) survival group. There was no significant difference in the number of cells from the thoracic segments between experimental groups.

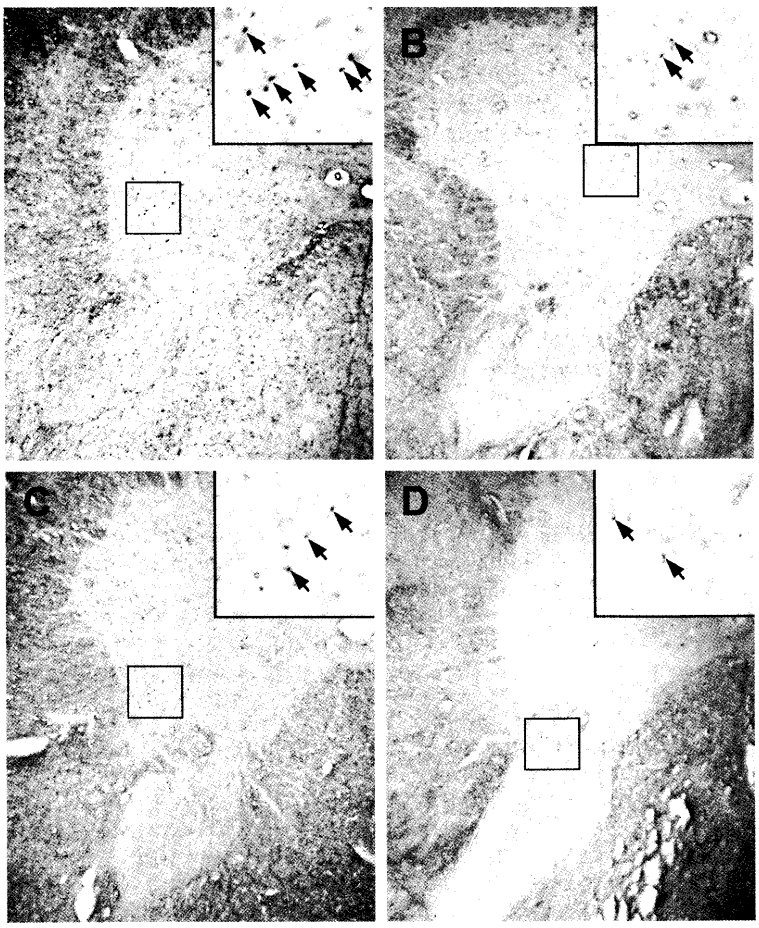

Fig. 2. Micrographs of BrdU+ cells in the spinal cord at various time points after BrdU injection: **A** – 2 hours, **B** – 2 weeks, **C** – 5 weeks, **D** – 10 weeks. Arrows indicate BrdU+ cells in the boxed areas, x20.

In the anterior column, more BrdU+ cells were present at 2h after BrdU in all segments. In the lateral column, the number of *de novo* generated cells was increased only in the cervical and thoracic segments of the short-term (2h) survival group. There was no difference in the number of cells in the dorsal column of all four experimental groups at all investigated levels.

In the other experimental groups, there was no significant difference in the total number of positive cells between the gray and white matter at all levels of the spinal cord with a few exceptions. In the third experimental group (5 weeks after injection), an increased number of *de novo* generated cells was found in the ventral horns of gray matter and anterior column of white matter in cervical segments. In the fourth experimental group (10 weeks after injection), the total number of BrdU+ cells in cervical and lumbar segments was increased both in the gray and white matter. In the gray matter, more cells were found in its ventral and dorsal horns. In the white matter, proliferative cells were concentrated in its anterior and lateral columns.

Discussion. We present the first analysis of *in vivo* cell proliferation in normal adult primate spinal cord. We found more *de novo* generated cells at 2h after BrdU than at 2/5/10 weeks. More BrdU+ cells were registered in cervical than in thoracic or lumbar segments. Increased number of *de novo* generated cells was found only in the gray matter of cervical segments and it was at the expense of more proliferating cells in the ventral horns. The presence and distribution of BrdU immuno-positive cells is indicative for an existing proliferation occurring at a higher rate in the gray matter and mainly at cervical level of the spinal cord. Our findings are consistent with data from other mammals [5, 7, 8]. The higher number of positive cells 2h after BrdU application compared to other groups corresponds to the division rate of newly generated cells that incorporate BrdU. We consider that the possible origin of stem cells in the spinal cord might be the ependymal zone as suggested by others [2, 4, 6]. It remains to be determined what is the cellular lineage of the proliferating cells, their pathways of migration and differentiation.

References

1. Chiasson, B. J., V. Tropepe, C. M. Morshead, D. van der Kooy, 1999. Adult mammalian forebrain ependymal and subependymal cells demonstrate proliferative potential, but only subependymal cells have neural stem cell characteristics. – J. Neurosci., 19, 4462– 4471.
2. Cizkova, D., M. Nagyova, L. Slovinska, I. Novotna, J. Radonak, M. Cizek, E. Mechirova, Z. Tomori, J. Hlucilova, J. Motlik, I. Jr. Sulla, I. Vanicky, 2009. Response of ependymal progenitors to spinal cord injury or enhanced physical activity in adult rat. – Cell Mol. Neurobiol., 29, 999–1013.
3. Doetsch, F., I. Caille, D. A. Lim, J. M. Garcia-Verdugo, A. Alvarez-Buylla, 1999. Subventricular zone astrocytes are neural stem cells in the adult mammalian brain. – Cell, 97, 703–716.
4. Hamilton, L. K., M. K. Truong, M. R. Bednarczyk, A. Aumont, K. J. Fernandes, 2009. Cellular organization of the central canal ependymal zone, a niche of latent neural stem cells in the adult mammalian spinal cord. – Neuroscience, 164(3), 1044-1056.
5. Horner, P. J., A. Power, G. Kempermann, H. G. Kuhn, T. D. Plamer, J. Winkler, L. Thal, F. Gage, 2000. Proliferation and differentiation of progenitor cells through the intact adult rat spinal cord. – J. Neurosci., 20(6), 2218–2228.
6. Meletis, K., F. Barnabé-Heider, M. Carlén, E. Evergren, N. Tomilin, O. Shupliakov, J. Frisén, 2008. Spinal cord injury reveals multilineage differentiation of ependymal cells. – PLoS Biol. 6(7), e182.
7. Shihabuddin, L. S., J. Ray, F. H. Gage, 1997. FGF-2 is sufficient to isolate progenitors found in the adult mammalian spinal cord. – Exp. Neurol., 148, 577–586.
8. Weiss, S., C. Dunne, J. Hewson, 1996. Multipotent CNS stem cells are present in the adult mammalian spinal cord and ventricular neuroaxis. – J. Neurosci., 16, 7599–7609.

Institute of Experimental Morphology, Pathology and Anthropology with Museum
Bulgarian Anatomical Society

Acta morphologica et anthropologica, 19
Sofia • 2012

Thymocyte microenvironment reorganization during leukemia transformation (structural and immunocytochemical data)

Ts. Marinova[1], L. Spassov[2]

[1]*Department of Biology, Medical Genetics and Microbiology,* [2]*Department of Surgery, Medical Faculty, Sofia University "St. Kliment Ohridski"*

A lot of experimental and clinical investigations of different kinds of mouse leukemia and leukemic patients have shown the important role of the thymus in the pathogenesis of lymphoid leukemia and the obligatory participation of the thymic epithelial cells in the intrathymic leukemogenesis. We have previously reported that the lympho-epithelial cell complexes seem to be a unique striking example of very close lymphoid/stromal cells interaction involved in thymic microenvironmental plasticity during chemically induced leukemogenesis. Our results provide new structural and immunocytochemical evidence for intermediate filaments alterations in cortical epithelial cells of mouse leukemia thymus. They suggest simultaneous cytokeratin/Nerve growth factor immunoreactivity modulation of thymic epithelium, which is probably involved in thymocyte microenvironment reorganization during leukemogenesis.

Key words: thymocyte microenvironment, experimental lymphoid leukemia

Introduction

Accumulating evidence shows that the thymus is involved in the pathogenesis of mouse lymphoid leukemia, but the precise role of the thymic microenvironment, including epithelial cells (EC) and their intermediate filaments (IF) proteins cytokeratins (CK) is unclear [1, 2].

We have previously reported that the lympho-epithelial cell complexes seem to be a unique striking example of very close lymphoid/stromal cells interaction involved in thymic microenvironmental plasticity during chemically induced leukemogenesis [3, 4, 5].

The present study was focused on IF reorganization and some immunocytochemical features (distribution and co-localization of CK and Nerve growth factor-NGF immunoreactivity) of the thymic microenvironment in mice with experimental chemically induced acute *L1210* lymphoid leukemia.

Material and Methods

Leukemic DBA/2 inbred mice with chemically induced L1210 lymphoid leukemia and control mice were investigated simultaneously [2, 4].

Four primary antibodies (Ab) were used for the first step of the immunocytochemical study: 1. Anti-pan cytokeratin (mouse, Mo Ab; Cat. Nr. C 1801, Sigma Chemical Co.); 2. Anti-Cytokeratin Ab (Mo, BioGenex Lab USA); 3. Anti-NGF Ab (NGF H-20, r-p, SC-548); 4. Anti-CD 14 Ab (mouse monoclonal Ab; UCH-M1, Cat. Nr. SC-1182, Santa Cruz Biotechnology); Secondary Antibodies: ABC Staining Systems (mouse-sc 2017 and rabbit-sc 2018, Santa Cruz Biotechnology) were used as secondary antibodies for immunohistochemistry at the light microscopic level. Anti-mouse IgG (coupled with 10-nm gold particles) and anti-rabbit IgG (coupled with 5-nm gold particles) gold-conjugated Ab (whole molecule, Sigma Chemical Co.) were applied for immunoelectron microscopy.

Routine methods for transmission electron microscopy, immunoperoxidase, and immunogold electron microscopy were applied according to the earlier described standard protocols [2, 4, 5]. To define the nature of the thymic cell types that expressed CK/NGF, serial tissue sections were stained with anti-pan-cytokeratin and anti-CD 14 Ab, which are known to detect epithelial cells and monocyte/ macrophages, respectively. Control experiments (negative and positive) were carried out in parallel.

Results

Intermediate filament accumulation and disassembly in large cytoplasmic areas, "elongated" desmosomes and nucleus reorganization were found in leukemia thymus (Fig. 1).

Fig. 1. Electron micrograph of EC from leukemic thymus showing IF accumulation and disassembly (Orig. magn. X 24 000).

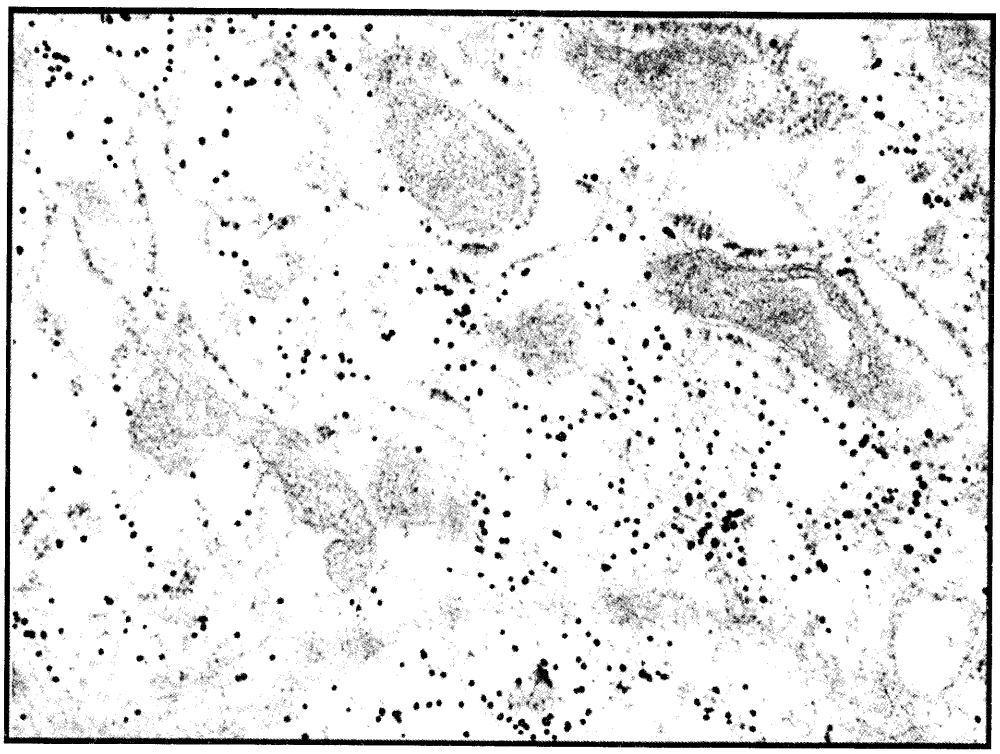

Fig. 2. Ultrastructural data for overexpression of CK in immunopositive leukemic EC. Immunogold localization of CK-binding gold granules in IF/mitochondria rich areas of EC (Orig. magn. X 28 000).

Immunogold labelling showed overexpression of CK in mitochondria rich areas of leukemic EC (Fig. 2). The increased CK immunoreactivity of epithelial cells correlated with lympho-epithelilal cells (LEC) complex formation, including thymic nurse cell-like structures and rosettes in the external cortex. Polarization of CK-binding gold granules at sites of both EC-EC and EC-LC contacts was subcapsulary and subseptaly observed. Ultrastructural data for co-localization of CK (10 nm binding gold granules) and NGF (5 nm binding gold granules) were found by immunogold electron microscopy in double binding CK/NGF-immunopositive EC processes.

Discussion

A lot of experimental and clinical investigations of different kinds of mouse leukemia and leukemic patients have shown the important role of the thymus in the pathogenesis of lymphoid leukemia and the obligatory participation of the thymic epithelial cells in the intrathymic leukemogenesis. However, the mechanisms by which EC induce "abortive" differentiation and leukemic transformation of the thymocyte precursors of the bone marrow, are still unknown [2, 6, 7].

The results of the present study provide new structural and immunocytochemical evidence for IF alterations in cortical EC of mouse leukemia thymus.

EC may be able to meet the requirements of an altered milieu by modulation their intermediate filaments proteins. The data suggest simultaneous CK/NGF

immunoreactivity modulation of thymic epithelium, which is probably involved in thymocyte microenvironment reorganization during leukemogenesis. It seems likely that the modulation of CK/NGF coexpression may be one of the mechanisms by which the double-immunopositive cortical EC are involved in local regulation of thymus plasticity and T-cell development in leukemic thymus.

Acknowledgements: The authors thank Dr. T. Toshev from the Bulgarian Academy of Sciences, Sofia, for providing the thymus specimens.

References

1. Anderson, G., E. J. Jenkinson: Lymphostromal interactions in thymic development and function. – Nat. Rev. Immunol., 1, 2001, 31-40.
2. Valkov, I., Tz. Marinova, M. Davidoff, L. Takacs. Structural and histochemical features of cortical thymic epithelial cells in mice with chemically-induced lymphoid leukemia. – Thymus, 12, 1988, 39-50.
3. Marinova, Ts., P. Angelova, I. Christov: Thymic lymphoepithelial complex formation in mice with chemically-induced lymphoid leukaemia. – CR Acad. Bulg. Sci., 52, 1999, 129-132.
4. Marinova, Ts., M. Markova, L. Aloe. NGF overexpression and distribution in cortical thymic epithelial cells of mice with experimentally induced leukaemia. – In Vivo, 20, 2006, 259-264.
5. Marinova, Ts. Epithelial framework reorganization during human thymus involution. – Gerontology, 51, 2005, 14-18.
6. Marinova, Tz., N. Valkov. Ultrastructural characheristics of the cytoskeleton in thymus epithelial cells with oncornaviruses. – CR Acad. Bulg. Sci., 37, 1984, 533-335.
7. Turrini, P., M. L. Zaccaria, L. Aloe. Presence and possible functional role of nerve growth factor in the thymus. – Cell Mol. Biol., 47, 2001, 55-64.

Institute of Experimental Morphology, Pathology and Anthropology with Museum
Bulgarian Anatomical Society

Acta morphologica et anthropologica, 19
Sofia • 2012

Characterization of mouse oocytes and oocyte-cumulus complexes extracted for nuclear matrix and intermediate filaments (NM-IF)

V. Nikolova, R. Zhivkova, M. Markova, T. Topouzova-Hristova, A. Mitkova**, S. Delimitreva*

Department of Biology, Medical Faculty, Medical University of Sofia
**Department of Cytology, Histology and Embryology, Faculty of Biology, Sofia University St. Kliment Ohridski*
***Molecular Medicine Center, Medical University of Sofia*

The extraction for nuclear matrix and intermediate filaments (NM-IF) is a three-step procedure removing most proteins while preserving essential cell architecture. We, for the first time, studied systematically mouse oocytes and oocyte-cumulus complexes after NM-IF extraction. Subjected to electrophoresis, they displayed a distinct pattern of bands. Light microscopy of extracted oocyte-cumulus complexes at germinal vesicle (GV) stage showed that much of their content was lost, leaving mainly skeletal structures. However, the general appearance, position of oocyte nucleus, zona pellucida, distribution of cumulus cells and their projections were preserved. In mature oocytes, extraction destroyed the structural organization completely. Our study shows that GV oocyte-cumulus complexes possess interconnected skeletal structures preserving the morphology even after extraction. This stability is lost in maturing oocytes, presumably due to cytoskeletal reorganization and disconnection from cumulus cells after GV breakdown.

Key words: oocyte, nuclear matrix, intermediate filaments, microscopy

Introduction

The extraction for nuclear matrix and intermediate filaments (NM-IF) is designed to preserve only these highly resistant skeletal structures, dissolving most proteins while retaining essential architectural features. It removes membranes and soluble content by non-ionic detergent, microtubules and microfilaments by high salt extraction, and chromatin by nuclease digestion [2]. The NM-IF extraction has been performed on many somatic cell types as well as spermatozoa [5]. However, no systematic study of NM-IF structures in oocytes has been published. An attempt to apply the procedure to hamster oocytes [7] produced only preliminary results due to methodological problems (cells failed to adhere on slides). Kadam et al. [3] found by immunoblotting a particular protein (MYH9) in mouse oocytes extracted for NM-IF, but did not focus on the total

protein profile. We detected by immunofluorescence keratins and vimentin in partially extracted mouse oocytes [6]. However, while immunocytochemistry is informative about selected components, it does not provide comprehensive morphological data. In the present work, we performed NM-IF extraction on immature and mature mouse oocytes and oocyte-cumulus complexes in order to study their light microscopic morphology and electrophoretic protein profile.

Materials and methods

Prepubertal virgin BALB/c females were hormonally stimulated as described in [6]. Cells were obtained by puncturing oviducts and ovaries, then washed in phosphate-buffered saline (PBS), pH 7.2. Those processed for microscopy were briefly treated with 0.5 mg/ml hyaluronidase to remove outer layers of cumulus.

Extraction for NM-IF was performed as described earlier [5, 6]. Oocytes and oocyte-cumulus complexes were placed in cytoskeletal buffer with 0.5% Triton X-100 and then in high-salt extraction buffer containing 250 mM $(NH_4)_2SO_4$ (both steps for 10 min at 4°C). Then cells were treated with 0.2 mg/ml DNase I and 0.1 mg/ml RNase A at room temperature for 20 min. $(NH_4)_2SO_4$ was added to 250 mM for additional 5 min. Some oocytes were left unextracted as controls.

For light microscopy, cells were fixed on slides with methanol and stained with 5% Giemsa in PBS (pH 7.0) for 40 min. Sodium dodecyl sulphate (SDS) electrophoresis was carried out according to [4] on 12% gels under reducing conditions, followed by silver staining as described in [8].

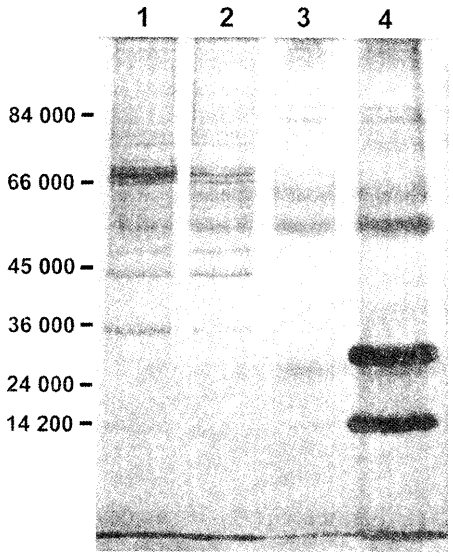

Fig. 1. Proteins from oocyte-cumulus complexes: unextracted controls (1), after cytoskeletal buffer (2), high salt (3) and nucleases (4) on silver-stained electrophoretic gel. At left, positions of molecular weight standards are indicated. The two most prominent bands on lane 4 are DNase I (Mr = 31 300) and RNase A (Mr = 13 700) used for chromatin digestion.

Results

Electrophoresis showed that after NM-IF extraction, a small fraction of the original proteins were preserved, forming a distinct pattern of bands (Fig. 1). Only the most prominent of them (Mr = 57 000) was visible also in unextracted controls.

Light microscopy showed very different effects of extraction on immature and mature oocytes (Fig. 2). Immature oocytes at germinal vesicle (GV) stage were surrounded by cumulus cells with well visible projections through zona pellucida (Fig. 2A). Extracted GV oocyte-cumulus complexes had lost much of their content, retaining mainly skeletal structures. However, the general appearance of the complex, position of oocyte nucleus, zona pellucida, distribution of cumulus cells and their projections were preserved (Fig. 2B).

Oocytes at metaphase I and metaphase II had lost their surrounding cumulus cells while being processed for microscopy. In

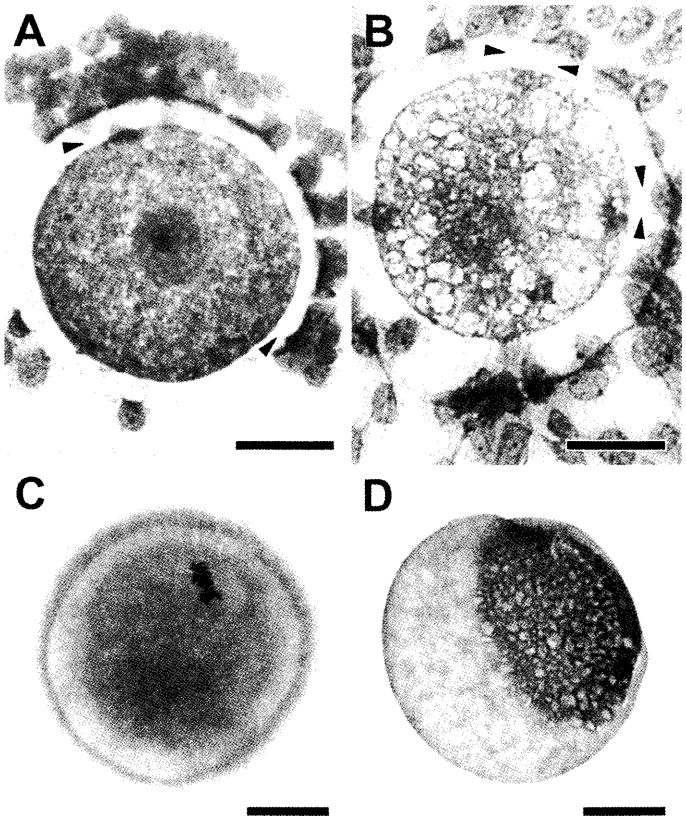

Fig. 2. Micrographs of Giemsa-stained oocytes, bars = 20 μm. **A**. Unextracted control oocyte-cumulus complex at GV stage. Arrowheads indicate projections of cumulus cells. **B**. Extracted oocyte-cumulus complex at GV stage. **C**. Unextracted control mature oocyte. The metaphase II plate is well visible. **D**. Extracted metaphase oocyte. The remaining cytoplasm has formed a sphere without any visible structure.

unextracted controls, cytoplasm had homogenous appearance, with the condensed chromosomes located at the cell periphery (Fig. 2C). Extraction of metaphase oocytes resulted in complete loss of structural organization and collapse of the remaining cytoplasmic content (Fig. 2D).

Discussion

Comparison of protein profiles after SDS electrophoresis showed that in oocyte-cumulus complexes, as in other tissues, proteins resistant to NM-IF extraction are few in number and make up only a small percentage of total protein content. The band with Mr 57 000 probably corresponded to intermediate filament proteins, known to be present in both oocytes and cumulus cells [6].

In our microscopic study, in contrast to the early report in [7], extracted GV oocyte-cumulus complexes retained their general morphology. At this stage, they appar-

ently possess well developed and interconnected skeletal structures allowing preservation of structural features even after disruptive chemical dissection. The importance of intercellular interactions in cell complexes, described for other tissues by different researchers [1, 9], in our case is best illustrated by the projections connecting cumulus cells to the GV oocyte. In later stages of oogenesis, the stability and resistance of supporting structures are lost, presumably due to reorganization of oocyte cytoskeleton and disconnection from cumulus cells after GV breakdown.

Acknowledgement: This study was supported by Medical University of Sofia grant No.15/2009.

References

1. Evangelatov, A., R. Skrobanska, A. Kyumurkov, R. Pankov. Three-dimensional environment stimulates RhoA Activation in fibroblast cells. – C.R. Acad. Bulg. Sci., 64, 2011, 553-558.
2. Fey, E. G., K. M. Wan, S. Penman. Epithelial cytoskeletal framework and nuclear matrix-intermediate filament scaffold: three-dimensional organization and protein composition. – J. Cell Biol., 98, 1984, 1973-1984.
3. Kadam, K.M., S. J. D'Souza, A. H. Bandivdekar, U. Natraj. Identification and characterization of oviductal glycoprotein-binding protein partner on gametes: epitopic similarity to non-muscle myosin IIA, MYH 9. Mol. Hum. Reprod., 12, 2006, 275-282.
4. Laemmli, U. K. Cleavage of structural proteins during the assembly of the head of bacteriophage T4. Nature, 227, 1970, 680-685.
5. Markova, M. D. Electron microscopic observations of human sperm whole-mounts after extraction for nuclear matrix and intermediate filaments (NM-IF). – Int. J. Androl., 27, 2004, 291-295.
6. Nikolova, V., S. Delimitreva, R. Zhivkova, I. Chakarova, D. Dimitrova, M. Markova (2011). Cytoskeletal changes during mouse oocyte maturation revealed by a variation of nuclear matrix and intermediate filaments (NM-IF) extraction. – C.R. Acad. Bulg. Sci., 64, 2011, 1571-1576.
7. Plancha, C. E., M. Carmo-Fonseca, J. F. David-Ferreira (1989). Cytokeratin filaments are present in golden hamster oocytes and early embryos. Differentiation, 42, 1989, 1-9.
8. Sasse, J., S. R. Gallagher (2003). Staining proteins in gells. Curr. Protoc. Mol. Biol., 10, 2003, 10.6.1-10.6.27.
9. Valkov, I., T. Marinova, M. Davidorff, L. Takács. Structural and histochemical features of cortical thymic epithelial cells in mice with chemically-induced lymphoid leukemia. Thymus, 12, 1988, 39-50.

Institute of Experimental Morphology, Pathology and Anthropology with Museum
Bulgarian Anatomical Society

Acta morphologica et anthropologica, 19
Sofia • 2012

Variable position of some structures in the neck. A case report

S. Novakov[1], N. Yotova[1], A. Fusova[1], Ts. Petleshkova[1], P. Timonov[2]

[1]Department of Anatomy, histology and embryology, [2]Depertment of Forensic Medicine, Medical University – Plovdiv, BG

Variations ranging from subtle to remarkable affect every part of the human body. They may have important influences on predisposition to illness, symptomatology, clinical examination and investigation, and patient management including operative surgery. In our case we present several varieties of some neck structures: 1. Heterotopic submandibular gland; 2. Cleidohyoideus muscle (one belly omohyoid attached to the clavicle); 3. Superficial cervical veins varieties; 4. Positional varieties in hypoglossal nerve and lingual artery. Multiple varieties are not unusual and it's often that one abnormality is followed by another which could be explained by factors that affect one and the same period of development. Anatomic anomalies are supported by an underlying embryological basis and manifest their clinical impact. In conclusion, precise morphological evaluation is necessary for each findings considered pathological if only visual diagnosis is made. Sometimes normal structure with heterotopic position may mislead the clinician to consider it as pathological one.

Key words: human anatomy variations, trigonum Pirogovi, heterotopic submandibular gland, external jugular vein, cleidohyoideus muscle

Introduction

It is important to understand that no two living organisms are structurally or functionally identical – animals or plants (Bergman R.A., 2006)! In anatomy, normality embraces a range of morphologies and includes those that are most common and others called variations which are less frequent but not considered abnormal. Variations ranging from subtle to remarkable affect every part of the human body. They may have important influences on predisposition to illness, symptomatology, clinical examination and investigation, and patient management including operative surgery (Willan P.L., 1999, Novakov, S., 2003). Sometimes variety is so unnoticeable that we don't consider it as important for discussion during student dissection. But from a clinician point of view it could be surprising during routine interventions.

Description

In our case we present several varieties of some neck structures:

– Glandula submadibularis heterotopica – During 2nd year student dissection of an adult male cadaver after removing skin and superficial cervical fascia (subcutaneous fat) we noticed a swelling in the right carotid triangle, which doesn't correspond to the known normal structures in this region (Fig.1). The continuation of the dissection revealed that this was the submandibular gland in a heterotypical position – more than half of the gland was placed in the carotid triangle overlapping the deep structures of the region (Fig. 2). On the other side the position of the gland was similar but a little bit higher and closer to its usual one.

Fig. 1

Fig. 2

– Cleidohyoideus (one belly omohyoid attached to the clavicle) – Next variety could be classified as more sufficient one. It was a rare cleidohyoid muscle variety found on the right side of the neck (Fig. 3). First we saw the atypical attachment of the muscle to the middle third of the clavicle and later, when the whole muscle was dissected it became clear that it was a one belly omohyoid starting from its usual origin – hyoid bone (Fig. 4).

– Superficial cervical veins – the veins are the most variable anatomical structures. In this case the two anterior jugular veins were missing and there was a variety in external jugular, which was providing a larger medial tributary with a course along the lower third of anterior border of sternocleidomastoid muscle and ending in suprasternal space. The facial vein drains into the external jugular (Fig. 1).

Fig. 3

– N. hypoglossus – with its almost entire cervical course in digastric triangle. After releasing the submandibular gland on the left side and removing the investing layer of cervical fascia we found out that the loop of hypoglossal was lying above the digastric muscle (Fig. 5).

– A. lingalis – superficial to hyoglossal muscle – Usually the Pirogovi triangle possesses its main artery deep to the hyoglossus muscle. In the described case it's obvious that the lingual artery was lying superficial to the muscle and pierced the origin of the hyoglossus instead of passing beneath the posterior border of the muscle.

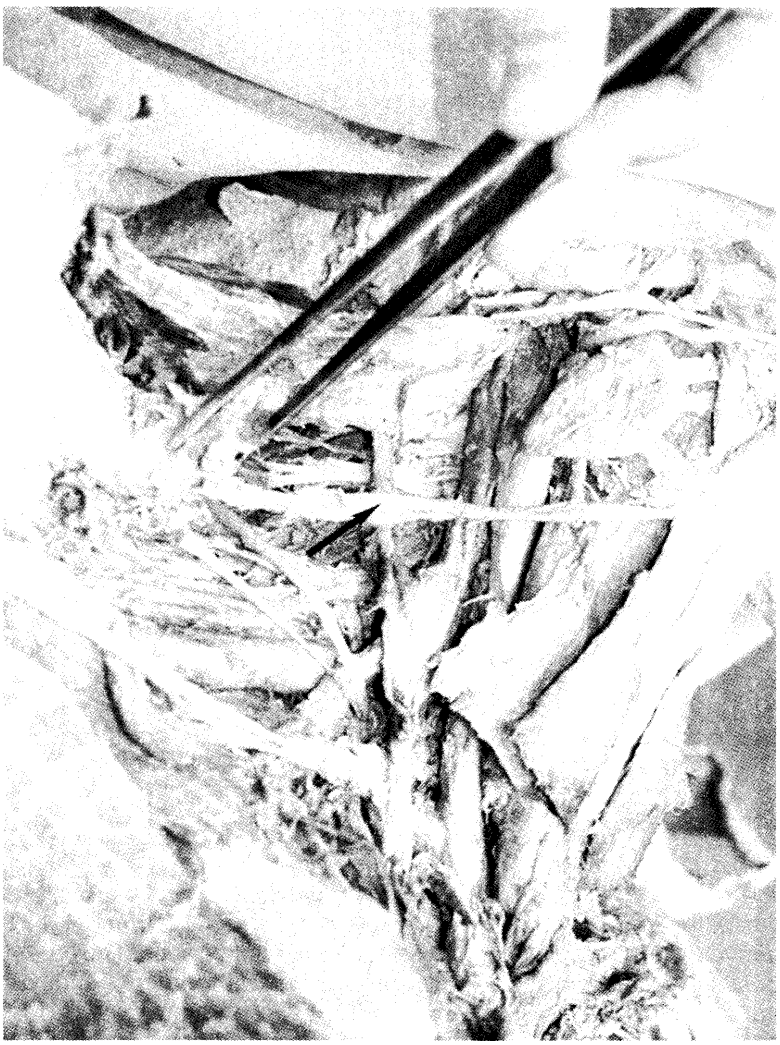

Fig. 4

Discussion

Multiple varieties are not unusual and it's often that one abnormality is followed by another which could be explained by factors that affect one and the same period of development. Anatomic anomalies are supported by an underlying embryological basis and manifest their clinical impact. The external jugular vein is used as venous manometer, while both the external and internal jugular veins are used for intravenous (IV) catheterization to conduct diagnostic procedures or IV therapies. The variations are important for interventional radiologists who perform transjugular procedures, such as port implantations and the transjugular intrahepatic portosystemic shunt or selective venous blood samplings in patients with hyperparathyroidism of unknown origin (Sanli

Fig.5

E.C., 2010, Daniel E., 2005). Tumor or cyst on the neck could be discussed in this case with submandibular gland displacement into carotid region (Triffonov M., 2005). There is no doubt that cleidohyoideus muscle is of clinical importance. The omohyoid muscle is an important landmark in the neck because it divides the anterior and posterior cervical triangles into smaller triangles (Moore K.L., 1992, Cummings, W.C, 1993). Because of its structure and relationship to the large cervical vessels, the omohyoid muscle deserves attention (Ziolkowski M., 1983). The omohyoid muscle is important for radical neck dissection as it is a landmark for this operation (Fukuda, H., 1998). The position of lingual artery in Pirogoff's triangle is important for the clinical practice and its ligation during mouth bleeding makes this region an important landmark for finding the artery (Homze EJ, 1997).

Conclusion

1. Precise morphological evaluation is necessary for each findings considered pathological if only visual diagnosis is made. Sometimes normal structure with heterotopic position may mislead the clinician to consider it as a pathological one.

2. The heterotopic position could also be of serious importance during surgical operations.

References

1. Bergman, R. A., A. K. Afifi, R. Miyauchi, 2006. Illustrated Encyclopedia of Human Anatomic Variation. Opera. URL:http://www.anatomyatlases.org/AnatomicVariants/AnatomyHP.shtml [accessed May 2012].
2. Cummings, W. C., M. J. Fredricson, A. L. Harker; 1993. Otolaryngology-Head and Neck Surgery 2, 2nd ed., Missouri, USA, Mosby-Year Book, 1539–1540, 1649–1650.
3. Daniel, E., W. F. Sr McGuirt, 2005. Neck masses secondary to heterotopic salivary gland tissue: a 25-year experience. – Am J Otolaryngol., 26, 96–100.
4. Fukuda, H., K. Onizawa, T. Hagiwara, H. Iwama, 1998. The omohyoid muscle: a variation seen in radical neck dissection. – Br. J. Oral. Maxillofac. Surg., 36, 399–400.
5. Homze E. J., S. D. Harn, B. J. Bavitz, 1997. Extraoral ligation of the lingual artery: an anatomic study. – Oral Surg Oral Med Oral Pathol Oral Radiol Endod., 83(3), 321-324.
6. Moore, K. L.; 1992. Clinically Oriented Anatomy, third ed, Baltimore, Williams & Wilkins A Waverly Company,.797.
7. Novakov, S., N. Yotova, 2003. Some variations in an embalmed dissected cadaver. – Anatomical Collection, 85th Anniversary of the Department of Anatomy and Histology, 71-72.
8. Sanli, E. C., N. C. Oztürk, A. Polat, H. Oztürk, 2010. Bilateral and symmetrical heterotopic submandibular glands in the upper neck: case report. – Surg Radiol Anat., 32(10), 979-982.
9. Triffonov, M., N. Yotova, S. Novakov, Hr. Shipkov, 2005. Accessory salivary tissue in the face. – Union of scientists in Bulgaria-Plovdiv, Series D. Medicine, Pharmacy and Stomatology, volume V, 287-9.
10. Willan, P. L., J. R. Humpherson, 1999. Concepts of variation and normality in morphology: important issues at risk of neglect in modern undergraduate medical courses. – Clin Anat, 12(3), 186-190.
11. Ziolkowski, M., J. Marek, J. Oficjalska-Mlynczak, 1983. The omohyoid muscle during the fetal period in man. – Folia. Morphol. (Warsz)., 42, 21–30.

Institute of Experimental Morphology, Pathology and Anthropology with Museum
Bulgarian Anatomical Society

Acta morphologica et anthropologica, 19
Sofia • 2012

Characteristics of milk cells

V. Pavlova, B. Alexieva, E. Nikolova

Institute of Experimental Morphology, Pathology and Anthropology with Museum, Bulgarian Academy of Sciences, Sofia

Human colostrum and milk represent complex biological liquids containing different immunoactive agents that change during lactation. These include immunocompetent cells like macrophages and lymphocytes with blood origin. Morphological characteristics of human leucocytes were assessed by the use of light microscopy, scanning electron microscopy and transmission electron microscopy. Additional characteristics of milk cells in colostrum were, investigated using membrane markers after lectins, Ag I/II or MBB activation. These examinations proved lymphocytes and macrophages as potential antigen presenting cells.

Key words: milk cells, colostrum, mucosal immunity.

Introduction

Human colostrum and milk represent complex biological liquids containing different immunoactive agents that change during lactation. Among them milk cells exist, in concentration of 1-3x10^6 in ml cells. These immunocompetent cells are neutrophils, macrophages and lymphocytes which have blood origin. Their range varies among individuals and time of lactation. T-lymphocytes are more abundant in comparison to B-lymphocytes that could be no more than 6% of total number of lymphocytes.

Materials and Methods

Light and electron microscopy

For the characterization of leukocyte population 512 samples of human breast milk from healthy donors were collected. Samples were taken between 2nd and 30th days post partum. Centrifugation at 200g was performed for 20 min to isolate leucocytes, followed by PBS washing. Afterwards cells were processed for light microscopy (LM), transmission electron microscopy (TEM) and scanning electron microscopy (SEM).

Observation under LM was performed on cell smears after the method of Wright-Farbung [1]. Eosin methylene blue was added to cell smears and left for one min, then 1 ml of distilled water was added and left another 3 min. Slides were dried at room temperature.

For SEM, cells were washed three times in PBS and left to adhere on cover slips for 20 min. They were then fixed in 2, 5% glutaraldehyde, dehydrated in graded ethanol solutions and covered with gold. Observation was performed under JEM-35 scanning electron microscope. For TEM observation milk samples were diluted three times with cold PBS and centrifuged three times at 1000g. Then cells were resuspended in 3% agarose in PBS and put on ice and fixed in 2,5% glutaraldehyde and post fixed in 1% OsO_4. Then samples were dehydrated in graded ethanol solutions and embedded in resin. Ultra thin sections were cut and observed under transmission electron microscope Opton EM 109.

Cultivation and Proliferation

Human milk samples were centrifuged at 200g for 20 min. and washed 4 times in PBS supplemented with 10% fetal calf serum (FCS). (1 x 10^6) cells were incubated in RPMI 1640 medium containing 10% FCS for 24, 48 and 72 hours in presence of 10 μg MBB, 5 μg Con A or 0, 1 μg Ag I/II at 37C, 5% CO_2. Control samples contained only cells, cultured in RPMI 1640 medium and 10% FCS. For proliferation assay cells were incubated with 1 μCi ^{3}H-Thy. Labeled DNA was harvested onto DEAE filters and triplicate sample readings were obtained by scintillation counting /Beckman/.

Indirect Peroxidase Technique

1 x 10^6 cells were stimulated with mitogens or antigens and cultured in presence of the following mAb: mB1, CD-71, CD-3, CD-4, RFD-7 and MA-5. Then cells were washed in PBS and cultured in presence of anti mouse Ig conjugated with peroxidase. 200 cells were counted on each sample and colored after Wright for cytological examination. For DNP and RNP activation of milk cells we performed methylene blue fast green method [2].

Results and Discussion

Human neutrophils and macrophages from breast milk showed regular morphology, compared to those, obtained from peripheral blood but had more granules, impregnated with lipids and carbohydrates. (see Fig. 1 and Fig. 2). Lymphocytes showed no morphological differences to those found in peripheral blood.

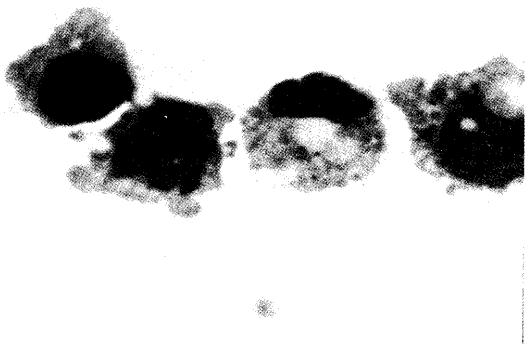

Fig.1. Macrophages from human colostrum, with pinocitotic vesicles or with microclasmatozes. (x 1000)

Fig.2. Leukocyte in human colostrum (x 1000)

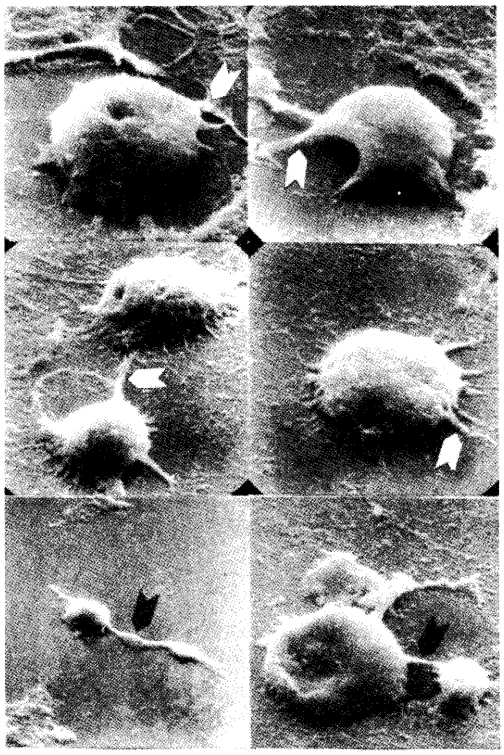

Fig.3.SEM micrograph of milk cells, with protrusions. Originally x 10000.

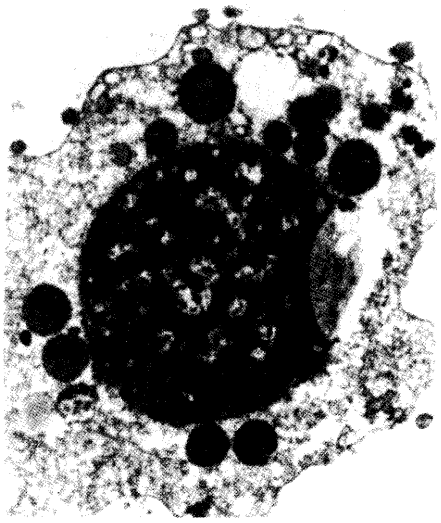

Fig.4. TEM micrograph of milk macrophage. Originally x 12000

Both TEM and SEM confirmed morphological characteristics of peripheral blood cells. Visibly (Fig. 3), cells possessed protrusions enabling their close contact with each other. TEM micrographs (Fig.4) represented typical neutrophils with plenty of lipid and carbohydrate granules and often with activated nuclei.

Activation of milk cells with Con A or MBB was performed and expression of several markers was assessed. The highest expression was found on second and third days of activation as visible in Fig 5.

ConA/MBB stimulation	DAY 0 to 4				
Marker	0	1	2	3	4
HLA-DR	14/14	72+/69+	58+/58+	43+/44+	20/20
CD71	2/2	21+/27+	62+/57+	78+/61+	40+/36+
CD3	12/12	50+/59+	72+/58+	76+/59+	47+/33+
CD4	10/10	28+/26+	29+/34+	40+/43+	25+/20+
3H-Thy Incorporation	-/-	4,1++/2,1++	7,0++/4,5++	6,1/6,6++	3,8+/6,2+

Fig.5. Expression of markers after ConA or MBB stimulation of milk cell.

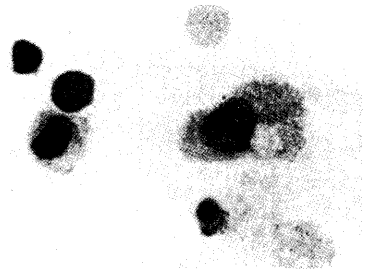

Fig.6. DNP and RNP staining of milk cells after Zvetkova E. et al. (x250).

mAb	Specificity	Day0	Day2	Day4
RFD7	macrophages	65±4	38±11	0±5
MA5	blood monocytes	26±3	84±8	93±6
mB1	antiHLA-DR	25±9	80±12	90±4

Fig.7. Expression of macrophages markers after *in vitro* stimulation with AgI/II.

After activation with AgI/II antibody, up regulation of RFD7 expression was observed, mostly in tissue macrophages and MA5 and mB1 were present only in 20% of cells (Fig.7)._Expression of the latter two markers increased with time of cultivation, which means macrophages in human colostrum were capable of inducing *de novo* synthesis and differentiation after activation with mitogens. The observation was confirmed by another cytological method. DNP and RNP staining of milk cells (see Fig. 6) revealed nuclear activation and possibility of *de novo* synthesis in milk macrophages.

Previous studies have proved that milk cells could pass the neonatal intestinal barrier. The precise mechanisms of crossing the intestinal mucosa have not been established yet [3]. After ingestion the maternal cells populate the lymph nodes, and could be often found in other tissues of the newborn. Thus they express their immunomodulating effects on neonates [4, 6]. Major histocompatibility complex (MHC) Class II antigens are fully expressed on newborn human intestinal mucosa [5]. MHC represents membrane glycoproteins, present on the cell surfaces of leucocytes. Class II antigens have limited expression- they are present only on mononuclear phagocytes and B-lymphocytes. Activation of milk cell with Con A, MBB or AgI/II demonstrated that maternal macrophages and lymphocytes expressed MHC Class II antigens *in vitro*, which means they are potential antigen-presenting cells. Activation with other antigens [7] showed similar to our results: colostral lymphocytes cross intestinal mucosa of newborn and remain immunologically active.

In conclusion the neonate intestine represents a unique system, unaffected by any antigens. Newborns receive adult antigen-presenting cells from maternal colostrum and milk. These cells are not recognized as foreign. Thus immune responses in neonates could be modulated in order of their survival.

References

1. Crago S, S. Prince, T Pretlow, J. McGhee, J. Mestecky. Human colostral cells. I. Separation and characterization. – Clin Exp Immunol, 38, 1979, 585-597.
2. Zvetkova E, J Jelinek. Methylene blue fast green staining of hemopoetic colonies in agar cultures. – Gegenbaurs Morphol Jahrb, 135, 1989, 779-793.
3. Jan C Le. Cellular components of mammary secretions and neonatal immunity: a review. – Vet Res., 27, 1996, 403-413.
4. Rognum T, PThrane, LStoltenberg, AVege, PBrandtzeag. Development of intestinal mucosa immunity in fetal life in the first postnatal months. – Pediatr Res., 32, 1992, 145-149.
5. Weaver E, H Tsuda, A Goldblum, C Davis. Relationship between phagocytosis and immunoglobulin release from human macrophages. – Infect Immun, 38, 1982, 1073-1077.

6. Williams P. Immunomodulating effect on intestinal absorbed maternal colostral leukocytes by neonatal pigs. – Can J Vet Res. 57, 1993, 1-8.
7. Tuboly S, S Berath, R Glavits, A Kovacs, Z Megyeri. Intestinal absorption of colostral lymphocytes in newborn lambs and their role in the development of the immune status. – Acta vet Hung, 43, 1995, 105-115.

Institute of Experimental Morphology, Pathology and Anthropology with Museum
Bulgarian Anatomical Society

Acta morphologica et anthropologica, 19
Sofia • 2012

Effect of sodium nitrite on sperm count in mature rats

E. Pavlova, D. Dimova, E. Petrova, Y. Gluhcheva, V. Ormandzhieva, D. Kadiysky, N. Atanassova

Department of Experimental Morphology, Institute of Experimental Morphology, Pathology and Anthropology with Museum, Bulgarian Academy of Sciences
Sofia 1113, Acad. G. Bonchev Str., Bl. 25, E-mail: e_bankova@yahoo.com

Sodium nitrite ($NaNO_2$) is a common food additive used as a color fixative and preservative in meats and fish. It is also known as hypoxia inducible agent and hypoxia has been shown to affect testicular functions. The aim of the present study is to investigate the effect of $NaNO_2$ on the sperm count in mature rats. Four-month-old male Wistar rats were intraperitoneally injected with $NaNO_2$ at 50 mg/kg b.w. Treated animals were sacrificed at different time intervals (days 5, 10 and 20) following the administration. Testes and epididymides were sampled. Spermatozoa were isolated from both vasa deferentia and counted. Reduction in the sperm count was observed in all experimental groups after $NaNO_2$ administration. The gonado-somatic index was elevated on the fifth day and returned within the normal range at later stages. Future studies would elucidate if $NaNO_2$-induced quantitative changes in the testicular structure are supported by histopathological findings.

Key words: sodium nitrite, rat sperm count

Introduction

Humans are constantly exposed to $NaNO_2$ through food and drinking water, with a minor contribution from air [5]. Sodium nitrite is known as E250 in the food industry. Other sources of $NaNO_2$ are various industries including agricultural, chemical industry, textile processing industry, disinfectants, colouring agents, etc. [4]. In the circulation $NaNO_2$ causes conversion of hemoglobin to methemoglobin, which is incapable of transporting oxygen to the body's tissues and organs and can cause hemic hypoxia.
The widespread use of sodium nitrite in the food industry contributes to the potential health risk if not handled cautiously and arouses the necessity of studying its effects. There is evidence of developmental and reproductive toxicity of $NaNO_2$ in experimental animal studies. However, available literature data for the impact of $NaNO_2$ on the testis are insufficient. In this respect, the aim of the present study is to investigate the effect of $NaNO_2$ on the sperm count in mature rats.

Materials and Methods

The experiments were carried out on four-month-old male Wistar rats. The animals were divided into three $NaNO_2$-treated groups (n=15 rats per group) and age-matched control group (n=16). Rats were maintained in the institute's animal house in standard hard bottom polypropylene cages at 23°C±2°C and 12:12 h light/dark cycle with free access to laboratory chow and tap water throughout the study.

In brief, $NaNO_2$ was injected intraperitoneally at 50 mg/kg body weight (1 ml dosing volume). Treated animals were sacrificed at different time intervals following the administration (days 5th, 10th and 20th) under light anesthesia. The control rats were injected with the same volume of distilled water. Testes and epididymides were sampled and weighed. Spermatozoa were isolated from both vasa deferentia and counted using Buerker's chamber. Data were statistically processed using Student's *t*-test.

The animal experiments were performed in accordance with the animal protection guidelines approved by the Ethics Committee for Experimental Animal Use at IEMPAM, BAS.

Results and Discussion

Toxicity to humans and animals is documented in nitrite overexposure including impairment of reproductive function. Literature data for the effect of sodium nitrite on the male reproductive system are controversial. Several studies provide some evidence of testicular changes at the histopathological level in male rats, but the observed effects

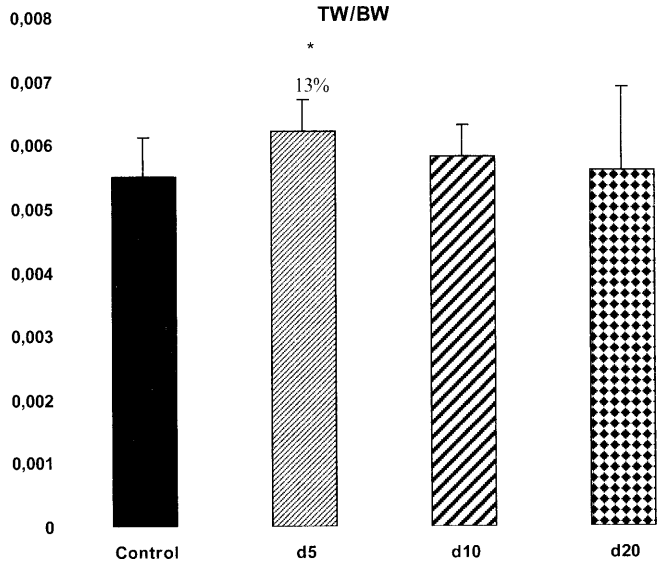

Fig. 1. Changes in rat gonado-somatic index (ratio of testis weight to body weight) at different time intervals after $NaNO_2$ treatment. Data represent mean value ± SDs (* $p < 0.05$; ** $p < 0.01$; *** $p < 0.001$).

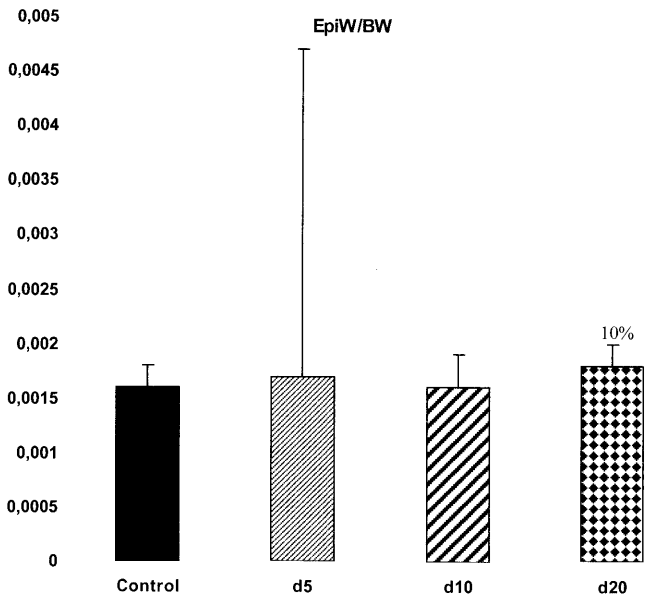

Fig. 2. Changes in rat epididymal index (ratio of epididymal weight to body weight) at different time intervals after $NaNO_2$ treatment. Data represent mean value ± SDs (* $p < 0.05$; ** $p < 0.01$; *** $p < 0.001$).

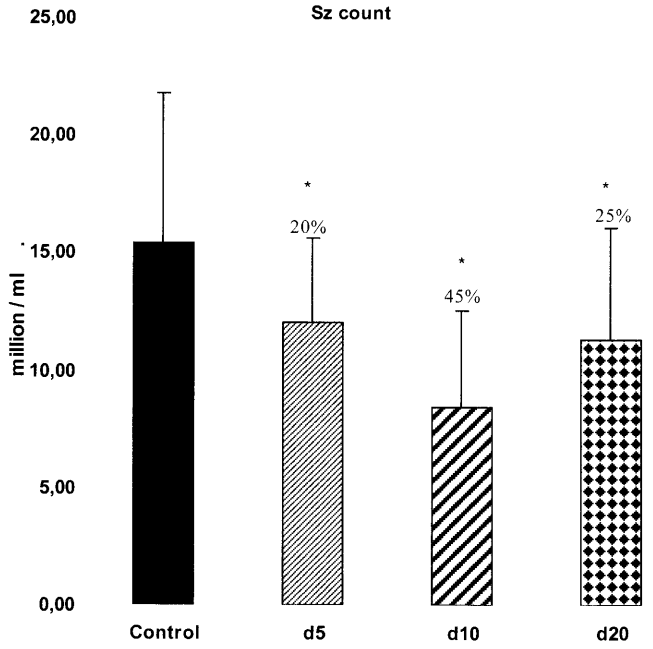

Fig. 3. Changes in rat sperm count at different time intervals after $NaNO_2$ treatment. Data represent mean value ± SDs (* $p < 0.05$; ** $p < 0.01$; *** $p < 0.001$). Sz count – spermatozoa count.

could not be confidently attributed to $NaNO_2$ exposure [3]. Sperm-head abnormalities after treatment of differentiating spermatogonia are reported in mice [1]. In contrast, no evidence of testicular pathology is identified in animals subjected to a 3-day regimen of $NaNO_2$ injections [2].

In the present study we report a decrease in the rat sperm count after different periods of sodium nitrite treatment. The gonado-somatic index (ratio testicular weight to body weight) was elevated on the fifth day (13%) and returned within the normal range at later stages (Fig. 1) whereas epididymal index (ratio epididymal weight to body weight) remained at normal values in all investigated periods (Fig. 2). Elevated gonado-somatic index in our study could be due to increased testicular fluid volume which may be associated with vascular permeability and disturbances of water-salt balance. Hormonal changes resulting from dysfunction in the hypothalamo-hypophysial-gonadal axis could be another possible cause for the elevated index. Our data also suggest that the testis is more sensitive to the effect of $NaNO_2$ in the first days after administration in comparison to epididymis.

We can conclude that $NaNO_2$ affects some weight indices and sperm count in mature rats. Our future work would elucidate if $NaNO_2$ administration provokes changes in the testicular morphology and morphometric parameters.

Acknowledgments: This work is supported by a grant No DMU 03/18 for Young scientists from the Bulgarian National Science Fund.

References

1. Alavantić, D., I. Sunjevarić, J. Pecevski, D. Bozin, G. Cerović. In vivo genotoxicity of nitrates and nitrites in germ cells of male mice. I. Evidence for gonadal exposure and lack of heritable effects. – Mutat. Res., 204, 1988, №4, 689-695.
2. Bond, J. A., J. P. Chism, D. E. Rickert, J. A. Popp. Induction of hepatic and testicular lesions in fischer-344 rats by single oral doses of nitrobenzene. – Fundam. Appl. Toxicol., 1, 1981, 389-394.
3. Reproductive and Cancer Hazard Assessment Section (RCHAS), Office of Environmental Health Hazard Assessment (OEHHA), California Environmental Protection Agency (CAL/EPA). Evidence on Development and Reproductive Toxicity of Sodium Nitrite. 2000.
4. U. S. Department of Health and Human Services. Toxicology and Carcinogenesis Studies of Sodium Nitrite. Drinking Water Studies. 2001.
5. WHO. Nitrate and nitrite in drinking water. Background document for development of WHO Guidelines for Drinking-water Quality. 2007.

Institute of Experimental Morphology, Pathology and Anthropology with Museum
Bulgarian Anatomical Society

Acta morphologica et anthropologica, 19
Sofia • 2012

Immunohistochemical expression of ghrelin and leptin in newborn rats

N. Penkova, P. Atanasova

Deparment of Anatomy, Histology and Embryology, Medical University, Plovdiv

Ghrelin is produced in the stomach, stimulates the release of GH from the anterior pituitary through the GH receptors, thus activating hunger. Using different methods the hormone is identified in the endocrine cells of the stomach and the Langerhans islands, but the phenotype and the morphological characteristics of the ghrelin-producing cells have not yet been discovered. Leptin is a hormone produced by the adipocytes. It plays a role in body weight regulation by signaling to the brain to reduce hunger and burn more calories. The complex interactions of ghrelin and leptin in appetite regulation are not yet elucidated. The aim of the present work was to study the morpho-functional link of ghrelin and leptin by finding out immunohistochemical expression presence and localization of both homones in rats. Immunohistochemical reactions for leptin and ghrelin by the ABC method with primary polyclonal antibodies (Santa Cruz, USA) were fulfilled on paraffin sections of fragments of subcutaneous adipose tissue and stomach of newborn Wistar rats. Our study demonstrated positive expression of leptin in the adipose cells of the subcutis but not in the stomach mucosa cells. Immunohitochemical reaction for ghrelin was detected in some of the cells of the stomach glands in the newborn rats. Adiopocytes did not express ghrelin. Our results, revealing the localization and activity of leptin and ghrelin in the investigated tissue, suggest their close relations and interaction in the regulation appetite and metabolism from birth.

Key words: ghrelin, leptin, gastrointestinal tract, rat

Introduction

The morphological structure and functions of the gastrointestinal tract are yet to be completely studied. This is demonstrated by the discovery of a new hormone, produced by the gastrointestinal cells, called ghrelin. Ghrelin is an oligopeptide, composed of 28 aminoacids, isolated for the first time from a rat stomach [1]. Its secretion increases when the stomach is empty. Diet rich in lipids decreases ghrelin's plasma level while a low protein diet increases it [2]. Through specific receptors ghrelin binds with diencephalon nuclei and stimulates the feeling of hunger [3,4]. It is known that ghrelin is a releasing factor for growth hormone, acts as a ligand for the secretory receptors of growth hormone (GH-R) in adenohypophysis. As a releasing factor for the growth hormone it takes part in the regulation of metabolism. Ghrowth hormone itself stimulates the growth of bones and soft fissues, acts on protein, lipid and carbohydrates metabolism. Ghrelin was identified by the methods of immunochemistry and RT-PCR in the endocrine cells of ventricular mu-

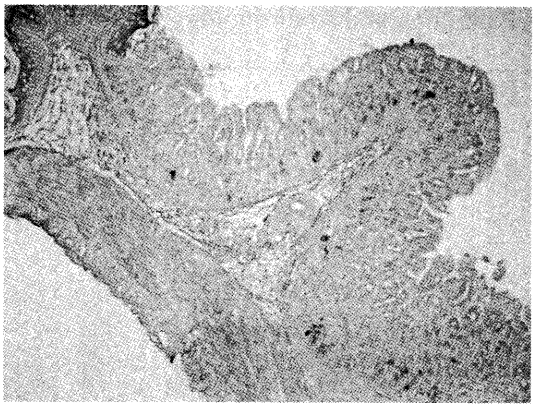

Fig. 1. Stomach of an one-day-old newborn rat. The mucosa of the esophagus passes in the mucosa of the stomach. We can observe pars cardiaca and part of the fundus of the stomach. All tissue layers of the gastric wall are formed. (x 10).

cosae and Langerhans isled in human [5]. But the type of the endocrine cells that secrete it has not yet been identified. Leptin is a hormone produced by the adipocytes. It plays a role in body weight regulation by signaling to the brain to reduce hunger and burn more calories. The aim of the present work was to study the morpho-functional link of ghrelin and leptin by finding out immunohistochemical expression presence and localization of both homones in rats.

Material and methods

The study is carried out on from fragments of subcutaneous adipose tissue and stomach of 10 one-day-old newborn Wistar rats. Paraffin sections of the stomach and the subcutaneous tissue were investigated by the ABC method for 12 hours using primary antibodies for: 1.ghrelin (rabbit polyclonal antibody Ghrelin – Santa Cruz Biotechnology, USA) dilution 1:100 at 4◦C and 2. primary polyclonal rabbit antibody for leptin (Santa Cruz Biotechnology, USA) dilution 1:200 at 4◦C. DAB was used as a chromogen. Leptin was expressed by brown granular substance and ghrelin was expressed by black granular substance in the cytoplasm of the cells. Negative controls, with buffer (PBS) or normal non-immune serum used instead of the specific antibodies, were used to verify the specificity of the immunohistochemical reactions to any examined antigen. In those samples no product from the corresponding reaction was present.

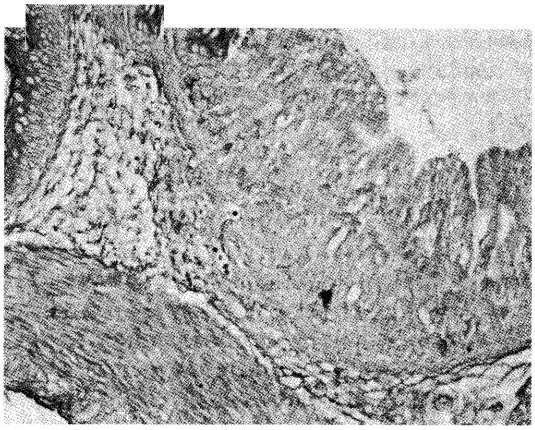

Fig. 2. Stomach of an one-day newborn rat – pars cardiaca. Single ghrelin-positive cell in the bottom of the cardia`s gland. We observe an immunohistochemical reaction of moderate intensity. The cytoplasm in the enlarged basal part of the cell is filled with fine black granules Paraffin preparation (x 20).

Results

From the sectors under study of the digestive tract – esophagus, stomach and intestine, expression of ghrelin was received only in fragments from the stomach. The morphological characteristic of the gastric wall shows the typical picture of a tubular organ. All tissue layers of mucosa are well formed. The couvering epithelium is a single-breasted cylindrical secretorius. In the home plate the glands are tightly arranged. Two or three rows of smooth muscle cells highlight the underlying loose connective tissue of the submucosa. In the thick muscular sheath are distinguished smooth muscle layers with circular, longitudinal

and oblique direction (Fig. 1). In the initial part of the stomach – pars cardiaca is established expression in single cells located on the bottom of the cardiacus glands. Immunohistochemical reaction was of moderate intensity. The black granules fill the entire cytoplasm of the endocrine cell (Fig. 2). In the fundus of the stomach is established a positive reaction in many cells from the bottom of the main glands. The expression of ghrelin in them is from weak to moderate (Fig. 3). Ghrelin positive cells are present in the body of the stomach. Here we observe a large number of endocrine cells with moderate intensity, as well as single cells with high intensity of immunohistochemical reaction. In these black granules tightly fill the entire cytoplasm of the cell (Fig. 4). Our immunohistochemical study demonstrated positive expression of leptin in the adipose cells of the subcutis. It is detected as a brown staining in the cytoplasm of the adipocytes which were typical mature unilocular cells – with one lipid drop occupying the whole cell and cytoplasm and nucleus pushed to the cell periphery. Subcutaneous adipocytes are not demonstrate positive immunohistochemical staining for ghrelin (Fig. 5.). Our study discovered positive expression of leptin in the subcutaneous adipose cells but none in the stomach mucosa. Immunohistochemical reaction of ghrelin was esltablished in some cells of the stomach glands in newborn rats. Adipocytes did not express ghrelin.

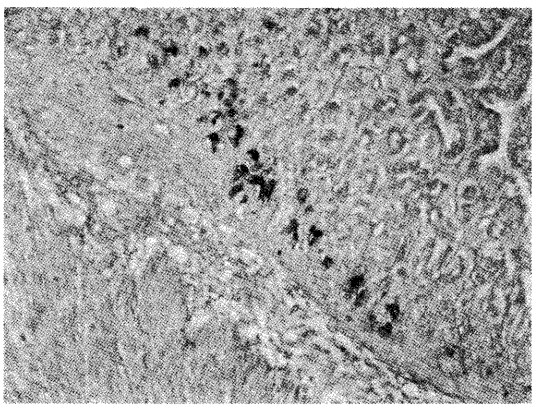

Fig. 3. Stomach of an one-day newborn rat – fundus. A large number of ghrelin-positive cells in the bottom of the main gland – gll. gastricae propriae. Immunohistochemical reaction with mild to moderate intensity. Paraffin preparation. (x 20).

Discussion

Many authors do not find expression of ghrelin in stomach cells of newborn rat fetuses despite the presence of high plasma levels of ghrelin in the fetus. Nakahara et al. explain this fact with high permeability of the hematoplacentar barrier for ghrelin. The hormone comes from the mother. It is established that the ghrelin which comes from the mother is one of the important factors that regulate the weight of the fetus during the late stages of pregnancy [6]. Hayashida T. et al. discover that the level of ghrelin in the postnatal period of newborn rats increases. Peak levels are reached during the second and third week after birth [7]. Our results also demon-

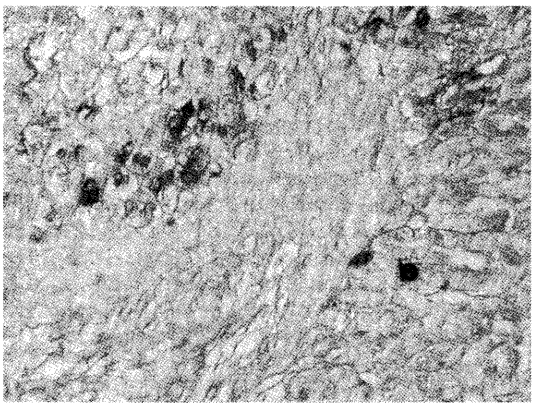

Fig. 4. Stomach of an one-day newborn rat – corpus. An area with a large number of endocrine cells with weak to moderate intensity of immunohistochemical reaction. Single ghrelin-positive cells with high intensity – the black granules tightly fulfil throughout the cytoplasm of the cell. Paraffin preparation. (x 40).

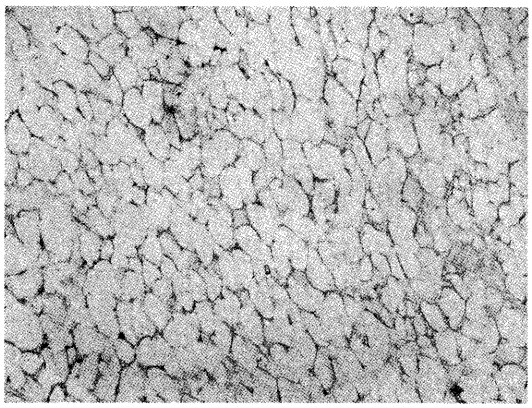

Fig. 5. Biopsy specimens from the subcutis. Leptin-positive adipose cells. Brown staining in the cytoplasm of the mature unilocular adipocytes. Paraffin preparation. (x20).

strate positive immunohistochemical expression of ghrelin in the stomach of one day old rats. K. Choi et al establish adipogenic effect of ghrelin on the white adipose tissue in vitro [8]. Other authors describe ghrelin as an inhibitor to some types of lipolisis [9]. W. Zhang et al. published opposite results on the activity of ghrelin on preadipocytic differentiation and proliferation. Study on cell lines with super expression of ghrelin revealed an inhibitory effect on adipogenesis [10].

Conclusion

Differentiated ghrelin producing cells are present in the wall of gastrointestinal tract during the early neonatal period. Positive immunihistochemic activity of leptin is established in adipocytes from the subcutaneous fat tissue of experimental animals. Further studies on the receptors for both of those hormones and the cells that express them would shed some light on the debatable question about the lack or presence of direct effect of ghrelin on adipocytes and its direction – stimulating or inhibitory.

References

1. Dornonville de la C., M. Bjorkqvist, A.K.Sandvik, I. Bakke, C.-M. Zhao, D. Chen, R. Hakanson. A-like cells in the rat stomach contain ghrelin and do not operate under gastrin control. – Regulatory Peptides, June 2001, **99**, 141-150.
2. Lee H., G. Wang, E. W. Englander, M. Kojima, G. H. Greeley Jr. Ghrelin, a new gastrointestinal endocrine peptide that stimulates insulin secretion: enteric distribution, ontogeny, influence of endocrine, and dietary manipulations. – Endocrinology, **143**, 2002, 185-190.
3. Chartel N., M. Kojiwa, K. Kandawa, H. Vaudry. Immunohistochemical localization and biochemical characterization of the frog Rana esculenta. – J. Comp. Neurol., 450, 2002, 34 – 44.
4. Fukumoto K., K. Nakahara, T. Katayama, M. Miyazatao, K. Kangawa, N. Murakami. Synergistic action of gastrin and ghrelin on gastric acid secretion in rats. – Biochemical and Biophysical Research Communications, **374**, 2008, 60-63.
5. Svenson H., H. Mulder, F. Sundler. The ghrelin cell: a novel developmentally regulated islet cell in the human pancreas. – Regul. Pept., **107**, 2002, 63 – 9.
6. Nakahara K., M. Nakagawa, Y. Baba, M. Sato, K. Toshinai, Y. Date, M. Nakazato, M. Kojima, M. Miyazato, H. Kaiya, H. Hosoda, K. Kangawa, N. Murakami. Maternal ghrelin plays an important role in rat fetal development during pregnancy. – Endocrinology, **147**, 2006, 1333-1342.
7. Hayashida T., K Nakahara, M S Mondal 1, Y Date 1, M Nakazato 1, M Kojima 2, K Kangawa 2 and N Murakami. Ghrelin in neonatal rats: distribution in stomach and its possible role. – Journal of Endocrinology, **173**, 2002, 239–245.
8. Choi, K., Roh, S. G., Hong, Y. H., et al. The role of ghrelin and growth hormone secretagogues receptor on rat adipogenesis. – Endocrinology, **144**, 2003, 754–759.
9. Muccioli, G., Pons, N., Ghe, C., et al. Ghrelin and des-acyl ghrelin both inhibit isoproterenol-induced lipolysis in rat adipocytes via a non-type 1a growth hormone secretagogue receptor. – Eur J Pharmacol., **498**, 2004, 27–35.
10. Zhang, W., Zhao, L., Lin, T. R., et al. Inhibition of adipogenesis by ghrelin. – Mol Biol Cell., **15**, 2004, 2482–2491.

Institute of Experimental Morphology, Pathology and Anthropology with Museum
Bulgarian Anatomical Society

Acta morphologica et anthropologica, 19
Sofia • 2012

Gender differences of the external nose in Bulgarians examined by 3D laser scanning

T. Petleshkova[1], P. Timonov[2], S. Sivkov[1], M. Manev[4], M. Yordanova[5], S. Yordanova[5], B. Vladimirov[3], Y. Zhecheva[6], I. Ivanova-Pandourska[6]

[1]*Department of Anatomy, Histology and Embryology, Medical University – Plovdiv*
[2]*Department of Pathoanatomy and Forensic Medicine, Medical University – Plovdiv*
[3]*Department of Maxillofacial Surgery, Medical University – Plovdiv*
[4]*Department of Orthodontics, Medical University – Plovdiv*
[5]*Faculty of Mathematics and Informatics, Plovdiv University "PaisiiHilendarski"*
[6]*Institute of experimental morphology, pathology and anthropology with museum, Bulgarian Academy of Sciences*

The aim of the study was to investigate the morphology of the external nose in young healthy male and female individuals of Bulgarian origin. Thirty nine subjects (16 male and 23 female) were included in the study. Their mean age was 26 years, mean weight – 70 kg and mean height – 172 cm. The surface of the face was scanned by a laser scanner (FastSCAN) with the head in Frankfort horizontal plane. The following anthropometric points were marked on the three-dimensional model: n, prn, sn and al (right and left). Each point was characterized by x, y and z values. The following measurements were calculated: volume of the external nose (mm^3), areas of nasal surfaces (mm^2), linear distances (mm), and angles (degrees). It was found that male nasal dimensions were greater than female and all measurements demonstrated racial differences.Sexual dimorphism is found in nasal width, volume of the external nose and areas of nasal surfaces.

Key words: gender differences, external nose, 3D laser scanning, Bulgarians, three-dimensional model

Introduction

The external nose is a human body structure that undergoes dynamic changes throughout life. It has relevance to various diagnostic, clinical and forensic procedures [1]. A number of cross-sectional and longitudinal investigations by foreign authors found that older individuals possessed noses with larger dimensions compared to younger people of the same sex and race. The external nose was also found to be larger in men than in women of the same age and race group [2, 3, 4]. Abnormal nose form and dimensions are found in congenital anomalies of the upper lip and palate, in certain genetic disorders like Down's syndrome and hypohidrotic ectodermal dysplasia [5, 6]. Detailed assessment of the nasal morphology is especially important for the

restoration of the facial profile by surgical reconstructive procedures. The changes of nasal form and dimensions associated with sex and age could be of help for forensic anthropologists in the identification of alive or diseased people. The aim of the present study was to investigate the morphology of the external nose in young healthy male and female individuals of Bulgarian origin. The mean dimensions were to be compared with the results from investigations by foreign authors on different population groups of the same age and sex. Another aim of the study was to look for association between some dimensions of the nose and height and weight of the studied individuals.

Material and methods

Thirty nine subjects (16 male and 23 female) were included in the study. Their mean age was 26 years, mean weight was 70 kg and their mean height – 172 cm. The subjects were selected to be above 20 years because of the slower rate of nasal change after this age as well as more pronounced gender differences in nasal shape and dimensions. The exclusion criteria were as follows: cranio-maxillofacial trauma, congenital anomalies, surgical interventions in the nasal area, genetic and psychiatric disorders. The surface of the face was scanned by a laser scanner (FastSCAN) with the head in standard position (Frankfort horizontal plane). The following anthropometric points were marked on the three-dimensional model: n, prn, sn and al (right and left). Each point was characterized by x, y and z values. The method was generally based on the so-called geometric morphometry [19, 20]. The separate objects in space are characterized by specific shape and size. For example a football and a tennis ball have the same shape but different size, whereas a balloon with certain size can have different shapes depending on modeling [19]. Therefore both shape and size must be taken into account in order to compare objects, including the nose.

The following measurements were calculated:

1. Volume of the external nose (mm^3) as the sum of the volumes of two pyramids with a common base (the first pyramid was defined by points n, prn, alr and als (V1) and the second – points sn, prn, alr and als (V2).
2. Areas of nasal surfaces (mm^2) – area of the left lateral side (n-prn-als (S1), area of the right lateral side (n-prn-alr (S2), and the sum of the two areas.
3. Linear distances (mm) – nasal width (alr-als), nasal height (n-sn), length of nasal bridge (n-prn), nasal tip protrusion (sn-prn).

Fig. 1. Anthropometric landmarks on the external nose.

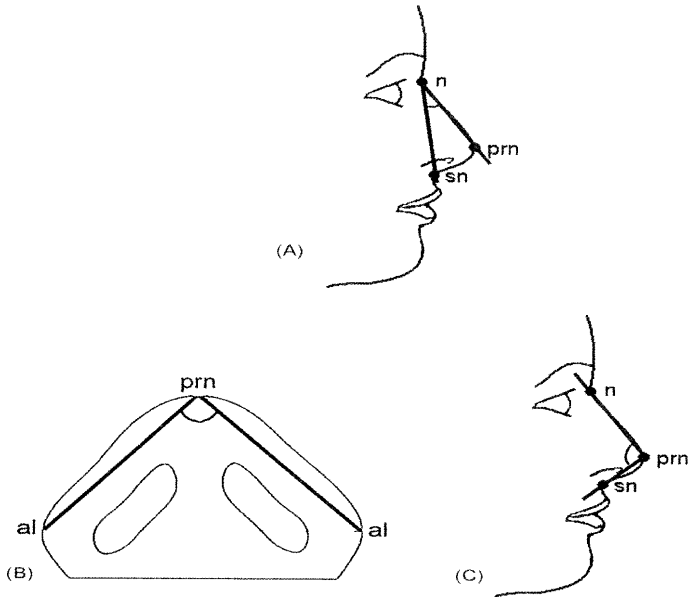

Figure 2. Angels measured.

4. Angles (degrees) – nasal convexity (sn-n-prn) (A1), inter-alar angle (alr-prn-all), nasal tip angle (n-prn-sn) (A3).

The results were analyzed statistically by the SPSS 17.0 software. Paired-samples t-test was used to compare left and right measurements. The distribution of the variables was tested by the Kolmogorov-Smirnov test. The Independent Samples test and Mann-Whitney test were used to analyze the differences between genders, as well as to test for correlation between nasal measurements and height and weight of the subjects. The level of significance was set at $p < 0.05$.

Results

Mean values of the studied variables for both genders are shown in table 1. Table 2 demonstrates results from laser scanning of the faces of healthy Italian and Chinese subjects in the same age group [1, 22].

It was found that male nasal dimensions were greater than female and all measurements demonstrated racial differences. Theses findings confirmed the results in other studies [1, 22].

Paired samples t-test showed no significant difference between S1 and S2 ($p=0.338$), which proved that there was no nasal asymmetry.

All studied variables except V1, A3 demonstrated normal distribution ($p=0.013$, $p<0.001$, $p=0.001$, $p<0.001$).

Significant differences between the following normally distributed variables in males and females were found using independent samples t-test – nasal width, S1, S2, S1 + S2 and V1 + V2. Therefore they can be used to discriminate between sexes (table 2).

Table 1. Volumes, areas and angles measured.

Variable	Males	Females
V1, mm3	6507,9	4421,8
V2,mm3	1085,6	922,77
V1+V2	7593,2	5344,6
S1, mm2	699,16	548,52
S2, mm2	671,35	551,26
S1+S2	1370,5	1099,8
A1, degrees	22,1000	24,3100
A2, degrees	72,97	75,48
A3, degrees	96,15	95,07

Table 2. Linear distances in different ethnicities.

Measurements	Male Bulgarians	Male Italians	Male Chinese	Female Bulgarians	Female Italians	Female Chinese
Nasal width	35,52	32,31	39,49	32,05	28,9	37,63
SD	6,94	3,1	2,95	2,88	3,3	3,47
Nasal height	53,39	55,65	50,15	49,83	51,17	46,93
SD	3,18	3,31	4,16	6,88	3,57	3,3
Nasal bridge length	47,1	51	43,65	44,06	46,46	40,04
SD	4,53	3,91	4,5	5,73	3,99	3,62
Nasal tip protrusion	20,31	19,17	17,68	19,58	17,69	16,69
SD	2,71	2,15	1,66	3	1,92	2,01

Table 3. Variables with significant sexual dimorphism in Bulgarians.

Gender	Male	Female		
N	16	23		
Nasal width	35,52±6,94	32,05±2,88	t=2,152	p=0,038
S1	699,16±177,75	548,52±72,9	t=3,662	p=0,001
S2	671,35±197,95	551,26±94,95	t=2,531	p=0,016
S1+S2	1370,5±369,76	1099,8±154,51	t=3,152	p=0,003
V1+V2	7593,2±4439,3	5344,6±1156,5	t=2,330	p=0,025

The Mann-Whitney test showed that the variable V1, which did not have normal distribution, was also significantly different between males and females (p=0.005). Therefore it can be used to discriminate between sexes too.

A positive correlation existed between nasal height and the subject's height (r=0.330, p=0.04), as well as between the subject's weight and S1 (r=0.347, p=0.03), S2/ r= 0.431, p= 0.009/, S1+S2/r= 0.379, p= 0.017/, V1/r= 0.406,p= 0.01/, V2/r= 0.362,p= 0.023/ andV1+V2/r= 0.403,p= 0.011/.

Conclusion

The creation of three-dimensional models is necessary for different clinical and experimental purposes.

In plastic and maxillofacial surgery they are important for the correction of hard and soft tissues in malformations or after trauma.

They may also be useful in the diagnosis of genetic and psychiatric disorders.

In forensic anthropology these models may have various uses – for facial reconstruction, the descriptive construction of a "portrait" or as an identification aid.

Acknowledgements: Data are from a survey research project DDVU 02/25 20.12.2010 "Cephalometric examination and 3D virtual modeling of the face aiming at construction and visualization of 3D facial statistics and creating cephalofacial database" funded by the National Science Fund of the Ministry of Education, Youth and Science.

References

1. Sforza Ch., G. Grandi, M. De Menezes, G. M. Tartaglia, V. F. Ferrario. Age- and sex-related changes in the normal human external nose. – Forensic Science International, **204**, 2010, 205.e1–205.e9
2. Gualdi-Russo E. Longitudinal study of anthropometric changes with aging in an urban Italian population – Homo, **49**, 1998, 241–259.
3. Pecora N.G., T. Baccetti, J.A. McNamara. Jr. The aging craniofacial complex: a longitudinal cephalometric study from late adolescence to late adulthood. – Am. J. Orthod. DentofacialOrthop. **134**, 2008, 496–505.
4. Zankl A., L. Eberle, L. Molinari, A. Schinzel. – Growth charts for nose length, nasal protrusion, and philtrum length from birth to 97 years. – Am. J. Med. Genet, **111,** 2002, 388–391.
5. Dellavia C., F. Catti, C. Sforza, G. Grandi, V.F. Ferrario. Noninvasive longitudinal assessment of facial growth in children and adolescents with Hypohidrotic Ectodermal Dysplasia. – Eur. J. Oral Sci. **116**, 2008, 305–311.
6. Ferrario V.F., C. Dellavia, A. Colombo, C. Sforza. Three-dimensional assessment of nose and lip morphology in subjects with Down syndrome. – Ann. Plast. Surg. **53,** 2004, 577–583.
7. De Angelis D., R. Sala, A. Cantatore, M. Grandi, C. Cattaneo. A new computerassisted technique to aid personal identification. – Int. J. Legal Med., **123,** 2009, 351–356.
8. Fraser N.L., M. Yoshino, K. Imaizumi, S.A. Blackwell, C.D. Thomas, J.G. Clement. A Japanese computer-assisted facial identification system successfully identifies non-Japanese faces – Forensic Sci. Int., **135**, 2003, 122–128.
9. Heidari H., H. Mahmoudzadeh-Sagheb, T. Khammar, M. Khammar. Anthropometric measurements of the external nose in 18–25-year-old Sistani and Baluch aborigine women in the southeast of Iran. – Folia Morphol, **68,** 2009, 88–92.
10. Roelofse M.M., M. Steun, P.J. Becker. Photo identification: facial metrical and morphological features in South African males. – Forensic Sci. Int., **177**, 2008, 168– 175.
11. Rynn C., C.M. Wilkinson. Appraisal of traditional and recently proposed relationships between the hard and soft dimensions of the nose in profile. – Am. J. Phys. Anthropol., **130,** 2006, 364–373.
12. Sforza C., G. Grandi, M. Binelli, D.G. Tommasi, R. Rosati, V.F. Ferrario. Age- and sexrelated changes in the normal human ear. – Forensic Sci. Int., **187**, 2009, 110.e1– 110.e7.
13. Sforza C., G. Grandi, F. Catti, D.G. Tommasi, A. Ugolini, V.F. Ferrario. Age- and sexrelated changes in the soft tissues of the orbital region. – Forensic Sci. Int., **185,** 2009, 115. e1–115.e8.
14. Shi J., A. Samal, D. Marx. How effective are landmarks and their geometry for face recognition? – Comput. Vis. Image Understand, **102**, 2006, 117–133.
15. Smith S.L., P.H. Buschang. Midsagittal facial soft-tissue growth of French Canadian adolescents. – Am. J. Hum. Biol., **14,** 2002, 457–467.
16. Stephan C.N., M. Henneberg. Predicting mouth width from inter-canine width—a 75% rule. – J. Forensic Sci., **48,** 2003, 725–727.

17. Stephan C.N. Position of superciliare in relation to the lateral iris: testing a suggested facial approximation guideline. – Forensic Sci. Int., **130**, 2002, 29–33.
18. Farkas L.G., T.A. Hreczko, M.J. Katic, Craniofacial norms in North American Caucasians from birth (one year) to young adulthood, in: L.G. Farkas (Ed.), Anthropometry of the Head and Face. – Raven Press, New York, 1994, pp. 285
19. Hennessy R.J., McLearie S., Kinsella A., Waddington J.L. Facial Shape and Asymmetry by Three-Dimensional Laser Surface Scanning Covary With Cognition in a Sexually Dimorphic Manner. – J Neuropsychiatry ClinNeurosci, **18**, 2006, 73-80.
20. Hennessy R.J., Baldwin P.A., Browne D.J., Kinsella Anthony., Waddington J. L. Frontonasal dysmorphology in bipolar disorder by 3D laser surface imaging and geometric morphometrics: Comparisons with schizophrenia. – Schizophr Res., **122,** 2010, 63–71.
21. www.fastscan3d.com
22. Aung S.C., C.L. Foo, S.T. Lee, Three dimensional laser scan assessment of the Oriental nose with a new classification of Oriental nasal types. – Br. J. Plast. Surg., **53,** 2000, 109–116

Institute of Experimental Morphology, Pathology and Anthropology with Museum
Bulgarian Anatomical Society

Acta morphologica et anthropologica, 19
Sofia • 2012

Comparison of the effect of acute LiCl intoxication on rat and mouse brain

E. Petrova, M. Dimitrova, St. Dimitrova, Y. Gluhcheva, V. Kolyovska, D. Deleva, D. Kadiysky

Department of Experimental Morphology, Institute of Experimental Morphology, Pathology and Anthropology with Museum, Bulgarian Academy of Sciences
Sofia 1113, Acad. G. Bonchev Str., Bl. 25, E-mail: dimkad@bas.bg

Morphological changes in the rat and mouse brain following acute lithium administration were studied using silver-copper impregnation for neurodegeneration. Vacuolization was observed in all the studied brain regions – cerebral cortex, cerebellar cortex and medulla oblongata of lithium-treated animals. Loss of Purkinje cells was seen in the cerebellum. Impregnated nerve fibres were observed to show a substantial damage of neuronal processes. No differences were noticed in the pattern of brain morphological changes between both species. Thus, rat and mouse models can be equally successful for the study of lithium salts effects on the brain.

Key words: lithium intoxication, rat, mouse, brain morphology, silver-copper impregnation

Introduction

Lithium is extensively used in psychiatric practice for the prevention and treatment of manic-depressive disorders. However, neurotoxicity of lithium salts within therapeutic dose has been reported in patients manifested by transient or persistent neurological deficits. Animal models are not sufficiently exploited for the study of lithium-affected brain morphology which restricts the possibility to follow up the pathological changes at an early stage. Cerebellar spongiform degeneration has been documented in a rat model of acute lithium intoxication [4] and these data correlate well with findings in humans [1]. Experimental data for the neurotoxic effect of lithium salts in mice are scarce.

The aim of the present study is to follow up the morphological changes in the rat and mouse brain provoked by acute lithium intoxication and to compare the effect of LiCl between both species.

Materials and Methods

Mature Wistar rats (four-month-old) and Balb/c mice (three-month-old) were subjected to acute lithium intoxication by a single dose of lithium chloride (250 mg/kg body

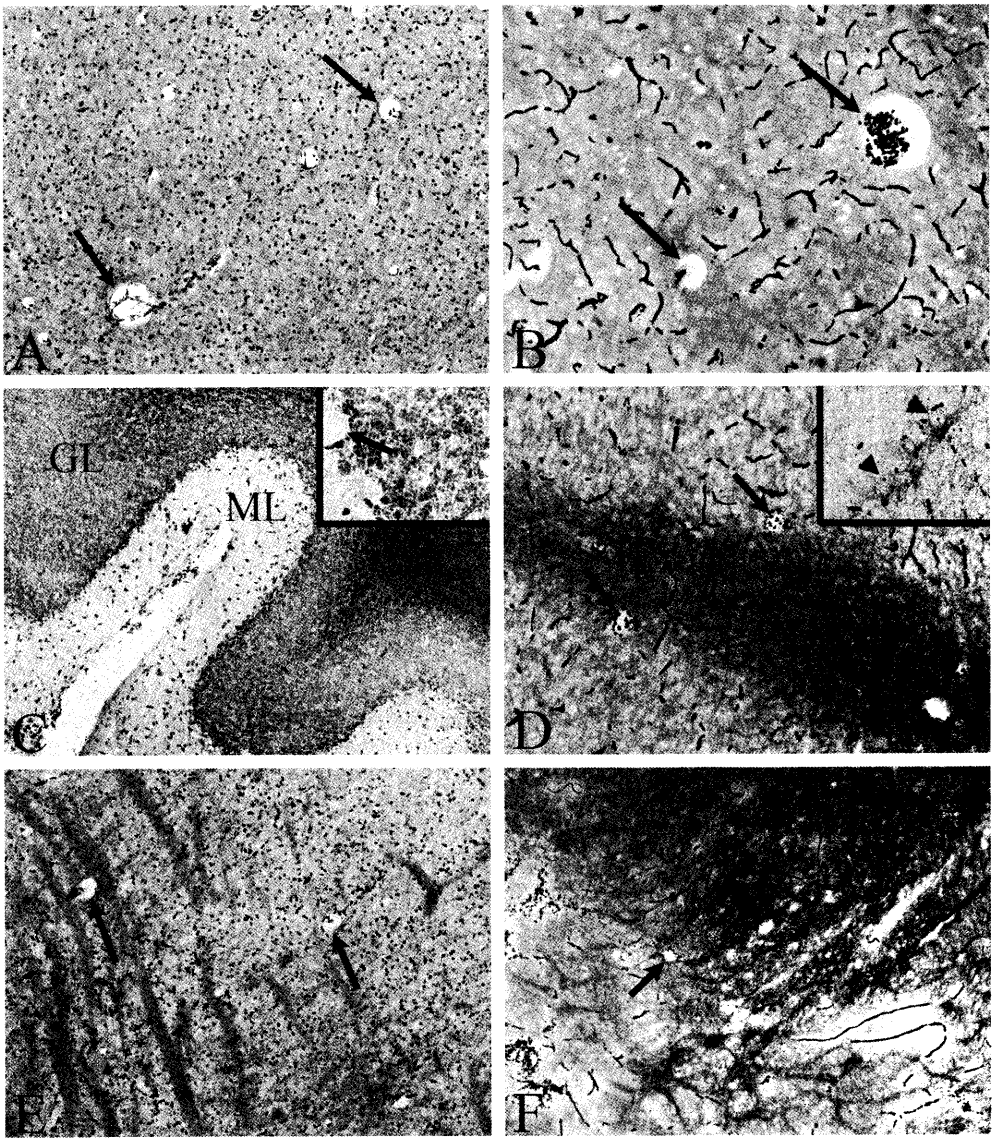

Fig.1. Morphological changes in different regions of mouse and rat brain following acute LiCl intoxication as detected by silver-copper staining. Similar vacuolization in the mouse (A) and rat (B) cerebral cortex (arrows). Preserved granular (GR) and molecular (ML) layers in the mouse cerebellar cortex (C), but empty spaces (arrow) of missing Purkinje cells (inclusion in C). Vacuoles of different size (arrows) in deeper zones of the granular layer of rat cerebellar cortex (D) and empty spaces (arrows) of lost Purkinje cells (inclusion in D). Sparsely located small vacuoles (arrows) in the mouse (E) and rat (F) medulla oblongata. A, B, D, E, F 200 X; C 100 X; inclusions 400 X.

weight, 0.2 ml dosing volume in saline, i.p.). Treated animals were sacrificed 24 hours following the administration under light anesthesia.

Different regions of the CNS were studied histologically – cerebral cortex, cerebellum and medulla oblongata using silver-copper staining for neurodegeneration. The silver impregnation was carried out exactly as described by De Olmos and Ingram [3]. All the sections were studied under Leica DM50008 (New York, USA) microscope.

Results and Discussion

Acute lithium intoxication in patients might be due to accidental (or deliberate) overdose of lithium-based drugs. In such cases, neuropathological changes found at autopsy prove to be similar to those in animal models of lithium toxicity. On the other hand, animal models allow following up the earliest histopathological signs of the intoxication. Our present investigation is prompted by the scanty morphological studies in experimental models of lithium-induced neurotoxicity. Most of the available data emphasize on biochemical, physiological, and behavioral effects of lithium, while brain histopathological changes are poorly investigated. Recently, we developed experimental rat and mouse models of lithium intoxication based on acute lithium administration. The silver-copper impregnation technique of de Olmos and Ingram [3] proved to allow precise localization of the morphological changes in the animal CNS and their topographic distribution in the brain.

Similar changes were observed in the mouse and rat cerebral cortex (Fig. 1 A, B). This brain region proved to be the most affected by the acute lithium intoxication. Vacuoles of different size (5-50 μm) were observed both in the outer and deeper cortical layers in the two species studied. Cell debris was visible inside the vacuoles. Significant loss of Purkinje cells was found in the cerebellar cortex of both species (Fig. 1 inclusions in C and D). However, in the mouse cerebellum no signs of vacuolization were observed (Fig. 1 C). In contrast, vacuoles of different size were detected in the deeper zones of rat cerebellar granular layer (Fig. 1 D). Data about the effect of lithium salts on the cerebellum morphology are rather controversial. Thus, no structural changes in the rat cerebellum have been reported by Licht et al. [5], whereas a widespread vacuolization was detected by Dethy et al. [4]. Much less pronounced vacuolization was registered in the medulla oblongata both in mouse and rat (Fig. 1 E, F). The formation of vacuoles in all brain regions is considered a common manifestation of brain neurodegeneration both in pathological conditions and during normal brain aging [2, 6].

In conclusion, acute lithium intoxication provokes similar pattern of changes but of different intensity in the rat and mouse brain. Therefore, rat and mouse models can be equally successful for studying the effects of lithium salts on the brain. Animal models of adverse brain impacts would be beneficial for the clinical trials because of the opportunity of detecting the early pathological signs.

Acknowledgments: This study was supported by the National Science Fund of Bulgaria under Contract № DNTS Macedonia 01/12 and by EC under Contract № COST Action BM1007.

References

1. Bejar, J. M. Cerebellar degeneration due to acute lithium toxicity. – Clin. Neuropharmacol., **8**, 1985, №4, 379-381.
2. Brandner, S. CNS pathogenesis of prion diseases. – Br. Med. Bull., **66**, 2003, №1, 131-139.
3. De Olmos, J. S., W. R. Ingram. An improved cupric-silver method for impregnation of axonal and terminal degeneration. – Brain Res., **33**, 1971, 523-529.

4. Dethy, S., M. Manto, E. Bastianelli, V. Gangji, M. A. Laute, S. Goldman, J. Hildebrand. Cerebellar spongiform degeneration induced by acute lithium intoxication in the rat. – Neurosci. Lett., **224**, 1997, 25-28.
5. Licht, R. W., J. O. Larsen, D. Smith, H. Brændgaard. Chronic lithium treatment with or without haloperidol fails to affect the morphology of the rat cerebellum. – Eur. Neuropsychopharmacol., **13**, 2003, 173-176.
6. Özsoy, Ş. Y., R. Hazirogˇlu. Age-related changes in cat brains as demonstrated by histological and immunohistochemical techniques. – Rev. Med. Vet., **161**, 2010, №12, 540-548.

Institute of Experimental Morphology, Pathology and Anthropology with Museum
Bulgarian Anatomical Society

Acta morphologica et anthropologica, 19
Sofia • 2012

Morphological investigation in a rat model of hemic hypoxia

E. Petrova, V. Ormandzhieva, B. Eremieva, D. Kadiysky

Department of Experimental Morphology, Institute of Experimental Morphology, Pathology and Anthropology with Museum, Bulgarian Academy of Sciences
Sofia 1113, Acad. G. Bonchev Str., Bl. 25, E-mail: emiliapetrova@abv.bg

In this study, we report rat brain morphological changes after sodium nitrite-induced acute hemic hypoxia. Male Wistar rats at the age of four months were intraperitoneally injected with sodium nitrite ($NaNO_2$) at 50 mg/kg. Treated animals were sacrificed at different time intervals (1h and 48h) following the administration. Brain sections were stained using routine histological methods and examined under a light microscope. Vacuolization was observed in corpus callosum of the hypoxic brains. Increased number of the dark epithelial cells of plexus choroideus, macrophages and dark pyramidal neurons in the cortex were the most prominent histopathological changes indicating that $NaNO_2$-induced hypoxia results in rat brain injury.

Key words: hemic hypoxia, sodium nitrite, rat brain morphology

Introduction

Insufficient oxygen or hypoxia produces a great physiological stress inducing cellular responses that result in deleterious effects on certain tissues [7]. Hypoxia is one of the major pathological events causing neuronal cell injury, neurodegeneration and cell death. The brain is the most hypoxic vulnerable of all vertebrate tissues because of its high rate of aerobic metabolism and limited antioxidant defense systems [4]. The pathogenesis of cerebral hypoxia has been associated with a time dependent cascade of molecular events including rapid fall in intracellular adenosine triphosphate with consequent increase in adenosine, anaerobic glycolysis, activation of calcium-stimulated enzymes, mitochondrial dysfunction and formation of reactive oxygen species (ROS) that contribute to the oxidative brain damage [2]. Hemic hypoxia is characterized by reduced oxygen-transport capacity of the blood often due to deficit of hemoglobin and altered transport, binding and delivery of O_2 by the hemoglobin.

Literature data for the effect of hemic hypoxia on brain morphology are insufficient. The present investigation is undertaken to follow up the rat brain morphological changes after $NaNO_2$-induced acute hemic hypoxia.

Materials and Methods

The experiments were carried out on four-month-old male Wistar rats. The animals were maintained in the institute's animal house in standard hard bottom polypropylene cages at 23°C±2°C, 12:12 h light/dark cycle and free access to laboratory chow and tap water throughout the study. Rats (n=10) were subjected to acute hemic hypoxia by a single intraperitoneal injection of $NaNO_2$ at 50 mg/kg body weight (1 ml dosing volume). Treated animals were sacrificed at different time intervals following the administration (1h and 48h) under light anesthesia. The control rats (n=5) were injected with the same volume of distilled water.

Fig. 1. Light microscopic micrograph of choroid plexus from hypoxic rat brain with dark epithelial cells (➡) and macrophages (►). HE, x20

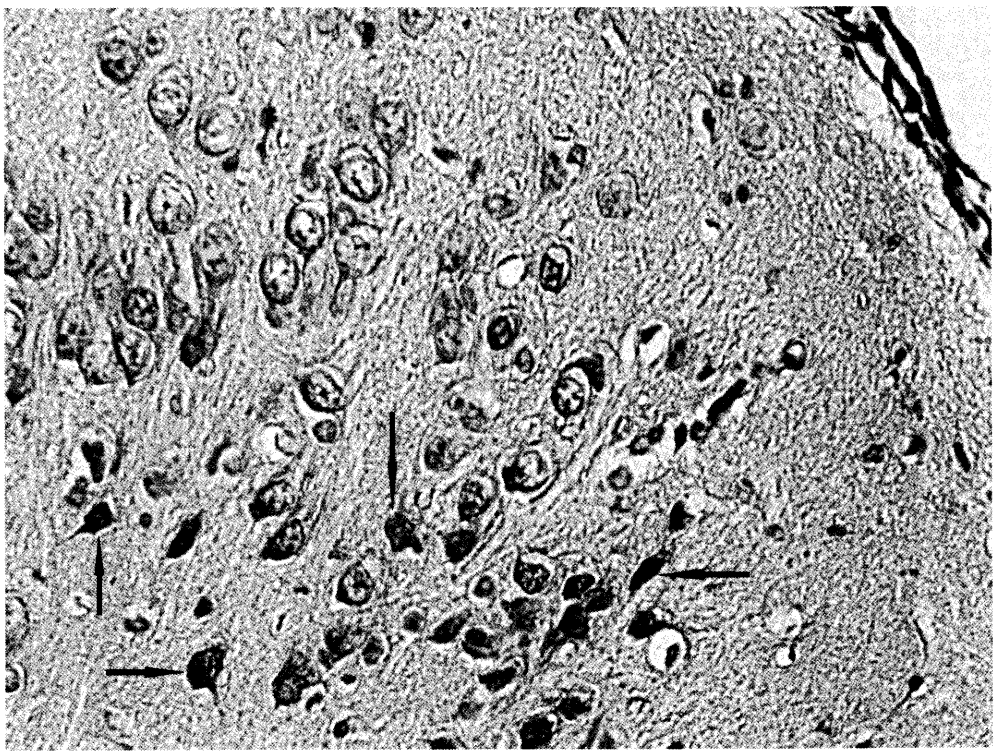

Fig. 2. Light microscopic micrograph of cerebral cortex from hypoxic rat brain with dark pyramidal neurons (➡). HE, x40

Brains were sampled, fixed and embedded in paraffin using routine histological practice. Tissue coronal sections (7 μm) were stained by hematoxylin-eosin *and* examined under light microscope.

The animal experiments were performed in accordance with the animal protection guidelines approved by the Ethics Committee for Experimental Animal Use at IEMPAM, BAS.

Results and Discussion

It is known that brain hypoxia generates a series of biochemical events with several cellular and functional consequences, such as plasma membrane structural damage and delayed cell death [6]. Several experimental models have been used to simulate the human cerebral hypoxia syndrome. In our experiments we have developed a model of acute sodium nitrite-induced hemic hypoxia. Sodium nitrite, an inorganic salt with both harmful and healthful effects, is known as hypoxia inducible agent. In the circulation it causes conversion of hemoglobin to methemoglobin, which is incapable of transporting oxygen to the body's tissues and organs. Thus the oxygen-carrying capacity of the blood is reduced. The administration of $NaNO_2$ in high concentrations may cause brain inflammation, ischemia and impaired cerebral energy [8].

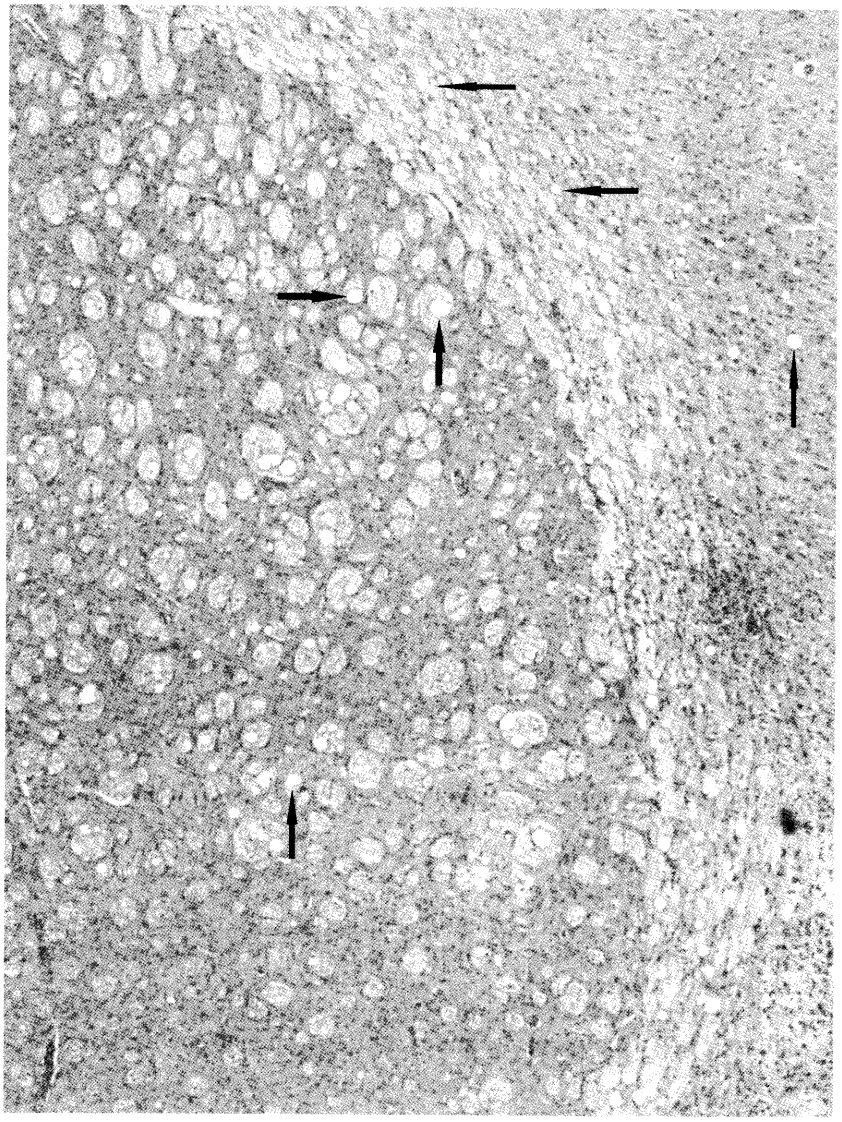

Fig. 3. Light microscopic micrograph of corpus callosum from hypoxic rat brain with vacuoles (⟶). HE, x5

One hour following $NaNO_2$-induced hypoxia, we found increased number of the dark epithelial cells of plexus choroideus in the area of the fourth ventricle (Fig. 1). They are generally considered to be modified ependymal cells with epithelial cell characteristics and referred to as choroidal epithelial cells. Moreover, the number of macrophages was also increased. In the cerebral cortex, a large number of dark pyramidal neurons was observed (Fig. 2). These changes may be indicative of impaired secretory transport and represent a compensatory mechanism against hypoxic injury. Further transmission electron microscopic studies would elucidate the observed histopathological findings.

Morphological changes in the rat brain after $NaNO_2$-induced hypoxia are also documented by Zaidi [9]. Degenerating nerve cell bodies with pyknotic nuclei and vacuolar spaces in dentate gyrus, as well thinning of hippocampal and dentate gyrus blades have been demonstrated at the first hour following $NaNO_2$ injection. Extensive cerebellar Purkinje cell damage is also documented with swollen, autolytic and shrunken cells [8]. It is concluded that Purkinje cells are very vulnerable to hypoxic insult and $NaNO_2$-induced hypoxia results in a significant excitotoxic degeneration of these cells.

In our experiments vacuolization was observed 48 hours after $NaNO_2$ injection, mainly in corpus callosum and the deeper structures beneath it (Fig. 3). Changes in the vascular endothelium were also found though they would be characterized in detail by electron microscopy. The underlying mechanism of $NaNO_2$ influence on the brain is not clearly understood. Nitrite is known to cause free radical generation [5], as it can stimulate oxidation of ferrous ions in oxyhemoglobin to form methemoglobin as well as various ROS [1, 3].

In conclusion, the results of the present work are indicative of rat brain injury following acute hemic hypoxia. Future studies would elucidate the morphological changes at later stages, as well their reversibility.

Acknowledgments: This work is supported by a grant No DMU 03/18 for Young scientists from the Bulgarian National Science Fund.

References

1. Baky, N. A. A., Z. F. Zaidi, A. J. Fatani, M. M. Sayed-Ahmed, H. Yaqub. Nitric oxide pros and cons: The role of l-arginine, a nitric oxide precursor, and idebenone, a coenzyme-Q analogue in ameliorating cerebral hypoxia in rat. – Br. Res. Bull., **83**, 2010, 49-56.
2. Endres, M., D. Biniszkiewicz, R. W. Sobol, Ch. Harms, M. Ahmadi, A. Lipski, J. Katchanov, P. Mergenthaler, U. Dirnagl, S. H. Wilson, A. Meisel, R. Jaenisch. Increased postischemic brain injury in mice deficient in uracil-DNA glycosylase. – J. Clin. Invest., **113**, 2004, №12, 1711-1721.
3. Gladwin, M. T., J. H. Crawford, R. P. Patel. The biochemistry of nitric oxide, nitrite, and hemoglobin: role in blood flow regulation. – Free Rad. Biol. Med., **36**, 2004, 707-717.
4. Halliwell, B., J. M. C. Gutteridge. Oxygen radicals and the nervous system. – Trends Neurosci., **8**, 1985, 22-26.
5. Kohn, M. C., R. L. Melnick, F. Ye, C. J. Portier. Pharmacokinetics of sodium nitrite induced methemoglobinemia in the rat. – Drug Metab. Dispos., **30**, 2002, №6, 676-683.
6. Northington, F. J., R. Chavez-Valdez, L. J. Martin. Neuronal cell death in neonatal hypoxia-ischemia. – Ann. Neurol., **69,** 2011, №5, 743-758.
7. Sarada, S. K. S., P. Dipti, B. Anju, T. Pauline, A. K. Kain, M. Sairam, S. K. Sharma, G. Ilavazhgan, K. Devendra, W. Selvamurthy. Antioxidant effect of beta-carotene on hypoxia induced oxidative stress in male albino rats. – J. Ethnopharmacol., **79**, 2002, 149-153.
8. Zaidi, Z. F. Effects of sodium nitrite-induced hypoxia on cerebellar Purkinje cells in adult rats. – Pak. J. Med. Sci., **26**, 2010, №2, 261-266.
9. Zaidi, Z. F. Sodium nitrite-induced hypoxic injury in rat hippocampus. – Pak. J. Med. Sci., **26**, 2010, №3, 532-537.

Institute of Experimental Morphology, Pathology and Anthropology with Museum
Bulgarian Anatomical Society

Acta morphologica et anthropologica, 19
Sofia • 2012

Effect of hemic hypoxia on the cholesterol content of rat brain synaptosomal membrane

E. Petrova, E. Vasileva, V. Ormandzhieva

Bulgarian Academy of Sciences, Institute of Experimental Morphology, Pathology and Anthropology with Museum, Department of Experimental Morphology
Sofia 1113, Acad. G. Bonchev Str., Bl. 25, E-mail: emiliapetrova@abv.bg

In this study we report changes in the cholesterol content of rat brain synaptosomes following hemic hypoxia. Male Wistar rats at the age of three months were subjected to sodium nitrite-induced hemic hypoxia. The synaptosomal fraction was isolated and lipids were extracted. The cholesterol content was measured by gas-liquid chromatography.

In the synaptosomes of hypoxic brains, we found increased levels of total cholesterol (10.8-fold), free cholesterol (6-fold), and esterified cholesterol (26-fold). These changes indicate a disturbance of cholesterol homeostasis. The cholesterol accumulation may be interpreted as a physiological adaptive response to hypoxia.

Key words: cholesterol, synaptosomes, rat brain, hemic hypoxia

Introduction

Cholesterol is the main mammalian membrane-active sterol, and also the most studied one. It is largely present in the plasma membranes of glial cells and neurons and in the specialized membranes of myelin. Among the variety of biological functions, cholesterol is suggested to enhance the production of presynaptic components including synaptic vesicles [12] and release sites [4].

The insufficient oxygen supply has been shown to promote cholesterol accumulation in cells [5] but little is known about the cholesterol subcellular distribution in the hypoxic brain. As the membrane lipid environment is essential for the development and regulation of the synaptic functions, it is of great interest to study how the synaptosomal cholesterol pool is affected by hypoxia.

Materials and Methods

Three-month-old male Wistar rats were subjected to sodium nitrite-induced hypoxia. Sodium nitrite was administered intravenously at 20 mg/kg body weight. Hypoxic rats were lightly anesthetized and sacrificed by decapitation.

The synaptosomal fraction was isolated by discontinuous two-step sucrose gradient centrifugation of rat brain homogenate according to the method of Venkov [15]. Lipids were extracted according to the method of Kates [16] using the following eluates: chloroform:methanol 1:2 (v/v) and chloroform:methanol:water 1:2:0.8 (v/v/v).

The cholesterol content was determined by gas-liquid chromatography as we have previously described [7].

Results are reported as mean values ± SD and statistically analyzed by Student's *t*-test.

The animal experiments were performed in accordance with the animal protection guidelines approved by the Ethics Committee for Experimental Animal Use at IEMPAM, BAS.

Results and Discussion

In the present study, we examined the effect of hemic hypoxia on the cholesterol content of rat brain synaptosomal membrane.

The appearance of sterols in biological membranes is considered to be an important step in membrane evolution [1]. Cholesterol is the main sterol present in the animal tissues. It is required for many physiological functions such as cell membrane construction, cell proliferation and biosynthesis of vital hormones [5]. The level of cholesterol in the membrane strongly affects the barrier properties of membranes as well as many other physicochemical properties of lipid bilayers. Cholesterol regulates the activity of membrane-bound transporters, ion channels, signalling molecules, and transport vesicles [3].

Cholesterol levels strongly influence the establishment and maintenance of synaptic connections and the basic synaptic processes and plasticity [8, 9]. A number of investigators report that cholesterol turnover is most intensive in synaptosomes and support the hypothesis about local synthesis of cholesterol in the synaptic terminals. The majority of brain cholesterol is in unesterified form [13] which finds good support in our observations in control rats. Our findings in control rat brains indicated the predominant presence of free cholesterol (0.67±0.13 mg/g dry lipid residue/ml; mg/g/ml) in the synaptosomal fraction. Esterified cholesterol (0.23±0.02 mg/g/ml), as well as small amounts of lanosterol (0.03±0.001 mg/g/ml) were also found.

Cholesterol homeostasis is very important for human and animals. The dynamic equilibrium between free and esterified cholesterol in the brain is controlled by the activity of the respective sterol ester hydrolases. It is reported that hypoxia may disturb this balance and promote cholesterol accumulation in cells. Moreover, selective sensitivity of synaptosomal membrane function to cerebral cortical hypoxia is demonstrated [10].

In our experiments we applied a model of sodium nitrite-induced chemical hypoxia. It refers to hemic hypoxia – a condition in which there is a reduction in hemoglobin's ability to transport oxygen. Sodium nitrite converts hemoglobin to methemoglobin and unlike the ferrous form of hemoglobin, methemoglobin does not bind oxygen strongly. Thus the oxygen-carrying capacity of the blood is reduced. As a result, the total cholesterol significantly increased in the synaptosomal subcellular fraction (from 0.93±0.1 to 9.988±0.12 mg/g/ml). The levels of free and esterified cholesterol were 6-fold (4.04±0.06 mg/g/ml) and 26-fold (5.95±0.08 mg/g/ml) above the control values, respectively (Fig. 1). The esterified cholesterol pool accounted for 60% of the total cholesterol. We have previously reported similar changes of the mitochondrial cholesterol content in the hypoxic and ischemic rat brain [6, 7]. Obviously, the hydrolysis of membrane phospholipids during hypoxia disrupts the integrity of the

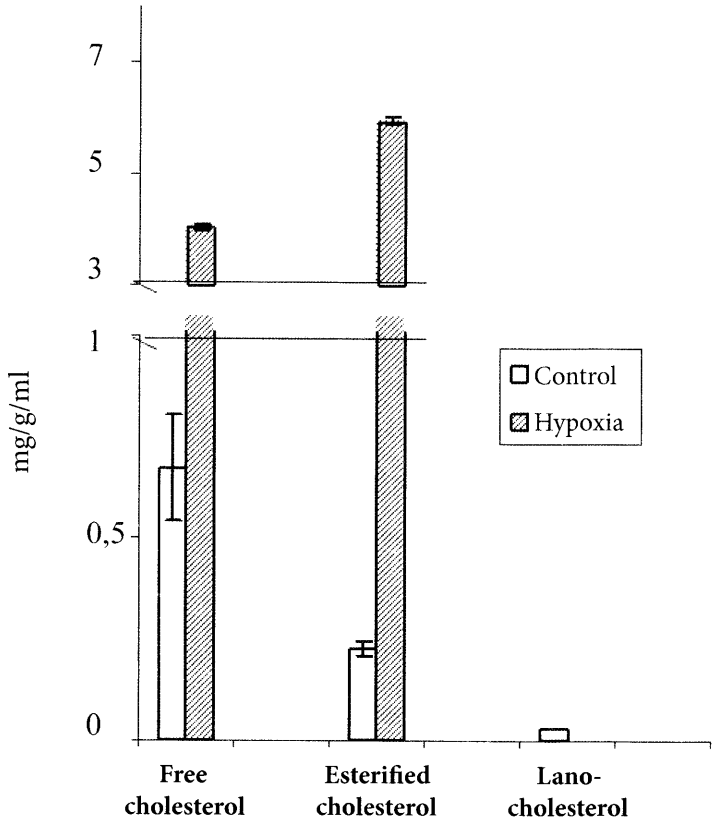

Fig. 1. Synaptosomal cholesterol content of hypoxic rat brain. Values are expressed in mg/g dry lipid residue/ml. $p<0.001$

membrane which can lead to the release of active cholesterol whose esterification can be stimulated by free fatty acids.

The cholesterol accumulation in cells is considered to depend on the balance of complex factors: the extracellular cholesterol uptake via the LDL (low-density lipoprotein) receptor pathway, de novo cholesterol synthesis, intracellular cholesterol trafficking (among organellar, cytosolic, and plasma membrane pools), cellular efflux, and cholesterol esterification/deacylation reactions [2]. Under hypoxic conditions, the activity of acyl-CoA:cholesterol acyltransferase (ACAT) is increased, which leads to a decrease in cholesterol efflux and cholesterol is accumulated in the esterified form [5]. Lipoprotein uptake by LDL receptors is not shown to play an important role in cellular cholesterol accumulation.

The high concentration of sterol esters can apparently be explained with the role of the ester to serve as a carrier and storage site for the otherwise toxic free fatty acids. It is reported that the accumulation of cholesterol and cholesterol esters represents a durable adaptive response to different forms of cell injury [14]. Nevertheless, excess cholesterol must be avoided because it can form solid crystals which can be toxic to cells. Excess cholesterol can also cause many adverse effects such as atherosclerosis or neurological degenerative disease [11].

In conclusion, our data provide evidence that sodium nitrite-induced hypoxia affects the cholesterol content in rat brain synaptosomal membrane which results in

its accumulation. These changes indicate the disturbances in cholesterol biosynthesis, intercellular transport and intracellular distribution of cholesterol, and may be implicated in the cell survival pathways.

References

1. Barenholz, Y. Cholesterol and other membrane active sterols: from membrane evolution to "rafts". – Progr. Lipid Res., **41**, 2002, №1, 1-5.
2. Johnson, W. J., M. C. Phillips, G. H. Rothblat. Lipoproteins and cellular cholesterol homeostasis. – Subcell. Biochem., **28**, 1997, 235-276.
3. Kristiana, I., H. Yang, A. J. Brown. Different kinetics of cholesterol delivery to components of the cholesterol homeostatic machinery: implications for cholesterol trafficking to the endoplasmic reticulum. – Biochim. Biophys. Acta, **1781**, 2008, №11-12, 724-730.
4. Lang, T., D. Bruns, D. Wenzel, D. Riedel, P. Holroyd, C. Thiele, R. Jahn. SNAREs are concentrated in cholesterol-dependent clusters that define docking and fusion sites for exocytosis. – EMBO J., **20**, 2001, №9, 2202-2213.
5. Mukodani, J., Y. Ishikawa, H. Fukuzaki. Effects of hypoxia on sterol synthesis, acyl-CoA: cholesterol acyltransferase activity, and efflux of cholesterol in cultured rabbit skin fibroblasts. – Arterioscler. Thromb. Vasc. Biol., **10**, 1990, №1, 106-110.
6. Petrova, E., E. Vasileva, A. Dishkelov. Changes of the cholesterol content in rat brain subcellular fractions in experimental model of cerebral ischaemia. – Compt. rend. Acad. bulg. Sci., **58**, 2005, №7, 839-842.
7. Petrova, E., E. Vasileva, A. Dishkelov. Effect of hypoxia on the cholesterol content in rat brain mitochondria. – Compt. rend. Acad. bulg. Sci., **65**, 2012, №3, 359-364.
8. Pfrieger, F. W. Role of cholesterol in synapse formation and function. – Biochim. Biophys. Acta, **1610**, 2003, №2, 271-280.
9. Pfrieger, F. W, N. Ungerer. Cholesterol metabolism in neurons and astrocytes. – Prog. Lipid Res., **50**, 2011, 357-371.
10. Razdan, B., P. J. Marro, O. Tammela, R. Goel, O. P. Mishra, M. Delivoria-Papadopoulos. Selective sensitivity of synaptosomal membrane function to cerebral cortical hypoxia in newborn piglets. – Brain Res., **600**, 1993, №2, 308-314.
11. Tan, Q. Thesis: Inhibition of cholesterol biosynthesis under hypoxia, Texas: Texas A&M University; 2005.
12. Thiele, C., M. J. Hannah, F. Fahrenholz, W. B. Huttner. Cholesterol binds to synaptophysin and is required for biogenesis of synaptic vesicles. – Nature Cell Biol., **2**, 2000, №1, 42-49.
13. Vance, J. E., H. Hayashi, B. Karten. Cholesterol homeostasis in neurons and glial cells. – Semin. Cell Dev. Biol., **16**, 2005, 193-212.
14. Zager, R. A., T. Andoh, W. M. Bennett. Renal cholesterol accumulation. A durable response after acute and subacute renal insults. – Am. J. Pathol., **159**, 2001, №2, 743-752.
15. Венков, Л. Получаване на обогатени фракции на елементи, изграждащи нервната тъкан. – Съвр. пробл. невроморфол., **11**, 1983, 1-60.
16. Кейтс, М. Техника липидологии. Москва, Мир, 1975, 322.

Institute of Experimental Morphology, Pathology and Anthropology with Museum
Bulgarian Anatomical Society

Acta morphologica et anthropologica, 19
Sofia • 2012

Comparative analysis of relapsing bladder urothelial cancer

H. Popov, P. Ghenev

Department of General and Clinical Pathology, Medical University – Varna, St Marina University Hospital

Bladder cancer is a problem in the practice with the high percentage of relapsing. At microscopic level, there are no objective criteria for evaluation of the tendency for local relapsing. In this regard, possible signs could be derived from the peculiarities of the stroma. Stromal reaction, manifested by inflammatory infiltration in the tumor is referred to the biological behaviour of the cancer , with special attention to the presence of eosinophil leukocytes. The present study was carried over156 cases of primary cancers. Tumor-associated tissue eosinophilia (TATE) was traced at the initial foci of 78 case with recurrent cancer and compared to the same number of cases without relapsing, matched for gender and age. The cases that relapsed in the future contained statistically significant greater numbers of eosinophils in the primary cancer. These results suggest that TATE may be one of the probable prognostic signs for local relapsing of urothelial cancer.

Key words: cancer, recurrency, stroma, TATE

Introduction

Tumors of bladder consist of 90-95% of all neoplasms in the urogenital system. Their frequency is 12,4:100 000 people (1).
Bladder cancer represents a problem in the clinical practice with the high percentage of relapsing, even in high-grade cancer. At microscopic level, there are no convincing objective criteria for evaluation of the tendency for local relapsing, invasion in the wall and/or metastases. In this regard, possible signs could be derived from the peculiarities of the stroma, such as presence of eosinophil leukocytes, mast cells, lymphocytes, plasmocytes, fibroblast and myoepithelial cells. Increased numbers of eosinophil leukocytes is described in many malignant tumors and their presence is considered either with good or poor prognosis in the different cancer locations. The exact role of these cells in the anti-tumor immunity is not clear. Their activity is connected with: secretion of cytotoxic proteins (2); and basal membrane damage by eosinophil-derived cation proteins and peroxidase (3). Thus, products released by eosinophils interfere in the majority of processes of tissue remodeling, including the biological behaviour of tumors (4).

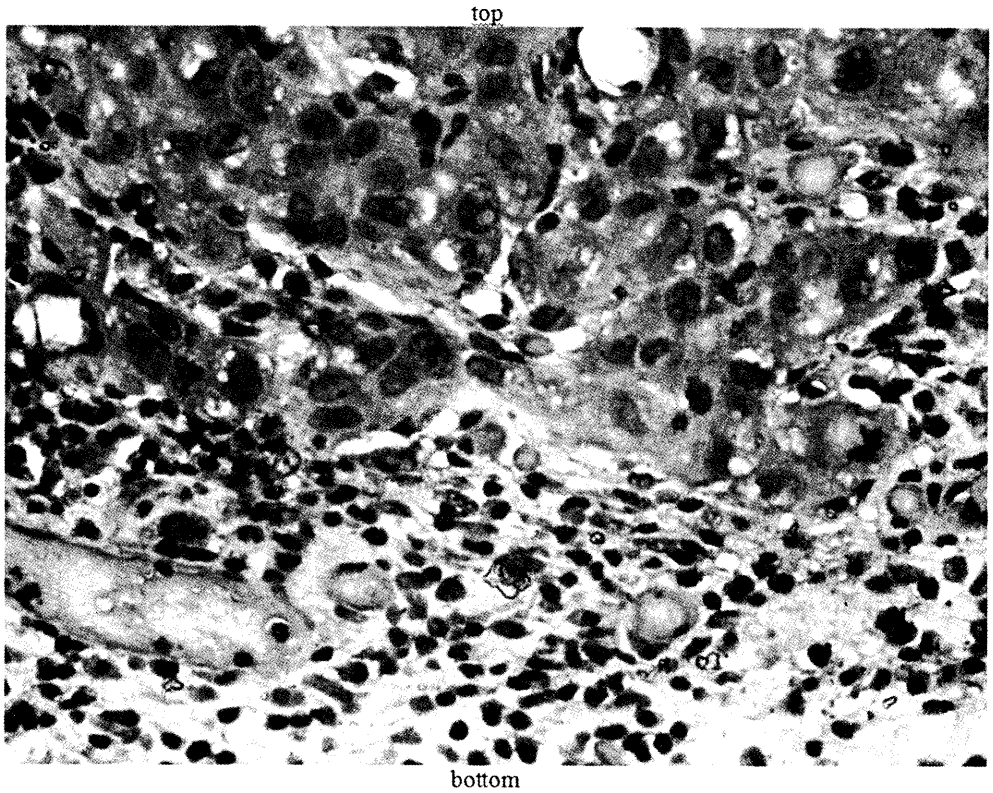

Fig. 1. Case № 30, 65 year old man with urothelial carcinoma High Grade; abundant eosinophilis in the stroma, around the tumor nests, XE, original magnification x20.

Aim

The aim of the present study is to evaluate the significance of tumor-associated tissue eosinophilia (TATE) by comparing the presence of eosinophils in two groups of primary urothelial cancers; relapsing and without relapsing.

Methods and materials

A retrospective analysis for a period of 5 years (2007-2011) was performed. Bladder cancer was diagnosed in 632 patients – out of them 78 developed relapsing tumor for a mean period of six months. TATE in this patients was compared to control group of non-relapsing tumors of 78 patients, matched according to gender and age. All observations were performed on hematoxylin-eosin stained sections of the paraffin blocks from the archive. Non-parametric analysis was used to evaluate the data.

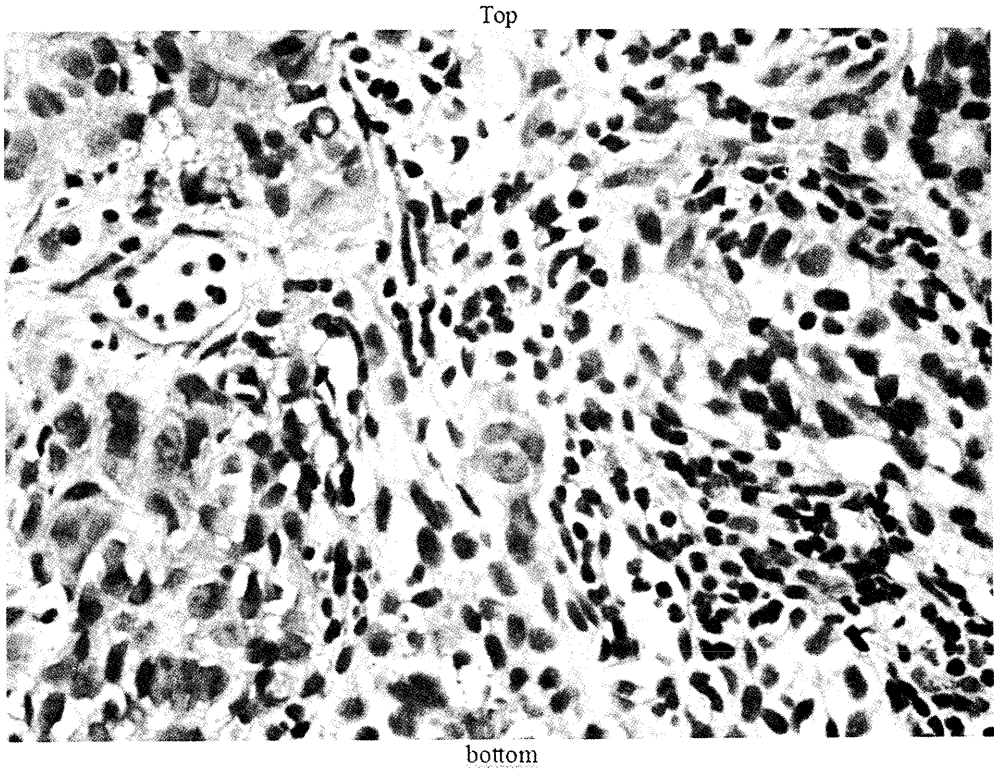

Fig. 2. Case № 60, 57 year old man with urothelial carcinoma High Grade; without eosinophil leukocytes in the stroma reaction around the tumor nests, XE, original magnification x20

Results

TATE was considered as positive when eosinophils were present in the stroma of the bladder cancer (Fig 1) and as negative when no eosinophils were seen (fig 2) TATE was established in 52 patients of the relapsing group, versus 31 of the controls (table 1).

Table 1. Distribution of tissue eosinophilia in primary urothelial carcinomas outbreaks with and without subsequent relapse.

$\chi^2 = 23,26$ p<0,001	Without TATE	With TATE	Total
Recurrency	17	47	78
Non-recurrency	61	31	78
Total	78	78	156

Conclusions

The findings show that cases that relapsed in the future contained statistically significant greater numbers of eosinophils in the primary cancer, compared to the control group. These results suggest that TATE may be one of the probable prognostic signs for local relapsing of urothelial bladder cancer.

References

1. Chernozemski, I., S. Karanov, H. Valerianova. Diagnosis, treatment and monitoring of patients with malignant neoplasms, Sofia, 2003, 312-322.
2. Lowe, D., C. Fletcher, R. Gower. Tumour-associated eosinophilia in the bladder. J Clin Pathol 1984, 37(5):500-2.
3. Filipović, M., S. Cekić. The role of eosinophils in asthma. Facta Universitatis. – In Series: Medicine and Biology Vol.8, No 1, 2001, pp. 6 – 10.
4. Pereira. M., D. Oliveira, L. Kowalski. The role of eosinophils and eosinophil cationic protein in oral cancer. A review. Arch Oral Biol, 2011, 56(4):353-8.

Institute of Experimental Morphology, Pathology and Anthropology with Museum
Bulgarian Anatomical Society

Acta morphologica et anthropologica, 19
Sofia • 2012

Postpartum sudden death by right atrial cyst

D. Radoinova[1], K. Kalchev[1], A.Angelov[2], Y. Yotov[2], P. Shivachev[3]

[1]Department of Pathology and Forensic medicine
[3]Clinic of Cardiology
[4]Clinic of Pediatrics
Medical University "Prof. Dr. Paraskev Stoyanov" – Varna, Bulgaria

Heart cysts are usually congenital. They are asymptomatic and thus found incidentally in relation to other conditions. Sometimes their size determines life-threatening complications. Surgical treatment is successful. We represent a case with a fatal outcome in a 28-years-old woman who had given birth by Caesarean section. The patient had been hospitalized 13 days after delivery in relation to sudden chest pain, fever and ultrasonographic (USG) examination that revealed pericardial effusion and a cystic formation of the right atrium. She had died suddenly on the second night of hospitalization before transfer into cardiac surgery department for further diagnostic procedures and surgical treatment. At autopsy a ruptured cyst of the right atrium and interatrial septum with relative tricuspid valve stenosis, pericarditis, myocarditis, haemorrhage in rupture and cardiac tamponade had been found.

Introduction

Giant Blood Cyst (GBC) [1, 2, 3, 4, 5] are usually congenital, asymptomatic affecting mostly valvular structures. They are rarely seen after the 2 years of age as they spontaneously regress over time, although in some cases they are found in adults [4, 5]. The most common size of GBC is microscopic [1], but sometimes their large size determines complications – valvular and ventricular dysfunction, thromboembolic myocardial infarction, pulmonary embolism or obstruction of the coronary arteries. The most common treatment is surgery [2, 3], after which there is a full recovery. [5]

Clinicomorphological case report

We present a case of a 28-y-o woman who had been admitted to Cardiology clinic with complaints of increasing during inhalation chest pain and fever up to 38,5°C that started suddenly the day before hospitalization. On the day of admission a cardiologist had found echocardiographic data of pericardial effusion and cystic formation in the

right atrium and directed her to hospital for further treatment. Thirteen days before that she had delivered a child by C-section for reasons of fetal distress. She had been taken L-thyroxine for hypothyroidism in Hashimoto's thyroiditis for a period of one year. At the time of admission her general condition had been satisfactory, with low-grade fever of 37,6°C and sounds of pericardial friction. The new echocardiography showed 300 ml of pericardial effusion and thin-wall cyst in the right atrium with a diameter of 65 mm, occupying about 50% of atrial volume, not participating in blood circulation, covering a large part of the interatrial septum near the tricuspid valve protruding into the left atrium, causing relative tricuspid stenosis. There had been serological evidence of adenovirus infection – anti-adenovirus IgM (+)/IgG (+), and exacerbated chronic pyelonephritis.

After the start of medication an improvement of symptoms had been noticed. Series of consultations had been performed. MRI and transfer to the Department of Cardiac Surgery had been planned, but prior to that, on the second night of the stay, the nurse on duty found the patient with no signs of respiration and heartbeat. Full CPR had been performed, but without success.

At autopsy 850 ml of bloody fluid and blood clots was found in the pericardial sac. The heart was enlarged, soft weighing 450 g. The right atrium was dilated, with a cystic formation with a diameter of 6.5 cm, 2-3 mm thick wall, located in the interatrial septum and front atrial wall, protruding to the atrioventricular tract. When opened, a 15 mm slit-like laceration on the right auricle wall was found, corresponding to a 7 mm laceration and haemorrhages on the outer surface of the auricula. This laceration communicates with the pericardial sac. No contents of the cyst was found. Histologically in the myocardium was found a diffuse lymphocytic inflammatory infiltrate in the rupture

Fig. 1. Echocardiographic image of a cyst of the right atrium.

Fig. 2. Gross appearance of the cyst protruding over the tricuspid valve, which caused relative valvular stenosis.

Fig. 3. Gross appearance of the cyst – notice the granular inner surface.

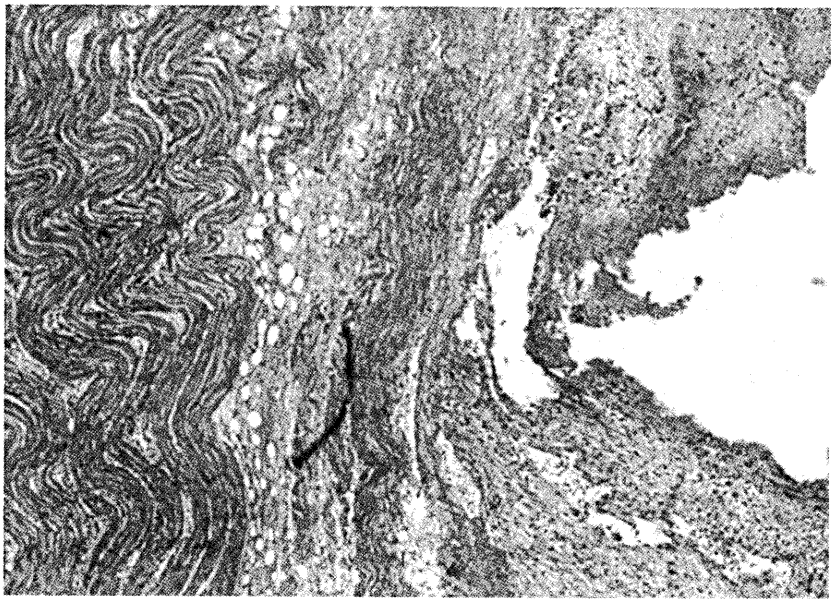

Fig. 4. Part of the cyst (right) area with a laceration and lymphocytic inflammatory infiltration between the myocardial fibres in the cyst wall.

area with formation of granulation tissue. The visceral pericardium was infiltrated with non-specific polymorphonuclear inflammatory cells.

Edema and single hemosiderin-laden macrophages were found in the lungs. The organs of the great circle of circulation were congested. Uterus showed early changes of birth delivery by C-section and a small, clinically insignificant myomatous nodule.

The cause of death was an acute heart failure after cardiac tamponade due to rupture of the cyst causing atrial haemorrhage and leakage of it's contents into the pericardial sac.

Another interesting fact is that the fetus had prenatal cardiac rhythm and conduction disorders. After birth tumor formations in the septum of the heart of the infant were found after USG examination, identified as rhabdomyomas, situated in the apical part of the interventricular septum on the right and the left ventricular surface, with maximum size of 12/5 mm, without hemodynamic significance. Bradicardic heart rate of 70-80 bpm had been found, due to blocked extrasystolic bigemeny. Reduction of the extrasystoly and normalization of heart rate had been achieved with age. Transfontanel USG have not shown any changes in the brain. The follow-up physical development of the child was satisfactory, without heart failure and cyanosis, persisting supraventricular extrasystoles and reductoin of cardiac tumors' size. At last follow-up examination the relatives reported of absence seizures, staring and temporary loss of consciousness. The child had been consulted with a pediatric neurologist and had been hospitalized for suspection of tuberous sclerosis and performance of brain CT and EEG.

Discussion

This case raises interesting issues for discussion – whether it is a hereditary heart abnormality or damage to the heart of the mother and the fetus in relation to the adenovirus infection found before. A positive IgM means an active infection which was confirmed morphologically, but positive IgG implies chronic viral disease which could be associated with both mother and child's heart conditions.

Another interesting question is whether there is a link between heart disorders of mother and infant to the clinical manifestation and treatment of Hashimoto's thyroiditis. It could be assumed that the thyroid hormonal imbalance (due to the lower than conventional dose of L-thyroxine that the mother had been taking) may lead to changes in the heart morphology and function of the fetus. A fact, indirectly supporting this assumption, is the regression of cardiac formations in the baby with age.

References

1. Centella, T., J. L. Moya, M. Muñoz and E. M. Reguero. Giant Endocardial Blood Cyst in the Right Atrium: Echocardiographic and Magnetic Resonance Imaging Features. Circulation., **117**, 2008, 3250-3251.
2. Chong, Z., H.U. Jian, N.I. Yi-ming, J. Zhi-nong and X.U. He-yun. Giant blood cyst tumor in the left ventricular outflow tract. Chinese Medical Journal. **120 (12)**, 2007,1109-1110.
3. Dencker, M., T. Jexmark, F. Hansen, P. Tydén, A. Roijer, C. Lührs. Bileaflet blood cysts on the mitral valve in an adult. J. Am. Soc. Echocardiogr., **22(9),** 2009:1085.
4. Dumantepe, M., K. Ak, U. Mungan, I. Alp, B. K. Inan, A. T. Yilmaz. Blood Cyst of the Right Ventricle Presenting as Recurrent High Fever and Chills in an Adult. Thorac Surg. **87**, 2009, 638–40.
5. Gallucci, V., P. Stritoni, G. Fasoli, G. Thiene. Giant blood cyst of tricuspid valve. British Heart J., **38**,1976, 990-992.

Institute of Experimental Morphology, Pathology and Anthropology with Museum
Bulgarian Anatomical Society

Acta morphologica et anthropologica, 19
Sofia • 2012

Cytopathological effects of *Suid herpesvirus 1* (strain A_2) in cell line DEC 99

Y. Ralinska, I. Ivanov, R. Peshev, M. Alexandrov*

Institute of Experimental Morphology, Pathology and Anthropology with Museum – Bulgarian Academy of Sciences, Sofia
**National Diagnostic and Research Veterinary Institute, Sofia*

Cytopathological effects of the *Suid herpesvirus 1,* strain A_2 (SuHV-1/A_2) were studied in cell cultures from permanent cell line DEC 99. Rounding of the cell, formation of syncytia with different number of nuclei and destruction of the cell layer were the main cytopathological changes detected. Double staining of the cells with acridine orange and ethidium bromide revealed many apoptotic cells at different cell dead levels. Condensation and fragmentation of the chromatin as well as a great number of full and empty virus particles were observed by means of electron microscopy. It was concluded that the data concerning virus morphogenesis are insufficient. Therefore further investigations in this field have to be carried out to demonstrate the interactions between DEC 99 cell line and SuHV-1/A_2.

Key words: apoptosis, Aujeszky's disease, DEC 99, *Suid herpesvirus 1,* syncytia.

Introduction

Aujeszky's disease is an important viral disease in swine with high economic impact. The causative agent *Suid herpervirus 1* (SuHV-1) is a member of family *Herpesviridae,* subfamily *Alphaherpesvirinae,* genus *Varicellovirus* [5]. Like the other alphaherpesviruses SuHV-1 produces distinct cytopathic effects in susceptible cell cultures including rounding of cells, destruction of the cell layer and in some cases formation of syncytia [3]. Numerous types of cell lines or primary cell cultures are susceptible for propagation of SuHV-1 [7], including chick embryo cells [10]. However permanent cell lines from mammalian origin have been predominantly used for studying the characteristics of the virus. Therefore the aim of the present investigations was to study the cytopathological effects of the SuHV-1, strain A_2 in cell cultures from permanent duck cell line DEC 99.

Materials and Methods

Cell cultures. Cell cultures (CCs) from the permanent cell line DEC 99 were cultivated in a CO_2 incubator (5% CO_2, 37,5°C and 95% humidity) in a combination of Medi-

um 199 and Iskove's modification of Dulbecco's medium (IMDM), containing 25mM HEPES buffer (Sigma), supplemented with 10% fetal bovine serum (FBS) (Sigma) and antibiotics in usual concentrations.

Virus stock. Virulent strain A_2 of *Suid herpesvirus 1* (SuHV-1/A_2) was used, kindly supplied by the Department of Virology at the National Diagnostic & Research Veterinary Institute, Sofia, Bulgaria.

Cell infection with SuHV-1/A_2. DEC 99 cells were exposed to SuHV-1/A_2 ($10^{5.3}$ $TCID_{50}$/ml) after the confluence of cell monolayers reached 50%. The virus adsorption was performed for 40 min in tissue culture flasks and plates and after that the maintenance medium was added. Experimental controls including uninfected monolayers were used in all studies.

Double vital staining of DEC 99 cells with acridine orange (AO) and ethidium bromide (EB). In this study, DEC 99 cells uninoculated and inoculated with the SuHV-1/A_2 (third passage on DEC 99 cells, $10^{5.3}$ $TCID_{50}$/ml) were grown in 24-well plates on specially prepared glass lamellas (20×20 mm). At 6, 12, 24, 36, 48, 60 and 72 h p.i. lamellas with DEC 99 cells were harvested, washed in PBS and double-stained by mounting with cell monolayers down on microscope slides using a drop of a double vital staining solution. The solution was prepared by adding 100 μL of 1 mg/mL EB (Sigma) and 100 μL of 1 mg/mL AO (Sigma) to 10 mL of PBS. The investigations were performed on fluorescent microscope Leika DM 500B (Wetzlar, Germany) equipped with the FITC combination of filters.

Electron microscopy (EM). For transmission EM (TEM) infected cells with third passage on DEC 99 cells SuHV-1/A_2 (48 h p.i.) were fixed overnight at 4°C in 2.5% glutaraldehyde, postfixed for 2 h in 1% osmium tetraoxide, dehydrated in graded alcohol and embedded as pellet in Durcupan (Fluka). Yellow-gold ultrathin sections (70–100 nm thick) were prepared and mounted on 400 mesh copper grids and stained with saturated solution of uranyl acetate followed by lead citrate according to the standard technique. All electron microscopy examinations were carried out on an electron microscope JEOL 1200 EX at an accelerating voltage of 80 kV and an instrumental magnification of 2,000–75,000×. Electron micrographs were taken on Kodak EM Film 4489, 6½ x 9cm. The negatives were scanned directly on a HP Scanjet 4890 scanner at 600 dpi resolution using the "SCAN FILM" option.

Results

Double vital staining cytological assay. Normal, uninfected DEC 99 monolayers were composed of closely packed elongated or polygonal morphologically heterogeneous fibroblast like cells **(Fig.1, a)**. The nuclei exhibited dull-green fluorescence and contained 1-7 well-defined nucleoli. The cytoplasm was with dull-green fluorescence and contained large perinuclear accumulations of lysosomal granules. At the 6th h p.i. many cells were shrunken and rounded with enriched number of lysosomes or with lysosomal fusions **(Fig. 1, b)**. After 12 hours of infection the cells were rearranged and formed grape-like clusters where a lot of cells were with late apoptotic nuclei and the cells at periphery were with severe plasma membrane blebbing **(Fig. 1, c)**. At the 24th hour they were cell aggregates composed of intact dead cells **(Fig. 1, d)** and syncytia connected with cytoplasmic tails **(Fig. 1, e)**. At the 36th and 48th hours many nuclei were with dissolved nucleoli. The cytoplasm of many of these cells was stained homogeneously red due to the destruction of the lysosomes **(Fig. 1, f)**. Single viable cells and numerous syncytia were found on the 60th-72nd h p.i. Many syncytia were with decreased number or missing lysosomes **(Fig. 1, g)**. In some cells nuclei exhibited bright fine granular

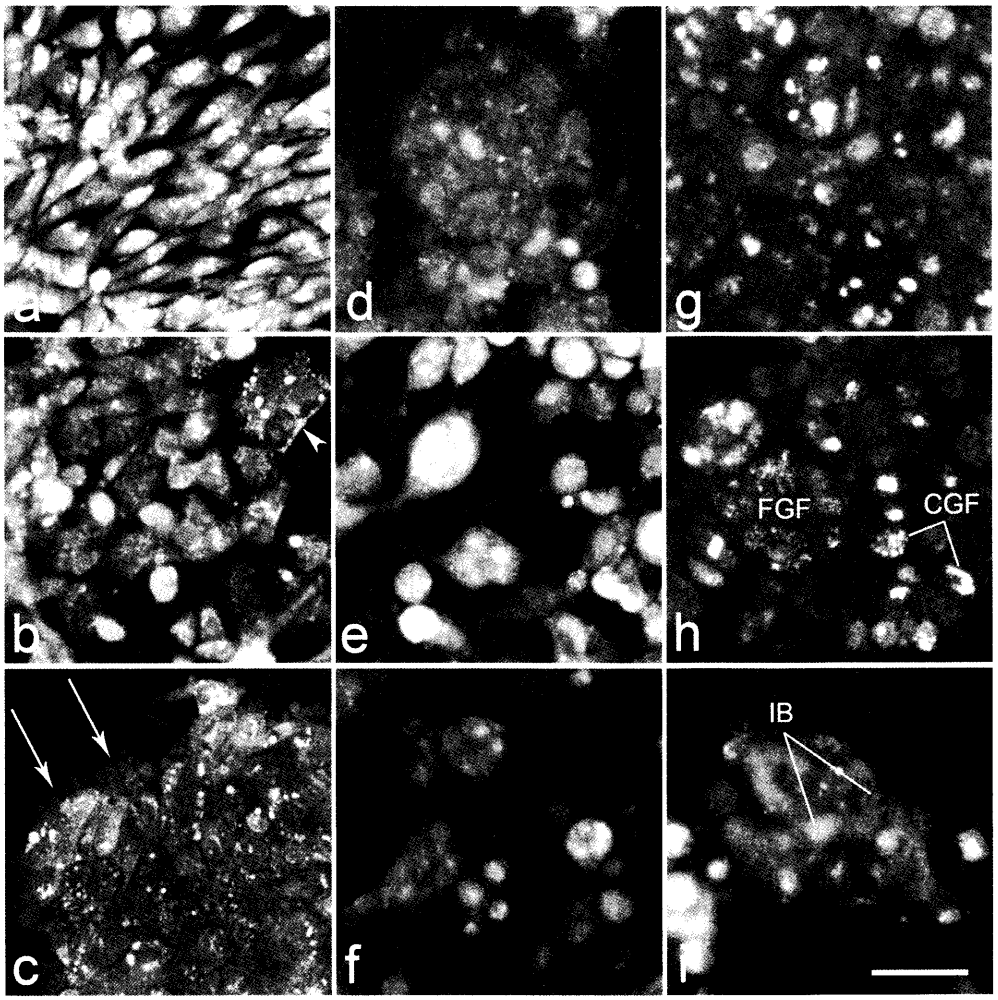

Fig. 1. Cell cultures from cell line DEC 99 infected with SuHV-1/A_2. Normal, uninfected DEC 99 at the 24th h p.i. (a). Shrunken and rounded cells with enriched number of lysosomes or with lysosomal fusions generating largest lysosomal granules (arrowhead) at 6th h p.i. (b). Cells with late apoptotic nuclei and cells with plasma membrane blebbing (arrows) in grape-like clusters at the 12th h p.i. (c). Cell aggregates composted of dead cells (d) and syncytia with cytoplasmic tails between (e) at the 24th h p.i. Cells with dissolved nucleoli and homogeneously red stained cytoplasm at the 36th h p.i. (f). At the 60-72 hour p.i. (g – i): Syncytia with lytic nucleoli and decreased number or missing lysosomes (g); Cells with bright fine granular yellow-green (FGF) or coarse granular (CGF) nuclear fluorescence (h) and nuclei with rearrangement of the chromatin in reticular pattern thus forming different intranuclear inclusion bodies (IB) (i). Vital acridine orange-ethidium bromide staining. Bar = 50 μm.

fluorescence, while other ones were with coarse granular fluorescence **(Fig. 1, h)**. There were also nuclei with rearrangement of the chromatin in reticular pattern thus forming different intranuclear inclusion bodies **(Fig. 1, i)**.

Electron microscopy. The ultrastructural features included condensation or margination of chromatin as well as dense irregular or granular aggregates in the nuclei.

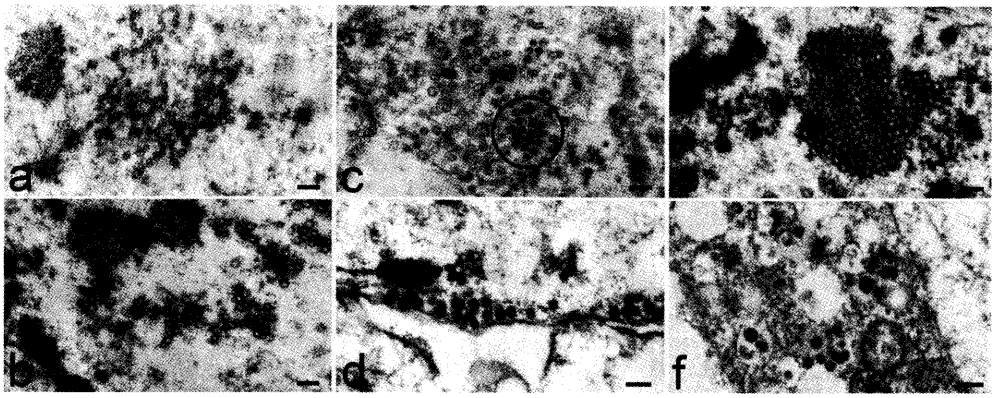

Fig. 2. Electron micrographs of ultrathin sections from DEC 99 cell cultures infected with SuHV-1/A_2 at the 48th p.i. SuHV-1/A_2 virions with different shape and different amount of electron-dense material in the nuclei (a – e). Predominantly naked empty (type A particles) capsids (b). Predominantly naked capsids with electron lucent cores (type B particles). The circle enclose naked capsids with electron dense (type C particles) cores (c). Completely assembled virions near the inner nuclear membrane (d). Viral particles arranged in paracrystalline arrays in the nucleus of an infected cell (e). Cytoplasmic viral aggregates enclosed in vacuoles (f). Uranyl acetate-lead citrate staining. Bars = 200 nm.

The observed SuHV-1/A_2 particles were naked empty capsids (type A particles) **(Fig. 2, a)** or capsids enclosing electron lucent (type B particles) **(Fig. 2, b)** or electron dense (type C particles) cores **(Fig. 2, c)**. The completely assembled virions were usually found located near the inner nuclear membrane or enclosed between inner and outer nuclear membranes **(Fig. 2, d)** Viral particles in various stages of assembly were also frequently found within the cytoplasm. They were associated with smooth membranous structures or accumulated in different in size and shapes aggregates. In addition, paracrystals composed of viral capsids enclosing a variety of electron dense material were frequently observed in the nuclei of DEC 99 cells **(Fig. 2, e)**. Some cytoplasmic viral aggregates were enclosed in irregularly shaped vacuoles **(Fig. 2, f)**.

Discussion

The results of the present studies are in agreement with those of other authors studying the SuHV-1 in primary or permanent cell lines from different origin [4, 9, 10]. By means of double staining of the DEC 99 cells with AO/EB have been revealed typical cytopathological changes characteristic for alphaherpesviruses [3, 10] including detachment, shrinking and rounding of the cells and formation of syncitia. The AO/EB technique revealed also enrichment of the number of lysosomes or lysosomal fusions at the 6th h p.i. and destruction of lysosomes after the 36th h p.i., but the interaction between SuHV-1 and lysosomes remain unclear. It is necessary to note here that the used technique have not been widely used in virological studies. It was developed to establish life and death cells on the basis of the cell membrane integrity and specific intercalation of the used fluorophores with the cell DNA [2]. However as it could be concluded from the present study and earlier [8] the AO/EB (or AO and propidium iodide) staining could be very useful for studying the cytopathological changes induced by viruses in cell cultures as it has been for SuHV-1/A_2 in DEC 99 cells and *Caprine herpesvirus 1* in MDBK cells.

According to the current knowledge A-, B-, and C-type capsids are usual findings during the herpesvirus assembly [1] and results in agreement with that were obtained in the present study. On the other hand herpesvirus virions with morphologically similar shape and structure were simultaneously established within the nucleus and the cytoplasm. This finding could be due to the DEC 99 cell culture properties which have been developed from a duck embryonic cell origin [6] but the data are insufficient. It is considerably different from that described by other scientists who studied the morphogenesis of the SuHV-1 using cell culture lines from mammalian origin [4]. However several successful passages of SuHV-1/A_2 performed in DEC 99 cells (unpublished data) undoubtedly indicate that despite the differences in the morphogenesis an infectious virus progeny is produced. Finally we are well aware of the problems inherent the difficulty to establish a dynamic process from the limited static electron micrographs and we are convinced that further investigations in this field have to be carried out to demonstrate more detailed peculiarities of the SuHV-1/A_2 propagation within DEC 99 cell line.

References

1. Baines, J.D., S.K. Weller. Cleavage and packaging of Herpes simplex virus 1 DNA. Herpesvirus assembly. – In: Viral genome packaging machines: Genetics, structure, and mechanism (Ed. C.E. Catalano). Molecular Biology Intelligence Unit. 2005, 135-150.
2. Duke, R.C. Methods of analyzing chromatin changes accompanying apoptosis of target cells in killer cell assays. – In: Apoptosis methods and protocols. Humana Press. 2010, 47-50.
3. Fenner's veterinary virology, 4th Edition, N.J. MacLachlan, E.J. Dubovi (eds.). Academic Press. 2011, 22-24.
4. Granzow, H., F. Weiland, A. Jons, B.G. Klupp, A. Karger, T.C. Mettenleiter. Ultrastructural analysis of the replication cycle of pseudorabies virus in cell culture: a reassessment. – J. Virol., 71, 1997, 2072-2082.
5. International Committee on Taxonomy of Viruses. Virus Taxonomy: 2009 release, http://www.ictvonline.org/index.asp. 2009.
6. Ivanov, I., A. Kril. Establishment and characterization of a permanent duck embryo cell line. – Exp. Pathol. and Parasitol., 4, 2000, 41-44.
7. OIE Terrestrial Manual. Aujeszky's Disease. Manual of diagnostic tests and vaccines for terrestrial animals. Chapter 2.1.2. 2011, 145-157.
8. Sirakov, I.N., R. Peshev, M. Alexandrov, E. Gardeva. Immunofluorescence and cytopathological features induced by Caprine herpes virus 1 in MDBK cells. – Rev Med Vet, 4, 2012, 167-173.
9. Šmíd, B., L. Valíček, A. Sabó. Morphogenesis of Aujeszky's disease virus in pig lung macrophage cultures. Acta Vet. Brno, 50, 1980, 79-87.
10. Žuffa, A., J. Matis, V. Pleva. Studies on several strains of pseudorabies (Aujeszky) virus showing different virulence by means of the immuno- and acridine orange fluorescence. – Arch Gesamte Virusforsch, 24(4), 1968, 396-405.

Institute of Experimental Morphology, Pathology and Anthropology with Museum
Bulgarian Anatomical Society

Acta morphologica et anthropologica, 19
Sofia • 2012

Quantitative assessment of remodeling in thigh blood vessel walls as a part of the complex approach to peripheral arterial disease

D. Stavrev[1], V. Kniajev[2], G. Marinov[1]

[1]Department of Anatomy, Histology and Embryology, Medical University, Varna, [2]University Clinic of Vascular Surgery, Hospital "St. Anna", Varna,

The data presented for the thickness of the intima and the media of thigh segments of the FA, VF and GSV are part of a complex comparative analysis of morphological remodeling of the vessel wall of the highway in the lower extremity PAD. They can serve as a basis for interpretation and comparison of results obtained by modern imaging methods and tools for visualization and assessment of the vascular system in patients with PAD of the lower limb undergoing surgery, as well as for a selection criterion of adequate venous graft material in the reconstructive surgery for the treatment of PAD of the lower limb

Key words: TASC for PAD, FA, VF, GSV, remodeling

Introduction

Recommendation 76 of The Trans-Atlantic Inter-Society Consensus for the peripheral arterial disease (TASC for PAD) indicates that close cooperation between different disciplines is essential for timely diagnosis and treatment of patients with critical limb ischemia [1]. The therapeutic tactic in this disease requires an integrated approach involving systematic monitoring of general health status, mode of life, and vasoactive antilipidemic drugs, gene therapy and timely surgical intervention. The high effective results from the application of Endovascular Surgery (EVS) initially in the central vascular regions as aorta, coronary and carotid blood vessels [4] creates a natural desire for rapid transfer of these new medical techniques and technologies in a larger range of blood vessels segments [6], including and surgical treatment of PAD [8]. Without ignoring the surgical bypass, as a „gold standard" for treatment of occlusive disease, EVS, including Percutaneous transluminal angioplasty (PTA) and stent placement are used more often in patients with risk of underlying disorders, and the combination of surgical bypass with PTA increases [3]. At the same time a transfer of EVS from one anatomic region to another requires not only developing new instruments and equipment but also a new approach to the study of morphological changes of the blood vessels subject to intervention. Thus, in the recent years, the remodeling of the blood ves-

sels from the various segments of the vascular system in the various stages of life, more often are the objects of the study [5].

The aim of this study is to trace the process of remodeling of the vascular wall, through objective metric data on thickness of the intima and media of highway vessels of the thigh in different stages of PAD.

Material and methods

The study covered the 139 biopsies taken from the thigh segments of the Femoral artery, the Femoral vein and Great saphenous vein, during the surgery in the University Clinic of Vascular Surgery, Hospital „St. Anna", Varna, belonging on the 82 patients with PAD of the lower limb. For the control the necropsies from the analogous blood vessels were taken in the Department of Anatomy, Histology and Embryology, Medical University, Varna. The biopsies and the necropsies were fixed in 10 % formaline solution. Representative parts were embedded in Histowax or in Parafin. Using paraffin microtome 7 mm thick sections were prepared. Staining with Haematoxylin-Eosin and the both three-chrome stainings after van Gieson and after Mason were used to evaluate the histological structure.

Measuring the size of vascular sheaths on photomicrography was done through the program Image Tool 3.00 (The University of Texas Health Science Center in San Antonio). The measuring of the thickness of both tunica intima and tunica media, that are clearly distinguishable, both from each other and from adventitia was performed. In the intima the distance was measured between the internal contour of luminal endothelium and the internal contour of the muscle circular layer of the media. In the media the distance was measured between the innermost contour of the circular muscle layer and the outermost contour of the circular muscle layer. In this method sequentially and separately 2600 measurements were conducted. The obtained metric results were documented in worksheets for every one arterial and venous segment, which was measured, according the clinical diagnosis and performed surgery. Mathematical processing of results was done using the Excel program from Microsoft and was calculated in order:

1. minimum and maximum thicknesses measured in fixed number of areas for the every one layer of the every one artery and vein;
2. calculation of average arithmetic value of the thickness of the every one layer of the every one artery and vein – for the individual and for the group;
3. coefficient of variation for the group.

Results

The results of this study based on morphometric analysis showed that in the three studied vessels the intima is most affected layer of the vascular wall by the process of remodeling. This process is expressed more strongly in the AF intima than in VSM and VF intima. Coming in the underlying section of the wall transformation makes the boundaries between tissues lining the wall difficultly discernible.

Therefore, early signs of remodeling of the intima can be analyzed only in areas in which this layer is with sufficiently well preserved structure. In the lower extremity PAD the thickness on the intima of the AF generally increase. Its average thickness in patients with reconstruction exceeds that of the control by 141% against it. In patients with amputation also intima exceeds that of control but only by 131% against it (Fig.1). Thickening of intima of VSM and VF is an essential element in the remodeling of the

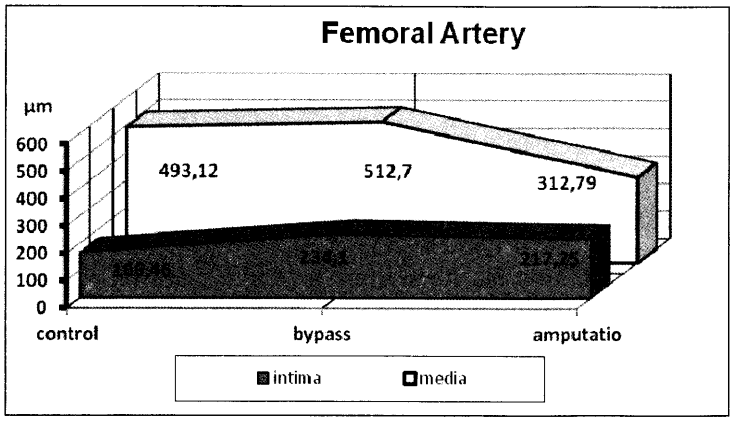

Fig. 1

walls in PAD. Thickness of the intima in the VSM in patients with PAD is uneven and the measured values vary widely. The average thickness of the intima increases and this process is more pronounced in advanced stages of disease. The average thickness of the intima in patients with VSM reconstruction exceeds that of the control by 114% against it. The average thickness of the intima of the VSM in patients with amputation exceeds that of control and is 164% against it Fig.2). Thickness of the intima of VF in patients with PAD is also uneven and measured values vary widely. In the final stages of PAD the average thickness of the VF intima increases significantly in patients with amputation than that of control, being 167% against it (Fig.3). Comparison of the measured digital characteristics of medium thickness of the intima of the VSM and VF in PAD shows that they have similar values, but their growth is almost two times more intense than that of AF.

The media in AF initially keeps its thickness, but with the progression of PAD significantly reduces. In patients with reconstruction, it is similar to that of control – 104% against it. In patients with amputation the media is significantly thinner – 63% against it. The average thickness of the media of VSM in patients with PAD also increases its thickness and in patients with reconstruction, it is 123% compared to controls. In

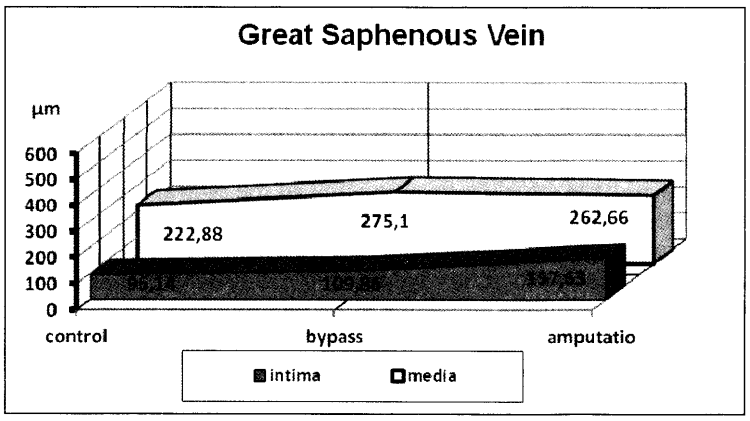

Fig. 2

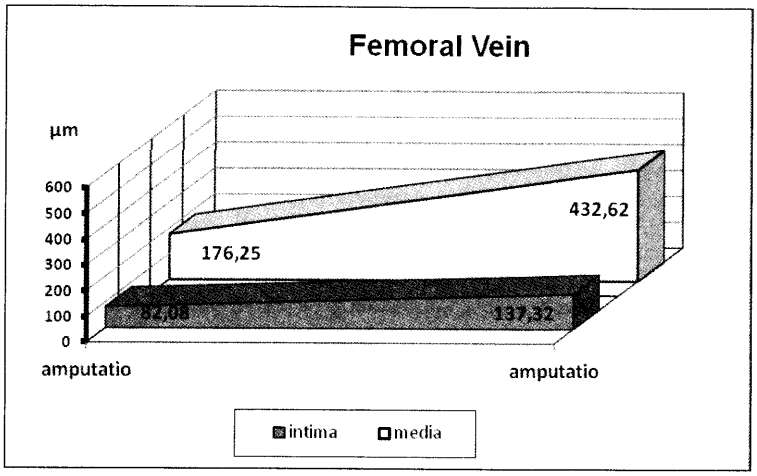

Fig. 3

patients with an amputation, it is 118% compared to controls. The media of VF also greatly increases its thickness and in patients with amputation its average thickness is 245% compared to controls. Thickening of the media of VF wall in patients with amputation is much more pronounced than in the VSM.

Discussion

The process of remodeling of the walls of the thigh vessels at the development of PAD lead to substantial changes in their construction. They have specific quality characteristics in each artery and vein. The proper and accurate interpretation, and evaluation of their effects on the vascular system of the limb, is necessary to be demonstrated through quantitative assessment, first of intima-media thickness. Widespread application of ultrasound measurement of intima-media thickness of carotid arteries, showed the important diagnostic and prognostic value of this approach [2].

1. In all studied patients with PAD, the average thickness of the media of vessels studied is greater than the average thickness of the intima.
2. The intima of the AF in patients who had great amputation is thicker compared to patients with reconstructions, while the media is much thinner.
3. The intima of VSM in patients who had major amputation is thicker compared to patients with reconstructions, while the media did not show significant differences.
4. The thickness of VF intima in patients who had a high amputation showed no significant differences with that of the VSM, while media of VF is thicker.
5. The media is the main and most thick layer of AF, VSM and VF. Our results show, that this layer has a much greater resistance to remodeling of its structure than intima. This resistance can be connected with the fact that media is ontogenetic older than intima.
6. VSM and VF the both had preserved largely its morphological structure and biomechanical properties, and are therefore suitable for use as graft material in reconstructive vascular surgery. In addition, the VF is not only the venous graft with increasing role in the surgery of the lower limb, but it has a great potential for widespread use as material in other vascular segments, too [9, 10].

References

1. Barandon L., L. Leroux, P. Dufourcq, P. Plagnol, C. Deville, C. Duplaa, T. Couffinhal, Pessac and Langen, Gene Therapy for Chronic Peripheral Arterial Disease: What Role for the Vascular Surgeon? An. Vas. Surg., 18(6), 2004, 758-765.
2. Collin C. O. Kim-Thanh, H. Beaussier, S. Laurent, P. Boutouyrie. Valeur prédictive de l'épaisseur intima-média de l'artère carotide commune sur le risque de survenue d'événements cardiovasculaires. Sang Thrombose Vaisseaux, 20(8), 2008, 393-403
3. De Sanctis J.T. Percutaneous interventions for lower extremity peripheral vascular disease. Am. Fam. Physician., 64(12), 2001, 1965-1972.
4. Hassantash S-A., B. Bikdeli, S. Kalantarian, M. Sadeghian, H. Afshar. Pathophysiology of aortocoronary saphenous vein bypass graft disease. Asian Cardiovasc. Thorac. Ann. 16, 2008, 331-336.
5. Kafetzakis, A.,G. Kochiadakis, A. et al. Laliotis. Association of subclinical wall changes of carotid, femoral, and popliteal arteries with obstructive coronary artery disease in patients undergoing coronary angiography. Chest, 128, 2005, 2538-2543.
6. Met R., U.P. Van Lienden, M.J.W. Koelemay, S. Bipat, D.A. Legemate, J.A. Reekers. Subintimal angioplasty for peripheral arterial occlusive disease: a systematic review. Cardiovasc. Intervent.Radiol., 31, 2008, :687–697.
7. Mizia-Stec K., Z. Gąsior[1], B. Zahorska-Markiewicz[2], M. Holecki[2], M. Haberka[1], M. Mizia[1], S. Gomułka[1], A. Żak-Gołąb[2] and A. Gościńska[1] The indexes of arterial structure and function in women with simple obesity: a preliminary study Heart and Vessels, 23(4), 2008, 224-229.
8. Puato, M., C. Piergentili, M. Zanardo, et al. Vascular remodeling after carotid artery stenting. Angiology, 58,(5), 2007, 565-571.
9. Schulman M.L., L.G. Schulman, A.M. Liedo-Perez. Unusual autogenous vein grafts. Vasc. Surg. 26, 1992, 257-264.
10. Stavrev D., G. Marinov, V. Knyazhev. Femoral vein wall remodeling in chronic arterial insuffiency of the lower limb. Acta Morph. and Anthrop., 10, 2005, 78-82.

Institute of Experimental Morphology, Pathology and Anthropology with Museum
Bulgarian Anatomical Society

Acta morphologica et anthropologica, 19
Sofia • 2012

Using of plastinated anatomical preparations in preclinical and clinical education of medical students

D. Sivrev[1], A. Usovich[2]

[1]Department of Anatomy, Faculty of Medicine, St. Zagora, Bulgaria
[2]Department of Anatomy, State Medical University, Vitebsk, Belarus

Plastination is a new technology for anatomical specimen preservation without toxic materials. Biodur S10 is a classic polymer for anatomical objects preservation. The process during eight weeks. The preparations are safety, non odorous, they can preserve at ordinary conditions and use for medical students education.

Plastinated organs can be used for anatomical training of medical students and the practical training of graduate students in clinical educational subjects. S10 plasination technique because of the low hardness of preparations allows small operations in the field of ophthalmology and oto-rhino-laryngology.

Keywords: Biodur, plastination, preservation, anatomy, brain slices.

Introduction

The Human Society needs of high level physicians and other medical specialists. The anatomy is a base of all medical educational subjects.

Dissection is a very important method in medical education from old ages to this day. Solution of formaldehyde 3-10% used for fixation is very noxious for humans. It causes inflammation of respiratory system, allergic reaction etc.

Plastination is a new revolutionary technology to create safe and durable anatomical preparations stored under normal conditions. Plastinated organs can be used for anatomical training of medical students and the practical training of graduate students in preclinical educational subjects as well as in clinics. S10 plasination technique because of the low hardness of preparations allows small operations in the field of ophthalmology and oto-rhino-laryngology too.

Material and Methods

We use S10 plastination technique for production of anatomical preparations for medical student education.

Fixation of **hearts**, **brains**, **livers**, **joins** etc. is in 10% formalin at room temperature. If specimen is tick infiltration is necessary. Dehydration, forced impregnation and curing phase are standard [12].

For plastination of the **eyeball** we used a combination of two different technologies – S10 plastination technique of von Hagens [12] and impregnation by Steinmann [10].

Replacing tissue water with polymer is performed by forced impregnation, but with polyethylene glycol – by the method of molecular substitutions.

Pig eyes were used for model development. Hylase (Farma Dessau, Gbm, Germany) 300 UI was injected into the vitreous chambers to help liquification of the vitreous body [6].

Fixation of specimen is necessary for successful plastination. We used standard fixation with formalin 5% for 4 days because eye walls are thin and fixative penetrates all parts of the object. Eye wall doesn't need of formalin infiltration but it is necessary to inject fixative into vitreous body.

Acetone 100% is dehydration liquid in stepwise freeze substitution. Procedure continues 5 days at -25°C. Acetone contains until 90% water at the first step, but no water at the last step.

Biodur S10/S3/S6 (100:1:0.7) silicone [6] was injected into the chambers until they were full. Specimens were then placed in the polyethylene glycol and stored at 5°C to permit the curing of the silicone.

For plastination of the **internal ear** we used applications of surgery techniques on human skull. The temporal bone was plastinated with S10 technique [9].

Results

After gas-curing durable, flexible and safety whole organs: hearts, brains, livers, joins etc. are made. We use them in anatomical education of medical students.

Vessels, valves and muscles of the heart are detailed. Papillary muscles, chordae tendineae and valves of the heart are discernable and coronaries are easy of access to study.

Full particulars of brain surface are pronounced. Whole brains keep their special features. Lobes, fissures, sulcus and gyri are in a good condition. The central and lateral sulcus are apparent and students can study the brain morphology on plastinated preparations.

The liver has a stable consistence and all its details are distinguish one thing from another. Gall bladder, ducts and portal vessels look like real. Four hepatic lobes and ligaments are with well-defined outlines and well preserved.

After drying, the eye specimens is soft, life-like and suitable to be used in the educational process. The appearance of the plastinated specimens is similar to their natural condition. Eye muscles and optical nerve are in good shape and students can study the eye morphology on plastinated preparations. The cornea of eye is damaged anytime.

Discusion

We can make whole organs and their parts in field of anatomy, pathology and forensic medicine [1] obey the rules of the ethics of using human remains [2]. We can plastinate whole brain and brain slices as well as joint and muscle preservations [8, 9, 12].

We use plastinated organs in medical education of first and second year students. Plastinated bones and joins are suitable for first year students as well as whole organs, brains and muscles for second year.

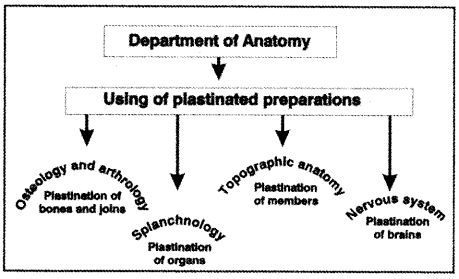

Fig 1. Using of plastinated preparations

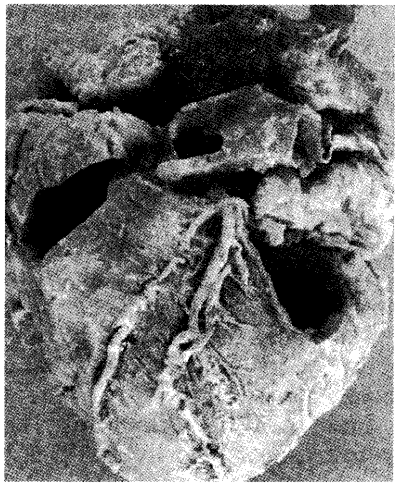

Fig 2. Heart plastination

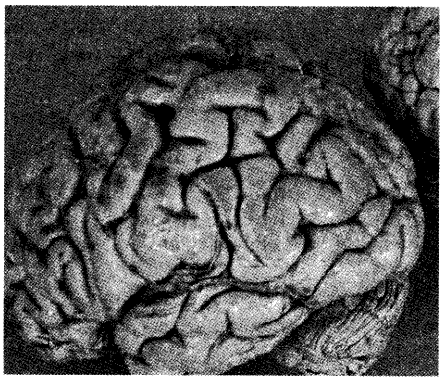

Fig 3. Brain plastination

Fig 4. Liver plastination

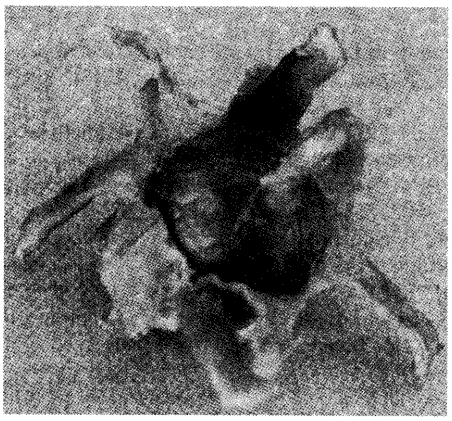

Fig 5. Plastination of eyeball

Fig 6. Damage of cornea

Our heart plastination results are according with experiments of other autors [5], but we combined two different methods for heart plastination. Some autors plastinated bones, joins and ligaments too [4, 7, 8]. Usually Biodur P40 is use for brain slices plastination [3, 11]. We used Biodur S10 and had good results – low price, good appearance and stability.

The vitreous body of eye was replaced by Biodur S10 and eyeball wall was impregnated by polyethylene glycol. The polymer prevents the retina from detaching when the eye is placed under vacuum during the subsequent phases of the impregnation process. This makes the pig eye a good surgery model similar to living human eyes.

We found the combination of the two different polymers as an excellent method for the preparation of the eyeball for education of medical students and specialists.

Plastinated internal ears are safe for student. They are suitable for storage at room temperature in ordinary conditions without submersion in formaldehyde-containing fixatives in glass jars.

Brain slices have all details. The polymer trace out the border between white and gray matter, nuclei and fibres.

Conclusion

The students can use anatomical preparations in their preclinical and clinic education. Preparations are safety, non odorous and they can preserve at ordinary conditions.

References

1. Alpar, A, T. Glasz, M. Kálmán. Plastination of Pathological Specimens – A Continuing Challenge. Journal of the International Society for Plastination, 20, 2005, 8-12.
2. Barilan, Y. Bodyworlds and the ethics of using human remains: a preliminary discussion. Bioethics, 20(5), 2006, 233-247.
3. Frohlich, I., A. Probst, M. Polgar, M. Sora, H. König. Plastic-embedded brain slices of the dog – a basis for clinical examination with modern diagnostic imaging. Wien Tierärztl Mschr, 90(3), 2003, 62-66.
4. Johnson, G., M. Zhang, D. Jones. Dorsal and ventral portions of ligamentum nuchae are not independent of each other. Clinical Anatomy, 17(2), 2004, 158-160.
5. Oostrom, K. Plastination of the heart. Journal of the International Society on Plastination, 1(2), 1987b, 12-19.
6. Sivrev, D., J. Kayriakov, Z. Trifonov, D. Djelebov and M. Atanasov. Combined Plastination Methods for Preparation of Improved Ophthalmologic Teaching Models. J Int Soc Plastination Vol 12, No 2, 1997, 12-14.
7. Sora, M., B. Genser-Strobl. The sectional anatomy of the carpal tunnel and its related neurovascular structures studied by using plastination. European Journal of Neurology, 12(5), 2005, 380-384.
8. Sora, M., B. Genser-Strobl, J. Radu, S. Lozanoff. Three-dimensional reconstruction of the ankle by means of ultrathin slice plastination. Clinical Anatomy, 19, 2006, 196-200.
9. Steinke, H., S. Pfeiffer, K. Spanel-Borowski. A new plastination technique for head slices containing brain. Annals of Anatomy, 184(4), 2002, 353-358
10. Steinmann W: Die Polyethilenglykol-Impregnation. Wienn, 1986.
11. Weiglein, A. Sheet plastination of brain slices according to the P35 and P40 profcedures. Journal of the International Society on Plastination, 13(2), 1998, 27-42.
12. von Hagens G: Heidelberg Plastination Folder: Collection of all technical leaflets for plastination. Anatomische Institut 1, Universitat Heidelberg, Heidelberg, Germany, 1985, 1-36.

Institute of Experimental Morphology, Pathology and Anthropology with Museum
Bulgarian Anatomical Society

Acta morphologica et anthropologica, 19
Sofia • 2012

Bone morrow microvascular dencity in chronic mieloproliferative neoplasms in patients with and without *jak2* (v617f) mutation

M. Tzaneva, N. Zgurova, L. Gercheva, A. Zhelyazkova**

Departmennt of General and Clinical Pathology, Medical University, Varna
**Clinic of Haematology, MBAL "Sveta Marina", Varna*

The incidence of *JAK2* (V617F) mutation in myeloproliferative neoplasms (MPNs): polycythemia vera (PV), essential thrombocythemia (ET) and chronic idiopathic myelofibrosis (MF) is very high, which leads to constitution activation of *JAK2* and an independent growth of the haemopoetic cell lines.

Angiogenesis in MPNs was studied by an endothelial marker (CD34) and bone marrow microvessel density (MVD) compared in patients with and without *JAK2* (V617F) mutation.

MVD in *JAK2* mutation was 16.48±8.77 (per high-power microscopy field – HPF), 12.51±5.59, 20.51±7.77 for PV, ET and MF, respectively. Patients without mutation had MDV 11.32±5.74, 12.80±5.40 and 15.00.±7.57 for PV, ET and MF, respectively. There was no difference ($p>0.05$) in mean MVD in ET, while MVD was higher in PV and MF patients with *JAK2* mutation ($p< 0.01$).

These results show pronounced angiogenesis in the bone marrow of MF and PV patients with *JAK2* mutation. Probably it is induced by the activation of the *JAK2* signaling pathway.

Key words: bone marrow microvessel density, polycythemia vera, essential thrombocythemia, chronic idiopathic myelofibrosis, *JAK2* (V617F) mutation

Neoangiogenesis is an integral part in the progression of solid tumors and the microvascular density in tumor tissue correlates well with its growth and its capacity to metastasize (10). Increased number of bone morrow blood vessels is established in various hematologic disorders, such as acute lymphoid or myeloid leukemia, myelodysplastic syndrome, chronic myeloid leukemia and plasma cell proliferative disorders (3, 9). In normal conditions, human bone marrow is supplied by a relatively smaller number of blood vessels.

Marked neoangiogenesis is a characteristic feature of myeloproliferative neoplasms (MPNs): polycythemia vera (PV), essential thrombocythemia (ET), and chronic idiopathic myelofibrosis (MF) (3, 10). These Philadelphia-negative (Ph_) chronic MPNs display a high frequency of *JAK2* (V617F) mutation. It is an acquired somatic mutation in the *JAK2* gene resulting in a valine to phenylalanine substitution at position 617 (JAK2V617F) (7).

Currently available data indicate that *JAK2* (V617F) participates in the pathogenesis of these neoplasms, because the mutation leads to constitution activation of *JAK2* and thus haemopoetic cell lines acquire a potential for independent growth (10).

That is why we studied angiogenesis in MPNs and compared bone marrow microvessel density (MVD) in patients with and without *JAK2* (V617F) mutation.

Materials and Methods

Forty three patiens with MPNs were investigated (21 men and 22 women, 23 to 77 years of age).

Tissue specimens

Patients were selected based on the availability of well-preserved bone marrow biopsy specimens, suitable for additional stainings. Paraffin sections were stained with HE and Gomori. A histopathological diagnosis of the MPNs was made in accordance to WHO (9). Paraffin section (5 μm thick) was processed by peroxidase-antiperoxidase technique. Monoclonal antibody Mo a Hu CD34 class II clone QBEnd (Dako) was used for detection of microvessels. We counted the number of vessels per (HPF – 10 x 40) in the areas of most dense vascularization. Five areas were evaluated from each patient. MDV was determined as a median value of all measurings. The data are presented as the mean and standard deviation. Statistical comparisons using analysis of variance and Student's t-test was performed. $P<0.05$ was considered statistically significant.

JAK2 (V617F) mutation was determinate by reverse-transcribed polymerase chain reaction (RT-PCR method).

Results

Histology

Eighteen of the patients were with PV. In bone morrow there were an increased number of the erythroid precursors and the myeloid-erythroid ratio was usually decreased. The megakaryocytes were pleomorphic, grouped together and had deeply lobulated nuclei without atypical and dysplastic features.

ET was established in twelve patients. The bone morrow in ET was usually normocellular for age or moderately hypercellular with an increased number of either large or giant megakaryocytes. They showed hyperlobulated nuclei and/or appeared in clusters or were diffusely dispersed. The megakaryocytic clusters were found around the sinusoids or close to the bone trabeculae. Reticulin fibrosis was minimal or lacking.

MF was found in thirteen patients. Nine of them were in the cellular phase and four in fibrotic phase. In the cellular phase, the bone morrow was hypercellular and displayed panmyelosis. Megakaryocytes were atypical and often appeared in clusters around the sinusoids and/or bone trabeculae. Abnormal nuclear lobulation, naked nuclei, and large bizarre forms were frequently observed. Micromegakaryocytes were often present. MF patients in the fibrotic phase revealed various degrees of fibrosis and marked hypocellularity. Megakaryocytes had deeply lobulated and hyperlobulated nuclei, abundant mature cytoplasm, and smooth nuclear contours.

Bone morrow microvascular dencity

MVD in *JAK2* (V617F) mutation was 16.48±8.77 (10 x 40), 12.51±5.59, 20.51±7.77, respectively for the patients with PV, ET and MF (Fig. 1). Patients without mutation had MDV 11.32±5.74, 12.80±5.40 and 15.00.±7.57 for PV, ET and MF, respectively (Fig.2). There was no significant difference in mean MVD in ET between the groups

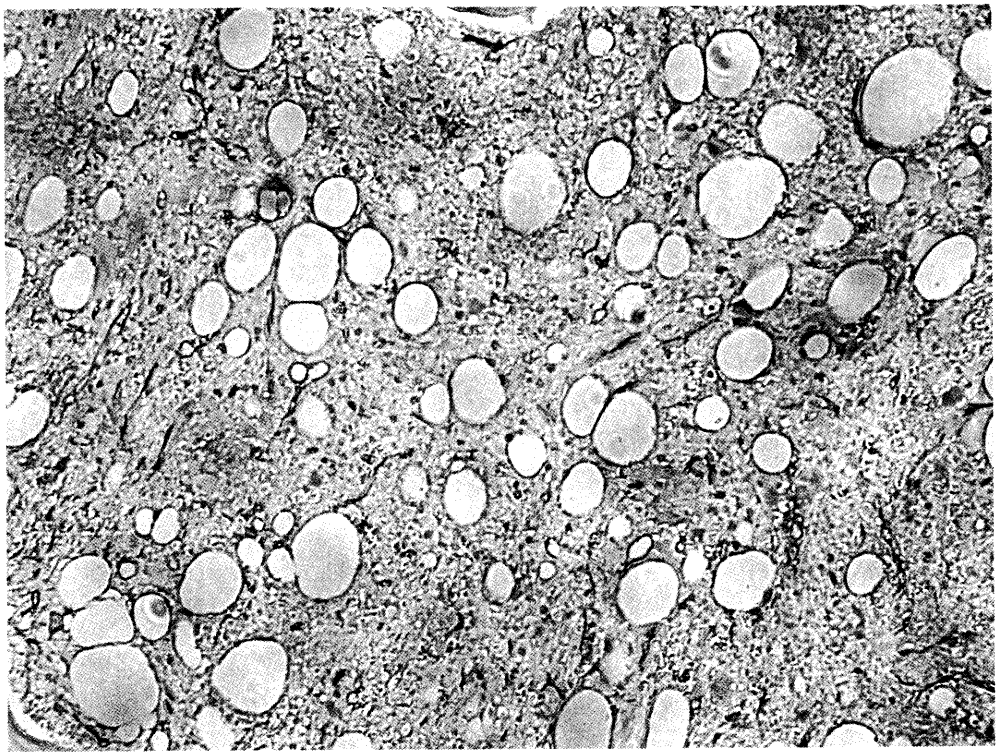

Fig 1. MPN in *JAK2* positive patient with PV.

($p>0.05$). MVD was higher in both PV and MF with *JAK2* (V617F) mutation as compared to *JAK2* (V617F) negative patients ($p<0.01$). The microvessels had moderate to high expression of CD34 in the cytoplasm of the endothelial cells. Scattered CD34 positive cells were also found, but the positive reaction was only in the nuclei.

Disscusion

An increased MVD in MPNs compared to controls has been already established (3, 4). Patients with MF had the highest MVD, followed by PV and ET. In addition, an altered vascular architecture has been established in MPNs (3). By confocal microscopy, tortuous and branched microvessels were observed in both PV and MF (3).

Our quantitative results considerably extend the results of previous studies and show a correlation between angiogenesis in bone morrow and *JAK2* mutation for patients with MF and PV. MF and PV patients with *JAK2* mutation had higher MVD than *JAK2* negative patients. This finding in patients is confirmed by in vitro studies, which show that angiogenesis is induced by activation of the *JAK2* signaling pathway, while vascular sprouting is inhibited by *JAK2* blockade (11).

JAK2 gene was mapped on the short arm of chromosome p24 in 1992 by Pritchard and his colleagues (5). It has 140 kb spanning 25 exons to form 1132 aminoacid JAK2 protein (7). *JAK2* mutation is implicated with mobilization of CD34-positive cells and

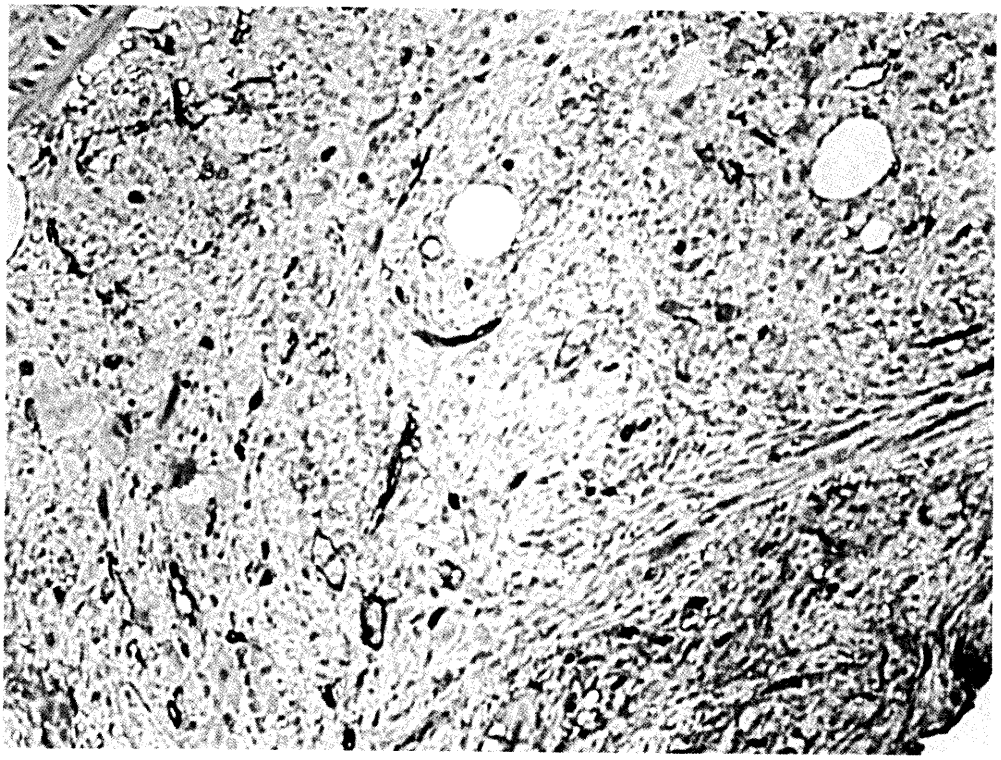

Fig 2. MPN in *JAK2* negative patient with PV.

MPNs progression (2). In this study endothelial cells were marked with CD34, but a set of haematopoietic cells also were CD34 positive. MPNs are thought to originate at the level of a primitive haematopoietic progenitor or stem cells (8). During embryogenesis endothelial cells and haematopoietic cells share a common cell origin (8). *JAK2* mutation is found in both endothelial hepatic venule cells and haematopoietic cells in patients with PV (8). The increased MVD in patients with *JAK2* mutation indicate that the endothelial cells are a part of the malignant transformations in MPNs.

We found that CD34 antibody visualized endothelial cytoplasm of microvessels. The scattered CD34 positive cells showed nuclear expression. CD34 expression was present only in the nuclei of haemopoietic stem cells with *JAK2*V617F mutation, while in their differentiated progeny, it remains mostly in the cytoplasm (6). The signals that are required for the translocation of normal and mutated *JAK2* to the nucleus remain unknown. It has been suggested that the activation of the kinase, coding from *JAK2* by phosphorylation may be the first step of several modifications which operate the nuclear translocation and when the cell undergoes differentiation these modifications are shut off, and mutated JAK2 protein remains predominantly in the cytoplasm. On the basis of these data we consider that the endothelial cells at least in part are differentiated cells.

We were unable to find a change in MVD between *JAK2* positive and *JAK2* negative patients with ET. Our results differ from other studies, which report an increased bone morrow angiogenesis in ET (4). According to Medinger et al. (2009) CD105 is

more reliable marker for newly formed vessels than CD34. On the other side, this probably indicates that angiogenesis is not involved, at least during the early stages of ET.

In conclusion, the formation of blood vessels is pronounced in MF and PV in bone marrow of patiens with *JAK2* mutation. Whether this is a major oncogenic event or a consequence of clonal haematopoietic cell proliferation remains to be clarified.

Reference

1. Ahmed, A., C. C. Chang. Chronic idiopathic myelofibrosis. Clinicopathologic features, pathogenesis, and prognosis. – Arch. Pathol. Lab. Med. **130,** 2006, 1133-1143.
2. Kralovics, R., F. Passamonti, A.E. Buser, S. S. Teo, R. Tiedt, J. R. Passweg., A. Tichelli, M. Gazzola, R. C. Skoda. A gain-of-function mutation in myeloproliferative disorders. – New Eng. J. Med. **352,** 2005. 1779-1790.
3. Lundberg, L.G., R. Lerner, P. Sundelin, R. Rogers, J. Folkman, J. Palmblad. Bone marrow in polycythemia vera, chronic myelocytic leukemia, and myelofibrosis has an increased vascularity. – Am. J. Pathol. **157**, 2000, 15-19.
4. Medinger, M., R. Skoda A. Gratwohl, A. Theocharides, A. Buser, D. Heim, S. Dirnhofer, A. Tichelli., A. Tzankov. Angiogenesis and vascular endothelial growth factor-/receptor expression in myeloproliferative neoplasms: correlation with clinical parameters and JAK2-V617F mutational status. – British J Haematol. **146,** 2009, 150–157.
5. Pritchard, M., E. Baker, D. F. Callen, G. R. Sutherland, A. F. Wilks. Two members of the JAK family of protein tyrosine kinases map to chromosomes 1p31.3 and 9p24. – Mammalian Genome **3,** 1992, 36-38.
6. Rinaldi, C. R., P. Rinaldi., A. Alagia., M.Gemei., N. Esposito., F. Formiggini., V. Martinelli., V. Senyuk., G. Nucifora., F. Pane. Preferential nuclear accumulation of JAK2V617F in CD34 but not in granulocytic, megakaryocytic, or erythroid cells of patients with Philadelphia-negative myeloproliferative neoplasia. – Blood. **116,** 2010, 6023-6026.
7. Saltzman, A., M. Stone, C. Franks, G. Searfoss, R. Munro, M. Jaye, Y. Ivashchenko. Cloning and characterization of human Jak-2 kinase: high mRNA expression in immune cells and muscle tissue. -Biochem Biophys. Res. Commun. 246, 1998, 627-633.
8. Sozer, S., M. I. Fiel, T. Schiano, M. Xu, J. Mascarenhas, R. Hossman. The present JAK2V617F mutacion in the liver endothelial cells of patients with Budd-Chiari syndrome. – Blood, **113,** 2009, 5246-5249.
9. Steven. H.S., E. Campo, N. L. Harris, E. S. Jaffe, S. A. Pileri, H. Stein. J. Thiele, J. W. Vardiman. WHO classification of tumours of haematopoietic and lymphoid tissues. **4th edition,** 2008, 1-439.
10. Weidner, N. Tumor angiogenesis: review of current applications in tumor prognostication. – Seminars Diagnostic Path. **10,** 1993, 302-313.
11. Zhu, K., M.A. Amin., Y. Zha., L.A. Harlow., A.E. Koch. Mechanism by which H-2g, a glucose analog of blood group Hantigen, mediates angiogenesis. – Blood **105**, 2005, 2343–2349.
12. Yoon, S.Y., A. Tefferl., C. Yang. Bone marrow stromal cell distribution of basic fibroblast growth factor in chronic myeloid disorders. – Haematologica **86,** 2001, 52-57.

Institute of Experimental Morphology, Pathology and Anthropology with Museum
Bulgarian Anatomical Society

Acta morphologica et anthropologica, 19
Sofia • 2012

Expression of MUC 1, MUC2, MUC5AC and MUC6 in gastric carcinoma

*M. Tzaneva, N. Zgurova, V. Tsvetkova**

Departmant of General and Clinical Pathology, Medical University, Varna

Gastric carcinoma is two main histological types: intestinal and diffuse type. The aim of this study was to evaluate the expression and the distribution of MUC1, MUC2, MUC5AC and MUC6 in the tumor and adjacent non-tumor epithelial tissue by immunohistochemistry in twelve cases of gastric carcinomas. MUC1 immunoreactivity in the cytoplasm of tumor cells was variable – from weak to moderate, while in non-tumor tissue it was very weak.

MUC5AC and MUC6 showed a low content in tumor cells as compared to non-tumor tissue. MUC2 expression was observed in seven intestinal and one diffuse carcinoma. In adjacent mucosa MUC2 positive goblet cells had in all intestinal carcinomas.

In conclusion, these results show that during the process of carcinogenesis the expression of gastric mucins MUC5AC and MUC6 is decreased and the expression of MUC2 is aberrant in areas of intestinal metaplasia. An increased MUC1 expression probably plays a role in the development of neoplastic gastric epithelium.

Key words: gastric carcinoma, mucin expression, gastric carcinogenesis

Introduction

Mucus, a gel-like substance that covers the mammalian epithelial surfaces is composed of mucin glycoproteins (10). Mucus acts as both a lubricant and as a protective barrier between the contents of the stomach and the mucosal epithelial surface (7). In human gastric mucosa three mucins have been identified: MUC1, MUC5AC and MUC6 (3). There are two structurally and functionally distinct classes of mucins: secreted gel-forming mucins (MUC2, MUC5AC, MUC5B and MUC6) and transmembrane mucins (MUC1, MUC3, MUC4, MUC12 and MUC17) (10). Alterations of their expression pattern have been described in carcinomas as well as in precursor lesions (2, 6, 8, 11). The aim of this study is to investigate the expression and the distribution of MUC1, MUC2, MUC5AC and MUC6 in tumor tissue and to compare this expression with the MUC profile in tumor adjacent mucosa of gastric carcinoma.

Materials and Methods

Twelve patients carcinoma surgically resected were investigated. The patients were 7 men, and 5 women. The age varied from 36 to 76 years.

Tissue specimens

Three or four tissue specimens were collected from surgically removed tumor and another two or three from adjacent non-tumor epithelial tissue. Paraffin sections were stained with HE, PAS and Alcian blue. A histopathological diagnosis of the carcinoma was made in accordance to Lauren (5). Paraffin sections (5 μm thick) were processed by peroxidase-antiperoxidase technique. The primary antibodies were: MUC1 (RB-9222-R7), Mucin2 Ab.2 (M53) (Ms 1037-R7), Mucin 5AC Ab-2(1-13ML) and MUC-6 Ab-1 (CLH5) (MS-1153-S) (LAB VISION THERMO)

Results

Histology.

Gastric carcinomas were divided into two main histological types (intestinal and diffuse) on the basis of their tendency of glandular formation. Ten of gastric carcinomas were from intestinal type and two had a diffuse growth pattern.

Light microscopic immunohistochemistry.

In non-tumor tissue MUC1 immunoreactivity was weak and was located in the apical membrane and the cytoplasm of parietal cells in the fundic glands It was also occasionally present in cytoplasm of the antral glands and antral surface mucous cells (Fig.1).

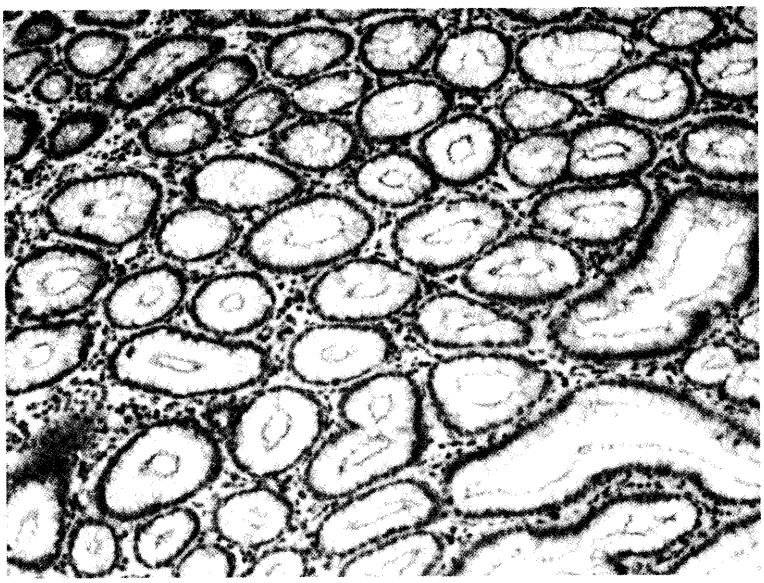

Fig.1. MVD in *JAK2* positive patients with PV

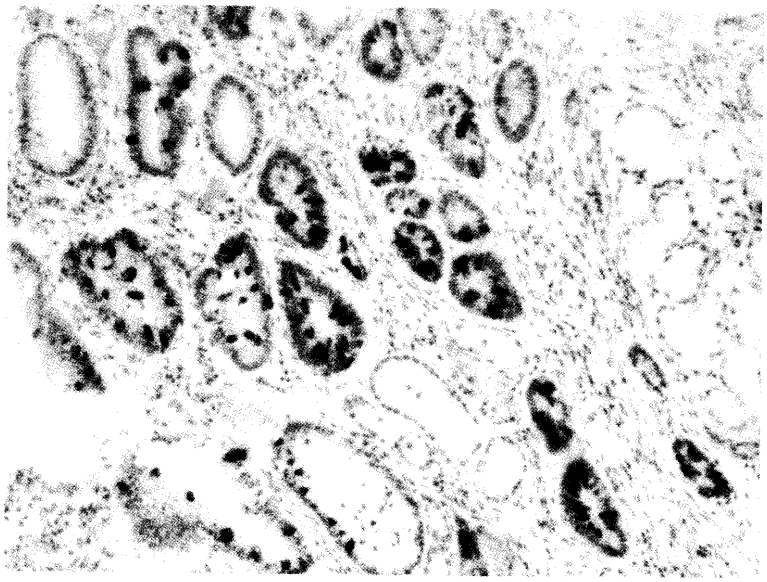

Fig.2. MVD in *JAK2* negative patients with PV

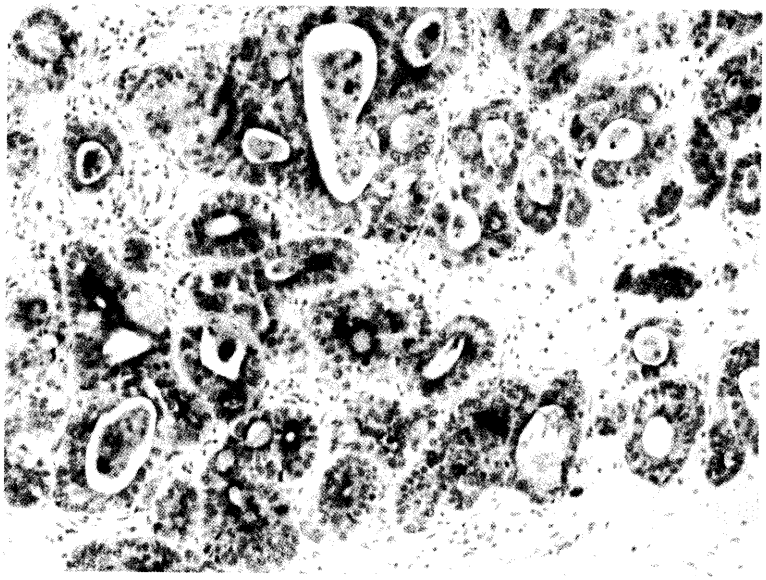

Fig.3. MUC1 in the cell tumor cytoplasm and in the lumen of the tumor glands

MUC5AC was highly expressed in foveolar epithelium and mucous neck cells of antrum. MUC6 was localized in the glands of the antrum and in some mucus neck cells. MUC2 was not detected in normal gastric mucosa. It was observed in goblet cells in intestinal metaplasia next to intestinal carcinoma only (Fig.2). In adjacent non-tumor mucosa MUC2 positive goblet cells had in all intestinal carcinoma.

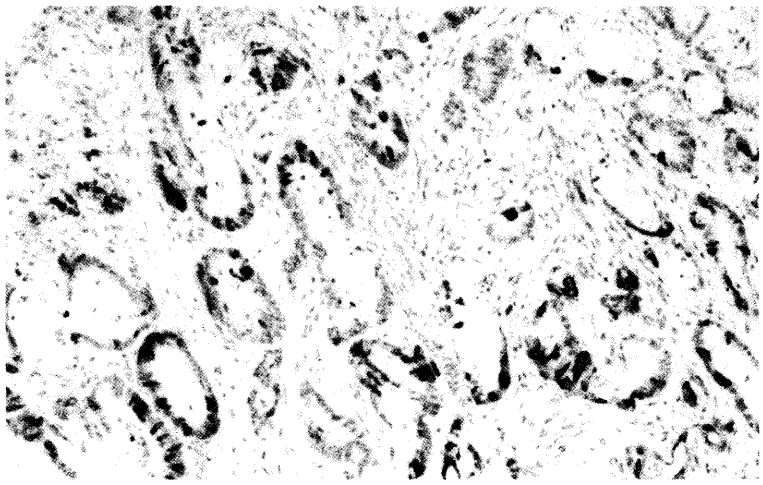

Fig. 4. MUC2 in the cell tumor cytoplasm in intestinal gastric carcinoma

In tumor tissue of the intestinal carcinoma MUC1 expression was weak to moderate and was localized mainly in cell tumor cytoplasm and sometimes in the lumen of the tumor glands (Fig.3). In diffuse carcinoma MUC1 positive expression in the tumor cell was weak, but present in almost all of the tumor cells. In the most of intestinal carcinomas we were not able to find MUC5AC expression in tumor cell or they showed a very weak expression. The tumor cells of the two diffuse carcinomas were moderately positive for MUC5AC. MUC6 expression was weak or lacking. Seven intestinal carcinomas and one diffuse carcinoma were MUC2 positive. MUC2 was found only in tumor cell cytoplasm (Fig.4).

Discussion

In this study, we established an altered expression of the gastric mucins: MUC1, MUC5AC and MUC6 in gastric carcinoma. Our results showed that the process of neoplastic transforwmation in human stomach is associated with a decrease of some gastric mucins: MUC5AC and MUC6 and an aberrant expression of mucins normally expressed by the intestine (MUC2).

Adenocarcinomas of the stomach can be classified into two major types (5). The "intestinal" type is composed of distinct glands with polarized cells resembling colon carcinoma. The "diffuse" type is composed of solitary cells or small clusters of cells. The intestinal type of gastric cancer is the predominant type in elderly populations and is preceded by well-defined precancerous lesions, such as intestinal metaplasia and atrophic gastritis. We found expression of MUC2 in goblet cells in adjacent non-tumor gastric mucosa only in intestinal carcinoma. The most of intestinal carcinomas showed MUC2 positivity in tumor cells. These results support the assumption that the intestinal metaplasia does represent a differentiation of the mucosa toward an intestinal phenotype of gastric carcinoma.

The diffuse carcinoma is not preceded by precancerous lesions (8). It is suggests that MUC2 is not expressed in diffuse carcinomas. We observed MUC2 in one of the two diffuse carcinomas. In the two diffuse carcinomas we did not detect immunohistochemically MUC2 in non-tumor tissue. We considered that MUC2 synthesis in diffuse

carcinomas may be reflects an altered synthetic ability and as a result diverse mucin products may appear in tumor tissue.

We found an increased expression of MUC1 in tumor tissue of all gastric carcinoma. It was localized mainly in tumor cell cytoplasm in contrast to non-tumor tissue, where it was detected in the apical membrane and cytoplasm of parietal cells in fundic glands. MUC1 expression was very weak in antral mucosa. It has been reported that MUC1 molecule participates in cell-cell and cell-substratum interaction (10). It is also known that MUC1 acts as docking protein for some signaling molecules (4). Immunohistochemical studies in human gastric carcinoma have shown that over-expression on carcinoma cells plays a role in metastatic process by inhibiting tumor cell adhesion and in escaping from immune surveillance (1). Our results suggest that the over-expression of MUC1 may be regarded as one of the factors, which play a role in the malignant transformation of gastric epithelial cells.

We found a decreased expression of gastric mucins (MUC5AC and MUC6) in the both types of gastric carcinoma. Similar data were also described (9). The present study shows that expression of MUC5AC and MUC6 is not associated with the histological type of the gastric carcinomas.

In conclusion, our results suggest that there is a decreased expression of gastric mucin MUC5AC and MUC6 together with an abberant expression of MUC2 in intestinal metaplasia, during the process of gastric carcinogenesis. A high MUC1 level probably plays a role in appearance of neoplastic gastric epithelium. The mucin profile in tumor cells is not different in both types of gastric carcinoma.

References

1. Agrawal, B., B.M.Longenecker. MUC1mucin-mediated regulation of human T cells. – International Immunology 17, 2005, 391-399.
2. Babu, S.D., V. Venkataraman, N. Devaraj, C. A. Reis., H. Devaraj. Expression profile of mucins (MUC2, MUC5AC and MUC) in Helicobacter pylori infected pre-neoplastic and neoplastic human gastric epithelium. Molecular Cancer, **5,** 2006, 5-10.
3. Byrd, J., R.S. Bresalier. Alterations in gastric mucin synthesis by Helicobacter pylori. – World J. Gastroenterol., **4**, 2000, 475-482.
4. Huang, L, D. Chen, D. Liu, L. Yin, S. Kharbanda, D. Kufe. Muc1 oncoprotein blocks glycogen synthase kinase 3β-mediated phosphorulation and degradation of β-catenin. – Cencer Res. **65,** 2005, 10413-10422.
5. Lauren, P. The two histological main types of gastric carcinoma: diffuse and so-called intestinal type carcinoma.- Acta Pathol. Microbiol. Scandinavica, **64,** 1965, 31-49.
6. Li, X. H., H.C. Zhen, Z. G. Wang, H. Takahashi, X. H. Yang, Y. F. Guan, Y.Takano. The clinicopathological and prognostic significance of MUC-1 expression in Japanese gastric carcinoma: an immunohistochemical study of tissue microarrays. – Anticancer Res., **28,** 2008, 1061-1068.
7. Magalhäls, A., C.A.Reis. Helicobacter pylori adhesion to gastric epithelial cells in mediated by glycan receptors. – Brazillian J. Medical Biolog. Res. **43,** 2010, 611-618.
8. McGrath, S.C., M. Ebert, C. Röcken. Gastric carcinoma: Epidemiology, pathology and patogenesis. – Cancer Therapy **5,** 2007, 877-894.
9. Reis, C.A., L. David., F. Carvalho., U. Mandel., C. De Bolós., E. Mirgorodskaya., H.Clausen., M.S. Simőes. Immunohistochemical study of the expression of MUC6 mucin and co-expression of other secreted mucins (MUC5AC and MUC2) in hunan gastric carcinoma. – J.Histochem. Cytochem. **48,** 2000, 377-388.
10. Sasaki, M., H. Ikeda, Y. Nakanuva. Expression profiles of MUC mucins and trefoil factor family (TTF) peptide in the intrahepatic biliary system: physiological distribution and pathological significance. – Progress Histochem. Cytochem. – **42,** 20007, 61-110.
11. Szachnowicz, S., I. Cecconello., U. Ribeiro, K,Iriya., R.E.Ibrahim., F.R.Takeda., C.E.Corbett., A.V.S.Ribeiro. Mucin pattern reflects the origin of the adenocarcinoma in Barret's asophagus: a retrospective clinical and laboratorial study. – World J. Surg. Oncol. **7**, 2007, 7-27.

Institute of Experimental Morphology, Pathology and Anthropology with Museum
Bulgarian Anatomical Society

Acta morphologica et anthropologica, 19
Sofia • 2012

Influence of Metal Compounds on Viability and Proliferation of Rat Insulinoma Cells

T. Zhivkova, L. Dyakova, B. Andonova-Lilova, R. Kalfin*, A. Tolekova**, E.- M. Mosoarca***, R. Tudose***, O. Costisor***, R. Alexandrova*

Institute of Experimental Morphology, Pathology and Anthropology with Museum, Bulgarian Academy of Sciences, Acad. Georgi Bonchev Str., Block 25, Sofia 1113, Bulgaria;
**Institute of Neurobilogy, Bulgarian Academy of Sciences, Sofia 1113, Bulgaria;*
***Deaprtment of Physiology, Pathophysiology and Pharmacology, Medical Faculty, Trakia University, Stara Zagora, Bulgaria;*
****Institute of Chemistry Timisoara of the Romanian Academy, 24 Mihai Viteazu Blvd, RO-300223, Timisoara, Romania*

In the present study the influence of ammonium vanadate (0.01-20 μg/ml) and Cu(I,II)complexes with Mannich-bases N,N'-bis(4-antipyrylmethyl)-piperazine and N,N'-tetra-(antipyryl-1-methyl)-1,2-diaminoethane (1–200 μg/ml) on viability and proliferation of RIN-38 rat insulinoma cells was investigated. The experiments were carried out by thiazolyl blue tetrazolium bromide (MTT) test after 72 h of treatment. Some of the Cu(II) complexes – $Cu_2(BAMP)I_3$ (TS-2) and $Cu(TAMEN)(NO_3)_2$ (TS-17), did not express cytotoxic activity. Ammonium vanadate decreased in a time- and concentration- dependent manner the viability and proliferation of RIN-38 cells.

Key words: RIN-38 rat insulinoma cells, ammonium vanadate, copper(I,II) complexes, cytotoxicity, diabetes mellitus

Introduction

The lifestyle changes characteristic to the second half of the 20 century, have evoked diabetes mellitus (DM) epidemic which drastically impairs the quality of life and is the underling cause of many demises. To treat DM, which has many severe complications, several types of insulin preparations and synthetic drugs for Type 1 diabetes and Type 2 diabetes, respectively, have been developed and are in clinical use. However, there are several problems concerning the insulin preparations and synthetic drugs, such as physical and mental pain due to daily insulin injections and defects involving side effects, respectively. Consequently, a new class of therapeutic agents is anticipated [2, 3]. The idea of using metal ions for the treatment of diabetes originated in the late 19th century. A wide class of vanadium, copper and zinc complexes was demonstrated to be effective for treating diabetes in experimental animals [2, 3, 4, 6]. As a first step in our search for new metal compounds with antidiabetic properties in this study we present

data about the influence of ammonium vanadate and three newly synthesized Cu(I,II) complexes with Mannich-bases N,N'-bis(4-antipyrylmethyl)-piperazine (BAMP) and N,N'-tetra-(antipyryl-1-methyl)-1,2-diaminoethane (TAMEN) on viability and proliferation of RIN-38 rat insulinoma cells.

Materials and Methods

Chemicals and other materials. Dulbecco's modified Eagle's medium (DMEM) and fetal bovine serum (FBS) were purchased from Gibco-Invitrogen (UK). Dimethyl sulfoxide (DMSO), and trypsin were obtained from AppliChem (Germany); thiazolyl blue tetrazolium bromide (MTT) was from Sigma-Aldrich Chemie GmbH (Germany). All other chemicals of the highest purity commercially available were purchased from local agents and distributors. All sterile plastic and syringe filters were from Orange Scientific (Belgium).

Compounds. The experiments were performed with amonium vanadate (NH_4VO_3, Valerus) and three newly synthesized complexes of Cu(I, II) with Mannich-bases N,N'-bis(4-antipyrylmethyl)-piperazine (BAMP) and N,N'-tetra-(antipyryl-1-methyl)-1,2-diaminoethane (TAMEN) – $Cu_2(BAMP)(NCS)_4$ (TS-1), $Cu_2(BAMP)I_3$ (TS-2), $Cu(TAMEN)(NO_3)_2$ (TS-17). The compounds were obtained according to the previous work [5]. Ammonium vanadate (Valerus) was dissolved initially in bidistilled water, sterilized by filtration (diameter of pores 0.2 μm) and then diluted in culture medium. The concentration of the compound in the stock solution was 1 mg/ml. Copper complexes were initially dissolved in dimethylsulfoxide (DMSO, Serva) and then diluted in culture medium. The concentration of DMSO in the stock solution (where the concentration of the copper complex was 1 mg/ml) was 2 %.

Cell cultures and cultivation. The permanent rat insulinoma cell line RIN 38 (Cell Culture Collection, IEMPAM – BAS) was used as experimental model in our study. The cells were grown as monolayer cultures in DMEM medium, supplemented with 5-10% FBS, 100 U/mL penicillin and 100 g/mL streptomycin. The cultures were maintained at 37 °C in a humidified CO_2 incubator (Thermo scientific, Hepa class 100). For routine passages adherent cells were detached using a mixture of 0.05% trypsin and 0.02% EDTA. The experiments were performed during the exponential phase of cell growth.

Cytotoxicity assay. The cells were seeded in 96-well flat-botommed microplates at a concentration of 1×10^4 cells/well. After the cells were grown for 24 h to a subconfluent state (~ 60-70%), the cells from monolayers were washed with phosphate buffered saline (PBS, pH 7.2) and covered with media modified with solutions, containing different concentrations of the compounds tested: 0.01-20 μg/ml (for NH_4VO_3) and 1 – 200 μg/ml (for Cu complexes). Each solution was applied into 4 to 6 wells. Samples of cells grown in non-modified medium served as controls. After 72 h of incubation, the effect of the compounds on cell viability and proliferation was examined by thiazolyl blue tetrazolium bromide (MTT) test as described by Mossman [1]. The method consisted of three hours incubation with MTT solution (5 mg MTT in 10 mL D-MEM) at 37 °C under 5% carbon dioxide and 95% air, followed by extraction with a mixture of absolute ethanol and DMSO (1:1, vol/vol). Optical density was measured at 540/620 nm using an automatic microplate reader (TECAN, Sunrise™, Austria). Relative cell viability, expressed as a percentage of the untreated control (100% viability), was calculated for each concentration. Concentration–response curves were prepared. All data points represent an average of three independent assays.

Statistical analysis. The data are presented as mean ± standard error of the mean. Statistical analysis was performed using one-way analysis of variance (ANOVA) followed by Dunnett post-hoc test (GraphPad 5.00 program – La Jolla, CA, USA).

Results and Discussion

In our investigations the compounds tested were applied for 72 h at concentrations of 0.01, 0.05, 0.1, 0.5, 1, 5, 10, 20 μg/mL (for NH_4VO_3) and 1, 10, 20, 50, 100, 200 μg/ml (for Cu complexes with Mannich bases). The obtained data about viability/proliferation of the treated RIN 38 rat insulinoma cells are summarized in Figures 1 and 2.

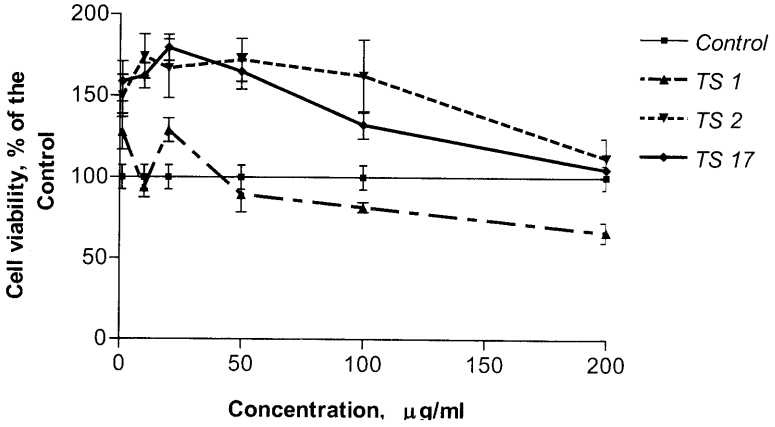

Fig. 1. Effect of Cu(I, II) complexes with Mannich-bases N,N'-bis(4-antipyrylmethyl)-piperazine (BAMP) and N,N'-tetra-(antipyryl-1-methyl)-1,2-diaminoethane (TA-MEN) on viability and proliferation of RIN-38 rat insulinoma cells. The compounds are applied at concentrations of 1, 10, 20, 50, 100, 200 for 72 h. The investigation was performed by MTT test. TS1 = $Cu_2(BAMP)(NCS)_4$; TS2 = $Cu_2(BAMP)I_3$; TS3 = $Cu(TAMEN)(NO_3)_2$ (TS-17).

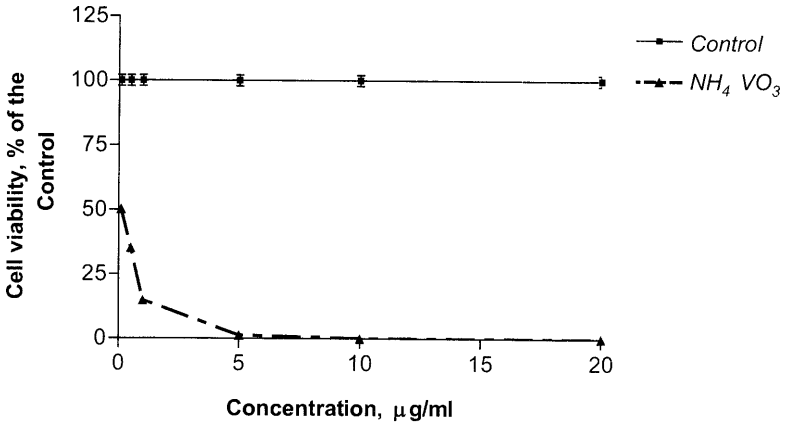

Fig. 2. Effect of ammonium vanadate on viability on viability and proliferation of RIN-38 rat insulinoma cells. NH_4VO_3 was applied at concentrations of 0.1 0.5, 1, 5, 10, 20 μg/mL for 72 h. The investigation was carried out by MTT test.

NH_4VO_3 was found to decrease in a time- and concentration- dependent manner the viability and proliferation of RIN-38 cells. Relatively higher survival rate was observed at concentrations $\leq$ 0.05 μg/ml ($\geq$ 75% viable cells, data not presented in Fig. 1). At the same time some of the Cu(II) complexes – $Cu_2(BAMP)I_3$ (TS-2) and $Cu(TAMEN)(NO_3)_2$ (TS-17), did not reduce the viability of the treated cells even when administered at concentrations of 100 and 200 μg/ml.

The permanent rat insulinoma cell line RIN-38, induced by high-dose X-ray irradiation, is one of the most widely used insulin-secreting cell lines and is appropriate for the development of new anti-diabetic strategies. Additional experiments are underway to examine the influence of the compounds tested (especially low toxic copper complexes) on insulin-secreting activity of these cells.

Acknowledgements: This study was supported by Grant DDVU-02-24/2010 from the National Science Fund, Sofia, Bulgaria; European Social Fund and Republic of Bulgaria, Operational Programme "Development of Human Resources" 2007-2013, Grant № BG051PO001-3.3.06-0048 from 04.10.2012.

References

1. Mosmann, T. Rapid colorimetric assay for cellular growth and survival: application to proliferation and cytotoxicity assays. – J. Immunol. Meth., **65**(1-2), 1983, 55-63.
2. Sakurai, H., A. Katoh, T. Kiss, T. Jakusch, M. Hattori. Metallo-allixinate complexes with anti-diabetic and anti-metabolic syndrome activities. – Metallomics., **2**, 2010, 670-82.
3. Sakurai, H., H. Yasui, Y. Adachi. The therapeutic potential of insulin-mimetic vanadium complexes. – Expert. Opin. Investig. Drugs. **12**, 2003, 1189-203.
4. Vanco, J., J. Marek, Z. Trávnícek, E. Racanská, J. Muselík, O. Svajlenová. Synthesis, structural characterization, antiradical and antidiabetic activities of copper(II) and zinc(II) Schiff base complexes derived from salicylaldehyde and beta-alanine. – J. Inorg. Biochem., **102**, 2008, 595-605.
5. Weinberger P., O. Costisor, R. Tudose, O. Baumgartner, W. Linert. A novel mixed valence copper(II)-Copper(I)-bis(antipyryl-methyl)-piperazine complex: synthesis, molecular structure and spectroscopic characterization. – J. Mol. Structure, **519**, 2000, 21-31.
6. Yasumatsu, N., Y. Yoshikawa, Y. Adachi, H. Sakurai. Antidiabetic copper(II)-picolinate: impact of the first transition metal in the metallopicolinate complexes. – Bioorg. Med. Chem., **15**, 2007, 4917-22.

Institute of Experimental Morphology, Pathology and Anthropology with Museum
Bulgarian Anatomical Society

Acta morphologica et anthropologica, 19
Sofia • 2012

Immunocytochemical Study of CB1 Receptors in Rat's Dorsal Striatum after Immobilization Stress

A. Bozhilova-Pastirova[1], K. Grancharska[2], N.Pencheva[2], B. Landzhov[1], Lina Malinova[1] and W. Ovtscharoff[1]

[1] Department of Anatomy and Histology, Medical University, Sofia 1407, Sofia, Bulgaria Prof. Anastasia Bozhilova-Pastirova
[2]Department of Kinesitherapy, South-West University, Blagoevgrad

The aim of this study was to examine the immunocytochemistry of the cannabinoid receptors CB1 in neuronal elements in the rat dorsal striatum after acute immobilization stress. First, CB1 immunoreactivity appeared as puncta and was found in neuronal cell bodies, axons and dendrites. Second, the morphometric analysis revealed that the density of CB1 receptors in neurons of the dorsal striatum increases in the acute immobilized rats comparing with control rats.

Key words: acute immobilization stress, CB1 receptors, dorsal striatum, rat

Introduction

Stress is defined as a state of threaten to homeostasis, evoking adaptive responses of the organism that can be specific or nonspecific to the stressor. The adaptive response are in response to the activation of specific circuits and is genetically programmed and permanently modulated by environmental factors [1, 2]. The adaptive responses in due to an acute stressor include the physiological and behavioral processes that are essential to reestablish homeostatic balance.

The immobilization stress causes variable physiological, behavioral and endocrine responses by activating motor, autonomic, and hypothalamic-pituitary-adrenal systems. The descending loop of the immobilization evoked stress pathway arises from cortical, limbic, hypothalamic, and some mesolimbic efferents, which activate motor and autonomic output system [2]. The basal ganglia are an important subcortical center for the integration and control of cognitive, motor and limbic processes. The striatum is the largest nucleus of the basal ganglia and receives associative, motor and limbic projections in territories segregated throughout its associative, sensorimotor and limbic extension [3]. The striatum is involved in the control of many aspects of stress and can influence motor response to stress [4].

One of the mechanisms known to play a part in the response of an organism to stress is activation of the endocannabinoid system [5, 6]. The endocannabinoid system

is a signalling system, comprising of the endogenous cannabis-like ligands anandamide and 2-arachidonoylglycerol, which bind to a family of G-protein-coupled receptors, called CB1 and CB2 [7]. On the other hand, the presence of CB1 receptors in stress-responsive neural circuits suggests that it may play a crucial role in regulating behavioral responses to stress [8].

Futhermore, in the light of the above data, the purpose of the present study was to examine the density of CB1 – immunoreactive neurons in the dorsal striatum of control and acute immuobilized rats.

Materials and methods

Animals: The experiments were carried out on male (n = 6) Wistar rats (180-200 g) kept under normal conditions at ambient room temperature (22°C). Each group (control and experimental) included three rats.

Acute model of immobilization stress: The animals were placed in a plastic tube with adjustable plaster tape on the outside so that the animals were unable to move 1 h. There were holes for breathing.

Immunocitochemistry: After the completion of the stress model, 24 hs later they were anaesthetized with Thiopental (40 mg/kg, i.p.). Transcardial perfusion was done with 4% parafomaldehyde in 0.1 M phosphate buffer, pH 7.2. The brains were removed from skulls and postfixed for 1 hour (h) in the same fixative at 4°C. Coronal sections were cut on a freezing microtom (Reichert-Jung) at 40 μm. Free-floating sections were preincubated for 1 h in 5% normal goat serum in PBS. Afterwards, incubation of the sections was performed in a solution of the primary antibody for 48 hs at room temperature. We used a polyclonal anti-CB1 antibody (, raised against the N-terminal, Santa Cruz, USA), in a dilution of 1:1000. Then sections were incubated with biotinylated anti-mouse IgG (dilution, 1:500) for 1 h and in a solution of avidin-biotin-peroxidase complex (Vectastain Elite ABC reagent; Vector Labs., Burlingame CA, USA; dilution 1:250) for 1 h. This step was followed by washing in PBS and then in 0.05 M Tris-HCl buffer, pH 7.6, which preceded incubation of sections in a solution of 0.05% 3,3′-diaminobenzidine (DAB, Sigma) containing 0.01% H_2O_2 for 10 min at room temperature for the visualization.

Morphometric analysis was performed by capturing images of) through a 40 objective using a microanalysis system Nikon photomicroscope ECLIPSE 80i (digital camera DXM 1200C and the measured area of 0.360185 mm^2). Data the entire drawings were entered in the computer program, recorded automatically, calculated and compared by Student's t-test. All values are presented as means ± standard error of the mean (S. E. M.).

Results and discussion

The staining patterns on coronal sections throughout the whole extension of dorsal striatum at levels of +2.2 to + 3.2 mm from bregma [9] were analyzed. The dorsal striatum in rodents (caudate – putamen) is not divided clearly into caudate and putamen and have a medial-lateral gradient of connectivity (ventromedial and dorsolateral), which is similar, but not identical to the connectivity in primates [10].

The principal findings were as follows. First, in the dorsal striatum there were numerous moderately stained CB1 immunoreactive neurons with punctated cytoplasm,

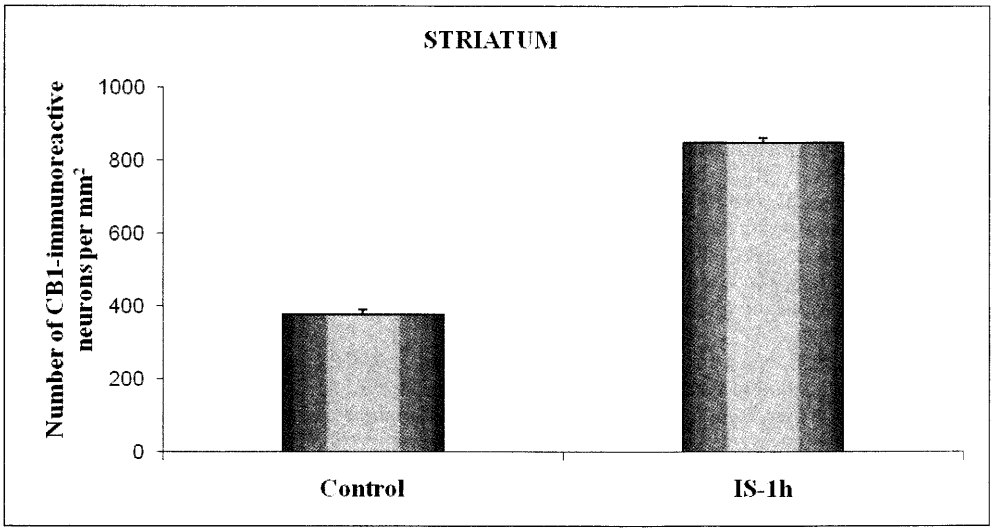

Fig. 1. The number of CB1-immunoreactive neurons in the dorsal striatum of control and acute immobilized rats (IS-1h), $P<0.01$. Values are presented as means ± S.E.M.

and unindented unstained nuclei. The distribution of the CB1-like immunoreactive neurons and neuronal elements generally coincided with that observed in previous studies that employed autoradiography. *in situ* hybridization and immunocytochemistry in CNS [11].

Second, in the dorsal striatum there was a lateral to medial density gradient and the lateral region being the more densely labeled. Third, our data provide the evidence about significant difference in the density of CB1 – immunoreactive neurons in the dorsal striatum between control and acute immobilized rats. Immubilized rats have greater density of CB1 – immunoreactive neurons than controls rats (Fig. 1). These results suggest that differences in the density of CB1-immunoreactive neurons in the immobilizes rat dorsal striatum can be related to the action of the stressers during the acute stages of immobilization [11].

Conclusion

In summary, our morphometric studies reveal differences in the number of CB1 – immunoreactive neurons in the rat dorsal striatum after acute immobilization. These new data may open the way to new studies in stress signalling in the dorsal striatum.

Acknowledgments: This work was supported by grant from Ministry of Education (*МОН НС"НИ" ДОО2-54/2008)*

Referenses

1. McEwen, B.S., L. Eiland, R G. Hunter, M.M. Miller. Stress and anxiety: structural plasticity and epigenetic regulation as a consequence of stress. – Neuropharmacology, 62, 2012, 3-12.

2. Pacák, K., M. Palkovits. Endocr Stressor specificity of central neuroendocrine responses: implications for stress-related disorders. – Rev., 22, 2001, 502-548.
3. McFarland, N.R., S. N Haber. Convergent inputs from thalamic motor nuclei and frontal cortical areas to the dorsal striatum in the primate. J. Neurosci. 20, 2000, 3798-3813.
4. Voorn, P., L. J. Vanderschuren, H. J. Groenewegen, T. W. Robbin, C. M. Pennartz. Putting a spin on the dorsal-ventral divide of the striatum. – Trends Neurosci., 27, 2004, 468-474.
5. McLaughlin, R. J., M. N. Hill, S S., Dang, S. R Wainwright, L. A. Galea, C. J. Hillard, B. B. Gorzalka. Upregulation of CB(1) receptor binding in the ventromedial prefrontal cortex promotes proactive stress-coping strategies following chronic stress exposure. -Behav Brain Res., 237C, 2012, 333-337.
6. Hill, M.N., B.S. McEwen. Involvement of the endocannabinoid system in the neurobehavioural effects of stress and glucocorticoids. – Prog. Neuropsychopharmacol. Biol. Psychiatry, 34, 2010, 791-797.
7. Pazos, M.R., E. Núñez, S. Benito, R. M. Tolón, J. Romero. Functional neuroanatomy of the endocannabinoid system. – Pharmacol. Biochem. Behav., 81, 2005, 239-247.
8. Ganon-Elazar, E., I. Akirav. Cannabinoids prevent the development of behavioral and endocrine alterations in a rat model of intense stress. – Neuropsychopharmacology, 37, 2012,456-466.
9. Paxinos, G., C. Watson. – In: The Rat Brain in Stereotaxic Coordinates (II Ed.), San Diego CA, 1986.
10. Voorn, P., L. J.Vanderschuren, H. J. Groenewegen, T.W.Robbins, C. M. Pennartz. Putting a spin on the dorsal-ventral divide of the striatum. – Trends Neurosci. 27, 2004, 468-474.
11. Tsou, K., B.S. Rown, M.C. Sañudo-Peña, K. Mackie, J.M. Walker. Immunohistochemical distribution of cannabinoid CB1 receptors in the rat central nervous system. Neurosci., 83, 1998, 393-411.

Institute of Experimental Morphology, Pathology and Anthropology with Museum
Bulgarian Anatomical Society

Acta morphologica et anthropologica, 19
Sofia • 2012

Interaction of Tyr-W-MIF-1 and Tyr-K-MIF-1 with in PAG with CB1-receptors during cold stress

L. Malinova[2], H. Nocheva[1], A. Bocheva[1], A. Bozhilova-Pastirova[2]

[1] Department of Pathophysiology, Medical University, Sofia
[2] Department of Anatomy and Histology, Medical University, Sofia 1407, Sofia, Bulgaria Prof. Anastasia Bozhilova-Pastirova

During an acute stress response, physiological processes are important to redirect energy utilization among various organs and selectively inhibit or stimulate various organ systems, or their components to mobilize energy reserves and to be prepared for exposure to additional, unpredictable challenges. Under stress conditions the hypothalamic-pituitary-adrenal (HPA) axis is stimulated. Exitation of opioid receptors within the PAG activates descending opioid inhibitory pathways and suppresses nociception. Tyr-W-MIF-1 and Tyr-K-MIF-1 are neuropeptides, neuromodulators, which are able to inhibit the expression of some forms of stress.

The aim of our study was to investigate the effects of Tyr-W-MIF-1 and Tyr-K-MIF-1 on CB 1 expression in PAG after cold stres in rats.

Introduction

The midbrain periaqueductal gray (PAG) is the cell group surrounding the midbrain aqueduct. Recent evidence suggests that the important functions which are associated with the PAG autonomic regulation and analgesia are integrated by longitudinal arranged columns of neurons (1, 3). The Tyr-MIF-1 family of peptides includes Tyr-W-MIF-1 and Tyr-K-MIF-1 are neuropeptides. Endogenous opioid peptides are substances which are produced in the body and its take part in the various functions as hormones or neuromodulators. These peptides can modulate pain and stress by antiopiate and mu-specific processes (4). The endogenous opioid peptides Tyr-W-MIF-1 and Tyr-K-MIF-1 belong to the Tyr-MIF-1 family of peptides and have been shown to be involved in a wide spectrum of physiological processes, including the development of stress (4). Literature data showed that members of Tyr-MIF-1 family are particularly attractive candidates for opiate modulators. Unlike the most other putative opiate-modulating peptides, they bind to the opiate receptors and to their own non-opiate sites. It is known that Tyr-K-MIF-1 showed little activity on opiate binding, while Tyr-W-MIF-1 acted as a mixed μ2-opioid receptor agonist and μ1-opioid receptor antagonist (2, 4, 5, 6, 7).

Material and methods

Acute model of cold stress: The animals were placed in a refrigerating chamber at 4° C for 1 h. The control group was not submitted to 1 h cold stress procedure.

Drugs and treatment: Tyr-W-MIF-1 and Tyr-K-MIF-1 (both in dose 1 mg/kg) were obtained from Sigma. The neuropeptides were dissolved in sterile saline (0.9% NaCl) solution and were injected intraperitoneally (i.p). After completion of the cold stress model the animals were injected with Tyr-W-MIF-1 or Tyr-K-MIF-1. 24 h later the animals were anaesthetized with Thiopental (40 mg/kg, i.p.) and perfused through the heart with fixative (4% paraformaldehyde in 0.1 M phosphate buffer, pH 7.2).Brains were removed and sectioned by a freezing microtome. Free-floating sections were preincubated for 1 h in 5% normal goat serum in PBS. Afterwards, incubation of the sections was performed in a solution of the primary antibody for 48 h at room temperature. We used a polyclonal antibody anti-CB1 antibody (Santa Cruz, USA) in dilution of 1:1000. Then the sections were incubated with biotinylated anti-mouse IgG (dilution, 1: 500) for 2 h and in a solution of avidin-biotin-peroxidase complex (Vectastain Elite ABC reagent; Vector Labs, Burlingame CA, USA; dilution 1:250) for 1 h. This step was followed by washing in PBS and then in 0.05M Tris-HCl buffer, pH 7.6, which preceded incubation of sections in a solution of 0.05% 3,30-diaminobenzidine (DAB, Sigma) containing 0.01% H_2O_2 for 10 min at room temperature for visualization. All procedures were approved by the Animal Care and Use Committee of the Medical University, Sofia.

Results and discussion

Our results showed that one-hour cold stress increases the expression of CB1-immunoreactive neurons in the periaqueductal grey compared with expression in intact animals. The results showed that after intraperitoneal treatment with Tyr-K-MIF-1 and Tyr-W-MIF-1 decreased the expression of CB1-immunoreactive neurons in the periaqueductal grey. In this investigation we have shown that changes in the expression of CB1 receptors are associated with cold stress. These findings correspond with several previous that the Tyr-W-MIF-1 and Tyr-K-MIF-1 exerted antiopioide effects under the different types of stresses (2, 5).

References

1. Bandler R, Shipley MT. Columnar organization in the midbrain periaqueductal gray: modules for emotional expression? Trends Neurosci 1994.17.379-389.
2. Bocheva A. I. , E. B. Dzambazova-Maximova. Effects of Tyr-MIF's family of peptides on immobilization stress-induced antinociception in rats. Folia Med. 2004;46.42-46.
3. Chrousos G. P. The role of stress and the hypothalamic-pituitary-adrenal axis in the pathogenesis of the metabolic syndrome: neuro-endocrine and target tissue-related causes. Int. J. Obes. Relat. Metab. Disord., 24, 2000, S50-5.
4. Kavaliers M. MIF-1 and Tyr-MIF-1 antagonize morphine and opioid but not non-opioid stress-induced analgesia in the snail, Cepaea nemoralis. Peptides, 8, 1987, 1–5.
5. Weihong P., A. J. Kastin. From MIF-1 to endomorphin: The Tyr-MIF-1 family of peptides. Peptides, 28, 2007, 2411-2434.
6. Zadina J.E., Kastin A.J., Krieg E.F., Coy D.H. Characterization of binding sites for N-Tyr-MIF-1 (Tyr-Pro-Leu-Gly-NH2) in rat brain. Pharmacol Biochem Behav., 1982, 17, 1193- 1198.
7. Zadina JE, Paul D, Gergen KA, Ge L-J, Hackler L, Kastin AJ. Binding of Tyr-W-MIF-1 (Tyr-Pro-Trp-Gly-NH2) and related peptides to μ1 and μ2 opiate receptors. Neurosci Lett., 215, 1996, 65-69.

Institute of Experimental Morphology, Pathology and Anthropology with Museum
Bulgarian Anatomical Society

Acta morphologica et anthropologica, 19
Sofia • 2012

Anthropology

Age Changes in the Topical Distribution of Subcutaneous Fat Tissue in Certain Body Parts and Areas in Adult Men Aged 20-50 Years

E. Andreenko

Plovdiv University "P. Hilendarski", Faculty of Biology,
Department of Human anatomy and physiology

The purpose of this study is to track the age changes in the topical distribution of SFT on some body parts and areas in adult men, aged 20-50 years. 801 clinically healthy men, aged 20-50 years, were the object of this study. Men are divided into six age groups, in 5-year intervals. The thickness of 9 SF of the body and limbs were measured with calipers. The topical distribution of SFT on certain body parts was evaluated basing on the five ratios according to formulas. The results showed that the thickness of SFT for the men of all age periods is greater on lower limbs than upper limbs, a greater torso, compared with the limbs, and greater in the lower torso in the compare with the upper torso.

Key words: skin folds, ratios, age, males.

Introduction

The quantity and topical distribution of subcutaneous fat tissue /SFT/ as characteristics of the physical development of individuals, and in particular, as characteristics of their body composition, are indicators that have an essential role in the etiology of obesity and a number of socially significant diseases [1, 2, 3]. The thickness of various skin folds help us to estimate the specificities of the "external" fat tissue and its changes under the influence of various external factors – physical activity, diet, health status, as well as the influence of age [4, 5, 6, 7, 8].

The purpose of this study is to track the age changes in the topical distribution of SFT on some body parts and areas in adult men, aged 20-50 years.

Material and Methods

801 clinically healthy men, aged 20-50 years, were the object of this study. Men are divided into six age groups, in 5-year intervals. The thickness of 9 SFs of the body and limbs were measured with calipers (subscapular SF, biceps SF, triceps SF, forearm SF, X rib SF, abdomen SF, suprailiac SF, thigh SF, and calf SF).

The topical distribution of SFT on certain body parts was evaluated basing on the following five ratios:

1. Ratio of SFT – *torso/limbs* through **4 SF** (by Rolland-Cachera et al., 1990)
(subscapular SF + suprailiac SF) / (triceps SF + biceps SF)

2. Ratio of SFT – *torso/limbs* through **6 SF** (by Malina-Bouchard 1988 and 1996);
(subscapular SF+ suprailiac SF + abdomen SF) / (triceps SF + biceps SF + calf SF)

3. Ratio of SFT – *upper/lower torso* through **4 SF** (by Malina-Bouchard 1988 and 1996);
(subscapular SF + X-rib SF) / (suprailiac SF + abdomen SF)

4. Ratios of SFT – *upper/lower limbs* (by Malina - Bouchard 1988 and 1996):
(1.First ratio) (triceps SF + biceps SF) / (thigh SF + calf SF)
(2. Second ratio) (triceps SF + forearm SF) / (thigh SF + calf SF)

The data were analyzed using SPSS statistical package. Reliability of intersexual and interage differences was checked by t-criterion of Student at the level of significance $P<0.05$.

Results and Discussion

1. RATIO OF SFT – ***TORSO/LIMBS*** through **4 SF** (Figure1).
The results show that throughout the period of research, from 20 to 50 years of age, the values of the ratio between SFT on the torso and limbs, calculated through 4 SFs, are over 1.00mm/mm, which means a greater accumulation of SFT on the body compared to limbs – a typical feature of adulthood. The tendency for a thicker layer of SFT on the body compared to that of limbs increases significantly after 30 years of age.

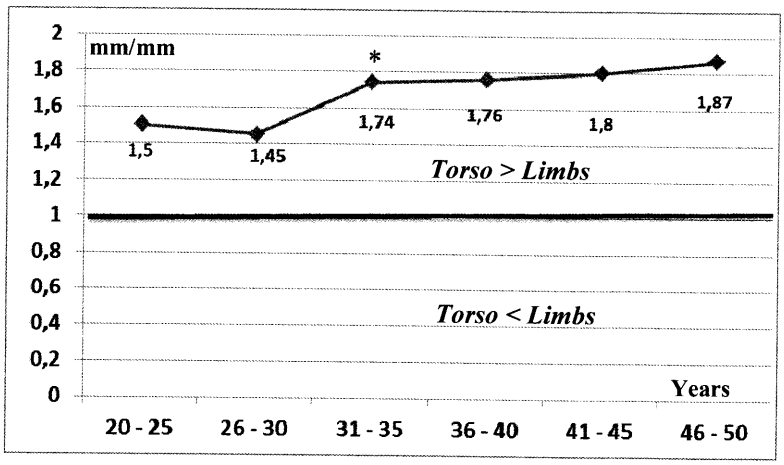

* statistical significance

Fig. 1. Ratio of SFT ***torso/limbs*** through **4 SF**

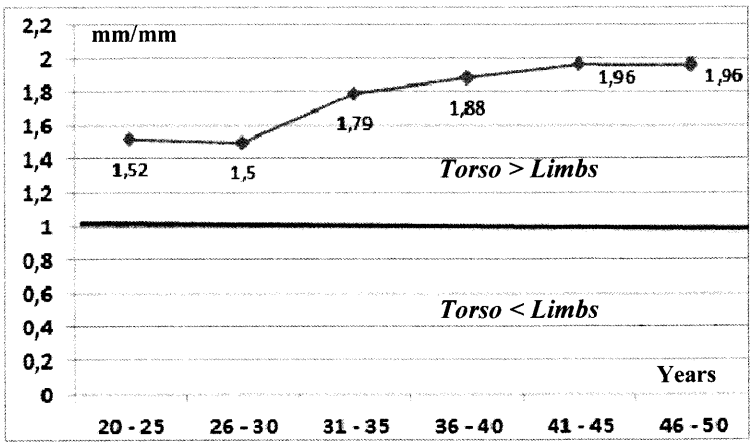

* statistical significance

Fig. 2. Ratio of SFT – ***torso/limbs*** through **6 SF**

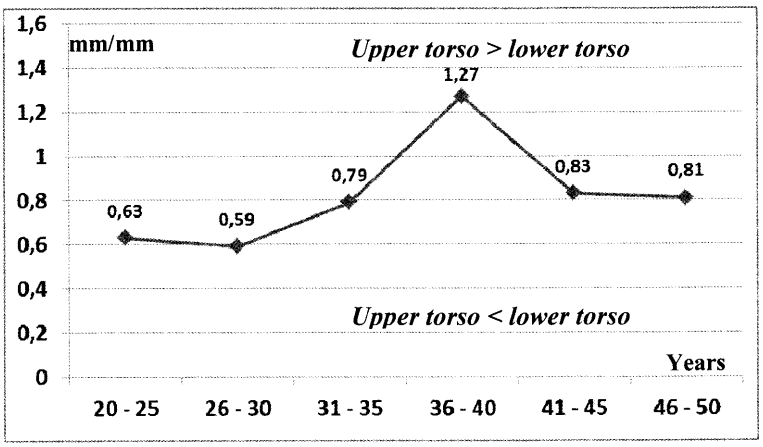

* statistical significance

Fig. 3. Ratio of SFT – ***upper/lower torso*** through **4 SF**

2. RATIO OF SFT – ***TORSO/LIMBS*** through **6 SF** (Figure 2).
The comparative analysis of the data, obtained for the ratio of SFT on the torso and limbs through 6 SFs, shows a similar result to that of the ratio torso/limbs through 4 SFs. Throughout the study period, the age curve is located above the level of 1.00 mm/mm and tends to increase with age advancing, which objectifies the greater increase of SFT on the torso than limbs.
3. RATIO OF SFT – ***UPPER/LOWER TORSO*** through **4 SF** (Figure 3).
The change in distribution of SFT on the upper and lower torso, with age advancing, in the men we studied was evaluated with the ratio of two chest SFs and 2 abdomen SFs. The results show proportionately thicker SFT in the abdomen area compared to the chest area, in the first half of the age period. Between 36-40 years, the accumulation

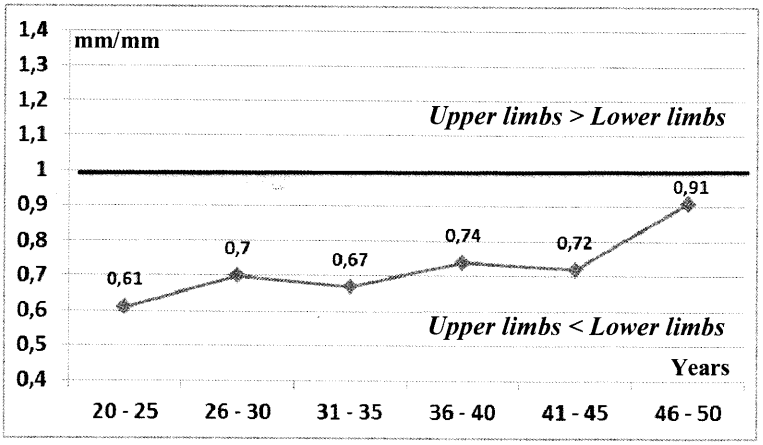

* statistical significance

Fig. 4. Ratio of SFT – ***upper/lower limbs*** **(1)**

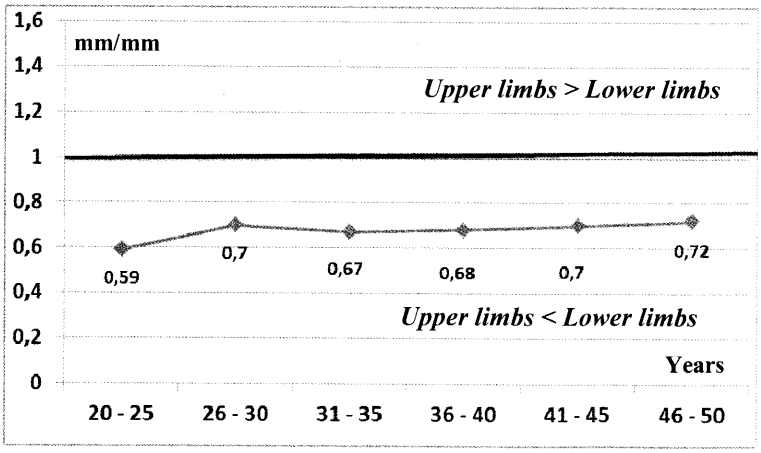

* statistical significance

Fig. 5. Ratio of SFT – ***upper/lower limbs*** **(2)**

of "external" fat tissue in the chest area significantly increases and exceeds that of the abdomen, leading to location of the curve over 1.00 mm/mm. In the second half of the age period, there is a redistribution of SFT, which is related to its reduction on the chest and its accumulation on the abdomen. The values of the ratio fall and they are below 1.00mm/mm but not reaching those from the beginning of the study.

4. RATIOS OF SFT – ***UPPER/LOWER LIMBS*** (Figure 4, Figure 5).

The results obtained in the two ratios show generally similar changes with age advancing, but there are some differences, too. In both ratios the values are below 1.00 mm/mm throughout the age period which shows a greater thickness of the SFT on lower limbs than upper. On the other hand, with the ratio [6, 7] from the beginning to the end of the age period of research, it seems to have a clear tendency of increasing values,

respectively proportional reduction of SFT on lower limbs, while with ratio [6, 8] there is a tendency to retaining and retention. The bigger number of statistically significant, interage differences that we found in ratio [6, 7] gives us reason to believe that it evaluates more accurately and objectively the topical distribution of SFT on upper and lower limbs in the men of the study.

Conclusions

1. Throughout the age period of research, from 20 to 50 years of age, there is a greater accumulation of SFT on the body compared to limbs, and after the age of 30, this trend grows significantly.

2. In the first half of the period of research, as well as at the end of it, there is a proportionately thicker layer of SFT on the abdomen, compared to that on the chest. A significant distribution of SFT on the trunk occurs in men aged 36-40 years. This is the period when there is an intense accumulation of "external" fat tissue on the chest area exceeding that on the abdomen.

3. For the men of all age periods, the thickness of SFT is greater on lower limbs than upper limbs, and there is a distinct trend towards topical redistribution with age advancing and progressive increase in the area of upper limbs.

References

1. Malina, R., C. Bouchard. Subcutaneous fat distribution during grow. – New York Plenum, 1988, 63-84..
2. Malina, R. Regional body composition: age, sex end ethnic variation. – Human Kinetics, 1996, 217-255
3. Rolland-Cachera, M, M. Sempte, M. Batail, E. Patois, F. Guggenbuhl, V. Fautrad. Adiposity indices in children. – Amer. J. Clin. Nutrition, 36, 1982, 178-184.
4. Te Velde S., J. Twisk, W. Mechelen, H. Kemper. Birth weight, adult body composition, and subcutaneous fat distribution. – Obes Res, 11, 2003, 202-208.
5. Tineshev. S. Estimating body composition in 18-year-old girls and boys through the method of bioelectrical impedance analysis. – Glasnik, ADS, 46, 2011, 67-72.
6. Митова, З. Антропологична характеристика на физическото развитие, телесния състав и телесната охраненост при 9-15 годишни деца и подрастващи от София. Автореферат дисерт. труд, 2009, София, 1-28.
7. Младенова С., Николова М., Д. Коджебашева. Развитие на подкожната мастна тъкан при деца и подрастващи от Смолянски регион. –Scientific research of the Union of scientists in Bulgaria-Plovdiv, Series C. Technics and technologies, Balkan Conference of Young Scientists, 16-18 June 2005, Plovdiv, 5, 2005, 248-256.
8. Младенова, С. Количество и разпределение на подкожната мастна тъкан в периода на растеж. – Сборник доклади от Международна научна конференция „Науката в условията на глобализацията през XXI век", Съюз на учените-Стара Загора, 1-2 юни 2006, 4, 2006, 68-74.

Institute of Experimental Morphology, Pathology and Anthropology with Museum
Bulgarian Anatomical Society

Acta morphologica et anthropologica, 19
Sofia • 2012

Assessment of Body Composition in 7-11-Year-Old Children from Smolyan (Bulgaria) throught Bioelectrical Impedance Analysis (Preliminary data)

S. Mladenova, I. Machokova

Plovdiv University „Paisii Hilendarski"– Branch Smolyan

The AIM of this work was to assess the age and gender variability of components of body composition in 7-11-year-old Smolyan children through bioelectrical impedance method. 362 children aged 7 to 11 years, of which 177 girls and 185 boys from Smolyan were the object of this study that measured transversally in the period January-May 2012 in four schools in the town of Smolyan. Children are divided into five age groups, and their average age was respectively 7.5, 8.5- to 11.5 years. The results of this study show that in the in body composition of the girls during the investigation period prevails absolute and relative quantity fats, as boys are characterized with bigger quantity free- fat mass quantity, i.e. with better skeletal - muscular development. In the two sexes the age changes at components of body composition were in relation with growth of levels of fat mass (FM) and free fat mass (FFM). The used bioelectrical impedance analysis is high-informational and reliable at population researches of assessment body composition and respectively for monitoring of deviations from normally physical development and body nurtitional status.

Key words: body composition, children, bioelectrical impedance analysis.

Introduction

It is known that the components of body composition are important and informative health indicators were used for monitoring of physical development and to diagnose deviations of normal nutritional status. For specialists one of the most important and disscussed problems was a question of the methods for accurate assessment of the quantities of body composition's components that can be used for diagnostic of deviations from normal physical development and particularly from normal nutritional status of the human body. Today in practice for assessment of body composition were used different methods, but one of the most advanced methods for population studies is the method of bioelectrical impedance analisys - BIA [1, 3, 5, 6, 7], became popular over the last decade. It is an objective, relatively accurate, noninvasive and easily applicable in practice evaluation method and fractionation of body composition.

The importance and relevance of studies related to body composition assessment in childhood for the monitoring of deviations in normal physical development and nutritional status defined the AIM of this work namely to assess the age and gender variability of components of body composition in 7-11-year-old Smolyan children through bioelectrical impedance method.

Material and methods

This work presents preliminary data from a study of the physical development of 362 children from Smolyan, aged 7 to 11 years, of which 177 girls and 185 boys. The study was performed transversally in the period January-May 2012 in four schools in the town of Smolyan. Children are divided into five age groups. For example, in the group of 8.5- year-olds included children aged 8.0 to 8.99 years. For convenience in analyzing the results of the age groups are given in integers. By Martin-Saler's method [4] of each person directly were measured two basic anthropometric indicators - height and weight. For assessment of body composition was used a two-component model of Behnke [2]. The relative values of body fat (% BF) were measured using bioelectrical impedance analysis (BIA) by body composition analyzer Tanita BC 453, an accuracy of 0.1%. Two main components of the body composition - fat mass (FM, kg) and and fat-free mass (FFM, kg) and the ratio between this two components (FM/FFM, kg) were calculated in addition. The collected data were processed using the statistical software package STATISTICA 6.0, by descriptive analysis. The differences between age and gender group were assessed by Student's t-test at significance level p= 0.05.

Results and discussion

The average values of the investigated indices in children of both sexes are shown in fig. 1-6.

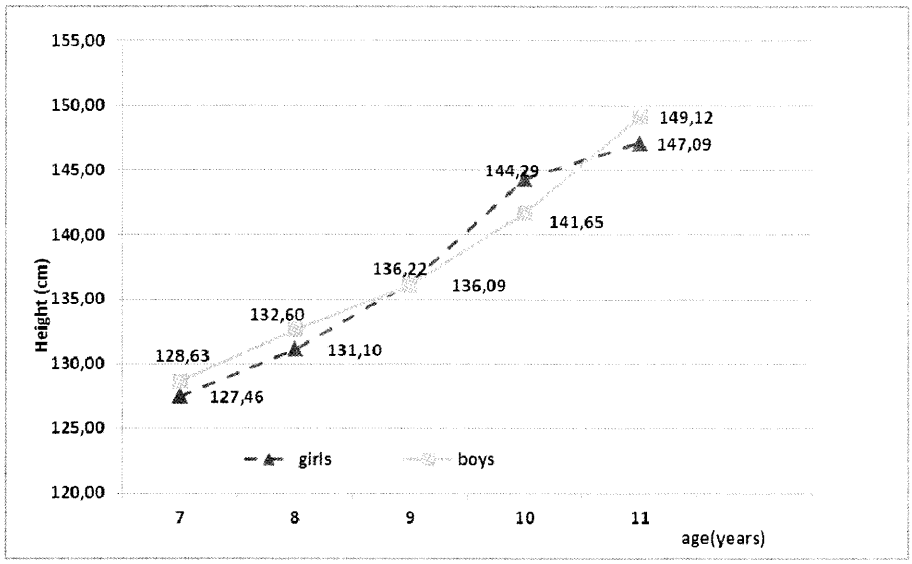

Fig. 1. Age and gender changes in the **height**

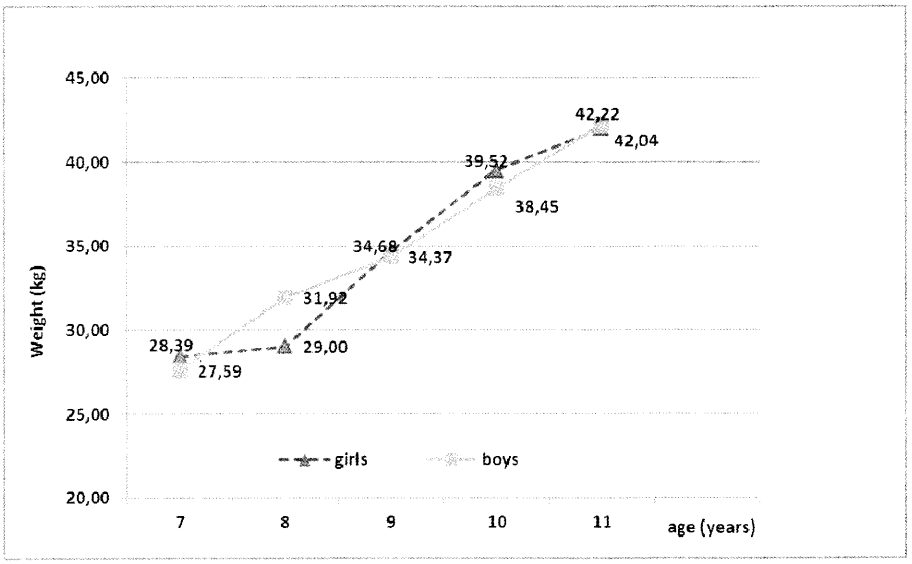

Fig. 2. Age and gender changes in the **weight**

Average **height** (Fig.1) of the contemporary generation of children in Smolyan during stidied period grows normally and continuously. The differences between separate age are statistically significant throughout the period ($p<0.05$). Differences between both sexes in this period are in boys` advantage, with exception of the 10th year of their life.

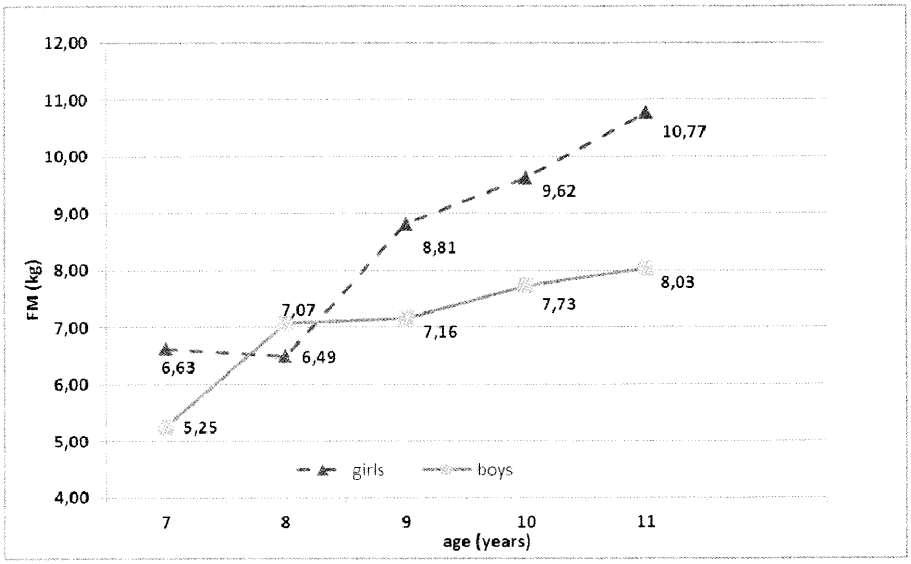

Fig. 3. Age and gender changes in **FM (kg)**

Similar results are show for **weight** (Fig.2). Significant increasing in the mean values observed in girls between 8-9th year (5.67 kg) and 9-10 years (4.84 kg) probably related to prepubertal growth acceleration. At boys statistically significant accumulation of body mass (4.2 кg) is seen between 7-8th and 9-10th year. The differences between sexes in body weight are non-significant and they are in girls` advantage. An exception is the 8th year which is probably connected with the simple.

One of the components of body composition with medical and biological importance is the relative part of the body fat. In our investigation for asses of % BF we used measuring of the bioelectrical impedance analysis. On the base of the relative values of BF are calculated absolute values of the body fat in kg i.e. fat mass (FM).

The **fat mass** (Fig.3) at the girls through the seen start school period grows general and middle with 4.14 kg, but at the boys- with 2.78 kg. Maximum accumulation of body fats in girls is seen between 8-9th year (2.32 кg), but in boys-between 7-8ht year (1.81 кg). The differences between sexes show predominating absolute part of body mass at girls, with exception of 8th year as reliable are differences only between 9th years old children ($p<0.05$).

Average values of other basic components of body composition, i.e. **fat-free mass (FFM)** (Fig.4) at boys are grown generally with 11.3 kg through the whole period. Maximum year accumulation of FFM at them is seen between 8-9th year (3.85 кg), but statistically significant interage differences in whole the period, with exception of 10-11th year. At girls accumulation of FFM is done with slow temps as general increasing for this period is 9.4 kg.

The data from our study for the two body components - fat mass and fat-free mass, are similar to the results for Sofia children [7, 8], independently of different method for assessment of body fat % - Slaughter equations used from Mitova [7] and BIA (Tanita) used in present study.

Through the observed age period changes in **boys body composition** (Fig. 5) mainly due to accumulation of active body mass, and very small extent of fat mass

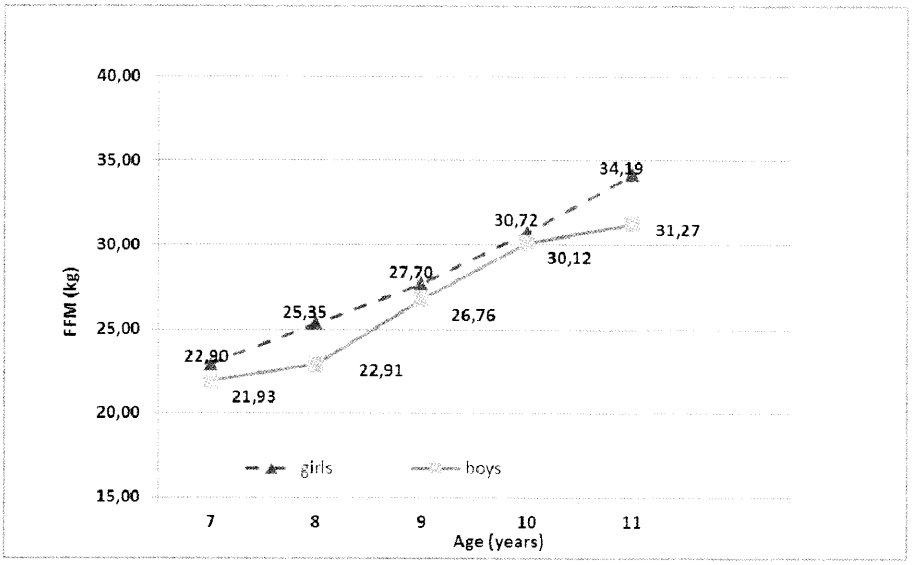

Fig. 4. Age and gender changes in **FFM (kg)**

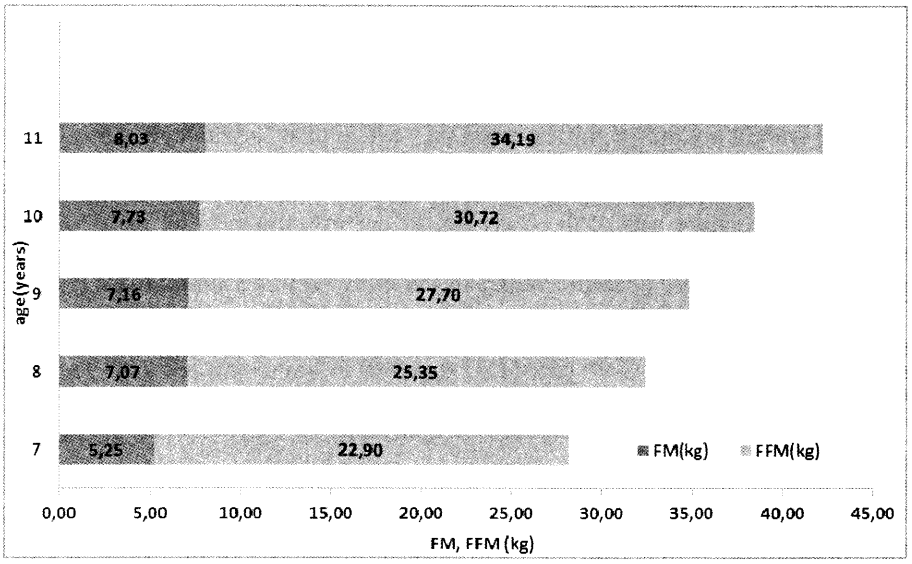

Fig. 5. Age changes in body composition **in boys**

(FM) as well. At girls, age changes in body composition (Fig.6) due to increase in lean, and fat component as well, especially after 8th year.

Another informative indicator is the ratio showing the distribution of body fat mass for a kilogram fat-free mass (BF/FFM, kg). The results of this ration showed that during the investigated period, girls put on bigger absolute amount of body fat mass for a kilogram fat–free mass than boys, with an exception of the 8th year. In intersexual plan

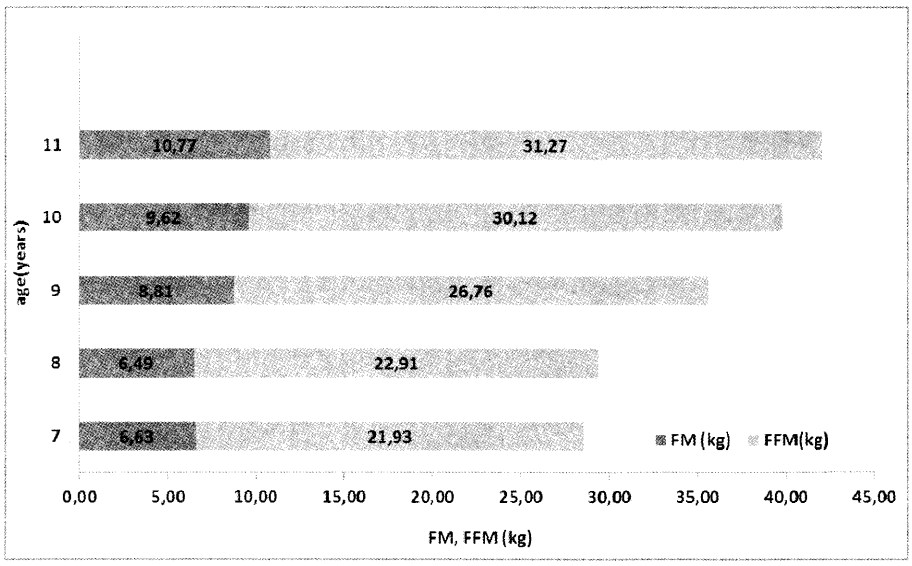

Fig. 6. Age changes in body composition **in girls**

the biggest differences are during the 11th year, when girls put on 1.1 kg amount of fat mass in a kilogram fat free mass (FFM) more than boys do.

In conclusion used bioelectrical impedance analysis is high-informational and reliable for population researches and assesment of body composition and respectively for monitoring of deviations from normally physical development and body nurtitional status.

References

1. Andreenko, E., M. Nikolova. Bioelectrical impedance analysis assessment of body composition of children and adolescents from Plovdiv (Bulgaria). – Glasnik, ADS, **46,** 2011, 59-65.
2. Behnke A. R. Anthropometric evaluation of body composition trough life. – Ann. N.Y. Acad. Sci., **110,** 1963, 450-464.
3. Khomyakova, I., E. Godina, L. Zadoroghnaya, A. Tretyak, E. Dorogova. Body composition in children and its Relationship with Sexual Maturation Level. – Acta Morph. et anthrop., **15**, 2010, 194-198.
4. Martin, R., K. Saller. Lehrbuch der Anthropologie. – Stuttgart, Custav Fisher Verlag, 1, 1957, 661.
5. Tineshev, S. Estimating body composition in 18-year-old girls and boys through the method of bioelectrical impedance analysis. – Glasnik, ADS, **46**, 2011, 67-72.
6. Topuzov, I., Z. Mitova, E. Kavdanski, N. Petrova, D. Dencheva (2002): Assessment of the obesity by means of the body and fat mass. - *Kineziterapy,* Sofia, **2**, 2002, 18-24.
7. Митова, З. Антропологична характеристика на физическото развитие, телесния състав и телесната охраненост при 9-15 годишни деца и подрастващи от София. – Автореф. на дис., София, 2009, 1-32.
8. Начева, Ан., Я. Жечева, Ив. Янкова, Зл. Филчева, З. Митова и Й. Йорданов Физическо развитие на деца и подрастващи в България на границата между XX и XXI век / Под ред. на Й. Йорданов/. – Изд. "Марин Дринов", 2012, София.

Institute of Experimental Morphology, Pathology and Anthropology with Museum
Bulgarian Anatomical Society

Acta morphologica et anthropologica, 19
Sofia • 2012

Nutritional Status in 9-15-years-old Schoolchildren from Sofia, Bulgaria /1984-2002/

Z. Mitova, R. Stoev, L. Yordanova

Institute of Experimental Morphology, Pathology and Anthropology with Museum, Bulgarian Academy of Sciences, Sofia

The aim of this paper is to identify trends in the frequency distribution of underweight (I+II+III degrees), normal nutritional status and overweight (incl. obesity) in children and adolescents from Sofia, tested in 1984/1987 in comparison with those of their peers in 2001/2002 year. As a result, in the beginning of 21st century among all boys the incidence and prevalence of underweight and that of overweight increases, whereas the frequency of normal nutritional status decreases. In girls, there are two trends – the same as in boys before puberty (age 9-10) and in those aged over 11 only the incidence of underweight increasesq especially in 14 and 15 years. The results in boys and in girls before puberty are similar to these observed in other Eastern European countries in recent pereiod.

Key words: Nutritional status, adolescents, children, underweight, overweight.

Introduction

One of the most discussed issues in auxology is the assessment of nutritional status (NS) in children and adolescents in population studies. In recent decades, for this purpose the most commonly used mean is body mass index (BMI). It has established national and ethnic differences. This requires the creation of both international standards and relevant national norms. Recently the most popular method for constructing normalized growth standards in anthropological and medical practices is the LMS method. On the basis of this method a set of cut-off point of BMI has been established to determine the type of NS in children, adolescents and adults – underweight, overweight and obesity [2, 3].

In Bulgaria there are not national standards of physical development from nearly 30 years. Data on the frequency distribution of different types of NS in children and adolescents are few and part of them relate to areas outside the capital of Bulgaria [5, 9], which led us to formulate the purpose of this communication, including:

The aim of this paper is to identify trends in the frequency distribution of underweight (I+II+III degrees), normal nutritional status and overweight (incl. obesity) in children and adolescents from Sofia, tested in 1984/1987 in comparison with those of their peers in 2001/2002 year.

Materials and methods

Data from two cross-sectional anthropometric studies of 9-15-year-olds schoolchildren in Sofia have been analyzed [7, 8]. The studies were conducted in 1984/1987 and in 2001/2002. The first study included 405 boys and 421 girls, and the second one – 569 boys and 573 girls, divided fairly evenly in one-year age groups. By standard anthropometric methods for each student are measured body height and body weight, additionally has been calculated body mass index (BMI=body weight$_{(kg)}$/body height$^2_{(m)}$). The distribution of students in the categories of NS is made after Cole et al. [2, 3]. Reliability of differences in BMI of boys and girls from the two surveys by age groups was determined by Student's t – test, and the differences in the frequency of students from two studies in each category NS (separately for both sexes) – respectively by χ^2 test.

Results and discussion

The results of the categorization of students in both studies present that with the exception of 9-year-old boys and 13-year-old girls underweight is more common in students surveyed in 2001/2002 (Tabl. 1). From the beginning to the end of the investigated age period there is a incresing trend of underweight by age, which at age 15 reaches ~ 20.0% in both sexes. This is significantly higher than in 1984/1987, when the highest incidence of underweight was in age of 13 – 10.0% of boys and 16.0% in girls. As for the category of overweight it was found that in most age groups of boys the incidence of overweight and obesity increased while in girls after age 11 it seems to exist an opposite trend – a decrease of its frequency by age, particularly sharp at 14 and 15 years.

As a result, in the beginning of 21st century among all boys the incidence and prevalence of underweight and that of overweight increases, whereas the frequency of normal NS decreases.

In girls, there are two trends. In the age of 9 and 10, ie in infantile and prepubertal stages of development, there is a simultaneous increase in the number of underweight girls and those with abnormal body feed (like boys). From 11 years onwards, however, only the incidence of underweight increases. Obviously the differences in distribution of NS types in girls before and after the onset of puberty are sexual related (whether biologically or genderly is another matter). By overlaying the two opposing tendencies in girls produce a rise in the frequency of individuals with underweight and reduction of this of overweight and obesity, and to virtually the same proportion of girls with normal NS (Fig. 1). As a final result, the differences between the general samples of girls surveyed in the 1980s, and in 2001/2002 are lower than for boys. There is a reduction in the number of subjects with normal body feed and increase of individuals with underweight and overweight in boys at all, and in girls before puberty. We believe that the above increase in the proportion of subjects with deviant NS may be due to the increased social differentiation during the transition period in Bulgaria, whose existence is not in doubt. A similar phenomenon has been observed in other countries of Eastern Europe [1, 4]. The increased expression of this phenomenon in boys may be related to the greater sensitivity of the male body to the factors of the social environment, long celebrated in the writings of many well known authors [6]. Regarding the absence of such a phenomenon in girls during and especially after puberty could be related with socio-cultural changes during this period, such as the widespread use of irrational nutrition, the reduced motor activity, the application of different diets among students and others.

Table 1. Distribution of the investigated schoolchildren into nutritional status categories.

Age (yrs)	N	Underweight		Normal		Overweight+Obesity	
		n	%	n	%	n	%
BOYS (1984/1987)							
9	30	2	6.7	24	80.0	4	13.3
10	54	4	7.4	39	72.2	11	20.4
11	84	7	8.3	66	78.6	11	13.1
12	72	6	8.3	53	73.6	13	18.1
13	69	7	10.1	55	79.7	7	10.1
14	60	1	1.7	52	86.7	7	11.7
15	36	2	5.6	29	80.6	5	13.9
GIRLS (1984/1987)							
9	34	1	2.9	29	85.3	4	11.8
10	66	7	10.6	50	75.8	9	13.6
11	65	5	7.7	50	76.9	10	15.4
12	58	8	13.8	40	69.0	10	17.2
13	86	14	16.3	58	67.4	14	16.3
14	49	4	8.2	31	63.3	14	28.6
15	63	6	9.5	50	79.4	7	11.1
BOYS (2001/2002)							
Age (yrs)	N	Underweight		Normal		Overweight+Obesity	
		n	%	n	%	n	%
9	81	2	2.5	64	79.0	15	18.5
10	79	11	13.9	57	72.2	11	13.9
11	82	9	11.0	54	65.9	19	23.2
12	83	10	12.0	59	71.1	14	16.9
13	76	12	15.8	52	68.4	12	15.8
14	83	14	16.9	54	65.1	15	18.1
15	80	16	20.0	56	70.0	8	10.0
GIRLS (2001/2002)							
9	81	7	8.6	59	72.8	15	18.5
10	80	11	13.8	51	63.8	18	22.5
11	80	8	10.0	60	75.0	12	15.0
12	85	13	15.3	64	75.3	8	9.4
13	83	9	10.8	63	75.9	11	13.3
14	82	14	17.1	58	70.7	10	12.2
15	82	17	20.7	64	78.0	1	1.2

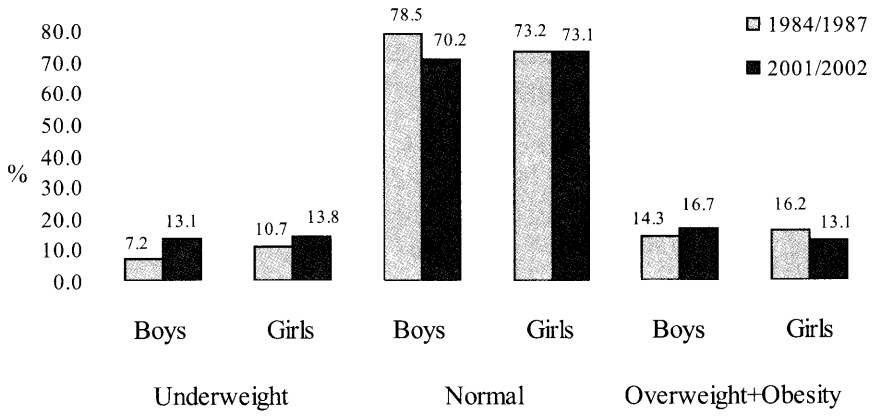

Figure 1. Frequency of the schoolchildren into nutritional status categories.

Conclusion

In the beginning of 21st century among all boys the incidence and prevalence of underweight and that of overweight increases, whereas the frequency of normal nutritional status decreases. In girls, there are two trends – the same as in boys before puberty (age 9-10) and in those aged over 11 only the incidence of underweight increasesq especially in 14 and 15 years.

The results of this paper outline a social problem in Bulgaria which has been neglected until now due to the fact that the focus of researchers, institutions and the public interest lies mostly in overweight and obesity. It confirms the need of further research, which will provide to relevant national standards for NS in the young generation of Bulgaria.

References

1. Bodzar, E., A. Zsakai, K. Tausz. The biological status of children living in disadvantaged micro-region of Hungary. – 18th Congress of EAA, Abstracts, Ankara, 2012, 73.
2. Cole T, M. Bellizzi, K. Flegal, W. Dietz. Establishing a standard definition for child overweight and obesity: international survey. – BMJ, **320**, 2000, 1240-1243.
3. Cole T., K. Flegal, D. Nicholls, A. Jackson. Body mass index cut offs to define thinness in children and adolescents: international survey. – BMJ, **335,** 2007, 194-201.
4. Lewandowska, J., H. Piechaczek, K. Busko, E. Kalka. Trends in the body fatness and nutritional status of Polish students of Warsaw Technical University over the period 1959 -2011. – 18th Congress of EAA, Abstracts, Ankara, 2012, 86.
5. Nikolova, M., E. Godina, D. Mollova. A comparison of Plovdiv and Moskow children's height, weight and BMI values. – Acta morph. et anthrop., **15,** 2010, 212-216.
6. Wolanski, N. Rozwoj biologiczny czlowieka. – Warszawa, PWN, 1985, 1-708.
7. Митова, З. Антропологична характеристика на физическото развитие, телесния състав и телесната охраненост при 9 – 15 годишни деца и подрастващи от София. – Дис., София, 2009, 1-225.
8. Стоев, Р. Антропологична характеристика на подрастващи – физическо развитие и полово съзряване във връзка със семейно-битовата среда. – Дис., София, 2007, 1-177.
9. Тинешев, Сл. Антропологична характеристика на деца и подрастващи. – Дис., Пловдив, 2009, 1-325.

Institute of Experimental Morphology, Pathology and Anthropology with Museum
Bulgarian Anatomical Society

Acta morphologica et anthropologica, 19
Sofia • 2012

Frequency of metopic suture in male and female medieval cranial series

Silviya Nikolova, Diana Toneva

Institute of Experimental Morphology, Pathology and Anthropology with Museum, Bulgarian Academy of Sciences, Sofia,

Each half of the adult frontal bone begins to ossify from a single centre. At birth, the frontal bone is composed of two symmetrical halves, which are separated from each other by the metopic suture. This suture normally closes between the 1st and 2nd year of life and is usually completely fused by the 3rd year, but it can remain patent to the 7th year. A major anomaly is the failure of the two halves to fuse during infancy or in early childhood, a condition known as a metopism or metopic suture. In the present study, an attempt is made to study, compare and assess the sexual differences of metopic suture in male and female medieval cranial series. A total of 318 crania of adult individuals from both sexes are investigated. It is established that metopism is more frequent among the female cranial series compared to the male one.

Key words: metopic suture, cranial series, sexual differences

Introduction

The adult frontal bone is an irregular, bowl-shaped bone. Each half of the frontal bone begins to ossify from a single centre, which appears in membrane between 6 and 7 weeks during the fetal life. At birth, the frontal bone is composed of two symmetrical halves, which are separated from each other by the metopic or frontal suture [9].

Metopic suture is a kind of dentate suture [1], which runs between the frontal bones of the fetus, from the ventral part of the anterior fontanelle to the *nasion*. It is considered to be an anterior extension of the sagittal suture. This suture normally closes between the 1st and 2nd year of life and is usually completely fused by the 3rd year, but it can remain patent to the 7th year [10]. The condition, in which the suture is complete and extends from *nasion* to *bregma* is usually referred to as metopism. Remnant of any part of the suture remaining after the age of about 2 years is usually called a sutura metopica persistens [9]. If the suture is not present throughout and occupies a small area between *nasion* and *bregma*, it is considered as an incomplete metopic suture. It is also called a median frontal suture and usually present between the two superciliary arches [7].

It has been reported by various workers that the incidences of metopism and metopic suture vary in different populations. The frequency may range from 1% to 12% and the incidence is slightly higher in the male population [10].

It is essential to know about metopism and metopic suture, because they can be easily misdiagnosed as vertical traumatic skull fractures extending in the mid-line in head injury patients or even for the sagittal suture in antero-posterior radiological images. It is also important for paleodemography and forensic medicine [2, 5]. In the present study, an attempt is made to study, compare and assess the sexual differences in frequency of metopic suture in male and female medieval cranial series.

Materials and methods

A total of 318 crania (159 males and 159 females) are investigated. All crania belonged to adult individuals from both sexes. The both cranial series consist of medieval bone material from the IEMPAM, BAS collection. Both the sex and age of the individuals are previously determinate by the metrical and scopical features of the crania and postcranial skeletons [6, 12, 13].

The metopic suture presence and appearance towards its length are assessed according to Movsesyan et al. [14] by the following codes (0-3): 0 – absence of metopic suture; 1 – remnant of metopic suture with length approximately about $^1/_3$ of the whole suture length; 2 – remnant of metopic suture with length approximately about $^1/_2$ of the whole suture length; 3 – metopism or metopic suture extending from *nasion* to *bregma*.

Statistical significance of the sexual differences is assessed by chi-squared test (χ^2-test) at $p < 0,05$.

Results and Discussion

A major anomaly of the frontal bone is the failure of the two halves to fuse in the midline during infancy or in early childhood [9], a condition known as a metopism or metopic suture.

Among the investigated medieval female series metopic suture extending from *nasion* to *bregma* is established in 10,1 % (table 1). Nevertheless, remnant of metopic suture with approximately about $^1/_3$ of the whole suture length, is established in only one case (0,6 %). The frequency of metopism among the medieval male cranial series (table 1) is lower (8,2 %) compared to female one. However, in male series there are not established cases of metopic suture remnants. These data are in accordance with other researcher results for incidence of metopic suture in Europeans, which range between 7 – 10 % [3, 4, 8].

Table 1. Frequency of metopic suture among the investigated medieval male and female cranial series.

Metopic suture	**Medieval female cranial series**		**Medieval male cranial series**	
	n	**%**	**n**	**%**
Absence (0)	142	89,31	146	91,82
Remnant with approximately length about 1/3 of the whole suture length (1)	1	0,63	0	0,00
Remnant with approximately length about 1/2 of the whole suture length (2)	0	0,00	0	0,00
Metopism (3)	16	10,06	13	8,18
Total	159	100,00	159	100,00

The comparison between both series shows that metopism is more frequent among the female series compared to male one, but the difference is not statistically significant. Furthermore, remnants of metopic suture are established only among the female series. Tavassoli [11] mentioned the fact that metopism appears more frequently among women than men and it is more prevalent in medieval times than today. The author believed that this is result of disorder in the ossification process due to the action of some biochemical factor, most probably a lack of calcium, which is related with malnutrition amongst women who have become pregnant and have given birth immaturely. Because of this, Tavassoli [11] believed that metopism is not merely an interesting morphological fact, or even a racial or genetic characteristic, but it is an indicator of a definite ossification and biochemical disorders, which are consequence of malnutrition due to intrinsic or extrinsic factors.

Conclusion

In summary, metopism is established with different frequency in both investigated medieval cranial series, but is more frequent among the female series compared to male one. Remnants of metopic suture are rare findings and are established only in female series.

Reference

1. Ajmani, M. L., R. K. Mittal, S. P. Jain. Incidence of the metopic suture in adult Nigerian skulls. – J. Anat., **137(1)**, 1983, 177-183.
2. Bademci, G., T. Kendi, F. Agalar. Persistent metopic suture can mimic de skull fractures in the emergency setting? – Neurocirugía, **18**, 2007, 238-240.
3. Breathnach, A. S. Frazer's Anatomy of the Human Skeleton. London, Churchill, 1958, 5th ed.
4. Bryce, T. H. Osteology and Arthrology. – In: Quain's Elements of Anatomy. 11th ed., London, Longmans Green, 1915, vol. 4, pt. I, p. 177.
5. Chakravarthi, K. K., N. Venumadhav. Morphological study of Metopic suture in adult South Indian skulls. – Int J Med Health Sci., **1(2)**, 2012, 23-28.
6. Martin R., K. Saller. Lehrbuch der anthropologie in sistematischer darstellung, I, Stuttgart, Gustav Fisher Verlag, 1957.
7. Murlimanju, B.V., L. V. Prabhu, M. M. Pai, A. A. Goveas, K. V. N. Dhananjaya, M S. Somesh. Median Frontal Sutures – Incidence, Morphology and Their Surgical, Radiological Importance. – Turkish Neurosurgery, **21(4)**, 2011, 489-493.
8. Romanes, G. J. Cunningham's Textbook ofAnatomy. London, Oxford University Press, 1972, 11th ed., p. 133.
9. Scheuer, L., S. Black. Developmental Juvenile Osteology. London, Academic Press, 2000, 587 pp.
10. Skrzat, J., J. Walocha, J. Zawilinski. A note on the morphology of the metopic suture in the human skull. – Folia Morphol., **63**, 2004, 481–84.
11. Tavassoli, M. M. Metopism: As an Indicator of Cranial Pathology; A Good Example from Iranian Plateau. – Acta Medica Iranica. **49(6)**, 2011, 331-335.
12. Алексеев, В.П. Остеометрия. – Москва, Наука,1966.
13. Алексеев, В.П., Г.Ф. Дебец. Краниометрия. – Москва, Наука,1964.
14. Мовсесян, А., Н. Мамонова, Ю. Рычков. Программа и методика исследования аномалий черепа. – Вопросы антропологии, **51**, 1975, 127-150.

Institute of Experimental Morphology, Pathology and Anthropology with Museum
Bulgarian Anatomical Society

Acta morphologica et anthropologica, 19
Sofia • 2012

Case of pott's disease in recently investigated middle age series

Victoria Russeva

Institute of Experimental Morphology, Pathology and Anthropology with Museum, Bulgarian Academy of Sciences

Find from skeleton found in grave B 50-1, necropolis N 3, Zlatna livada, IX-X c. AD, male, 40-50 years at death, is analyzed. On T 11 - T 12 is ascertained a pathological change, result of Pott's disease, most characteristic marker for tuberculosis infection on spinal cord. Find appears as a confirmation of presence of this infection in studied population, which is not a unique case for Bulgarian middle-age series.

Lytic changes on human skeletal remains are registered in many paleoanthropological series, providing information of development of bacterial-fungal infections in past populations [5, 10]. Pott's disease appears as most advanced form in development of lytic changes in vertebral column and these changes are emphasized as characteristic marker for presence of tuberculosis infection of individual and respectively, dissemination of this disease in population [10].

Key words: necropolis N 3, Zlatna livada, Middle Age, tuberculosis

Material and Methods

Recently investigated middle age series provided finds of vertebra with specific lytic changes, characteristic for developed Pott's disease. Skeleton from grave B 50-1, necropolis N 3, near village of Zlatna livada (Table 1), excavated in the season 2011, dated

Table 1. Available material, preservation. L – left; R – right

Bone	preservation	Bone		preservation	Bone		preservation
Cranial voult	fragmentary	Scapula	R	fragments	Pelvis	R	fragments
Face	fragmentary		L	fragments		L	fragments
Dentition	fragmentary	Clavicle	R	complete	Femur	R	fragments
Cervical vertebrae	5		L	complete		L	fragments
Thoracic vertebrae	complete	Humerus	R	complete	Tibia	R	none
Lumbar vertebrae	4		L	complete		L	complete
Ribs	fragments	Radius	R	complete	Fibula	R	none
Sternum	fragments		L	complete		L	fragments
Sacrum	fragments	Ulna	R	complete	T, MT, F	R	none
			L	complete		L	
		C, MC, F	R	P			
			L	P			

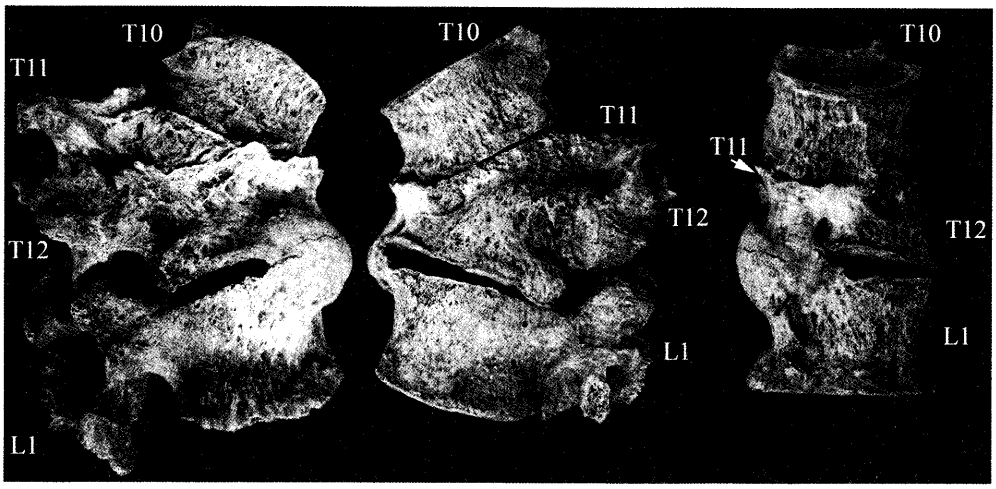

Fig. 1. T 10 – L 1, individual from grave B50/1, Zlatna livada, 3. Right and left lateral and frontal views

in IX-X c. AD [19] presents a similar find. Its age-sex identification is achieved after appropriate methods: auricular surfaces relief assesment [8]; cranial sutures obliteration stages after Olivier-Simpson [15]; complex of sexual dimorphism [1], cranial bones markers after Ferenbach et al. and Buikstra and Ubelaker, [15], standard tables for bone measurements [3, 7, 14]. Pathological changes were registered after methods, summarized in Aufderheide and Rodriguez-Martin and Ortner [2, 10].

Results and Discussion

The individual identifies as male, at 40-50 years at death. On the right parietal and on the occipital bone of the fragmented skull are found two button osteomas. The endocranial surface shows pronounced pits from arachnoid glands, the supraorbital region and scull vault are affected by *cribra cranii*, frontal and maxillary sinuses showed no changes. Dentition is affected by advanced caries, found on five teeth, high level of tooth abrasion and periodontal changes. Bones of the postcranial skeleton present developed arthrosis in shoulder, elbow and wrist, more pronounced in the left elbow and similar changes in hip, knee and left ankle joints, where bilateral asymmetry in development was not possible to assess, as bones of right side remained unrepresented. Vertebral column is affected by spondylosis, most pronounced in thoracic section. On femurs and tibiae is found hyperostotic layer.

In this skeleton T 11 and T 12 are ankylosed with characteristic change of form of T 11 with collapsed anterior wall and triangular form in lateral view (Fig. 1). On the T 12 are visible osteolytic changes with abscess openings, T 10 shows "woven" structure of cortical bone (Fig. 1). These changes on skeleton are characteristic for tuberculosis infection, especially for its type of Pott's disease. They are concentrated in one, most affected vertebra revealing unifocal development of reaction, pointed as typical for adults [10]. After these defects could be supposed long chronic period of the disease, in which, destruction of the spongious bone of the T 11 developed to eventual collapse of the frontal wall. As it is already noted by many authors [2], most frequently affected from skeletal manifestation of tuberculosis infection appears the spine cord, where changes

after Pott's disease are most pronounced. Investigation of cases with developed Pott's disease can't lead to real demographic distribution of tuberculosis infection in the population, but this lesion remains the surest marker of its presence [2, 10].

Four cases of Pott's disease and one of tuberculous coxitits are reported from other studied series, dated in Bulgarian Middle Age as Tuchovishte [4, 6], Kabile, the series from XII-XIII c AD [17], Kavarna, the series from the XV-XVII c. AD [4, 6] and Odartsi [16]. For series from territory of Hungary, dated in the middle ages, is reported a relative rising of cases of osteotuberculosis, including Pott's disease in the VII-IX c. AD [9, 11].

Conclusions

The studied find presents a case of tuberculosis infection, in necropolis of Zlatna livada 3, which ascertains, presence of this infection in population. Similar finds are reported for other Bulgarian middle age populations, revealing, that they did not differ to the known data for Hungary in the period and other European countries.

References

1. G. Acsádi, J. Nemeskéri. History of Human Life Span and Mortality. Budapest, Akademiai Kiado, 1970, 333
2. C. Aufderheide, C. Rodriguez-Martin. The Cambridge Encyclopedia of Human Paleopathology. Cambridge Univercity Press, 1998, 478.
3. Bass, W. Human Osteology: a Laboratory and Field Manual of the Human Skeleton. University of Missury, 1971, p. 281.
4. Goranov, I., P. Boev, N. Kondova, S. Cholakov. Paleopathological Data for the Spinal Column Diseases. Acta Morphologica, 4, 1983, 57-63.
5. Hershkovitz, I., B. Rothcshild, O. Dutour. Clues to Recognition of Fungal Origin of Lytic Skeletal Lesions. Am. J. Phys. Antropol. 106, 1998, 47-60.
6. KondovaN., Boev, P., Sl. Tcholakov. Paleopathology of the Medieval Bulgarian Population. Man and his Origins, Anthropols, Brno, 21, 1982, 379-382.
7. Kühl, R. Skelettreste aus prähistorische Brandbestattungen und ihre Aussagemöglichkeiten, mit Hinweisen auf spezielle Fragestellungen in Schleswig-Holstein. Mitteilungen der Anthropologischen Gesellschaft in Wien (MAGW), Band 115, 1985, 113-137.
8. Lovejoy, C., R. Meindl, T. Pryzbeck, R. Mensforth. Chronological Metamorphosis of the Auricular Surface of the Ilium: A new Method for the Determination of Adult Skeletal Age at Death. American Journal of Physical Anthropology, 1985, 68, 15-28.
9. Marcsik, A. Generalizált TBC Megbetegedés Diagnóyisa Egy Avrkori Csontváyon. Anthropol. Közl. 16, 1972, 2, 99-103.
10. Ortner: Ortner D. Identification of Pathological Conditions in Human Skeletal Remains. El;sevier, Sec. Ed, 2003.
11. Szelekovszky, M., A. Marcsik. Anthropological Analysis of Human Skeletal Matherial (7-9Th Century AD, East Hungary). Ann. Roum. Anthropol., 47, 3-15, 2010.
12. Ubelaker, D. Human Skeletal Remains: Excavation, Analysis, Interpretation (2 nd Ed.). Washington DC, Taraxacum, 1989.
13. Walrath D., P. Turner, J. Bruzek. Reliability Test of the Visual Assessment of Cranial Traits for Sex Determination. Am J Phys Anthropol, 125, 2004, 132-137.
14. Алексеев, В. Остеометрия, методика антропологических исследований. Москва, Наука, 1966, 252.
15. Алексеев, В., Г. Дебец. Краниометрия, методика антропологических исследований. Москва, Наука, 1964, 228.
16. Йорданов, Й., Б. Димитрова. Данни от антропологичното изследване на погребаните

в средновековния некропол № 2 при с. Одърци, Добричко, XI в. В: Дончева-Петкова, Л., Одърци. Некрополи от XI в. т. 2, 2005, 415-460.
17. Чолаков 1991: Чолаков, Сл., Н. Кондова, П. Боев. Биологична реконструкция на средновековното население от Кабиле. Кабиле, т. 2, 1991, 137-155.
18. Янков, Д., Р. Колева, Ч. Кирилов. № 54. Средновековно селище и некропол с. Златна ливада, км. 19+900-20+400 от АМ Марица. В: АОР за 2011 г. София 2012, 488-490.

Institute of Experimental Morphology, Pathology and Anthropology with Museum
Bulgarian Anatomical Society

Acta morphologica et anthropologica, 19
Sofia • 2012

Newborns from the series of necropolis n 2, zlatna livada – possible premature delivery cases

Victoria Russeva

Institute of Experimental Morphology, Pathology and Anthropology with Museum, Bulgarian Academy of Sciences

Anthropological material from necropolis N 2, Zlatna livada, XI-XII c. (119 complexes with 126 individuals) is investigated. In age-sex distribution is registered highest portion of infants in the age group Infans I (74.9 %), in which in first age group 0-4.9 years are recognized 88 individuals (70.97 %). Individuals at interval 0-1 years, with 60 skeletons, are the highest number in age interval 0-1 year. From them are ascertained 34 skeletons of newborns (56.67 %), aged less than one month. In these individuals is found a predominance of those, who show underdevelopment (measurements lower than means for tenth lunar gestation month).

Key words: Zlatna livada N 2, XI-XII c. AD, newborns

Evidence basis for reconstruction of mortality in past populations – skeletal remains from archaeological sites, has been debated for many years in relation to its representativeness [1]. High influence of burial ritual on the age-sex distribution of individuals in skeletal populations is emphasized pointing to its discriminative action to different age and sex groups in the population. Most influenced by burial ritual appears group of newborns and small children, at one side by restriction of such burials in regular necropolises, and from other side by less cautious manipulation of their remains, as preparation of grave construction and grave depth, which exposes skeletal remains to higher possibility of destruction by environmental conditions. Specifics of these skeletons, being with very small dimensions and lower calcification, also have negative influence to their representation in archeological complex.

Material and Methods

Necropolis N 2 in vicinity of the village of Zlatna livada, is fully investigated, dated in XI-XII c. AD. It appears as a part of a vast complex of settlement and other two necropolises, which developed from IX-X c. AD and represents a long surviving rural population, which inhabited the place [14, 15, 16]. Necropolis N 2 presents 119 complexes, in which are identified 126 individuals.

The anthropological investigation included all available material from skeleton after following methods in age-sex identification: dental development [8, 13], epiphyseal

Table 1. Age and sex distribution of identified individuals

	Infans I	Infans II	Juvenis	Adultus		Maturus		Senilis		Total
				M	F	M	F	M	F	
N	94	5	0	7	6	8	3	3	0	126
%	74.60	3.97	0	5.56	4.76	6.35	2.38	2.38	0	

Table 2. Age specific values of paleodemographic parameters*

	$D_{(x)}$	$d_{(x)}$	$l_{(x)}$	$q_{(x)}$	$e_{(x)}$	$a_{(x)}$		$D_{(x)}$	$d_{(x)}$	$l_{(x)}$	$q_{(x)}$	$e_{(x)}$	$a_{(x)}$
0-4.9	88	70,97	100,00	0,71	11,29	13,79	40-44.9	3,75	3,02	11,29	0,27	13,39	55,89
5-9.9	9	7,26	29,03	0,25	27,78	35,28	45-49.9	2,75	2,22	8,27	0,27	12,38	59,88
10-14.9	1	0,81	21,77	0,04	31,20	43,70	50-54.9	2,25	1,81	6,05	0,30	11,00	63,50
15-19.9	0	0,00	20,97	0,00	27,31	44,81	55-59.9	2,25	1,81	4,23	0,43	9,64	67,14
20-24.9	4,75	3,83	20,97	0,18	22,31	44,81	60-64.9	1,5	1,21	2,42	0,50	10,00	72,50
25-29.9	1,75	1,41	17,14	0,08	21,74	49,24	65-69.9	0,5	0,40	1,21	0,33	12,50	80,00
30-34.9	1,75	1,41	15,73	0,09	18,46	50,96	70-74.9	0	0,00	0,81	0,00	12,50	85,00
35-39.9	3,75	3,02	14,31	0,21	15,04	52,54	75-79.9	0	0,00	0,81	0,00	7,50	85,00
							80+	1	0,81	0,81	1,00	2,50	85,00

*mean values for adults with wider age determination

fusion [7], long bones lengths [2, 6]; identification of newborns [3]; pubic symphyseal surface relief after Todd [7], auricular surfaces relief [5]; cranial sutures obliteration [5, 10]; complex of sexual dimorphism [1, 10], cranial bones markers [7], standard tables for diameters of femoral, humeral and radial heads, femoral and humeral bicondylar breadth and clavicle length [2, 4, 11]. Results are processed after methods of paleodemography [1].

Results and Discussion

In the studied skeletal population is registered the highest portion of infants in the age group *Infans I* with 74.9 % (Table 1). In them are recognized 88 individuals (70.97 %) in first age group of 0-4.9 years (Table 2). The portion of individuals of first age interval influences in very negative way life expectancy in population at this age. Distribution of individuals in this age interval shows highest number of individuals at 0-1 years at death, with 60 skeletons, 64.52 %, from which are found 34 skeletons of newborns, aged less than 1 month, or 56.67 % (Fig. 1). In these individuals is ascertained a predominance of those, who show underdevelopment (measurements lower than means, characteristic for newborns at tenth lunar gestation month) or 61.76 %. Mean values of lengths of long bones from these skeletons fall in-between values, characteristic for 7.5 to 9.5 lunar months of gestation.

As a result, series from Zlatna livada, N 2, presents values of relative number of dead in the age 0-4.9 years of 70.97 %, much higher than mean values found in populations from XI-XII c. AD of 24.38 %, surpassing also values, found for series from near territories in the period. It appears as a unique middle aged complex in Bulgaria, which contains big portion of newborns at development under tenth gestational month.

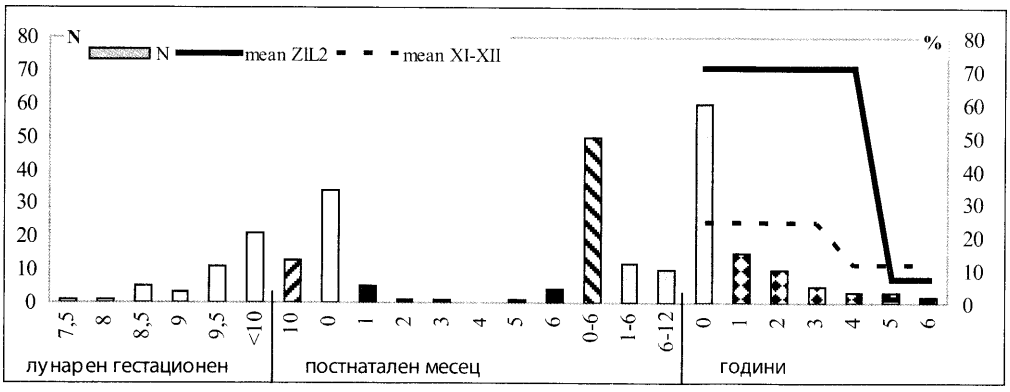

Fig. 1. Age distribution of individuals at the age 0-6 years at death

Conclusions

High number of newborns in the series, which exceed known values from all skeletal populations from regular middle aged necropolises from Bulgaria, could point to a period of specific use of the site for burials of newborns, most of them dead during, or after premature births. To similar interpretation leads also excavated grave of female with fetus in birth position, buried after possible death during birth. The site gives unique information about mortality of newborns and cases of premature delivery, after which survival in the period was extremely reduced. From cultural point of view – the age distribution could be a result of attention, given to the newborns, even ones with underdevelopment, for which other burial sites were possibly restricted.

References

1. G. Acsádi, J. Nemeskéri. History of Human Life Span and Mortality. Budapest, Akademiai Kiado, 1970, 333.
2. Bass, W. Human Osteology: a Laboratory and Field Manual of the Human Skeleton. University of Missury, 1971, 281.
3. Fazekas, I., F. Kosa. Forensic Fetal Osteology. Budapest: Budapest, Akademiai Kiado, 1978, 413.
4. Kühl, R. Skelettreste aus prähistorische Brandbestattungen und ihre Aussagemöglichkeiten, mit Hinweisen auf spezielle Fragestellungen in Schleswig-Holstein. MAGW, 115, 1985, 113-137.
5. Lovejoy, C., R. Meindl, T. Pryzbeck, R. Mensforth. Chronological Metamorphosis of the Auricular Surface of the Ilium: A new Method for the Determination of Adult Skeletal Age at Death. Am J of Phys Anthr, 1985, 68, 15-28.
6. Maresh, M. Measurements from roentgenograms. In: Ed. McCammon, R., Human Growth and Development, Springfield IL, C. C. Thomas, 1970, 157-200.
7. Schwartz, J. Skelleton Keys (An Introduction to Human Skelletal Morphology, Development and Analysis). New York, Oxford Press, 1995.
8. Ubelaker, D. Human Skeletal Remains: Excavation, Analysis, Interpretation (2 nd Ed.). Washington DC, Taraxacum, 1989.
9. Walrath D., P. Turner, J. Bruzek. Reliability Test of the Visual Assessment of Cranial Traits for Sex Determination. Am J Phys Anthropol, 125, 2004, 132-137.
10. White T., P. Folkens. The Human Bone Manual. Elsevier, 2005, 464.
11. Алексеев, В. Остеометрия, методика антропологических исследований. Москва, Наука, 1966, 252.

12. Алексеев, В., Г. Дебец. Краниометрия, методика антропологических исследований. Москва, Наука, 1964, 228.
13. А. Зубов. Одонтология. Методика антропологических исследований. Москва, Наука, 1968.
14. Янков, Д., Р. Колева, Ч. Кирилов. № 72. Спасителни археологически разкопки на обект "Средновековно селище и некропол", м. Бялата вода, с. Златна ливада, община Чирпан, (км. 19+900-20+250) АМ "Марица". АОР за 2009 г. София 2010, 611-613.
15. Янков, Д., Р. Колева, Ч. Кирилов. № 53. Средновековно селище и некропол с. Златна ливада, км. 19+900-20+400 от АМ Марица. АОР за 2010 г. София 2011, 513-515.
16. Янков, Д., Р. Колева, Ч. Кирилов. № 54. Средновековно селище и некропол с. Златна ливада, км. 19+900-20+400 от АМ Марица. В: АОР за 2011 г. София 2012, 488-490.

Institute of Experimental Morphology, Pathology and Anthropology with Museum
Bulgarian Anatomical Society

Acta morphologica et anthropologica, 19
Sofia • 2012

Changes in height in adult bulgarians from the end of 19th to the end of 20th century

Racho Stoev

Bulgarian Academy of Sciences, Institute of Experimental Morphology, Pathology and Anthropology with Museum, Sofia, Bulgaria

The data of body height in Bulgarians born since 1860-s to 1960s have been analyzed. Mean body height has been calculated and traced year by year. The results show that in the late nineteenth and early twentieth century, there was some deterioration in the socio-biological conditions, which is reflected in the stagnation and loss of height. In the interwar period this deterioration has been overcome and acceleration of adult height began and continued until the end of period under study. However, in this process, Bulgaria lags behind other European countries, which ahead Bulgarians in mean adult height.

Key words: anthropometric history, body height, Bulgaria, social influence on physical development

In recent decades, historical anthropometry has established itself as a method for assessing the socio-biological conditions in societies and periods with insufficient socio-economic data, such as societies with a large share of natural economy or of the informal economy etc. Based on it is examined the situation of the population of Russian and of Habsburg Empire, in the U.S. in the 19th century etc. [2, 3, 10, 11].

Material and Methods

The main sources of data for historical anthropometry are:

a) height measurements in recruits which in many European countries have been preserved partly or completely from the 17th century;

b) mass data from specialized anthropometric studies conducted during the 20th century [10].

In Bulgaria we have data on adult height for the period 1886-1942 (all recruits at 1897-1920 and three separate measurements at 1886, 1889 and 1942 [5, 12], and the results of four national-wide studies in 1960, 1970-71, 1980-82 and 1989-1993 [9, 13, 14, 15].

The data of stature in recruits were discussed in details in former papers [5, 12].

The nation-wide survey of 1960 gives mean heights in one-year age groups for men and women up to 26 years. Of the investigated, 2557 men aged 19-26 years and 3483 women aged 17 to 26 years can be considered adults [13].

The survey of 1970-71 gives mean heights in one-year age groups up to 24 years and then in five-year age groups up to 55-59 years. Of the investigated, 8489 men aged 18-59 years and 7980 women aged 17-59 years can be considered as grown [14].

The study of the years 1980-82 gives mean heights in one-year age groups up to 24 years and then in five-year age groups up to 65-69 years. Of them as adults can be considered 6,279 men 17 to 69 years, and 6,086 women of the same age [15].

The materials from the National Anthropological Program (NAP) give mean height of 2419 men and 2846 women aged 30 to 40 years, unfortunately, in a common age group [9].

The height by age were transformed in height by year of birth by subtracting the age of the peak years of the survey (1981 for the study 1980-82 and 1991 for NAP.

The mean heights in five-year age groups in the survey results from 1970-71 and 1980-82 years were brought to one year age groups using the formulas:

$$h_1(a) = H(A) + (a - A) / 5 \times (H(A+5) - H(A))$$

$$h_2(a) = h_1(a) \times 5H(A) / \sum_{k=-2}^{k=2} h1(A+k)$$

where: A – central age in a five-year age group;
H – mean height in a five-year age group;
a – age (one-year age group/
h_1 – mean height in one-year age group, first approximation
h_2 – mean height in one-year age group, second approximation

Results and Discussion

The analysis of the data shows that in men born in the late 19th century and matured up to 1920 a slight downward trend in height can be observed **(FIGURE 1).** It can be explained on the basis of the decline of the Bulgarian protoindustry and animal husbandry after the Liberation, leading to a reduction in GDP and national income per capita up to 1910, followed by an even worse war period 1912 -1918 [4, 8]

For those born in the twentieth century and reached maturity in the interwar period a pronounced increase in height (acceleration) can be observed. It occurs as well in men and women **(FIGURE 2)**. The data of mean height of 211 women measured by Vatev in 1899 do confirm that the reduction of the adult height in people born in the late nineteenth century also affected the women [7].

In the historical anthropometry greater adult height is associated with rising living standards and improving of the socio-biological conditions for children and adolescents. This increase in Bulgarians born in twentieth century can be connected with:

– the intensification of Bulgarian agriculture that began in the interwar period;

– the industrialization and urbanization of the country, which also began in the interwar period;

– the demographic transition – the sharp decline in fertility allows reduced number of children to receive better care; and others.

It is important to note that the acceleration of adult height, respectively, the improving of the socio-biological conditions for the development of children and adolescents began after World War I, but not after the Second World War, ie can not be associated with the social transformations after it. It is not noticeable, however, these transformations to have significantly impeded this process.

The comparison of data from different studies showed a defect of the 1980-82 national study. Although the published materials say that the survey has been carried out in the same sockets and by the same methodology as the previous 1970-71 survey [15], this is clearly not the case. As stated on earlier [6], if this was true, it would be expected the height of people over 20 years in the first study to not increase 11 years later. However such "increase" can be observed (**Fig.1, Fig.2).** Meanwhile, the results from the NAP have been published, which agreed well with the results of survey of 1970-71 year and badly with these from 1980-82 survey. Thus the measurement data from 1980-82 survey confirm the marked increase of adult height in Bulgarians born in the twentieth century, but the mean adult height in people born around 1960 has to be evaluated on the base of comparison with 1970-71 survey and of NAP – about 172 cm in males and 159 cm in females. This gives some 1 cm per 10 years growth of mean adult height – a rather moderate figure.

It is interesting to compare the data of adult height in Bulgaria and in some other countries (various data published in [1]) . The comparison shows that Italy and Greece, where young people were lagging behind their Bulgarian counterparts in the early twentieth century, later catch up and get ahead of Bulgaria's socio-biological conditions (**Figure 3).** The same is true for other relatively backward in the late 19th century, countries such as Portugal, Poland, Russia. On the other hand, the average height in

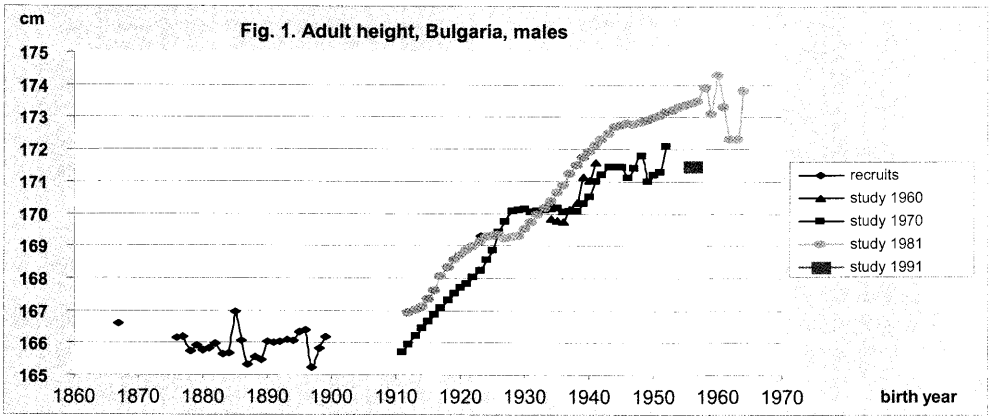

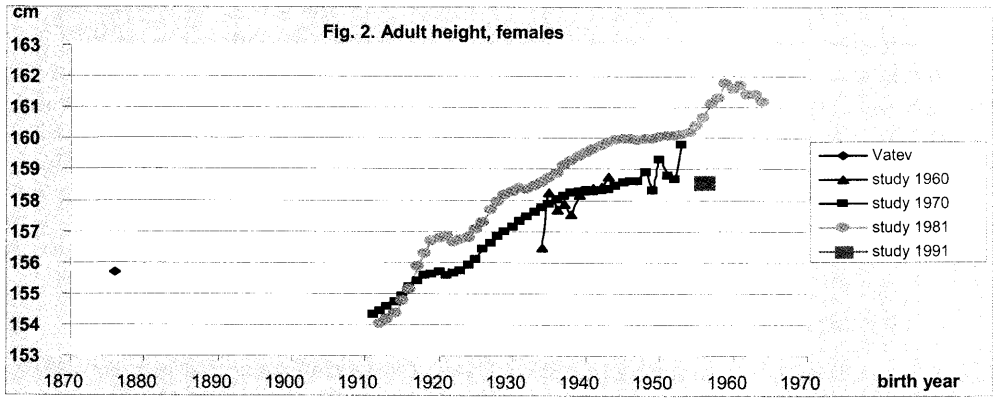

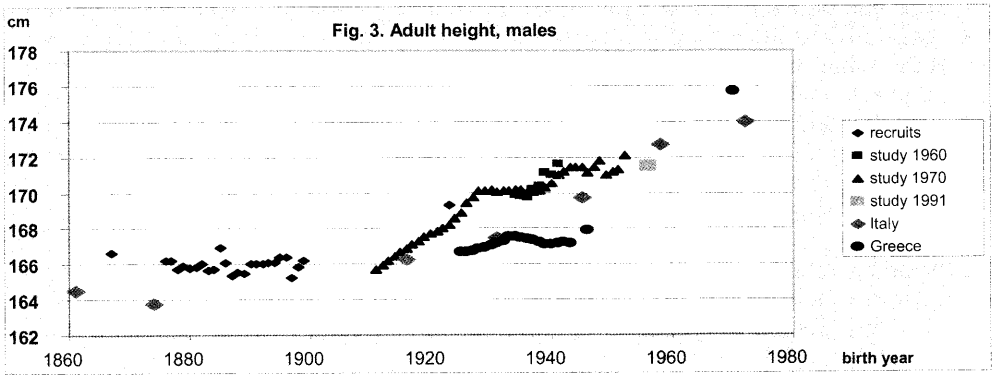

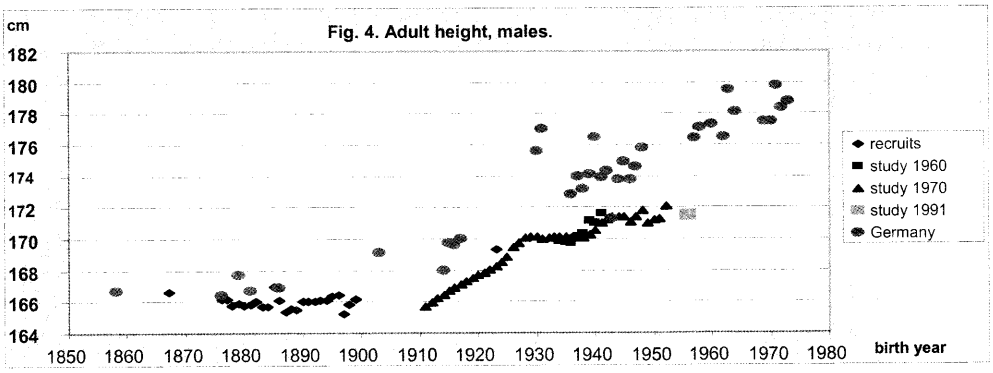

significantly more advanced Germany departs from level virtually identical to that in Bulgaria (about 166 cm (detaches and gradually surges higher (**Figure 4).**

Unfortunately, there are no representative data on mean adult height of Bulgarians born after the early 1960s, ie the main mass of the population in working and reproductive age.

Conclusion

Collected data on the mean adult height of Bulgarians of both sexes showed that in the late nineteenth and early twentieth century, there was some deterioration in the socio-biological conditions, which is reflected in the stagnation and loss of height. In the interwar period this deterioration has been overcome and acceleration of adult height began. However, in this process, Bulgaria lags behind other European countries, which ahead Bulgarians in mean adult height. Further studies are needed to trace secular changes in younger generations born after 1960.

References

1. Bodzsar, B.E., Susanne, C. (Eds). Secular Crowth Changes in Europe. Budapest, Eotvos University Press, 1998, 1-381.

2. K o m l o s, J. Nutrition and Economic Development in Eighteenth-Century Habsburg Monarchy. An Anthropometric History. Princeton Univ.Press, Princeton, 1989.
3. K o m l o s, J.. A History of Human Height from the 17th to the 21st Century. Paper presented on the Vth International Anthropological Congress of Ales Hrdlicka, Prague-Humpolec, 2009.
4. P a l a i r e t, M. The Balkan Economies, 1800-1914. Evolution without Development. Cambridge Univ.Press, Cambridge, 1997, 1-415.
5. S t o e v, R. Body height in recruits in Bulgaria (1897-1920). Acta morphologica et anthropologica, 18, 2012 (in press).
6. S t o e v, R., Y. Y o r d a n o v. Secular trend in Bulgaria. In: Bodzsar, B.E., Susanne, C. (Eds). Secular Crowth Changes in Europe. Budapest, Eotvos University Press, 1998, 65-73.
7. В а т е в, С т.. Антропология на българите. С., Друж. за нар. здраве, 1939, 1-179.
8. Д а с к а л о в, Р. Българското общество. 1878-1939. т.1, С., Гутенберг, 2005, 1-470 .
9. Й о р д а н о в и кол. Антропология на населението на България в края на XX век. С., Акад. Изд. "Проф.М.Дринов", 2006, 1-432.
10. М и р о н о в, Б.Н. Социальная история России периода империи (XVIII-начало XX в.), С.-Петербург, Дмитрий Буланин,1999, т.2, 1-566.
11. М и р о н о в, Б.Н. Благосостояние населения и революции в имперской России: XVIII-начало XX века. Москва, Новый хронограф, 2010,1-911.
12. С т о е в, Р. Ръст при новобранци в България, 1886-1942. IV Копривщенски морфологични дни, VIII Национална конференция по антропология, Копривщица, 2010 (устно съобщение).
13.Я н е в, Б и кол., Физическо развитие и дееспособност на населението в България от раждане до 26 години. С., Изд.БАН, 1965, 1-262.
14. Я н е в, Б и кол.Физическо развитие, физическа дееспособност и нервно-психическа реактивност на населението. С., Мед. и физк., 1982, 1-352.
15. С л ъ н ч е в, П. и кол., 1992л Физическо развитие, физическа дееспособност и нервно-психична реактивност на насеението на България. С., НСА, 1992, 1-336.

Institute of Experimental Morphology, Pathology and Anthropology with Museum
Bulgarian Anatomical Society

Acta morphologica et anthropologica, 19
Sofia • 2012

Age at Menarche in Sofia Girls /1984-2002/

R. Stoev, Z. Mitova, L. Yordanova

Institute of Experimental Morphology, Pathology and Anthropology with Museum, Bulgarian Academy of Sciences, Sofia

The purpose of this paper is to compare the results of two last cross-sectional studies of age at menarche in Sofia (1984-1987 and 2001-2002). The comparison shows that in the beginning of 21st century the mean age at menarche (calculated by probit analysis) in Sofia girls remains on the same level as in 1980s – 12.9±0.1 years. Its standard deviation is on the level of 1.3-1.4 years, typical for socially heterogeneous samples. A leveling of age at menarche in families with different number of children has been found, the causes of which need further study. The available data do not allow determining whether there was variation of the timing of puberty under the changes of social conditions between our researches and in the next decade.

Key words: age at menarche, socio-familial conditions, number of children in the family, acceleration, puberty.

Introduction

The appearance of first menstruation (menarche) is used as a relatively easy for study and objective indicator of the degree of sexual maturation in girls. The age at menarche (AM) itself is very sensitive to the influence of the environment and is used for evaluation of the social conditions equally with the adult height. It is most accurately determined on the basis of the proportion of menstruating girls by age from cross-sectional studies (see a review in [7].

The purpose of this paper is to compare the results of two last cross-sectional studies of AM in Sofia (1984-2002). They surround a period of great social changes and can serve as an indicator of how these changes affect the health and biological status of the young generation.

Material and methods

In 1984-87 by R. Stoev and L. Yordanova in a cross-sectional study 462 girls aged 9 to 16 years at the last birthday were examined in Sofia and in 2001-2002 – 565 girls aged 9 to 15 by Z. Mitova and L. Yordanova [4, 7]. They were distributed in one year age groups. Mean AM was calculated by probit analysis [2].

Table 1. Investigated and menstruating girls by age

Age (yrs) at last birthday	1984-1987			2001-2002		
	Girls	*menstruating*		*Girls*	*menstruating*	
	n	n_m	P, %	n	n_m	P, %
9	34	0	0	81	0	0
10	66	2	3.0	75	3	4.0
11	65	6	9.2	85	10	11.8
12	58	23	39.7	83	26	31.3
13	86	72	83,7	81	54	66.7
14	49	45	91.8	86	74	86.0
15	63	62	98.4	74	73	98,6
16	41	40	97.6	nd	nd	nd
total	462	250	54.5	565	240	42.5

Results and discussion

Of the girls investigated in 1984-1987 250 had menarche and of the surveyed in 2001-2002 – 240. The earliest cases of menstruating girls are in the 10 year age group and the latest single cases of girls without mensis – in the age groups 15 and 16 years (Table 1, Figure 1). Subjected to probit analysis these data show that mean AM in 1980s was 12.90±0.12 (SD=1.39) and at the beginning of 20th century – 12.92±0.09 (SD=1.28).

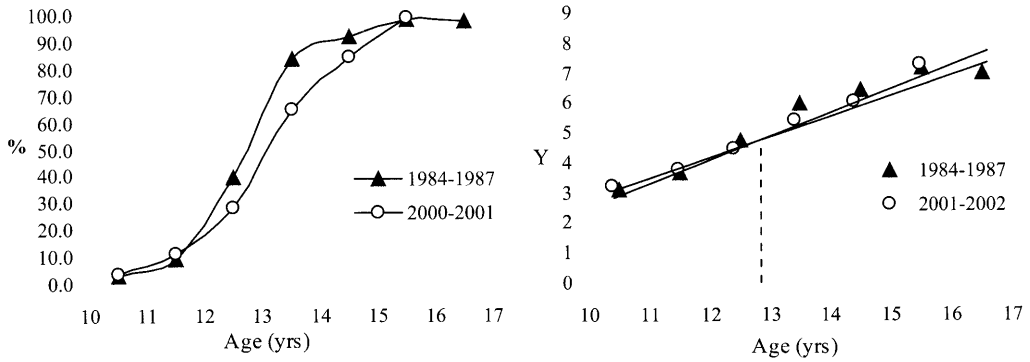

Fig. 1. Proportion of menstruating girls by age and its probit transformation Y.

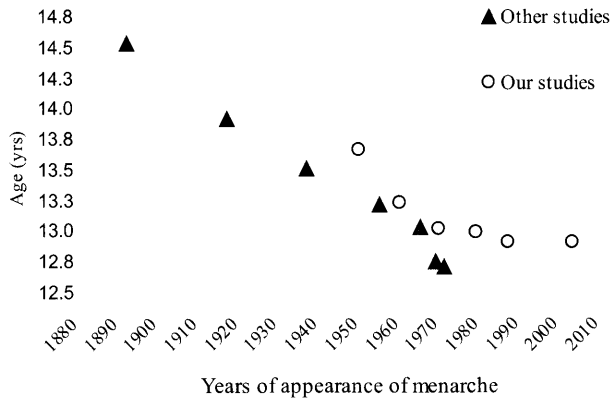

Fig. 2. Mean age at menarche in Sofia.

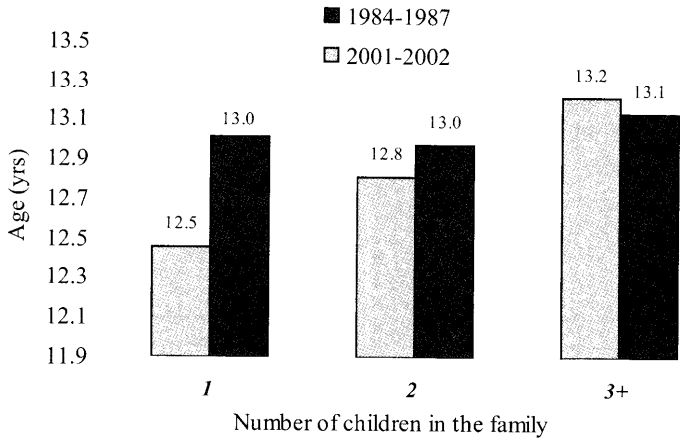

Fig. 3. Mean age at menarche by number of children in the family.

The mean AM is virtually the same, and the standard deviation is on the level typical for social heterogeneous samples [1].

The results of previous cross- sectional studies in which probit analysis can be made (even if it is not done in the original paper) show mean AM in Sofia of: 13.02 at 1963 [6] and of 12.74 at 1967 [3], statistically not different than these obtained by the authors. Retrospective studies in adult women and university students which also provide comparable, albeit less accurate results give mean AM in Sofia 13.00 around 1968 and 12.98 around 1977 [7] (Fig. 2).

All these results suggest a relatively stable average AM and therefore timing of puberty in Sofia from 1960s to 2002.

Meanwhile, in the smaller localities can be traced still a process of acceleration of the sexual maturation in the places for which comparable data exist (Haskovo – [3, 8]; Smolyan – [5, 7]).

Unfortunately, we do not have materials to see how the timing of sexual maturation changed in the extremely dynamic and socially difficult period of 1990s. On basis of studies in other countries AM during this period should have increased, reaching a maximum at the most difficult 1996-1997 and than declined, but our data are from before and after the crisis (see review in [7]).

The survey in 1984-1987 was accompanied by an extensive survey of socio-familial conditions, allowing tracing the relationship of the individual factors of the social environment with the terms of sexual maturation. Unfortunately, the survey in 2001-2002 was far less complete. Only the answers of the question about the number of the children in the family of the surveyed students can be used.

The results show that while in 1980s there is a strong correlation between the number of children in the family and AM, in the beginning of 21st century it disappears and the mean AM in families with one, two or three children differs within the statistical error (fig.3). Such a paradoxal lack of connection requires further research on the subject. Most likely it is related with the sharp decline of fertility in 1990s and the transition from two-children to one-child family model.

Conclusion

In the beginning of 21st century the mean age at menarche (calculated by probit analysis) in Sofia girls remains on the same level as in 1980s – 12.9±0.1 years. Its standard deviation is on the level of 1.3-1.4 years, typical for socially heterogeneous samples.

A leveling of age at menarche in families with different number of children has been found, the causes of which need further study.

The available data do not allow determining whether there was variation of the timing of puberty under the changes of social conditions between our researches and in the next decade.

References

1. W a n g e r m e z, J. L'age a la menarche. Variations dans l'espace et dans le temps. – Soc. d'anthrop. du Sud Ouest, Bull. trim., 16, 1981, 1, 51-63.
2. W e b e r, E. Grundriss der Biologischen Statistik. – Jena, Gustav Fischer Verlag, 1964, 1-582.
3. Д а м я н о в а, Цв. Показатели за нормален пубертет при момичетата. – Дис., София, 1974, 1-238.
4. М и т о в а, З. Антропологична характеристика на физическото развитие, телесния състав и телесната охраненост на 9-15 годишни деца и подрастващи от София. – Дис., София, 2009, 1-225.
5. М л а д е н о в а, С., Антропологична характеристика на растежа и развитието на деца и подрастващи от Смолянски регион в съвременните условия на живот. – Дис. Пловдив, 2003, 1- 193.
6. С е и з о в, Хр. Върху избързването на пубертетното развитие на учащите се в София в интервал от десет години. – Въпр. физ. култ., 3, 1964, 180-183.
7. С т о е в, Р. Антропологична характеристика на подрастващи – физическо развитие и полово съзряване във връзка със семейно-битовите условия. – Дис., София, 2007, 1- 177.
8. Т и н е ш е в, Сл. Антропологична характеристика на деца и подрастващи. – Дис., Пловдив, 2009, 1-325.

Institute of Experimental Morphology, Pathology and Anthropology with Museum
Bulgarian Anatomical Society

Acta morphologica et anthropologica, 19
Sofia • 2012

Sexual dimorphism in supero – inferior diameter of the femoral neck among the contemporary Bulgarian population

P. Timonov[1], I. Doychinov[1], K. Badiani[2]

[1]*Department of Forensic Medicine, Medical University – Plovdiv*
[2]*a student, Medical University – Plovdiv*

This study aims to demonstrate the accuracy of sex determination through use of the supero- inferior diameter of the femoral neck among the contemporary Bulgarian population and comparison of the yielded results with the data described by some international authors. An aggregate of 48 femora, 28 male and 20 female were studied. The Paired-Samples T-test proves the lack of significant difference between the two consecutive measurements ($p=0,137$) and between the left and right measurements ($p=0,137$). The Independent Samples Test reveals a significant difference between the variable of the two sexes ($p<0,001$). As a result, this landmark may successfully be used as a sex discriminant.

Key words: forensic anthropology, sexual dimorphism, femoral neck, supero-inferior diameter

Introduction

Each forensic anthropology examination of human skeletal remains is based on determining "the great four": sex, age, stature and race. When the whole skeleton, including pelvis and skull, is available, the accuracy rate of sex determination reaches up to 95 %. In case of a single bone available, except for a femur, sex determination is seriously impeded (5,8).

The significant sexual dimorphism of the femur is based on several facts:

1. Men are relatively physically stronger than women and they use their muscles more actively.
2. Men's axial skeleton is heavier than women's and this weight is normally distributed in the upper end of the two femora.
3. Due to its reproductive function the female pelvis differs in shape from male's, which is expected to result in a change in the upper part of the femora, forming the pelvic bones.

Studies on sex determination through use of various anthropometric landmarks of the femur have been carried out by a number of international researchers (1,3,4,5,7,8). Those authors do not quote equal values of a single index in the examination of differ-

ent population groups. This results from the influence of the differences in race, dietary regime, heredity, social and geographic factors.

This study aims to demonstrate the accuracy of sex determination through use of the supero- inferior diameter of the femoral neck among the contemporary Bulgarian population and comparison of the yielded results with the data described by some international authors.

Materials and methods

An aggregate of 48 femora, 28 male and 20 female were studied. They had been subject of forensic examination, and the sex of one part of said femora was known, while that of the others was determined through pelvic bones analysis. The bones included in this study fulfill the following criteria: – show no anomalies, deformations or abrasions, 2- have sustained no fractures previously, 3- have reached skeletal maturity. They belong to Bulgarians born after 1910; the average age of the known male bones is 56,8±13,44 years, and of the female ones 64.3±13,97 years (Mean±SD).

The mean studied is the supero – inferior diameter of the femoral neck (M 15). Two consecutive measurements were carried out in order to reduce errors in measurement. The Paired-Samples T-test was applied twice for the purpose of detecting the significant differences in the results from the two repeated measurements, as well as from the measurements performed on the left and right femoral necks of 19 pairs of bones. The means resulting from the two consecutive measurements of each bone undergo the Kolmogorov-Smirnov Test designated to indicate their distribution, and an Independent Samples Test designated to indicate any difference between the two sexes, and a Discriminant Function Analysis for the purpose of creation of a discriminant function for classification of the bones into male and female.

Results

The Paired-Samples T-test proves the lack of significant difference between the two consecutive measurements (p=0,137) and between the left and right measurements (p=0,137).

Therefore, the sample includes left or right femora of the respective pairs.

The means of the variable in our study of the male and female sex are shown in Figure 1. The mean of the male sex is bigger than that of the female.

Figure 2 shows the means resulting from this study and the means resulting from the previous studies covering contemporary Caucasians conducted by Alunni-Perret et al.)1) и Stojanowski and Seidemann (6), which prove the difference in the populations.

Sex	N	%	Mean	SD
M	28	58	**33,36**	3,56
F	20	42	**28,22**	1,77

Fig.1

Sex	Mean	SD	Mean	SD	Mean	SD
M	33,36	3,56	33,91	2,9	35,09	2,49
F	28,22	1,77	28,92	1,9	30,85	2,2

Fig.2

Sex	M	F		
N	28	20		
mean±SD	*33,36 ± 3,56*	*28,22 ± 1,77*	*t = 5,946*	*p <0,001*

Fig.3

Functions and variables	***Raw coefficient***	***Standart coefficient***	***Structure coefficient***	***Sectioning point***
M15	0,376	*1*	*1*	*- 0,16*
Constant	*- 11,733*			
Females < 30,79 < Males				

Fig.4

Percent correctly classified		
Male	***Female***	***Total***
95%	75%	89,60%

Fig.5

The Kolmogorov-Smirnov Test shows that the supero- inferior diameter of the femoral neck among the contemporary Bulgarian population is accurately distributed. (p=0,067).

The Independent Samples Test reveals a significant difference between the variable of the two sexes (p<0,001). As a result, this landmark may successfully be used as a sex discriminant. (Figure 3).

The acquired data is subjected to Discriminant Function Analysis and the studied index is involved as an independent variable. (Figure 4).

Based on this analysis the following function is created F= 0,376.M15 – 11,733 If F>-1,93 we assume that the bone is male and vice versa. As a result of this discriminant function the accuracy of sex determination of contemporary Bulgarian population is shown in Figure 5.

Conclusion

The mean of the anthropometric landmark examined is considerably bigger in men than in women, which is confirmed in the other foreign studies (1,2,6). Due to this characteristic, the supero-inferior femoral neck diameter may successfully be used for sex discriminant. The achieved result of accurate sex determination of 86,9 % matches the results achieved by foreign authors using the same landmark (1,6). On the other hand, differences are found in results comparison. Such population variations result from different social, genetic and climatic conditions. This necessitates the creation of contemporary standards for the different populations.

References

1. Alunni-Perret V., P. Staccini, G. Quatrehomme. Reexamination of a Measurement for Sexual Determination Using the Supero-Inferior Femoral Neck Diameter in a Modern European Population. – Forensic Sci, 48, 2003, No. 3.

2. A s a l a S. Sex determination from the head of the femur of South African whites and blacks. – Forensic Science International 117, 2001, 15-22.
3. I s ¸ c a n M. Y., P. M i l l e r - S h a i v i t z. Determination of sex from the femur in blacks and whites. – Coll. Antropol., 8, 1984, 169–175.
4. 5. I s ¸ c a n M.Y., S. D i n g. Sexual dimorphism in the Chinese femur. – Forensic Sci. Int. 74, 1995, 79-87.
5. K r o g m a n, W.M. Skeleton in forensic medicine. – Trans. Inst. Med. Chic., 16, 1946, 1554-167.
6. S t o j a n o w s k i CM, R.M. Seidemann. A re-evaluation of the sex prediction accuracy of the minimum supero-inferior femoral neck diameter for modern individuals. J Forensic Sci, 44(6), 1999, 1215–8.
7. T a y l o r J.V., R. D i B e n n a r d o. Determination of sex of white femora by discriminant function analysis: forensic science applications. J Forensic Sci, 27(2), 1982, 417–23.
8. Й о р д а н о в Й., Д. Р а д о й н о в а, Съдебномедицинска остеологична експертиза, Варна, Престиж Офис ООД, 2003, 88-90.

Institute of Experimental Morphology, Pathology and Anthropology with Museum
Bulgarian Anatomical Society

Acta morphologica et anthropologica, 19
Sofia • 2012

Bilateral asymmetry in metric features of human scapula

D. Toneva, S. Nikolova

Institute of Experimental Morphology, Pathology and Anthropology with Museum, Bulgarian Academy of Sciences, Sofia

The aim of the study is to perform a comparative assessment of the manifestations of asymmetry in the metric features of scapula as well as to seek for sexual differences in the direction and degree of the established asymmetry. The study includes measurements of whole scapulae and scapular fragments of 77 male and 91 female skeletons, belonging to adult individuals. Eleven directly measured features are investigated. The quantitative assessment of the bilateral asymmetry is made using the relative index of Wolanski for inter-group comparisons. All investigated metric features show bilateral differences, excepting the lower distance between processus coracoideus and cavitas glenoidalis in males.

Key words: scapula, asymmetry, metric features.

Introduction

The scarce data in the specialized literature on the asymmetry in human scapula determined the aim of this study, namely to perform a comparative assessment of the manifestations of asymmetry in the metric features of scapula as well as to seek for sexual differences in the direction and degree of the established asymmetry.

Material and methods

The anthropological investigation is performed on osteological material from archaeological excavations. The study includes measurements of whole scapulae and scapular fragments of 77 male and 91 female skeletons, belonging to adult individuals. Skeletal sex and age are determined by standard anthropological methods [1, 3, 4].

The investigation includes 11 directly measured features: Greatest breadth of *acromion scapulae* (9), GBAS; Length of *acromion scapulae* (10), LAS; Greatest length of *processus coracoideus* (11), GLPC; Length of *cavitas glenoidalis* (12), LCG; Breadth of *cavitas glenoidalis* (13), BCG; Depth of *cavitas glenoidalis* (14), DCG; Distance between *acromion scapulae* and *processus coracoideus*, DAS-PC; Upper distance between *acromion scapulae* and *cavitas glenoidalis*, UDAS-CG; Lower distance between

acromion scapulae and *cavitas glenoidalis*, LDAS-CG; Lower distance between *processus coracoideus* and *cavitas glenoidalis*, LDPC-CG. The first 6 features are measured after the methods of Martin – Saller, and the other ones are introduced by us. The reliability of established bilateral asymmetry is verified by Student's t-test at $P<0,05$. The quantitative assessment of the bilateral asymmetry is made using the relative index of Wolanski for inter-group comparisons [2]. The index is called Index for Asymmetry (IA): $IA = [2.(x_1 - x_2).100]/(x_1 + x_2)$, x_1 – mean value of the feature in right scapula, x_2 – mean value of the feature in left scapula. The positive sign of IA shows right-side asymmetry and the negative one – left-side asymmetry.

The degree of bilateral asymmetry is assessed by percentile analysis according to the data of IA. The border values are set at P_{25} ($P_{25} = 0,7$ IU) and P_{75} ($P_{75} = 2,1$ IU).

Results

The study is focused on the features, characterizing *acromion scapulae*, *processus coracoideus* and *cavitas glenoidalis*, as well as the distances between these bone structures. Basic statistic data for male and female scapulae are presented in Table 1. The results confirm presence of asymmetry in almost all investigated features of the scapula. Most measurements in both sexes are greater on the right side.

In accordance with the comparative assessment of the direction of asymmetry, as a whole the features of *acromion scapulae*, *processus coracoideus* and *cavitas glenoidalis* are with right-side asymmetry (Fig. 1). The distances to the upper point of *cavitas glenoidalis* are greater in left scapulae of both sexes, with the exception of the upper distance between *acromion scapulae* and *cavitas glenoidalis*, which is slightly greater on the right side in the female scapulae. The distances to the lower part of *cavitas glenoidalis* are greater in the right scapulae, excepting the lower distance between *processus coracoideus* and *cavitas glenoidalis* in males, which has the same measurements on both right and left sides.

According to the degree of bilateral asymmetry, the features with right-side asymmetry in both sexes are mainly of a moderate degree and a low degree of asymmetry is

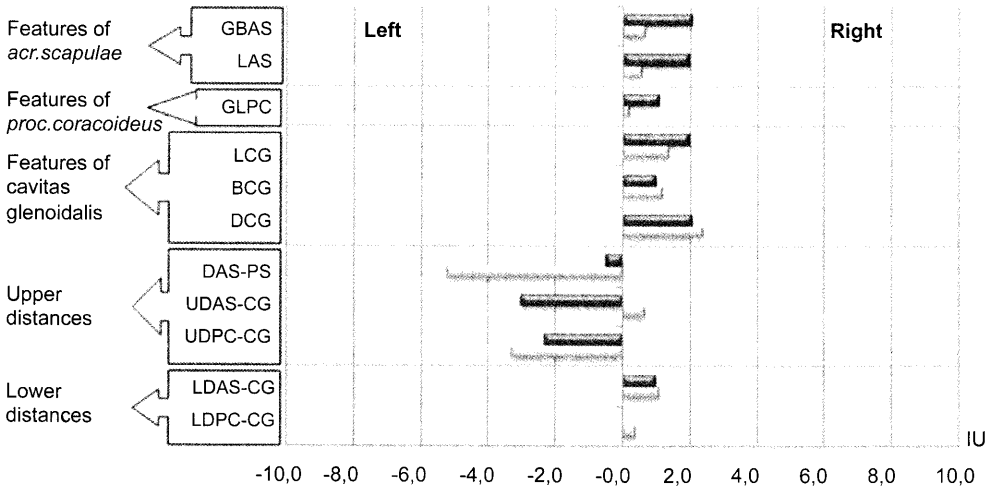

Fig. 1. Direction of the asymmetry in male and female scapulae

Table 1. Biostatistic data of measurements of male and female scapulae (n – number of pairs)

Features	Male scapulae						Female scapulae					
	n	$\bar{x}$ right	$\bar{x}$ left	Absolute difference	t-test	IA	n	$\bar{x}$ right	$\bar{x}$ left	Absolute difference	t-test	IA
GBAS	24	48,8	47,8	1,0	0,683	2,1	26	42,2	41,9	0,3	0,246	0,7
LAS	22	41,0	40,2	0,8	0,414	2,0	27	32,6	32,4	0,2	0,074	0,6
GLPC	30	46,0	45,5	0,5	0,624	1,1	29	42,2	42,1	0,1	0,126	0,2
LCG	57	41,4	40,6	0,8	2,006*	2,0	56	36,3	35,8	0,5	0,830	1,4
BCG	56	28,8	28,5	0,3	0,749	1,0	73	25,6	25,3	0,3	1,172	1,2
DCG	45	4,9	4,8	0,1	0,522	2,1	42	4,3	4,2	0,1	0,599	2,4
DBAS-PC	15	40,4	40,6	-0,2	-0,094	-0,5	17	35,7	37,6	-1,9	-1,260	-5,2
UDAS-CG	24	29,7	30,6	-0,9	-0,895	-3,0	27	27,6	27,4	0,2	0,244	0,7
UDPC-CG	31	30,4	31,1	-0,7	-0,874	-2,3	32	26,9	27,8	-0,9	-1,560	-3,3
LDAS-CG	17	60,0	59,4	0,6	0,476	1,0	17	53,5	52,9	0,6	0,584	1,1
LDPC-CG	21	50,3	50,3	0,0	-0,021	0,0	20	45,8	45,6	0,2	0,207	0,4

*- $P < 0,05$

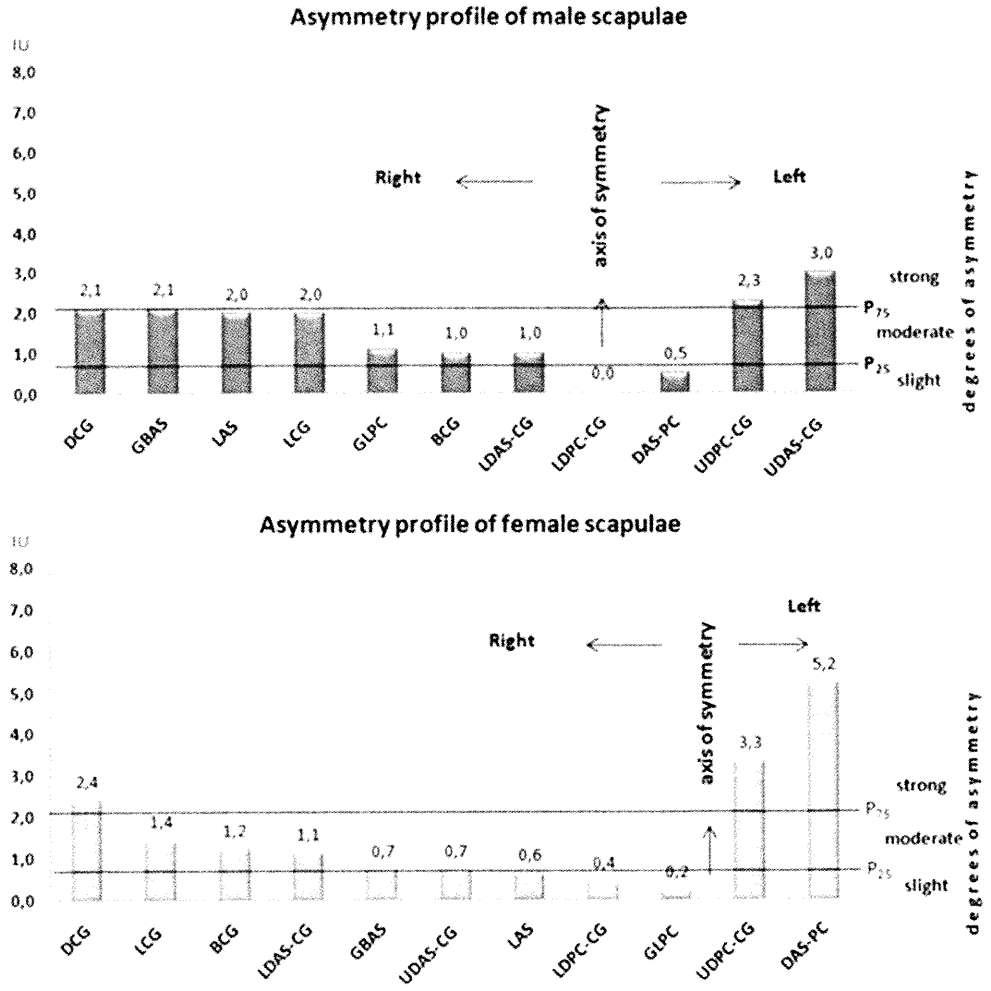

Fig. 2. Asymmetry profiles of male and female scapulae

often observed in females as well. In both sexes, the features with left-side asymmetry are predominantly of a high degree (Fig. 2).

The comparative assessment of the profiles of asymmetry shows that the right scapulae of both sexes have a vastly deeper *cavitas glenoidalis* from the left ones, and the right scapulae of males have also a wider *acromion scapulae*. Left male scapulae have greater distances from *acromion scapulae* to the upper point of *cavitas glenoidalis* in comparison with the right ones, and left female scapulae have greater distances between *acromion scapulae* and *processus coracoideus*.

Conclusions

In summary, all investigated features of the scapula show bilateral differences, excepting the lower distance between *processus coracoideus* and *cavitas glenoidalis* in

males. Some of the features show sexual differences in the direction and degree of asymmetry.

References

1. Martin, R., K. Saller. Lehrbuch der Anthropologie in systematicsher Darstellung. Band I, Stuttgart, Gustav Fischer Verlag, 1957.
2. Wolanski, N. A symmetria ciala czlwieka i jet zmiennosc w swiette funkcji konczyn. – Przegl. Anthrop., 23, 1957, 461 – 464.
3. Алексеев, В.П. Остеометрия. М., Наука 1966.
4. Никитюк, Б.А. Определение пола по скелету и зубам человека. – Вопросы антропологии, вып. 4, 1960, 135 – 139.

Institute of Experimental Morphology, Pathology and Anthropology with Museum
Bulgarian Anatomical Society

Acta morphologica et anthropologica, 19
Sofia • 2012

Secular changes in basic anthropometrical features of neonates and children in early childhood from Sofia

I. Yankova, Y. Zhecheva

Institute of Experimental Morphology, Pathology and Anthropology with Museum, Bulgarian Academy of Sciences

The aim is to analyze the changes in basic anthropometrical features of neonates and 3-6 years of age children from Sofia during XX century. Object of the study are 219 fullterm and healthy newborns investigated in 2001 and 640 preschool children investigated through 2004-2005. The secular changes in height, weight and head circumference are followed comparing our data with data from representative surveys conducted in 1907, 1960, 1970 and 1980/82. Data analyses of different generations' newborns and 3-6 year olds from Sofia in the XX century and early XXI century show periods of increase, abate or decrease of their growth. From early to mid twentieth century, stature, weight and head circumference in newborns changed slightly, and in preschool children stature and body weight increased significantly.

From 1960 to 1970 the anthropometric features of infants increased markedly. Next decade the acceleration changes subside, after that to the beginning of XXI century slow deceleration changes occurred.

Key words: secular changes, neonates, preschool children, stature, weight, head circumference

Introduction

Secular changes of somatometric and somatoscopic features in children are subject of many studies [1-4, 6-12]. These changes have fluctuating character and periods of acceleration, deceleration or even subsidence of the growth process are observed over the years [2]. Secular changes reflect the relationship between individual's genetic determination and environmental influences (socio-economic, environmental, geographic, etc.) in the realization of the human's physical shape [2, 6].

The first representative study of neonates, children, adolescents and adults in Bulgaria is conducted in 1907, followed by representative surveys in 1960, 1970 and 1980/82 [8, 11, 12, 13]. Surveys carried out in Sofia during 2001 of newborns and during 2004/05 of 3–6 years of age children provide the opportunity to assess the dynamics of secular changes over a period of nearly 100 years.

The aim of the study is to analyze the changes in basic anthropometrical features of neonates and 3-6 years of age children from Sofia during XX century.

Material and Methods

Object of the study are 219 fullterm and healthy newborns (110 boys and 109 girls) investigated through 2001, within 24 hours after birth, and 640 preschool children – 3-6 years of age (320 boys and 320 girls, evenly distributed into 4 age groups for both sexes separately) investigated through 2004-2005.

The secular changes in height, weight and head circumference are followed comparing our data with available data from representative surveys conducted in 1907, 1960, 1970 and 1980/82. The anthropometrical measurements were realized by Martin – Saller's classical methods [5].

Mathematical and statistical data processing are performed with SPSS 13.0. Statistically significant differences are established by Student's t-test in $P<0.05$.

Results

Secular changes in stature (Fig. 1)

From 1907 to 1960, the stature of newborn boys and girls increased with 0.5 cm. In 70's of the XX century the newborns were about 2.0 cm longer than those born in 1960. In the next decade, however, the acceleration decrease, and during the period 1980-2001 deceleration changes are observed, as newborns are about 2.0-2.5 cm shorter.
A similar trend is observed in stature of 3-6-year-old boys and girls. In the first half of the twentieth century, their stature increased by 10.0-15.0 cm or 2.0-3.0 cm/decade. Since 1960 till 1970 the mean values of stature increased with 2.0 to 4.0 cm. In the next ten years it not changed and during the period 1980-2004, already reported negative secular changes.

Secular changes in weight (Fig. 2)

In the first half of the twentieth century body weight of neonates is not changed, and from 1960 to 1970 it increased with 0.500 kg. In preschool children the increase is

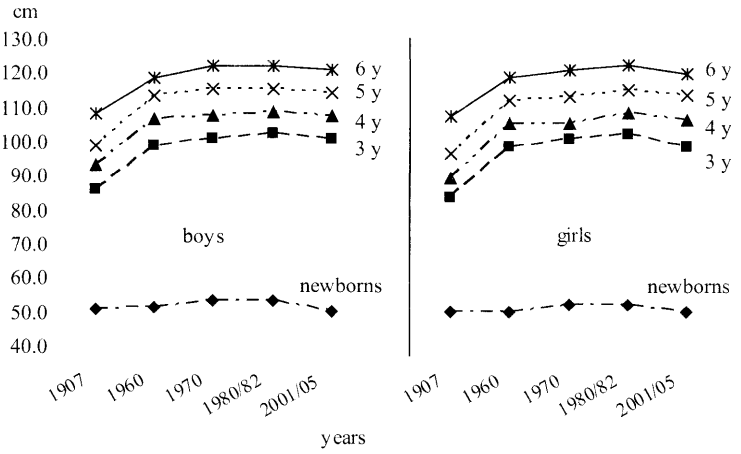

Fig. 1. Secular changes in stature of neonates and preschool children

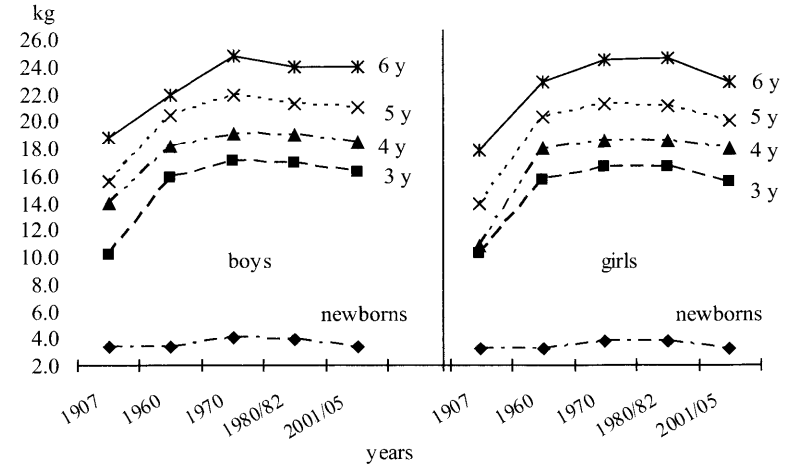

Fig. 2. Secular changes in body weight of neonates and preschool children

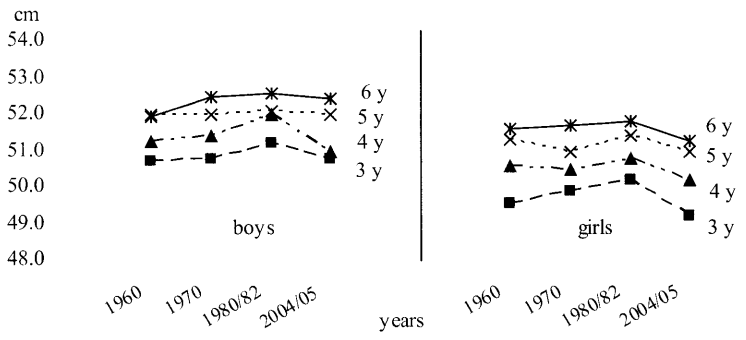

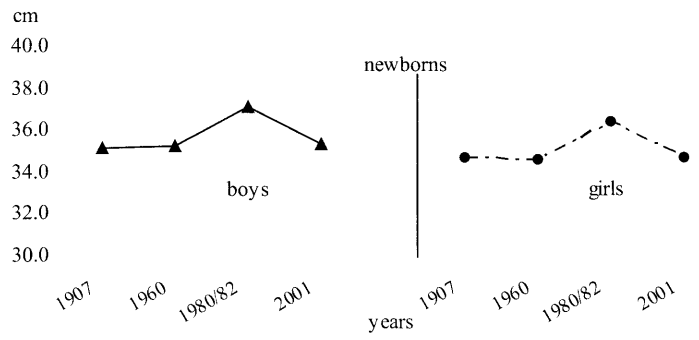

Fig. 3. Secular changes in head circumference of neonates and preschool children

about 1.000 kg/decade, as only in 6-year-old boys it reached to 3.000 kg during the period 1960-1970. After that the acceleration processes subside and begin deceleration changes which continued untill 2005.

Secular changes in head circumference (Fig. 3)

Until 60's of the twentieth century the secular changes in head circumference of newborns are not established, and for 3-6-year-old children no data. During the next twenty-year period the head circumference of newborns increased with about 2.0 cm, and in preschool children slow secular changes are established. After that, to the beginning of the XXI century markedly deceleration occurred in almost all ages with the exception of 5 and 6 year old boys.

Discussion

Since early XX century to 70's stature, weight and head circumference of children increased. In the next decade the acceleration changes abate and to beginning of the XXI century negativ secular changes are occured.

Investigating height, weight, head circumference and chest circumference of Bulgarian children from birth to 3 years, Dundova et al. [9] found significantly slower acceleration changes between 1970 and 1980 compared to the previous decade. They considered that in our country and in set of countries are observed subsidence of acceleration processes. The study of secular trend in weight and stature of newborns from Smolyan region also shows tendency to negative changes in the period 1975–1995. But in the last decade (1995 – 2008), a tendency toward positive secular changes in both measures is noticed, better expressed in newborn boys [10].

Secular trends in body dimensions of newborns and preschool children in various populations are contradictory [1, 2, 3, 4, 6, 7]. Many authors studied secular changes in different age groups of children and adolescents. They established similar trends, increases of stature and weight to the 70's or 80's of the XX century, after which the increase stops or appeared deceleration changes [2, 3, 4, 6, 7]. In Croatia, however, between 1983 and 2003 a positive secular trend in the birth weight of liveborn children is established [1].

Conclusions

The children in the early twenty-first century are shorter than their coevals in 1980.
At the beginning of the XXI century the children have almost equal body weight with the generation peers in 1960.

Newborns and preschool children in the early XXI century have smaller head circumference compared with the generation twenty years ago.

References

1. Bralić, I., U. Rodin, J. Vrdoljak, D. Plavec, V. Čapkun. Secular birth weight changes in liveborn infants before, during, and after 1991-1995 homeland war in Croatia. – Croatian Medical Journal, Vol. 47, Issue 3, 2006, 452-458.
2. Falkner F, J. M. Tanner. Human Growth – 2nd Edition. Plenum Press, New York and London, 1987, 1-537.
3. Godina, E. Z. Some latest trends in the somatic development of Moscow schoolchildren. – In: Karel Hajniš (ed.): Growth and Ontogenetic Development in Man IV. – Charles University, Prague, 1994, 123-128.

4. Godina, E. Secular trends in some Russian populations. – Anthrop. Anz., 68, 4, 2011, 367-377.
5. Martin, R., K. Saller. Lehrbuch der Anthropologie in sistematischer Darstellung. – Bd. I. Stuttgart, Gustav Fisher Vergal, 1957, 322-324.
6. Bodzsár, E., C. Susanne. (eds): Secular growth changes in Europe. – Eötvös Univ. Press, Budapest, 1998, 5-.381.
7. Vignerova J., P. Blaha, J. Kobzova et al. 2000. Growth and development of school children. – Centr. Eur. J. Publ. Health, 8 (3): 21-23.
8. Ватев С. Антропология на българите. София, 1939, 12-49.
9. Дундова, Р. Лонгитудинално проучване растежа на деца от 0 до 3 годишна възраст. – Дис. к.м.н., София., 1978.
10. Младенова, С., Ц. Ничева. Физическо развитие на новородените деца от Смолянски регион (1975-2008 г). – Сборник доклади от Юбилейна национална научна конференция с международно участие „Човекът и вселената". 6-9.10.2011, Смолян, 432-437.
11. Слънчев, П., Б. Янев, Ф. Генов, П. Щерев, П. Боев, Д. Сепетлиев, Б. Захариев. Физическо развитие, физическа дееспособност и нервно-психическа реактивност на населението на България (1980-1982). – Национална спортна академия, София, 1992, 1-336.
12. Янев Б., П. Щерев, П. Боев, Р. Семерджиева, Д. Сепетлиев. Физическо развитие и дееспособност на населението в България от раждане до двадесет и шест години. – БАН, София, 1965, 31-44.
13. Янев Б., П. Щерев, П. Боев, Ф. Генов, Д. Сепетлиев, И. Попов, Б. Захариев. Физическо развитие, физическа дееспособност и нервно-психическа реактивност на населението. – Медицина и физкултура, София, 1982, 7-348.

INSTRUCTION TO AUTHORS

SUBMISSION: Original papers and review articles written in English are considered and should be sent to the Editor-in-Chief.
Address: Bulgarian Academy of Sciences
Institute of Experimental Morphology, Pathology and Anthropology with Museum
Acad. G. Bonchev Str., Bl. 25,
1113 Sofia
Bulgaria
Our e-mail address is: <iemabas@bas.bg>
Manuscripts should not exceed 4 standard pages including abstract, captions, references and figures (3 copies — two copies in English and one copy in Bulgarian, and a disc using WINWORD 7.0, Times New Roman 12 pt).

CONDITIONS: In submitting a paper, the author should state in the covering letter that the article has not been published elsewhere and has not been submitted for publication elsewhere.
All manuscripts are subject to editorial review.

ARRANGEMENT:
Title page. The first page of each paper should indicate the title, the authors' names and institute where the work was conducted, followed by abstract and key words.
Abstract. It should contain no more than 150 words.
Key words. For indexing purposes, a list of up to 5 key words in English is essential.
Tables and illustrations. Tables and captions to the illustrations should be submitted on separate sheets. The proper place of each figure in the text should be indicated in the left margin of the corresponding page. All illustrations (photos, graphs and diagrams) should be referred to as "figures" and given in abbreviation "Fig.". The author's name, the number of the figure with indication of its proper orientation (top, bottom) should be slightly marked on the back of each figure. All illustrations should be submitted in duplicate too.
References. They should be indicated in the text by giving the corresponding numbers in parentheses. The "References" should be typed on a separate sheet. The names of authors should be arranged alphabetically according to family names, first the articles in Roman alphabet, followed by the articles in Cyrillic alphabet. Articles should include the name(s) of author(s), followed by the full title of the article or book cited, the standard abbreviation of the journal (according to British Union Catalogue), the volume number, the year of publication and the pages cited. For books - the city of publication and publisher. In case of more than one author, the initials for the second, third, etc. authors precede their family names. Example:
Tuohy, V. K., Z. Lu, R. A. Sobel, R. A. Laursen, M. B. Lees. A synthetic peptide from myelin proteolipid protein induces experimental allergic encephalomyelitis. — J. Immunol., 141, 1988, 1126-1130.
Norton, W. T., W. Cammer. Isolation and characterization of myelin. — In: Myelin (Ed. P. Morell), New York, Plenum Press, 1984, 147-180.
Further details. Use only standard symbols and abbreviations in the text and illustrations. Manuscripts, figures and diagrams should not be folded.
Full address. The exact postal address completed with postal code of the senior author must be given. If correspondence is handled by someone else, indicate this accordingly.

ISSN 0861-0509

AIMS AND SCOPE

Acta morphologica et anthropologica publishes original and review articles in the following sections:

Section A – Morphology:

1. Neurobiology; 2. Structure and Metabolism of the Cells;
3. Cell Differentiation and Kinetics; 4. Cellular Immunology;
5. Experimental Cytology; 6. New Methods; 7. Anatomy.

Section B – Anthropology:

1. Physical Development; 2. Somatotype and Body Composition;
3. Population Genetics and Medical Anthropology;
4. Paleoanthropology and Paleopathology.